

A Study of Salt Tolerance in *Arabidopsis thaliana* and *Hordeum vulgare*.

Al-Arbe M. Attumi

Thesis Submitted for the Degree of Doctor of Philosophy

**Division of Biochemistry and Molecular Biology, Faculty of Biomedical
and Life Sciences, University of Glasgow, U.K.**

December, 2007

© *Al-Arbe M. Attumi*

ABSTRACT

The original objective of this work was to compare the cellular processes in salt tolerant and salt sensitive plants cells to gain insight into the mechanisms that confer halotolerance. Halotolerant and salt sensitive cell lines were derived from the model glycophyte *Arabidopsis thaliana*; in addition cell suspension cultures from the dicot halophytes *Beta vulgaris* and *Atriplex halimus* were also generated. Unfortunately, severe disruptions were encountered following a serious fire; persistent power failures, and failures of new equipment hampered progress with this work. For this reason, only comparisons between the *Arabidopsis* cell lines were completed. The halotolerant (HHS) cell lines survival strategy is to prevent Na accumulation when grown in < 100 mM NaCl. Wild type (WT) cells grow faster than HHS cells in the absence of NaCl, but rapidly take up Na in 50 mM NaCl where their growth is severely affected, and fail to grow completely above 100 mM NaCl. No evidence was found to suggest this growth impairment arose from osmotic stress or nutrient ion deficiencies. Protein profiling of HHS cells identified a number of proteins whose abundance is regulated by salt stress. These included proteins involved in ion transport, central metabolism, and general stress responses. The implications of these findings are discussed.

In a separate project, a whole plant approach was taken to establish the physiological mechanisms that account for the reported difference in halotolerance between two commercially grown barley lines originating from China. Measurements on growth and development, plant water status, tissue ion profiling, photosynthesis rates, and transpiration rates suggested the tolerant line (Zhou 1) enters the reproductive phase of its life cycle approximately one week earlier than the sensitive line (Zhou 85), and this critical period allows floral development resulting in improved yields. This early

flowering is not associated with the well characterized *PpD-H1* locus controlling early flowering in cereals.

The main conclusion from this study is that for glycophytes that do not complete a full life cycle above 100 mM NaCl (which includes all of the world's major crops), it is the ionic component of salinity stress that impairs growth and yield. Further research on salinity stress in crops should focus on understanding the processes that control ionic balance rather than osmoregulation.



In the Name of Allah (God), Most Gracious, Most Merciful.

ACKNOWLEDGEMENTS:

Countless thanks and praise is to Allah for helping me to achieve this thesis and assisting me in this short life. Also I am indebted to my supervisor, doctor Peter Dominy, for the spiritual support, the guidance, the kindness, the opportunity, and his help in the preparation of this thesis ‘no a ward can describe his assistance’. Much thanks to him for giving me advice throughout the course of this undertaking. Special thanks are extended to Dr. Kimberley Mac-Kendrick for her assistance with protein analysis. I would also like to thank a lot Dr. Richard Burchmore for his useful advice and allowing me to use his lab for scanning and analysing gels. Dr. Robin Strang is thanked for his encouraging efforts and advices. Special thanks to all staff members, and students of the Plant Sciences Group for the warmth and kindness shown to me. In particular, I would like to thank a lot the people of Libya and the Ministry of Higher Education of Libya for the financial support in Libya and U.K.

Last but not least. I would like to express sincere thanks to my wife Zinab for playing a very important role especially during my studies. I also thank my sons Mohammed and Omar for their patient and creating a very nice environment. Finally, I am extremely grateful to my parents for their encouragement and support during my studies. Without the help of Allah and the help of all people mentioned above this work will not become true.

TABLE OF CONTENTS

Sections.....	Page
Title Page.....	0
Abstract.....	i
Acknowledgements.....	iii
Table of Contents.....	iv
List of Figures.....	xi
List of Tables.....	xiv
Abbreviations.....	xv
Declaration.....	xvii
Chapter 1: Introduction.	1
1.1 The Effect of Salinity on Agriculture.....	4
1.2 Plants Show a Wide Range of Tolerance of Salinity.....	4
1.3 The Definitions of Soil Salinity.	6
1.4 The Deleterious Effects of Salinity on Plant.....	7
1.5 Plant Strategies for Coping with High Salinity.....	8
1.6 K ⁺ & Na ⁺ Uptake Pathways.....	9
1.6.1 High Affinity Potassium Absorption.....	11
1.6.2 K ⁺ Transport within the Plant.....	12
1.7 The Role of Ca ²⁺ in Plant Salt Tolerance.....	13
1.8 Possible Mechanisms Conferring Salt Tolerance.....	14
1.9 The Importance of Turgor.....	14
1.10 Na ⁺ Requirement and Acquisition.....	17
1.10.1 Na ⁺ Requirements in Plants.....	17
1.10.2 Na ⁺ Uptake Mechanisms.....	18
1.10.3 The SOS Mechanism and Salt Efflux.....	19
1.11 Salt Stress Sensing in Plants.....	23
1.12 Na ⁺ Sequestration.....	23

1.13	Utilizing Model Plants to Study Salt Tolerance.....	24
1.14	Project Aims.....	26
Chapter 2: Comparison of Salt Tolerant and Salt Sensitive Arabidopsis Cell		
Lines.	28
2.1	Introduction.....	28
2.2	Materials and Methods.....	29
2.2.1	Arabidopsis Cell Suspension Cultures.....	29
	2.2.1.1 <i>Establishment of the Arabidopsis Habituated to High Salt (HHS) Cell Line</i>	30
2.2.2	Measurement of Growth Rates of Cell Cultures.....	30
2.2.3	Preparation of Cell Culture Material for ICP-OES Analysis.....	31
	2.2.3.1 <i>Standard Solutions</i>	31
	2.2.3.2 <i>Assessment of Ion Concentration in Plant Material</i>	32
2.3	Results.....	34
2.3.1	Comparison of WT and HHS Cell Cultures: Morphology.....	34
	2.3.1.1 <i>Fluorescein Diacetate (FDA) Staining</i>	34
	2.3.1.2 <i>Imaging Arabidopsis Cell Suspension Cultures</i>	34
2.3.2	Comparison of WT and HHS Cell Cultures.....	38
	2.3.2.1 <i>Effect of Salinity on the Growth of WT Cells</i>	38
	2.3.2.2 <i>Effect of Salinity on the Ion Content of WT and HHS Cells</i>	44
2.3.3	The Effects of Salt-Shock on the Growth and Ion Content of HHS Cells. 47	
	2.3.3.1 <i>Growth Rates of Salt-Shock HHS Cells</i>	47
	2.3.3.2 <i>Ion Content of Salt Shocked HHS Cells</i>	51
2.3.4	Assessment of Growth Limitation in WT and HHS Cell Cultures.....	52
2.4	Discussion.....	63

Chapter 3: Comparison the Proteome of Salt Tolerant and Salt Sensitive	
Arabidopsis Cell Lines.....	67
3.1	Introduction..... 67
3.1.1	Expression Profiling..... 67
3.1.2	General Aspects of Proteomics..... 68
3.1.3	Two-Dimensional Electrophoresis..... 69
3.1.3.1	<i>First Dimension Immobilized pH Gradient Gels.</i> 70
3.1.3.2	<i>Second Dimension SDS-PAGE.</i> 71
3.1.4	Mass Spectrometry..... 71
3.1.4.1	<i>MALDI-TOF.</i> 72
3.1.4.2	<i>Tandem MS.</i> 73
3.1.4.3	<i>Quantitative Proteomics.</i> 74
3.1.5	Integration of Genomic, Proteomics, and Bio-Informatics..... 75
3.2	Materials and Methods..... 76
3.2.1	Plant Material..... 76
3.2.2	Reagents and Apparatus..... 76
3.2.3	Experiment Setup..... 76
3.2.4	Sample Preparation..... 79
3.2.4.1	<i>Harvesting Arabidopsis Cells.</i> 79
3.2.4.2	<i>Protein Extraction.</i> 79
3.2.5	Determination of Protein Concentration..... 80
3.2.6	CyDye Labelling of Proteins..... 80
3.2.6.1	<i>Minimal Labelling.</i> 80
3.2.6.2	<i>1st Dimension Separation by Isoelectric Focussing.</i> 81
3.2.6.3	<i>2nd Dimension SDS Page Gel.</i> 84
3.2.6.3.1	<u>Preparation of Large Format Gels.</u> 84

3.2.6.3.1.1	Preparation of Gel Plates.....	84
3.2.6.3.1.2	Gel Casting.....	85
3.2.6.3.2	<u>Running the Second Dimension Gel</u>	86
3.2.7	Gel Scanning.....	87
3.2.8	Sypro Orange Staining.....	88
3.2.9	Spot Excision, Digestion, and Preparation for MS.....	90
3.2.9.1	<i>Spot Excision</i>	90
3.2.9.2	<i>Trypsin Digestion of Protein Samples</i>	90
3.2.10	Mass Spectrometry.....	91
3.2.10.1	<i>MALDI-TOF</i>	91
3.3	Analyses of Gel Images.....	92
3.3.1	Preparation of Gel Imaging.....	92
3.3.2	Spot Detection, Spot Matching and Generation of a Spot Map Using the Decyder V 5.01 DIA Module.....	92
3.3.3	Between-Gel Spot Matching, Determination of Protein Abundance, and Statistical Analysis Using the DeCyder V5.01 BVA Module.....	95
3.3.4	BVA Protein Table.....	96
3.3.5	Results.....	97
3.3.6	Spot Picking, MS and Protein Identification.....	98
3.3.7	Salt Stress Up-Regulated Proteins.....	100
3.3.8	Salt Stress Down-Regulated Proteins.....	101
3.3.9	Salt Stress Modulated Proteins (up and down-regulated).....	101
3.4	Discussion.....	103
3.4.1	Up-Regulated Proteins.....	104
3.4.1.1	<i>Transport proteins</i>	104
3.4.1.2	<i>Signalling Proteins</i>	106
3.4.1.3	<i>Stress Proteins</i>	107

3.4.1.4	<i>Senescence/Autophagy Proteins</i>	107
3.4.2	Down-Regulated Proteins.	108
3.4.2.1	<i>GST proteins (stress proteins)</i>	108
3.4.2.2	<i>Ambiguous Ferritin proteins</i>	108
3.4.3	Modulated (Down & up-regulated) proteins.....	109
3.4.3.1	<i>Transport proteins</i>	109
3.4.3.2	<i>Stress proteins</i>	109
Chapter 4: Comparison of Salt Tolerant and Salt Sensitive Barley Lines. ...		111
4.1	Introduction.....	111
4.1.1	The Barley Genotype Lines Used in This Study.....	112
4.2	Materials and Methods.....	113
4.2.1	Plant Material.....	113
4.2.2	Experimental Design.....	114
4.2.3	Preparation Barley Material for ICP-OES Analysis.	116
4.2.4	Photosynthesis.....	116
4.2.4.1	<i>Photosynthesis Measurements</i>	116
4.2.4.1.1	<u>CO₂ Response Curve</u>	117
4.2.4.1.2	<u>Light Response Curve</u>	121
4.2.4.2	<i>Modeling Photosynthetic Light Response</i>	125
4.2.4.2.1	<u>Rectangular Hyperbola Model (Linear)</u>	125
4.2.4.2.2	<u>Non Linear Model</u>	126
4.2.5	Assessment of Development.....	127
4.2.6	Assessment of Ppd-H1 Flowering Locus.....	127
4.2.6.1	<i>Isolating of Zhou 1 and Zhou 85 Genomic DNA for PCR Analysis</i> ..	127
4.3	Results.....	130
4.3.1	Growth Parameters.....	130

4.3.1.1	<i>Shoot and Root length.</i>	130
4.3.1.2	<i>Shoot and Root Fresh Weight.</i>	130
4.3.1.3	<i>Shoot and Root Dry Weight.</i>	130
4.3.1.4	<i>Number of Tillers per Plant.</i>	130
4.3.2	Grain Yield.....	137
4.3.2.1	<i>Spikes and Seeds per Plant.</i>	137
4.3.2.2	<i>Grain Yield and % Grain Yield.</i>	137
4.3.2.3	<i>Thousand Grain Yield.</i>	137
4.3.3	Plant Water Status.....	141
4.3.3.1	<i>Relative Water Content and Water Potential.</i>	141
4.3.3.2	<i>Water Use Efficiency (WUE).</i>	141
4.3.4	Ion Content Assessment.....	145
4.3.4.1	<i>K⁺ Content of Barley Shoot and Root.</i>	145
4.3.4.2	<i>Na⁺ Content of Barley Shoot and Root.</i>	145
4.3.4.3	<i>K⁺/Na⁺ Ratio of Barley Shoot and Root.</i>	146
4.3.4.4	<i>Ca⁺² Content of Barley Shoot and Root.</i>	146
4.3.5	Photosynthesis Measurements.....	151
4.3.5.1	<i>Photosynthesis Rates.</i>	151
4.3.5.1.1	<u>A_{max} and Alpha (α).</u>	151
4.3.5.1.2	<u>Photorespiration (Rl) and Dark Respiration (Rd).</u>	154
4.3.5.1.3	<u>V_{rubisco}.</u>	154
4.3.5.2	<i>Carbon Dioxide Supply.</i>	157
4.3.5.2.1	<u>Stomatal Conductance (gs) and Stomatal Control of Photosynthesis (L).</u>	157
4.3.6	Development Measurements.....	161
4.3.7	Assessment of Ppd-H1 Flowering Locus.....	161

4.3.8	Discussion.....	167
Chapter 5: General Discussion		169
5.1	Assessment of the Halotolerance of WT and HHS Arabidopsis thaliana Cell Suspension Cultures.....	170
5.2	Proteome Analysis of Arabidopsis HHS Cell Suspension Cultures Exposed to Salt Shock.....	175
5.3	Comparison of Salt Stress in Two Barley Lines.....	177
5.4	General Summary.....	179
Appendix.....		181
References.....		220

List of Figures

Fig. 1-1 Current Use of Potential Agricultural Land from the 13 Billion Hectares of Land Area on Earth.	3
Fig. 1-2 Possible Mechanisms Maintaining Ion Balance across the Plasma Membrane and Tonoplast of Salt-Tolerant and Salt-Sensitive Plant Cells.	16
Fig. 1-3 SOS Signalling Pathway for Na ⁺ Homeostasis in <i>Arabidopsis</i>	22
Fig. 2-1 Images of <i>Arabidopsis</i> HHS and WT Cells.	37
Fig. 2-2 Growth Curves of Wild Type <i>Arabidopsis</i> Cell Suspensions Exposed to Osmotic and Ionic Stress.	40
Fig. 2-3 Growth Curves of HHS <i>Arabidopsis</i> Cell Suspensions Exposed to Osmotic and Ionic Stress.	42
Fig. 2-4 Ion Content of WT and HHS <i>Arabidopsis</i> Cell Cultures.	46
Fig. 2-5 Growth Rates of HHS Cell Suspension Cultures Exposed to Ionic Stress.	49
Fig. 2-6 Ion Content of HHS <i>Arabidopsis</i> Cell Cultures.	55
Fig. 2-7 Sucrose Content of Basic Growth Media for <i>Arabidopsis</i> Cell Cultures.	56
Fig. 2-8 Ion Content of Basic Growth Media for <i>Arabidopsis</i> Cell Cultures.	57
Fig. 2-9 pH measurement of Basic Growth Media for WT and HHS <i>Arabidopsis thaliana</i> Cell Cultures.	58
Fig. 2-10 DAF-2DA Stained WT <i>Arabidopsis thaliana</i> Cell Suspension Cultures in 0 mM NaCl (BGM0-0.55).	59
Fig. 2-11 DAF-2DA Stained WT <i>Arabidopsis thaliana</i> Cell Suspension Cultures in 50 mM NaCl.	60
Fig. 2-12 DAF-2DA Stained HHS <i>Arabidopsis thaliana</i> Cell Suspension Cultures.	61
Fig. 2-13 DAF-2DA Stained HHS <i>Arabidopsis thaliana</i> Cell Suspension Cultures in 300 NaCl.	62
Fig. 3-1 Schematic Diagram of the Three Different Growth Conditions of HHS Cells Used for Proteome Analysis.	78
Fig. 3-2 Schematic diagram of CyDye protein labeling reaction.	83

Fig. 3-3 Images from a 2-D analysis showing two different samples plus the pooled Sample Image.....	94
Fig. 4-1 The Effect of Salinity on the Growth of Sixteen Commercial Barley Lines...	115
Fig. 4-2 Profile of Leaf Chamber Conditions Used to Collect CO ₂ - Response Curves.	119
Fig. 4-3 Carbon Dioxide Response Curve (CRC) of a Barley Leaf.....	120
Fig. 4-4 Profile of Leaf Chamber Conditions Used to Collect Light Response Curves.	123
Fig. 4-5 Light Response Curve of Barley Leaf.....	124
Fig. 4-6 Zhou 1 and Zhou 85 Barley Lines Exposed to NaCl.....	132
Fig. 4-7 The Effects of Salt Treatments on Primary Shoot and Root Length of Two Barley Lines (Zhou 1 and Zhou 85).....	133
Fig. 4-8 The Effects of Salt Treatments on Shoot and Root Fresh Weight of Two Barley Lines (Zhou 1 and Zhou 85).	134
Fig. 4-9 The Effects of Salt Treatments on Shoot and Root Dry Weight of Two Barley Lines (Zhou 1 and Zhou 85).	135
Fig. 4-10 The Effects of Salt Treatments on Number of Tillers of Two Barley Lines(Zhou 1 and Zhou 85).	136
Fig. 4-11 The Effects of Salt Treatments on Spikes and Seeds per Plant of Two Barley Lines (Zhou 1 and Zhou 85).	138
Fig. 4-12 The effects of salt treatments on the Grain Yield and % Grain Yields of two barley lines.	139
Fig. 4-13 The Effects of Salt Treatments on 1000-Grain Weight (g) of Two Barley Lines.....	140
Fig. 4-14 The Effects of Salt Treatments on Relative Water Content (RWC) and Water Potential (ψ_{H_2O}) of Two Barley Lines.....	143
Fig. 4-15 The Effect of Salt Treatment on the Water Use Efficiency of Two Barley Lines.....	144
Fig. 4-16 K Content of Salt Stressed Barley Shoots and Roots.....	147

Fig. 4-17 Na Content of Salt Stressed Barley Shoot and Root.	148
Fig. 4-18 K^+/Na^+ Ratios of Salt Stressed Barley Shoot and Root Tissue.	149
Fig. 4-19 Calcium Content of Salt Stressed Barley Shoot and Root.	150
Fig. 4-20 The Effects of Salt Treatments on CO_2 Assimilation and Quantum Efficiency, α of Two Barley Lines.	153
Fig. 4-21 The Effects of Salt Treatments on Photorespiration, R_i and Dark Respiration, R_d of Two Barley Lines.	155
Fig. 4-22 The Effect of Salt Treatments on $V_{rubisco}$ of Two Barley Lines.	156
Fig. 4-23 The Effects of Salt Treatments on Stomatal Conductance, (g_s) and Stomatal Control of Photosynthesis, (L) of Two Barley Lines.	159
Fig. 4-24 A_{max} <i>Versus</i> Stomatal Conductance (g_s) of two barley lines.	160
Fig. 4-25 Comparison of the Rate of Development of Zhou 1 and Zhou 85 Barley Lines.	164
Fig. 4-26 Genotyping Zhou 1 and Zhou 85 Barley Lines for the Early Flowering Locus Ppd-H1.	166

List of Tables

Table 2-1 The Final Concentration of Elements in the times 1 (X1) Standard Solution for Ion Analysis.....	33
Table 2-2 The Relative Growth Rates and Doubling Times of Wild Type and HHS Arabidopsis Cell Suspension Cultures Exposed to Osmotic and Ionic Stress.	43
Table 2-3 The Relative Growth Rates and Doubling Times of HHS Arabidopsis Cell Suspension Cultures Exposed to Ionic Stress.	50
Table 3-1 The Appropriate Laser and Wavelength Settings for Each Dye Scan.....	89
Table 4-1 Primers Used to Amplify SNP 22 of the Ppd-H1 Flowering Gene.	129
Table A 2-1 Linsmaier & Skoog Basal Medium (MSMO) is Components.....	181
Table A 3-1 Experimental Design of 2-D DiGE.....	182
Table A 3-2 Up-regulated Proteins in HHS <i>Arabidopsis</i> Cells Grown in High Salt.....	183
Table A 3-3 Down-regulated Proteins in HHS <i>Arabidopsis</i> Cells Grown in High Salt.	190
Table A 3-4 Modulated (Down & Up-regulated) Proteins in HHS <i>Arabidopsis</i> Cells Grown in High Salt.	193
Table A 4-1 Composition of 1/4 Strength Hoagland’s Nutrient Solution (SHNS) Ingredients.....	208
Table A 4-2 Raw Data of Two Barley Lines Development According to Zadok’s Scale.	215
Table A 4-3 Cereal Grain Development Stages by Zadoks, Feekes and Haun.....	217

List of Abbreviations

BGM	Basic Growth Media.
ABA	Abscisic Acid.
2,4-D	2,4-Dichlorophenoxyacetic Acid
A_{\max}	Maximum Photosynthesis Rate.
A_n	Net Photosynthesis Assimilation.
BLAST	Basal Local Alignment Sequencing Toll
BSA	Bovine Serum Albumin.
bp	Base pair.
C_a	Air CO ₂ Concentration
C_i	Internal CO ₂ Concentration
cDNA	Complementary Deoxyribonucleic Acid
CRC	CO ₂ Response Curve
CHAPS	3-[(3-Cholamidopropyl) Dimethylammonio] 1-Propane Sulfonate.
dS m^{-1}	deciSiemens per meter,
DTT	Dithiothreitol.
DiGE	Difference Gel Electrophoresis.
EC	Electrical Conductivity.
ESI-MS/MS	Electro Spray Ionization Tandem Mass Spectrometer.
EDTA	Ethylenediamine tetraacetic acid.
FAO	Food and Agricultural Organization of the United Nation.
FDA	Fluorescein Diacetate.
DAF-2DA	diaminofluorescein diacetate.
EnvZ	Inner Membrane Osmosensor.
GSTs	Glutathion-S-Transferase.
gDNA	genomic Deoxyribonucleic acid.
HHS	Habituated to high salt.
HKT1	<i>Triticum sativum</i> Gene Encoding a High-Affinity K ⁺ Transport.
ICP-OES	Inductively Coupled Plasma Optical Emission Spectroscopy.
IRGA	Infra Red Gas Analyzers.
LHCP	light harvesting chlorophyll–protein complexes.
LRC	Light Response Curve.
MALDI-ToF	Matrix Assisted Laser Desorption Ionisation Time of Flight.
MASCOT	Modular Approach to Software Construction Operation and Test

MPa	Mega Pascal.
MSMO	Murashige-Skoog-Basal Salt Medium.
NADPH	Nicotinamide Adenine Dinucleotide Phosphate-Oxidase.
NCBI	National Centre for Biotechnology Information.
NHX1	Gene Encoding Na ⁺ /H ⁺ antiporter.
OmpF	Outer Bacterial Membrane Protein F
PAGE	Polyacrylamide-Gel Electrophoresis.
ppm	Part Per Million.
pH	Hydrogen Ion Concentration Unit.
psi	Pounds Per Square inch.
PAR	Photosynthetic Active Radiation.
PPFD	Photosynthetic Photon Flux Density.
ppmv	parts per million by volume.
PMT	Photomultiplier tube
PTM	Post-Translational Modification.
Rd	Dark respiration.
ROs	Reactive Oxygen Species.
Rl	Photorespiration.
rpm	Revolution Per Minute.
RT-PCR	Reverse Transcriptase-Polymerase Chain Reaction.
Rubisco	Ribulose Bisphosphate Carboxylase-Oxygenase.
SDS-PAGE	Sodium Dodecyl Sulphate-Polyacrylamide Gel Electrophoresis.
SOS	<i>Arabidopsis</i> Salt Overly Sensitive.
TBE	Tris-Borate-Acid.
TEMED	Tetramethylethylenediamine.
Tween 20	Polyoxyethylelesorbitan Monolaureate.
V-H ⁺ -ATPase	Vacuolar H ⁺ -ATPase.
V-H ⁺ -PPase	Vacuolar H ⁺ -Pyrophosphate.
V-type	Vacuolar Type.
WT	Wild Type.

Declaration

I declare that this thesis for the degree of doctor of philosophy has been edited entirely by me and the work presented herein was performed by myself unless stated otherwise.

Signature

Date

Chapter 1: Introduction.

Over the last one hundred and fifty years global food production (agriculture production) has increased dramatically. This has occurred chiefly through the application of irrigation, chemical and organic fertilizers, agrochemicals to control weeds, pests and pathogens, genetics and plant breeding, and most recently bioengineering technology. All of these have increased food production globally (Huang *et al.*, 2002), and total cereal crop yield has practically doubled since 1960 (Kishore and Shewmaker, 1999). In Asia alone the improved crop yield from the Green Revolution reduced global hunger to 20% in the 1960s (Toenniessen *et al.*, 2003). However, it is likely that both increased yields and the acquisition of new arable land will be required to meet the needs of the 21st Century. Whatever technologies are developed and used, they must be sustainable in the long term.

Food production is not uniformly distributed across the globe due to the diversity of terrain, local climatic conditions, and the available agricultural expertise. Clearly, there is a limit to the amount of land available for food production, and to the theoretical limit on the maximum attainable yield of any given crop. At present, global food production is unbalanced; 183 nations in the world depend on food from outside their borders (food imports); this food comes from those countries with relatively low populations that practice intensive agriculture. Eighty-percent of cereal export is from the United States, Canada, Australia, and Argentina (World Resources Institute, 1992; US Census Bureau, 2004), but this will not be the case in the next 60 years if U.S. population continues to rise (double to 540 million people; United States Bureau of the Census, 1996). Overall based on realistic trends in food supply, these countries may no longer be in a position to export food by 2050 (Brown, 1995).

Salinity affects 7% of the world's land area, which amounts to 930 million ha (Szabolcs, 2004). It has been estimated that 20% of irrigated land suffers from salinity which if left untreated can render the land useless. Irrigation is important for agriculture, irrigated land which account for 15% of total arable land produces at least double that of rain-fed land. In total irrigated arable land produces 1/3 of the world food supply (Munns, 2002).

The world's population doubled between 1900 and 1960; by 2000, the population had reached 6 billion citizens, three-and-a-half times the population of 1900 (US Census Bureau, 2004). The World Bank and the United Nations FAO document that 1 to 2 billion people are now malnourished due to a combination of the inadequate food supply, low income, and unfair food distribution (Pimental *et al.*, 1997). Most of these live in Developing Countries, and includes one third of the population of sub-Sahara African (FAO, 2002).

An increasing population will result in an increase in environmental problems, to more conflict, and to social unrest (Brown and Nielsen, 2000; Carpenter and Watson, 1994; Jayne, 1999; Plant *et al.*, 2000). It is clear that an increasing population will require more food, and this needs the acquisition of more arable land. However, the practices of intensive mechanized agriculture are causing increased soil erosion and salinization, and the loss of arable land.

Globally, food and field crops are grown on 11% of the earth's inland area of 13 billion hectares Fig. 1-1 (Buringh, 1989; World Resources Institute, 1994). The total loss of land due to urbanization and highways ranges from 10 to 35 million hectares a year, about ½ of this loss coming from crop land (Doos, 1994).

■ arable ■ pasture ■ forest ■ urban ■ other

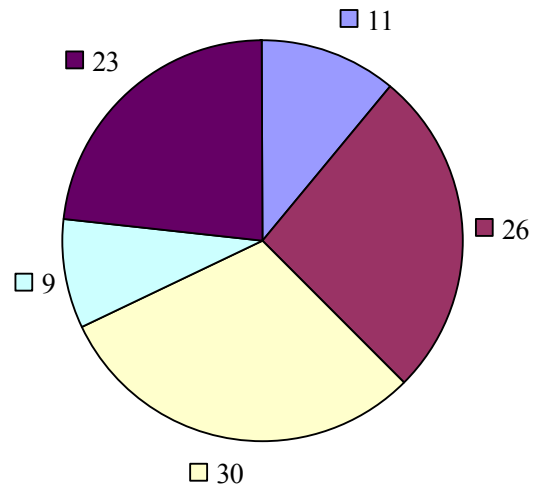


Fig. 1-1 Current Use of Potential Agricultural Land from the 13 Billion Hectares of Land Area on Earth.

The percentages in use are: ■ arable Land = 11%, ■ Pasture land =26%, ■ Forest land =30%, ■ Urban = 9%, and ■ Other = 23%. (Buringh, 1989; WRI, 1994).

Note, ‘Other’ means unsuitable for agriculture, pasture, or forests because the soil is too infertile or shallow to support plant growth, or the climate and land are too dry, cold, stony, steep, rocky or wet.

1.1 The Effect of Salinity on Agriculture.

The FAO reported in 1991 that more than 99% of world's food supply comes from land and less than 1% is from seas, oceans, and other aquatic habitats (FAO, 1991). The total arable land on the earth is approximately 13 billion ha of which 6 billion ha are located in arid and/or semiarid regions, and about 17% of this is severely affected by salt. In irrigated areas which constitute 230 million ha world-wide, 33% is affected by salt (Ashraf, 1994). Thus, the magnitude and the seriousness of the problem cannot be understated. Moreover, 40×10^3 ha of land world-wide is being lost every year from agriculture due to salinity (Al-Khatib *et al.*, 1993). It is also estimated that 250×10^3 ha of cultivated area in South Western Australia has become unproductive because of soil salinity (Malcolm, 1982).

The FAO also reported (FAO, 1990) that $2-3 \times 10^7$ ha of cultivated land is severely affected by salinity, and an additional $6-8 \times 10^7$ ha are affected to some extent. Only about 10% of total arable land on the earth can be considered as free from salt stress (Ashraf, 1994). In a survey on the distribution of 323 million ha of saline soils throughout the world, 54 million ha of the total is located in Africa, 17 million ha in Australia, 20 million in Mexico and Central America, 60 million ha in North America, 69 million ha in South America, 83 million ha in Southern Asia and 20 million ha in Southeast Asia (Massoud, 1974). In general, there is strong correlation between global agriculture yields and soil salinity.

1.2 Plants Show a Wide Range of Tolerance of Salinity.

Plants can be broadly classified into two groups according to their tolerance of salinity: (1) the salt sensitive plants, termed as 'Glycophytes': (2) the salt tolerant plants, or 'Halophytes'. Unfortunately, the major crops of the world are glycophytes that can not grow in saline habitats where salt concentrations are above ~ 100 mM NaCl. These

plants do not appear to possess mechanisms for adapting to the harmful effects of salinity. These glycophytes have evolved in habitats with very low soil Na^+ content, and may never have possessed the mechanisms or features to enable them to cope with the water deficits and ion levels prevailing in saline habitats (Greenway and Munns, 1980). Some classifications categorize plants as follows: tolerant, moderately tolerant, moderately sensitive, and sensitive, with respect of their response to salinity (Maas and Hoffman, 1977). For instance barley, cotton, and sugar beet are considered tolerant because they can grow in the salinity range of 6.9 to 8.0 dS m^{-1} (77-88 mM NaCl) without any apparent loss of yields, whereas most fruit trees, carrot, and onion are considered sensitive with yield loss thresholds of less than 2.0 dS m^{-1} (22 mM NaCl; (Maas and Hoffman, 1977). What is required is the development of major crop varieties that can grow in saline soils without losing their ability to produce high usable yields. The US Laboratory of Salinity define a saline soil as one with a saturation extract (the solution extracted from a soil at its saturation water content) electrical conductivity (EC) of greater than 4 deciSiemens m^{-1} , (equivalent to ~45 mM NaCl; Corwin *et al.*, 2003). The growth of many glycophytes is significantly limited in concentrations as low as 25-50 mM NaCl (Lessani and Marschner, 1978). In contrast, many halophytes grow well in high concentrations of NaCl, and complete their life cycle in full-strength sea water (~560 mM NaCl). Clearly, halophytes have the ability to avoid and/or get rid of toxic ions by mechanisms preventing them from accumulating at metabolic sites and impairing growth; many have specialized organs such as glands and bladders (Yeo, 1998). NaCl inhibits the *in vitro* activity of many enzymes (Blum, 1988; Greenway and Munns, 1980; Flower *et al.*, 1977). The cytoplasm of plant cells typically contain about 100 mM K^+ , and plant metabolism has, therefore, evolved to work efficiently at this concentration. Increased levels of Na^+ disrupt the ionic balance of the cytoplasm. As the

physicochemical properties of K^+ and Na^+ are similar, but not identical. As Na^+ levels in the cytoplasm rise, the ionic interactions within and between proteins, their co-factors, and substrates alters so that metabolism is no longer optimized. As a result, the activities of many enzymes operating in different pathways are perturbed (Flower *et al.*, 1977).

1.3 The Definitions of Soil Salinity.

Salt stress maybe defined as an excess of ions of soluble salts such as sodium (Na^+), chloride (Cl^-), calcium (Ca^{+2}), magnesium (Mg^{+2}), sulphate (SO_4^{-2}), and bicarbonate (HCO_3^-) in soil or in the culture medium that maybe have deleterious effects on plant growth (Lewis, 1984). Salinity is often expressed as concentrations (*e.g.* mM) or in electrical conductivities (EC). Salinity can be abbreviated as ECe (electrical conductivity of the extract) with units of electrical conductance (*e.g.* deciSiemens per meter, $dS\ m^{-1}$), or in the old units of electrical resistance (*e.g.* millimhos per centimeter, mmhos/cm), which is expressed in numerically equivalent units.

Along with the EC of soil extracts taken from the root zone, the EC of irrigated water, the solute (or osmotic) potential (ψ_s , measured in MPa), the total dissolved solids (TDS, $mg\ l^{-1}$), and total cation and anion content (TI, $mEq\ l^{-1}$) of the solution are also used for indices of salinity. The following relationships are often used: $\psi_s = 0.036\ EC$; $TDS = 640\ EC$; $TI = 10\ EC$, that is only if certain units are used (Fageria, 1992; United States Salinity Laboratory UC Riverside, 1954). The International System of Units (SI) of EC is deciSiement per meter ($dS\ m^{-1}$). For example, a soil extract with EC of one $dS\ m^{-1}$ has a concentration of roughly 11mM NaCl, and contains approximately 640 $mg\ L^{-1}$ total salts (Lewis, 1984). If soil extracts have an EC of greater than 4 $dS\ m^{-1}$ (46 mM NaCl) then the soil is considered to be saline (Troeh *et al.*, 1980). By definition, pure water at

STP (standard temperature and pressure) and air at 100% relative humidity has a water potential of zero.

1.4 The Deleterious Effects of Salinity on Plant.

Upon exposure, the primary effect of salt on plants is an osmotic stress (Jones, 1992) which causes dehydration and loss of turgor (within 1 hr). Subsequently, ingress of ions into cells can result in ion toxicity. Munns and co-workers (Munns *et al.*, 1995) tested wheat and barley genotypes for salt tolerance and noticed that there were two stages of growth response to salt stress. Initially, they identified a large decrease in growth rate, which arises from the loss of cell turgor. If the plant can regain turgor there is the potential to resume growth but, there is often a second reduction due to salt specific responses that originated from the accumulation of salt toxic levels within the cell. This may arise through disruption in the normal hormonal signals from roots (Munns, 2002). Under salt stress conditions, endogenous levels of a plant hormone, abscisic acid (ABA) increase (Gómez *et al.*, 1988), which appears acts as a signal to promote tissue acclimation (Chandler and Robertson, 1994). Elevated ABA levels have been correlated with increased tolerance to salt (Singh *et al.*, 1987), and exogenous application of ABA accelerated the adaptation of cultured tobacco cells to salt (LaRosa *et al.*, 1987), which provide further support for a role of ABA in the acclimation of plants to salinity and osmotic stress. The correlation between osmotic stress and change in the ABA level has been well established at the molecular level (Shinozki and Shinozaki-Yamaguchi, 1996).

In some plants, for example citrus, salt toxicity is due to Cl^- instead of Na^+ high concentration in the soil (Fernandez-Ballester *et al.*, 2003; Moya *et al.*, 2003). In plants chloride has two main roles: one as a counter anion for cation transport (Ca^{+2} , K^+ , Mg^{+2} , NH_4^+ *etc.*) for maintaining membrane potential: the second as a major osmotically

active solute for maintains both turgor and osmoregulation. Chloride is a micronutrient essential for healthy plant growth. A minimal requirement for crop growth of 1 g Kg^{-1} D Wt has been suggested, a quantity that can generally be supplied by rainfall (White and Broadley, 2001)

1.5 Plant Strategies for Coping with High Salinity.

Until recently strategies for solving the salinity problem in agriculture has tended to focus on soil reclamation. However, this has proved to be extremely expensive and untenable. In practice, land has been cultivated until salinity renders production uneconomic, at which point cultivation is switched to new areas. Recently, with the development of breeding and bioengineering, the focus has turned more towards developing salt-tolerant crops. However, this approach has its own drawbacks (Morpurgo, 1991). There is a view that salt tolerance in plants is a polygenic trait involving the co-ordinate expression of many genes, and that the prospects for bioengineering are therefore remote (Glenn *et al.*, 1999). However, recently this view has been challenged: salt resistant tomato (Zhang and Blumwald, 2001) and *Arabidopsis* (Apse *et al.*, 1999) plants have been produced by transformation with a single gene. Therefore, the prospects for overcoming salinity stress in crop plants using information derived from model system such as *Arabidopsis* and rice (*Oryza sativa*), may not be as bleak as once thought.

For example Gaxiola and co-workers (Gaxiola *et al.*, 1999) cloned the *A. thaliana* *NHX1* gene (encoding Na^+/H^+ antiporter) from a phage cDNA library of *A. thaliana* by probing with an EST (expressed sequence tag) (*Arabidopsis* Biological Resources Center, DNA stock Center contains a partial clone). The full length clone (2.1 Kb) is longer than the ORF (open reading frame) reported by the *Arabidopsis* Genome

initiative (ATM021B044) and has been deposited in GenBank (accession no AF106324).

Plants exposed to saline environments encounter three basic problems: (1) specific ion (Na^+ , Cl^- , *etc*) toxicity; (2) the need to maintain a favorable cell turgor pressure; (3) the need to obtain essential nutrient ions (*e.g.* K^+ , NO^-) in spite of the predominance of other chemically similar, potentially toxic ions (*e.g.* Na^+ , Cl^-) in the growth medium.

Salt tolerance in plants not only varies considerably among species, but also depends very much on the conditions under which the crop is grown (Maas, 1986). There are several factors that influence salt tolerance in plant. These include temperature, the composition and levels of salts, the growth phase of the plant, and the Leaching Fraction (LF) (Ayers and Westcot, 1976; Bauder, 2001; Fageria, 1992; Hanson *et al.*, 1999; Rhoades, 1977; USDA, 2002; Western Fertilizer Handbook, 1995).

Salinity has a negative impact on plant development and seed production. Flowering and maturity of rice is delayed by salt stress during both vegetative and reproductive growth stages (Castillo *et al.*, 2004). As little as 4g/l NaCl delayed flowering in iris plants by up to 3 days, and the delay of flowering continued after the salt stress was withdrawn (Zandt and Mopper, 2002) Plant tolerance to salinity is usually judged by three criteria: (1) the ability of the plant to survive on saline soils: (2) the growth rates and yields in saline habitats: (3) the relative growth rate or yield in saline compared with non-saline soils. The third criteria seems to provide the best estimate of plant salt tolerance (Mass and Grieve, 1987).

1.6 K^+ & Na^+ Uptake Pathways.

Unlike K^+ , Na^+ is not an essential mineral to plants in spite of its abundance in soil solutions. The high concentration of Na^+ and Cl^- in saline soils will disturb the acquisition of K^+ and other elements that are essential for plant growth, causing osmotic

stress and other problems such as oxidative stress (Zhu, 2001). Sodium inhibits many cytosolic enzymes as K^+ is normally required as a co-factor (Flower *et al.*, 1977; Wyn Jones and Pollard, 1983). Potassium uptake plays a very important role in plant growth and development (Ashley *et al.*, 2006; Mengel and Kirkby, 1982). Potassium flux in plant cells is essential for several physiological functions including: (1) enzyme activation: (2) osmoregulation: (3) control of membrane potential: (4) Turgor-controlled whole-leaf movements like heliotropism and stomatal function.

Not much is known about how plants absorb Na^+ from their surroundings but it is widely believed that Na^+ enters cells through K^+ channels and carriers located on the root cell plasma membranes (Schachtman *et al.*, 1997). This contention is supported by work on HKT1 (high-affinity K^+ uptake transporter) and LCT1 (low-affinity cation transporter) (Rubio *et al.*, 1995; Schachtman *et al.*, 1997).

Potassium uptake transporters in plant cells interact with some other metals such as Na^+ and Al^{3+} (Greenway and Munns, 1980). The absorption of K^+ is induced either by high-affinity or low-affinity mechanisms or a combination of both. High-affinity pathways are activated when the extra-cellular K^+ concentration is in the micromolar range and probably involves the utilization of a proton gradient and K^+/H^+ symporters. In contrast, the Low-affinity pathways operate when the extra-cellular K^+ concentration is in the millimolar range and involves ligand or voltage-gated channels (Assmann and Haubrick, 1996). The K_m values for K^+ uptake vary from 15 μM during K^+ starvation to 5 mM in cells growing at low millimolar K^+ concentrations (Ramos *et al.*, 1985; Rodriguez-Navarro and Ramos, 1984) to values as high as 50 mM in cells growing in K^+ concentrations exceeding 100 mM (Ramos *et al.*, 1994).

1.6.1 High Affinity Potassium Absorption.

High affinity K^+ uptake was first described by (Epstein *et al.*, 1963) and was named ‘Mechanism 1’. Although plants have an absolute requirement for K^+ , and Na^+ is toxic for many biological reactions in the cytoplasm, this is not the case if Na^+ is stored in the vacuole (Flowers and Lauchli, 1983; Subbarao *et al.*, 2003). High-affinity K^+ uptake is also essential for K^+ transport from the soil into plant roots (Epstein *et al.*, 1963; Epstein, 1966; Schroeder *et al.*, 1994). During the last decade many laboratories have attempted to identify plant genes encoding High-affinity K^+ uptake system that share characteristics with the fungal HAK transporters (Rodriguez-Navarro, 2000). Detailed analyses of HKT1 expressed in yeast and xenopus oocytes demonstrated two transport modes for HKT1, a saturatable high-affinity K^+ - Na^+ symporter activity and a low affinity Na^+ transport activity (Rubio *et al.*, 1995). High affinity K^+ uptake is stimulated by micromolar extracellular Na^+ concentrations. However, at high toxic extracellular Na^+ concentrations, K^+ uptake mediated by HKT1 is blocked and selective (low affinity) channel-like Na^+ uptake occurs (Gassmann *et al.*, 1996). HKT1 homologs have been isolated or detected from many plant species, including *Arabidopsis* (Uozumi *et al.*, 2000), rice (Fairbairn *et al.*, 2000) and the halophyte *Mesembryanthemum crystallinum* (Su *et al.*, 2003). The first K^+ channel was identified in yeast mutants using *Arabidopsis* cDNA libraries which belonged to class of inward-rectifier K^+ channels (Anderson *et al.*, 1992; Sentenac *et al.*, 1992). Eventually, a putative high-affinity barley transporter was identified with homology to the fungal HAK transporters (Santa-Maria *et al.*, 1997). The plant genes were named AtKT1 and At KUP (Fu and Luan, 1998; Kim *et al.*, 1998; Quintero and Blatt, 1997), or At HAK by (Santa-Maria *et al.*, 1997). Recently, BLAST searches of the plant genome database and the systematic use of the RT-PCR approach has led to the isolation of cDNA for HAK homologues from *Arabidopsis* (Rubio *et al.*, 2000), rice (Bañuelos *et al.*, 2002) and pepper (Martinez-

Cordero *et al.*, 2005). HKT transporters have two functions: (1) to take up Na^+ from the soil solution to reduce K^+ requirements when K^+ is a limiting factor, and (2) to reduce Na^+ accumulation in leaves by removing Na^+ from the xylem sap and loading Na^+ into the phloem sap (Rodriguez-Navarro and Rubio, 2006).

1.6.2 K^+ Transport within the Plant.

After entry into the root symplast, K^+ must be distributed to the rest of the plant, firstly by loading it to the xylem, and later moving it to the surrounding cells. In these movements K^+ crosses the plasma membranes of several types of cells, depending on the plant species. Moreover, fluxes into and out of the vacuole are also involved in cell K^+ homeostasis. It is obvious that K^+ channels mediate many of these fluxes (Véry and Sentenac, 2003), even when K^+ is taken up from low concentration solutions (Brüggemann *et al.*, 1999), but some other transporters are also involved. Interestingly, at the xylem/bundle sheath interface in maize leaves, the permeability for Rubidium (Rb^+) is at least as high as that for K^+ (Keunecke *et al.*, 2001), which is a characteristic of HAK transporters. This suggests that the function of high-affinity HAK-dependent K^+ uptake transporters is not restricted to K^+ uptake from the soil solution in root epidermal and cortical cells. Consistent with this notion is the observation that AtHAK5 is expressed in shoots (Ahn *et al.*, 2004; Rubio *et al.*, 2000) and in stellar root cells (Gierth *et al.*, 2005). In fact, most of the transporters of the KT/HAK/KUP family, 17 in rice (Bañuelos *et al.*, 2002) and 13 in Arabidopsis (Mäser *et al.*, 2001), do not belong to the cluster of the high-affinity transporters (Bañuelos *et al.*, 2002), and in some cases it has been argued that they are in fact low-affinity K^+ transporters (Senn *et al.*, 2001; Garcíadeblas *et al.*, 2002). A remarkable characteristic of KUP/HAK transports is that the range of K^+ concentrations at which they are active overlays with other types of transporters in bacteria, fungi, and plants. In *Escherichia coli*, the KUP transporters

exhibit low affinity transport (Bakker, 1993), whereas in fungi HAK transporters mediate high affinity K^+ transporters and seem to be redundant with other high-affinity K^+ transporters (Bañuelos *et al.*, 1995; Bañuelos *et al.*, 2000; Haro *et al.*, 1999). In plants, KT-HAK-KUP transporters have been associated with high-affinity K^+ uptake in root (Rubio *et al.*, 2000; Santa-Maria *et al.*, 1997)

1.7 The Role of Ca^{2+} in Plant Salt Tolerance.

Calcium is an essential macronutrient in plants and the content can be as high as 2.0% of the total dry weight (Benton-Jones, 1983). Calcium is generally taken up by the roots and travels with the transpiration stream until it reaches the leaves and other plant organs. Calcium deficiencies can occur in actively growing parts of the plant, while older parts may have an adequate amount. It is also effective in maintaining cell wall structure through its cross-linking between pectin polymers (Street and Opik, 2006). Calcium is also regarded as a very important second messenger involved in controlling many physiological processes and stress responses (*e.g.* stomatal movements, onset of senescence, pathogen attack, pollen tube growth, *etc.*; (Bush, 1995), and there is very good evidence that it directly or indirectly affects salt tolerance (Liu and Zhu, 1998; Shi *et al.*, 2000; Zhu *et al.*, 1998). Increased Ca^{2+} may protect the plants from NaCl toxicity by reducing the displacement of membrane associated Ca^{2+} (Cramer *et al.*, 1985) or by reducing Na^+ uptake and transport to the shoots (Cramer *et al.*, 1989; LaHaye and Epstein, 1971; Mass and Grieve, 1987). Ca^{2+} also improves K^+ uptake by plants exposed to high salinity (Cramer *et al.*, 1985; Cramer *et al.*, 1987), effectively increasing the K^+/Na^+ ratio in tissues, an important mechanism in salt tolerance (Greenway and Munns, 1980; Rengel, 1992).

1.8 Possible Mechanisms Conferring Salt Tolerance.

In general salinity is considered to be harmful when soil EC readings are greater than 4 dS m⁻¹, and of little concern at EC less than 2 dS m⁻¹. There are several key physiological features that are common in salt tolerant plants. First, the maintenance of a high cytoplasmic K⁺/Na⁺ ratio: second, the maintenance of a low concentration of Cl⁻ in cytoplasm (Fig. 1-2): third, the maintenance of turgor pressure in spite of low external water potentials (Blumwald *et al.*, 2000; Glenn *et al.*, 1999). These strategies are implemented by several mechanisms. These include the regulation of Na⁺/Cl⁻ transport from the roots to the shoot. Second, maintenance of low Na⁺ in the cytoplasm of cells by compartmentation within the cell (*i.e.* vacuole sequestration). Third, regulation of cytoplasmic net levels by the excretion from the cell and/or from tissues by specialized glands or bladders.

1.9 The Importance of Turgor.

Soft plant tissues (non-lignified) are supported by the pressure of cell contents against the cell walls. This is known as turgor pressure and is induced by the uptake of water into cytoplasm of the cells so that pressure is exerted by the plasma membrane on the cell wall. Water tends to move into the cell because of the osmotic effect of the low molecular weight solutes in the cytoplasm and vacuole. Water movement from the soil, through the plant, and into the air can best be understood from the concept of water potential, which is measured in pressure units (bars, Pascals etc.). Water always moves from high to low water potential whatever the cause of the difference in potential. By definition, pure water at S.T.P. (standard temperature and pressure) and air at 100% relative humidity have a water potential of zero. Because the growth (expansion) of cells of plant depends totally on turgor, decreased turgor is the factor most likely to inhibit plant growth when they are exposed to high salt (Ashraf, 1994). As a result,

transfer of a salt-sensitive plant from their original habitats to a high salt medium will produce a rapid water loss and wilting (Gorham, 1992a). Recently the plant cell vacuole has gained a lot of attention because of their multifaceted role in plant metabolism (*e.g.* recycling of cell components, regulation of turgor pressure, detoxification of xenobiotics, and accumulation of many storage substances (Maeshima, 2001). Moreover, the space-filling function of the vacuole is essential for cell growth, because cell growth is driven by the expansion of vacuole rather than that of the cytoplasm (Taiz, 1992). Osmotic adjustment by halophytes and other salt-tolerant plants to tolerate high saline conditions is a key strategy for survival and this can be achieved by ion uptake from the soil solution and sequestration in the vacuole, and by internal synthesis of compatible organic solutes in cytoplasm. A desiccated plant cell must reverse the water to potential gradient to survive, by forcing water flow back into the cell. Therefore, for plant cells to thrive in concentration above ~ 120 mM NaCl (\sim to -0.6 MPa, the water potential of plants in a well watered field), plants must develop a strategy to re-establish turgor pressure. Halophytes take advantage of their vacuoles to achieve this by accumulating enough osmotically-active solute in their vacuoles, to reverse the osmotic gradient so that water can be re-absorbed from the external medium. An energetically cheap way of accomplishing this is to take up Na^+ and Cl^- ions from the external medium and sequester them in the vacuole. If the solute potential (Ψ_s , or osmotic potential) of the vacuole (Ψ_s^{vac}) becomes more negative than that in the soil solution, water will flow into the cell and turgor will rise. However, for the cytoplasm to absorb water, it is necessary for the solute potential of the cytoplasm (Ψ_s^{cyt}) to decrease in parallel with Ψ_s^{vac} , and this can be achieved by the accumulation of non-toxic compatible solutes (*e.g.* glycine, betain, proline, and sugars; Flower *et al.*, 1977).

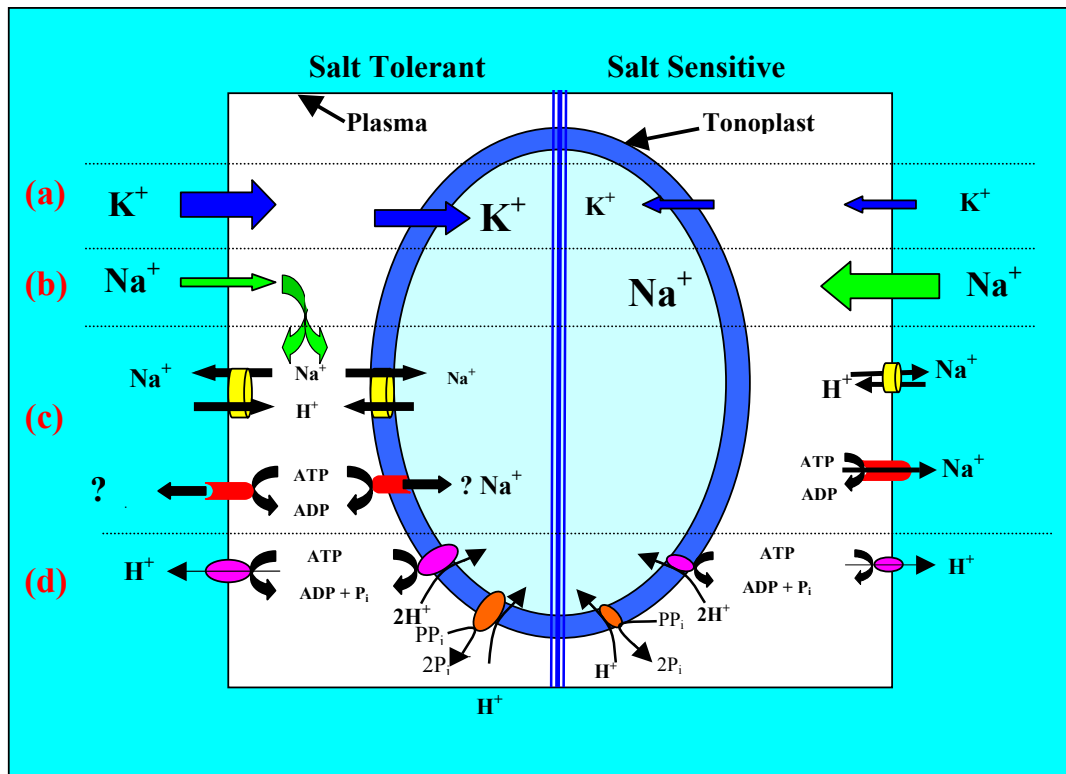


Fig. 1-2 Possible Mechanisms Maintaining Ion Balance across the Plasma Membrane and Tonoplast of Salt-Tolerant and Salt-Sensitive Plant Cells.

When compared with salt-sensitive plants, salt-resistant plants are believed to show increased levels of (a) potassium uptake, (b) decreased levels of sodium uptake, and (c) more efficient methods of sodium efflux by Na^+ -ATPases or Na^+/H^+ antiporters.

(d) H^+ pumping activity.

Na^+ , the major toxic cation found in saline soils, has a similar physiochemical structure to K^+ and competes for uptake, interfering with K^+ nutrition. There are two mechanisms of K^+ uptake in plants, the high affinity (K_m of 10-30 μM) to allow uptake at low external K^+ concentrations, (believed to be unaffected by external Na^+), and the low affinity mechanism that mediates K^+ uptake at high external K^+ concentrations (> 300 μM , K_m of >200 μM ; Buchanan *et al.*, 2000).

The mechanism for Na^+ uptake into plant cells is unknown, but has been assumed to occur through the K^+ pathway(s) or non-specific cation channels such as LCT1.

Na^+ efflux might occur through a Na^+ -ATPase (*cf. S. cerevisiae ENA1-4* system) or by a Na^+/H^+ antiporter (*e.g. SOS1*, Kamei *et al.*, 2005).

High K^+/Na^+ can be maintained by the controlled movement of these ions across the plasma membrane. Therefore, it is feasible that salt-resistant cells can discriminate more efficiently between K^+ and Na^+ with a stronger preference for K^+ uptake against Na^+ , or also, with effective Na^+ expulsion mechanisms.

The maintenance of favorable ion balance is dependent on the activity of H^+ pumps that drive active transport processes (d). these include the plasma membrane P-type H^+ ATPase, and tonoplast V-type H^+ ATPase and H^+ pyrophosphatase (Magnotta and Gogarten, 2002). Salt tolerance may depend on high densities and/or activities of these pumps.

1.10 Na⁺ Requirement and Acquisition.

1.10.1 Na⁺ Requirements in Plants.

The criteria for any element to be essential has been stated by (Arnon and Stout, 1939) the following conditions must be met for an element to be considered as “an essential nutrient for plants:” (1) the organism cannot complete its life cycle without it; (2) its action must be specific and cannot be replaced (completely) by any other element; (3) its effect on the organism must be direct, not indirectly through the environment. This set of criteria has been expanded by (Epstein, 1965) to include that if an element is part of an essential compound it must also be essential. Na⁺ has been shown to be essential for certain C₄ plant species, such as *Atriplex vesicaria*, *A. tricolor*, *Kochia childsii*, *Panicum miliaceum*, and *Distichlis spicata* L. In the absence of Na⁺, these C₄ plants grow poorly, showing visible deficiency symptoms such as chlorosis and necrosis, or fail to form flowers. Supplying 100 μM Na enhances growth and alleviated visual deficiency symptoms (Marschner, 1995; Pessaraki and Marcum, 2000; Pessaraki *et al.*, 2001; Brownell and Crossland, 1972).

It is generally considered that all higher plants show two contrasting responses to high external salt (NaCl) concentrations. One, is characterized by halophytes and involves high salt uptake with no damage within shoot organs, and is sometimes accompanied by salt excretion from leaves. The second, is typical of glycophytes; uptake occurs from the medium with subsequent upward movement through the shoot, but passage is restricted by mechanisms of varying effectiveness (Greenway and Munns, 1980; Läuchli, 1984). This second class of response is widespread among non-halophytic dicotyledons, particularly legumes, and usually relates specifically to exclusion of Na⁺, especially from leaves (Jacoby, 1964). Most species in this category are relatively sensitive to salt,

but others are notably more tolerant, e.g. *Lupinus luteus*, *L. angustifolius*, *Trifolium alexandrinum* (Läuchli, 1984).

1.10.2 Na⁺ Uptake Mechanisms.

A high K⁺/Na⁺ ratio in the cytosol is a very important and essential feature for normal cellular function in plants. Since living cells are not completely impermeable to Na⁺, the low concentration of Na⁺ in the cytoplasm requires its continuous exclusion normally against an electrochemical gradient (Rodriguez-Navarro *et al.*, 1994). Therefore, active exclusion of Na⁺ occurs either by a primary active Na⁺-pumping ATPase or by a secondary active (Na⁺ /H⁺ antiporter) mechanisms coupled to an electrochemical proton gradient Fig. 1-2 (Serrano and Gaxiola, 1994). Due to the physio-chemical similarity between K⁺ and Na⁺, it is generally assumed that K⁺ and Na⁺ compete for common absorption sites in the root. High affinity transporters are effective at very low external K⁺ concentrations and saturate when external K⁺ concentrations rise to 1 mM (Epstein, 1961). Sodium, even in 20-fold excess, fails to compete significantly with K⁺ for binding sites on High Affinity transporters. At higher concentrations of K⁺ (> 1 mM), Low Affinity transporters become important (Epstein, 1961; Epstein *et al.*, 1963), and some of these transporters do not discriminate well between K⁺ and Na⁺, and thus Na⁺ can competitively inhibit the absorption of K⁺ (Rains and Epstein, 1965).

Sodium uptake in plants is believed to be primarily through Low Affinity transporters (Rains, 1972). Recently K_{in} (inward rectifying K⁺ channels) channels have been reported in different root cells, including cortical, root hair, stellar and xylem parenchyma cells, that can sense external K⁺ concentrations (Blumwald *et al.*, 2000; Findlay *et al.*, 1994; Gassmann and Schroeder, 1994; Kim *et al.*, 1998; Maathuis and Sanders, 1995; Roberts and Tester, 1995; Vogelzang and Prins, 1994; Wegner and Raschke, 1994). These ion channels transport at rates between 10⁶ and 10⁸ ions per

second per channel protein. Transport is 'passive', where the diffusion of ions through the channel is a function of both the membrane voltage and the concentration difference across the membrane; thus uptake is not directly coupled to the input of other forms of free energy (Blumwald *et al.*, 2000; Maathuis *et al.*, 1997). Some argue plants should be termed according to their ability to absorb Na^+ and translocate it freely to the shoot. 'Natrophiles' take up and translocate Na^+ freely, whereas 'Natrophobes' desire to show a strong preference to absorb K^+ over Na^+ (Whitehead and Jones, 1972; Shone *et al.*, 1969; Smith *et al.*, 1980).

1.10.3 The SOS Mechanism and Salt Efflux.

Arabidopsis salt overly sensitive (SOS) mutants were identified by genetic screening of mutagenised seedlings for hypersensitivity to NaCl stress, and were characterized by retarded root growth (Liu and Zhu, 1998; Shi *et al.*, 2000; Shi *et al.*, 2002). In particular, the SOS1, SOS2, and SOS3 mutants were hypersensitive to Na^+ and Li^+ ions. Genetic and physiological data indicate that SOS1, 2 and 3 function within the same stress response pathway and lead to Na^+ tolerance (Zhu, 2003).

Under salt-stress conditions, *Arabidopsis* SOS mutants show a hypersensitive root growth. The SOS gene products are involved in ion transport and signalling processes. SOS1 encodes a plasma-membrane-localized Na^+/H^+ antiporter (Shi *et al.*, 2000) and is the principal target of the SOS pathway (Shi *et al.*, 2000; Shi *et al.*, 2003). SOS1 is the primary transport system responsible for cellular Na^+ efflux (Zhu, 2003) and controls Na^+ loading into the xylem of the root thereby restricting accumulation of the toxic ion in the shoot (Shi *et al.*, 2002). Furthermore, the SOS1 protein is localized in the epidermis, particularly in the root tip that are critical for growth and differentiation of the root and have an underdeveloped vacuoles so Na^+ sequestration is not feasible (Shi

et al., 2002). SOS1 has also been suggested to function as a Na⁺ sensor and is known to mediate control of target gene expression (Zhu, 2003).

SOS2 encodes a Ser/Thr protein (Serine/Threonine) kinase with sequence similarity to the catalytic domain of yeast SNF1, sucrose non-fermenting 1 (Halfter *et al.*, 2000). SOS2 is activated through the repression of autoinhibition (Halfter *et al.*, 2000; Guo *et al.*, 2001). Activated SOS2 is then recruited to the plasma membrane where it phosphorylates SOS1 leading to activation of its Na⁺/H⁺ antiporter activity (Quintero *et al.*, 2002). SOS3 encodes a Ca²⁺ binding protein with three predicted Ca²⁺ EF-hands (Liu and Zhu, 1998). SOS3 physically interacts with and activates SOS2. Thus the SOS3–SOS2 complex regulates the activity of SOS1 thereby regulating Na⁺ efflux from the cell (Qiu *et al.*, 2002). Several genes (*e.g.* At1g2190, At3g500601, At1g29500, and At4g37260) in the SOS mutants exhibit alterations in their expression patterns relative to those in wild-type plants (Gong *et al.*, 2001). (Kamei *et al.*, 2005) reported that SOS2 mutants were more sensitive under salt stress condition than those of SOS3 which suggests that the SOS pathway is more complicated than first thought (see Fig. 1-3).

In conclusion, the Salt-Overly-Sensitive (SOS) signalling pathway is a major regulatory cascade that controls Na⁺ homeostasis in response to high salinity. The gene encoding tonoplast Na⁺/H⁺ antiporter (*NHX1*) is induced by both salinity and ABA in Arabidopsis (Shi and Zhu, 2002), and rice (Fukuda *et al.*, 1999). The *AtNHX1* promoter contains a putative ABA responsive element (ABRE) between –736 and –728 from the initiation codon. *AtNHX1* expression under salt stress is partially dependent on ABA biosynthesis and ABA signalling through the ABA insensitive (ABI1) pathway. Salt-stress induced up-regulation of *AtNHX1* expression is lower in ABA deficient mutants (*aba2-1* and *aba3-1*) and in the ABA insensitive mutant, *abi1-1* (Shi and Zhu, 2002). Comparing tonoplast Na⁺/H⁺-exchange activity (mainly due to *AtNHX1*) between wild type and

mutant lines (*sos1*, *sos2* and *sos3*) shows that SOS2 also regulates tonoplast Na⁺ exchange (Chinnusamy *et al.*, 2005)

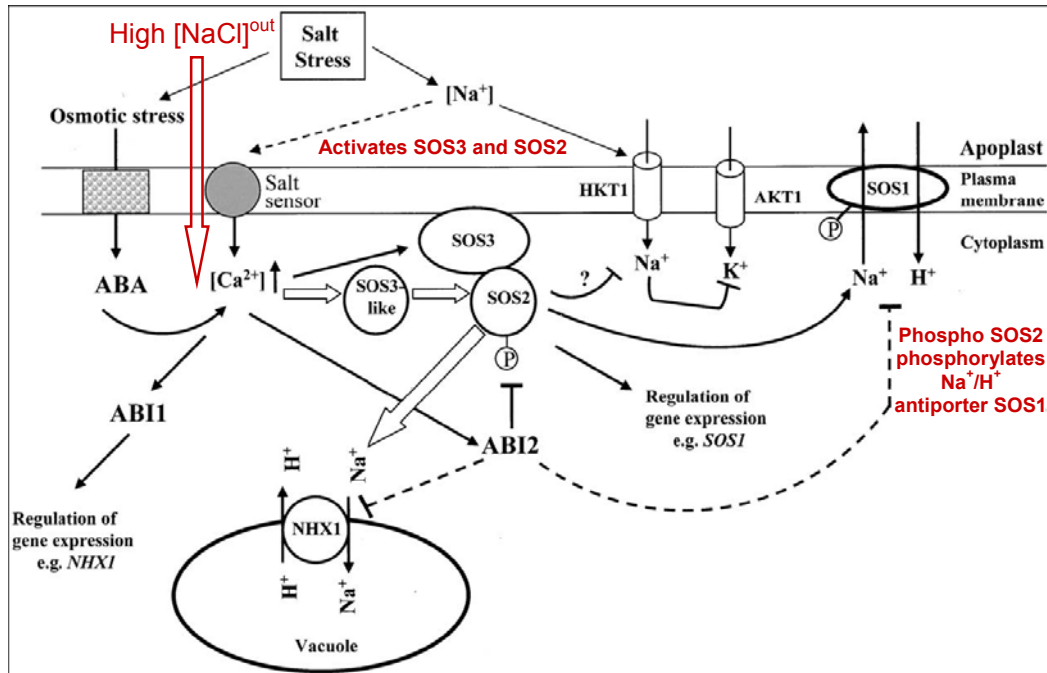


Fig. 1-3 SOS Signalling Pathway for Na⁺ Homeostasis in Arabidopsis.

Salt stress-elicited Ca²⁺ signals are perceived by SOS3, which activates the protein kinase SOS2. Activated SOS2 phosphorylates SOS1, a plasma membrane Na⁺/H⁺ antiporter, which then transports Na⁺ out of the cytosol. The transcript level of SOS1 is also regulated by the SOS3-SOS2 kinase complex. SOS2 also activates the tonoplast Na⁺/H⁺ antiporter that sequesters Na⁺ into the vacuole. Na⁺ entry into the cytosol through the Na⁺ transporter HKT1 may also be restricted by SOS2.

Abcisic acid (ABA) insensitive 1 (ABI1) regulates the gene expression of NHX1, while ABA insensitive 2 (ABI2) interacts with SOS2 and negatively regulates ion homeostasis either by inhibiting SOS2 kinase activity or the activities of SOS2 targets. Double arrow ⇔ indicates SOS-dependent and → indicates ABA-dependent pathways (Chinnusamy *et al.*, 2005).

1.11 Salt Stress Sensing in Plants.

Plants sense salt stress through ionic (Na^+) and osmotic stress signals. Therefore, excess Na^+ can be sensed either on the surface of the plasma membrane by a transmembrane protein or within the cell by membrane proteins or Na^+ sensitive enzymes (Zhu, 2003). In addition to its role as an antiporter, the plasma membrane Na^+/H^+ antiporter SOS1 (Salt Overly Sensitive 1), having 10 to 12 transmembrane domains and a long cytoplasmic tail, may act as a Na^+ sensor (Zhu, 2003). This dual role would be analogous to the sugar permease BglF in *Escherichia coli* and the yeast ammonium transporter Mep2p. When expressed in *Xenopus laevis* oocytes Na^+-K^+ cotransporters from *Eucalyptus camaldulensis* (Dehnh) show an increased ion uptake under hypoosmotic conditions while, their Arabidopsis homolog do not show this osmosensing capacity (Liu *et al.*, 2001).

1.12 Na^+ Sequestration.

A positive turgor is very important and essential for the expansion-induced growth of cells, and for stomatal functioning in plants. When plants are exposed to high salinity they desiccate, resulting in turgor loss. Plants have evolved an osmotic adjustment mechanism (active solute accumulation) that maintains water uptake and turgor under osmotic stress conditions. For osmotic adjustment, plants use inorganic ions such as Na^+ and K^+ and/or synthesize organic compatible solutes such as proline and soluble sugars. Vacuolar sequestration of Na^+ is an important and cost-effective strategy for osmotic adjustment, which also reduces the Na^+ concentration in the cytosol. Na^+ sequestration into the vacuole depends on expression and activity of Na^+/H^+ antiporters as well as on V-type V- H^+ -ATPase and V- H^+ -PPase. These phosphatases generate the necessary proton gradient required for activity of the Na^+/H^+ antiporters.

Overexpression of AVP1, a gene that encodes the vacuolar H⁺-pyrophosphatase in *Arabidopsis*, enhanced sequestration of Na⁺ into the vacuole and maintained higher relative water content in leaves. These plants also show higher salt and drought stress tolerance than that of wild type (Gaxiola *et al.*, 2001). The gene encoding tonoplast Na⁺/H⁺ antiporter (NHX1) is induced by both salinity and ABA in *Arabidopsis* (Shi and Zhu, 2002), and rice (Fukuda *et al.*, 1999). The AtNHX1 promoter contains a putative ABA responsive element (ABRE) between -736 and -728 from the initiation codon. AtNHX1 expression under salt stress is partially dependent on ABA biosynthesis and ABA signalling through ABA insensitive (ABI1). Salt-stress induced up-regulation of AtNHX1 expression is lower in ABA deficient mutants (*aba2-1* and *aba3-1*) and in the ABA insensitive mutant, *abi1-1* (Shi and Zhu, 2002). Comparing tonoplast Na⁺/H⁺-exchange activity (mainly due to AtNHX1) between wild type and mutants (SOS1, SOS2 and SOS3) shows that SOS2 also regulates the tonoplast exchange (Chinnusamy *et al.*, 2005).

1.13 Utilizing Model Plants to Study Salt Tolerance.

Plant biologists have reached the point where the genome sequencing of several higher organisms have been completed, including those of the model plant *Arabidopsis thaliana* and the important food crop rice (*Oryza sativa*). Within the next five years the genomes of several other important crop plants will be completed, and over the next decade the major challenge for plant biologists will be to make sense of the vast amounts of information that will be available. However, the complete genome data bases provide only a limited understanding of the biology of higher organisms as a whole.

First of all, it is clear from the completed genome data bases, (*Homo sapiens*, *Drosophila melanogaster*, *Arabidopsis thaliana*, etc.) that the function of only about a third of the putative genes is known with some certainty. The function of another third can be tentatively assigned using educated guesses based on weak homology with sequences from other organisms. The final third seem to be genes unique to the particular organism and their biological function is a complete mystery.

Second, it is believed that the patterns of global gene expression using DNA microarray technology will identify components of the signalling pathways and the resulting mechanisms that are activated in response to specific environmental stimuli. However, recent work suggests that about the third of the genes that are routinely identified as differentially regulated do not result in any changes in abundance at the protein level. Obviously, consideration of transcriptional regulation only can be very misleading (Gygi *et al.*, 2000; Gygi *et al.*, 1999; Mass and Grieve, 1987).

Third, gene sequence information gives no information at all on regulation of activity occurring at the protein level. It is now very well established that modification of proteins, such as phosphorylation /dephosphorylation impart on cells very complex and critically important mechanisms for the control of biological activity. This control can only be determined by direct studies on proteins. Moreover, recent studies have suggested that the proteome complexity of eukaryotes, including higher plants, may be as much as 10 times greater than the genome complexity (Aebersold *et al.*, 2000; Gygi and Aebersold, 2000) which again emphasize the importance of studying proteomes.

It has already been mentioned that salinity is a major determinant of crop production world-wide, and that most of the important field crops are glycophytes that will not complete a full life cycle above 100 mM NaCl. However there are wild plants (halophytes) which can tolerate full strength seawater (~500 mM NaCl). Understanding

the mechanisms that allow halophytes to survive high salinity may provide insights into developing salt tolerant crops. A lot of efforts have been focused on the effects of salinity on plants, but due to the recent trend of working with model plants (all of which are glycophytes including *Arabidopsis*), it is conceivable we may learn much about salt sensitivity and very little about salt tolerance. There is certainly, a great need to assess the genetic diversity of plants that occur in our environment, and to take up the more difficult challenge of identifying mechanisms in halophytes that cope with high salinity.

1.14 Project Aims.

The original objectives of this PhD project were to undertake a comparative study of the cellular processes of salt tolerant and salt sensitive plant cells. At Glasgow a salt tolerant cell suspension culture of *Arabidopsis thaliana* has been established. This line, named the HHS cell line (Habituated to High Salt) was established from wild type cell lines by continued exposure to salinity. Wild type cells grow best in basic nutrient media (MSMO media see Chapter 2, Section 2.2.1) but will not survive with the addition of 80 mM NaCl. In contrast, the HHS cells will grow vigorously in 300 mM NaCl, and survive extended periods at 380 mM NaCl.

The original plan was to thoroughly characterize the performance of these *Arabidopsis* cell lines exposed to a range of nutrient ions (K, Ca, and pH) and salinity concentrations. Parameters such as growth rates, ion profiling, membrane transport processes, transcript profiling, and protein profiling were to be measured. In addition, cell lines of the dicot halophyte *Atriplex halimus* were established to allow a comparison between the HHS and a genuine halophyte line. Unfortunately, due to the Bower Fire in 2001, this project was not completed. Whilst data has been collected on the growth rates, ion profiling and protein profiling of the HHS and WT *Arabidopsis* cell lines, repeated and continuous disruptions through 2003 and 2004 (attributable

mainly to irregular and frequent power failures in our temporary accommodation and the repeated failure of new incubators, there was a persistent loss of experiments, cultured cell lines, and harvested material. For this reason, a second whole plant project was started in 2005 comparing the physiological properties of two barley lines originating from China that were reported to be salt tolerant and salt sensitive. These lines were grown in the glasshouse and proved to be more durable than the cell suspension experiments. In this thesis, both sets of unrelated experiments are reported in their entirety.

Chapter 2: Comparison of Salt Tolerant and Salt Sensitive Arabidopsis Cell Lines.

2.1 Introduction.

Despite many decades of intensive research, it is still not clear how salt tolerant plant cells maintain ionic balance. There have been advances in our understanding of the regulation of ion transport in a few model glycophyte species such as Arabidopsis, rice and wheat *etc*, but the basic cellular mechanisms that maintain favourable ion gradients in halophytes exposed to high salinity are still not well known. In part, this is because of lack of research focus on halophyte species. Further, advances have been confounded by the complexity of the multi-tissue, whole root system; whilst there is an understandable desire to work with whole roots, the different age of cells and different tissues present generate experimental results that are often difficult to interpret. For instance, there may be important transport mechanisms residing on the plasma membrane of endodermal cells that are vital for regulating salt balance in the xylem, and therefore the shoot. The endodermal cells, however, represent ~1% of the mass of roots and so identifying transcripts and proteins that effect essential processes in the endodermis of whole roots is difficult. Further, reliable methods for isolating cells from different tissues have not been established.

It is difficult to characterise the kinetic properties of transport processes of specific cell types in complex tissues. Consequently, the studies are limited and confined, therefore, to reporting long-term changes (*i.e.* minutes to hours) where tissue specificity is uncertain.

In contrast, studies on cell suspension cultures may offer a major advantage over intact tissue for investigating salt tolerance, as the complexities superimposed by higher levels

of tissue organisation are not present. To survive in high salinity, unlike the intact root system of a plant, each cell in culture must be expressing the required traits for salt tolerance. There is a legitimate concern that cell suspension culture will generate results that contain artefacts not present in intact roots, but at least they will allow studies on single cells that show a range of sensitivities to salinity.

This chapter reports results from a series of experiments designed to investigate the responses of wild type (salt sensitive) and HHS (Habituated to High Salt) *Arabidopsis* cell cultures exposed to a range of salinities. Non-habituated *Arabidopsis* cell cultures will not survive in basic growth media supplemented with ~80 mM NaCl, whereas the HHS cells used in this study grow up to 380 mM NaCl. The intention was to use these resources to determine the cellular processes, particularly those associated with ion transport, that are involved in conferring salinity tolerance on *Arabidopsis* cells.

2.2 Materials and Methods.

2.2.1 Arabidopsis Cell Suspension Cultures.

Wild type *Arabidopsis thaliana* (L) Heynh var. Landsberg erecta photomixotrophic cell suspension cultures were a gift from Prof. Chris Leaver, University of Oxford and are fully described elsewhere (May and Leaver, 1993). Cells were grown in full-strength MSMO media (Sigma # M 6899, see Appendix Table A 2-1), supplemented with 0.5 mg l⁻¹ α -naphthalene acetic acid, 0.05 mg l⁻¹ kinetin, 3% (w/v) sucrose, and the pH adjusted to 5.8 using 0.2 M KOH. Throughout this thesis this media is referred to as Basic Growth Media (BGM). *Arabidopsis* cell cultures were grown under continuous light (PPFD 20 $\mu\text{mol m}^{-2} \text{s}^{-1}$) at 20 C°, and continuously shaken at 150 rpm in an illuminated / refrigerated orbital incubator (Sanyo Gallenkamp plc, Loughborough, U.K). The cultures were subcultured every seven days by transferring under sterile conditions 10 to 15 ml into 250 ml flasks containing 80 ml of autoclaved BGM.

2.2.1.1 Establishment of the Arabidopsis Habituated to High Salt (HHS) Cell Line.

Wild type Arabidopsis cell suspension cultures do not survive in BGM supplemented with 80 mM NaCl. Therefore, HHS cell lines were initiated from wild type cell suspensions by sub-culturing into BGM supplemented with 50 mM NaCl (BGM50_{-0.77}). The water potential of this media is -0.77 MPa. At this salt level wild type cells survive and grow slowly. Every week, two aliquots were removed from the BGM50_{-0.77} flasks and used to inoculate BGM media supplemented with 50 and 70 mM NaCl respectively (BGM50_{-0.77} and BGM70_{-0.86}). Growth was assessed after one week prior to subculture. Initially, each week the culture in BGM70_{-0.86} failed to survive, while those in BGM50_{-0.77} grew slowly. After 52 weeks of continuous habituation, however, one culture in BGM70_{-0.86} did survive, and was gradually coaxed over the next year to grow in progressively higher concentrations of NaCl (up to 380 mM, ~70% full-strength sea water).

2.2.2 Measurement of Growth Rates of Cell Cultures.

Growth rates of cell cultures were measured by determining the packed cell volume (PCV) of cells per ml of growth media with time. Cell cultures were mixed by gently swirling the flasks and quickly removing ~7ml aliquots under aseptic conditions. The aliquots were centrifuged at 291g for 3 min at 20°C in graduated 15 ml tubes (0.1 ml graduations), and both the total volume and the packed cell volume were noted; the volume of cells per ml media was then calculated.

The relative growth rates (RGR day⁻¹) and their reciprocal (Doubling Time, DT) were estimated from the slope of plots of the natural logarithm of PCV (ln PCV) *versus* days in culture. Both Arabidopsis WT and HHS cell lines were grown in Basic Growth Media supplemented with 0, 50 and 300 mM NaCl (BGM0_{-0.55}, BGM50_{-0.77} and

BGM300_{-1.96} respectively); in addition, to study the effect of osmotic stress alone, both cultures were grown in BGM supplemented with sorbitol to generate isotonic condition (*i.e.* BGM0_{-0.77}, BGM0_{-0.1.69}). HHS cells were also exposed to salt down shock conditions (1 week in BGM300_{-1.96}, and then transferred to BGM50_{-1.96} for a week), and salt up-shock (1 week in BGM300_{-1.96}, transfer to BGM50_{-1.96} for a week, transfer back to BGM300_{-1.96}) see Fig. 3-1.

2.2.3 Preparation of Cell Culture Material for ICP-OES Analysis.

Arabidopsis cell culture was mixed by hand swirling and a 7ml aliquot removed under aseptic conditions. Samples were harvested at daily intervals during growth (from inoculation, through the log phase of growth, to the stationary phase) from HHS cells grown in the full range of conditions (BGM300_{-1.96}, BGM50_{-1.96}, BGM50_{-0.77}, BGM0_{-0.55}, BGM0_{-0.77}, and BGM0_{-1.96}). Samples were then placed on a filter disc in a Buchner funnel connected to a vacuum pump. After briefly draining the growth media (~5s) the samples were then washed with 50 ml of ice-cold distilled water (~30s) to remove extracellular solution, and then transferred to a pre-weighed 15 ml sterile falcon tubes, dried for 72 hours at 75°C, and then re-weighed to determine the dry weight of the samples. Five ml (\pm 0.01 ml) of 10% (v/v) analytical reagent grade nitric acid was added to each tube and samples were then treated to three freeze-thaw cycles (-80°) to lyse the cells, and then left to digest for 4 days at room temperature on a shaking incubator. Ion content (Na, Fe, K, S, P, B, Mn, Mg and Ca) was measured using a Perkin Elmer Inductively Coupled Plasma-Optical Emission Spectrometer (ICP-OES) model optima 4300 DV (Perkin Elmer, Seers Green, Bucks., UK).

2.2.3.1 Standard Solutions.

Standard solutions were made in 1.6% HNO₃, exactly equivalent to the final concentration of HNO₃ in the samples after dilution. Ion concentrations in the standard

solution were chosen based on the expected concentrations in the plant material and the detection limits of the spectrometer. The final concentration of each element in the X1 Standard Solution is shown in Table 2-1. The standard curve was produced by six dilutions of the X1 Standard Solution (0, 0.01, 0.05, 0.10, 0.50 and 1.0). It is important to note that to achieve reproducible results, all analytes, both samples and standards, were prepared from the same batch of 1.6% HNO₃; this improves the resolution of trace elements as contaminants in the acid can be subtracted. Further, all dilutions were prepared by weighing using +/-1mg resolution, as this is more accurate than pipetting.

2.2.3.2 Assessment of Ion Concentration in Plant Material.

Ion content was measured with an Optical Emission Spectrometer (Perkin Elmer Optima 4300 DV) controlled by the software package (Win Lab32), Perkin Elmer Instruments, MA, USA). The standards were used to create a calibration curve to determine ion concentrations. The intensities of the emission at specific wavelengths from the diluted liquid samples were measured and the background compared with the standard curve, then the concentrations of the corresponding elements were determined. These data were then analyzed using Microsoft® EXCEL.

Table 2-1 The Final Concentration of Elements in the times 1 (X1) Standard Solution for Ion Analysis.

Element	K	Na	Ca	P	S	Mn	Mg	Fe	B
Conc. (mg/l)	45.08	59.01	36.59	11.38	4.44	1.39	1.97	3.44	0.18

2.3 Results.

2.3.1 Comparison of WT and HHS Cell Cultures: Morphology.

2.3.1.1 *Fluorescein Diacetate (FDA) Staining.*

Fluorescein diacetate dye is a colorless substance and often utilized to distinguish whether the population of cell is living or not. The dye is taken up as the neutral ion through the plasma membrane and then is cleaved by cytoplasmic esterases in the cell interior into fluorescein and acetate. The fluorescein ion is highly fluorescent and its charge prevents it from leaving the cell. Under ultraviolet light a bright green fluorescence is observed in viable cells with an intact plasma membrane and this is easily visualized with a fluorescent microscope. A 0.1% w/v stock of FDA was made up in acetone and the stock stored at -20 °C (McCabe and Leaver, 2000).

2.3.1.2 *Imaging Arabidopsis Cell Suspension Cultures.*

Figure 2-1 presents typical image of both wild type cells were grown in Basic Growth media (WT cells were grown in BGM0_{0.55} Fig. 2-1a, c, e) and habituated to high salt (HHS cells were grown in BGM300_{1.96} Fig. 2-1b, d, f). Cells were incubated for 2 min with 1 μ M FDA (fluorescein diacetate), and then washed 2 times in the same growth media. Cells were visualized with a fluorescence microscope (Zeiss Axioplan) fitted with fluorescein filters (panel a and b). Differences between the two cell lines are apparent. The WT cells were grown in BGM0_{0.55} took up stain into their cytoplasm, but not into their large central vacuoles which remained clear of fluorescence (Fig. 2-1a). HHS cells habituated to grow in BGM0_{0.55} showed a similar morphology (data not presented). In contrast, the HHS cells were grown in BGM300_{1.96} rapidly accumulated FDA (< 2 min) into a large numbers of what appears to be vesicles and/or small vacuoles; some staining of the cytoplasm was also apparent, and unstained large central vacuoles were also observed (Fig. 2-1b).

Figure 2-1 also presents confocal images that confirm these observations (panel c and d). In panels c and d the upper fluorescence images were taken from cells dual-labeled with the FDA (cationic dye) and LysoTrackerTM (anionic dye). The lower set of images in panels c and d are bright field micrographs without (left) and with (right) the merged fluorescence images. The merged images from the HHS cells were grown in BGM300_{1.96} clearly show some of the small vacuoles / vesicles fluoresce green (FDA accumulation) whilst other fluoresce red (LysoTrackerTM accumulation) indicating the interior of these endomembrane compartments are different and that they might have different functions. The fact that these vesicles / small vacuoles were largely absent from WT cells were grown in BGM0_{0.55} could indicate they have a role in conferring salinity tolerance on the HHS cells.

Thin section electron micrographs of WT cells were grown in BGM0_{0.55} and HHS cells were grown in BGM300_{1.96} (Fig. 2-1 panel e and f) clearly show the extensive ‘vesiculation’ observed under a light microscope. In addition, the nuclei of salt-stressed HHS cells appear to be disrupted; fragments of the electron dense nucleoli are observed suggesting the HHS cells may be aneuploid (Fig. 2-1e and f). Similar observations have been made in cell cultures of all halotolerant plant cells (*Atriplex halimus*, *Beta vulgaris*, *Aster tripolium*) and in intact root of *Distichlis spicata* (saltgrass), but not in the salt-sensitive cell cultures studied to date (*Arabidopsis thaliana*, and *Oryza sativa*). This proliferation in intracellular vesicles and small vacuoles may represent an important salinity de-toxification response in halotolerant plant cells.

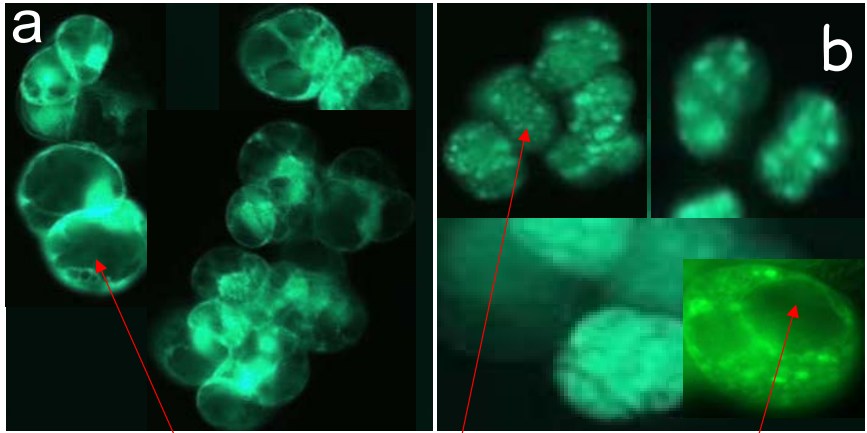
Fig. 2-1 Images of Arabidopsis HHS and WT Cells.

WT cells were grown in BGM0_{-0.55} media (panel a, c, and e) and HHS cells were grown in BGM300_{-1.96} (panel b, d, and f). For full description of Materials and Methods see section 2.2.1 and 2.2.2).

Fluorescence Light Microscopy: Cells from the WT cells were grown in BGM0_{-0.55} media (panel a) and HHS cells were grown in BGM300_{-1.96} (panel b) Arabidopsis cultures incubated with fluorescein diacetate (FDA). Note large central vacuoles in both WT and HHS cells, but the appearance of numerous small, brightly fluorescing small vacuoles / vesicles only in the HHS cells.

Confocal Fluorescence Microscopy: Images of WT cells (panel c) and HHS cells (panel d) Arabidopsis cells stained with FDA and LysoTracker™ red dyes. Large, non-fluorescing central vacuoles were observed in both cell lines, but small highly fluorescent vesicles were only found in salt tolerant cells. Images were taken with a Zeiss LSM 510 Laser Scanning Microscopes and 3-D images were digitally reconstructed using LSM 5 software, version 3.0. Note the appearance of small vacuoles / vesicles in the HHS cells that take up only FDA or only LysoTracker™ red.

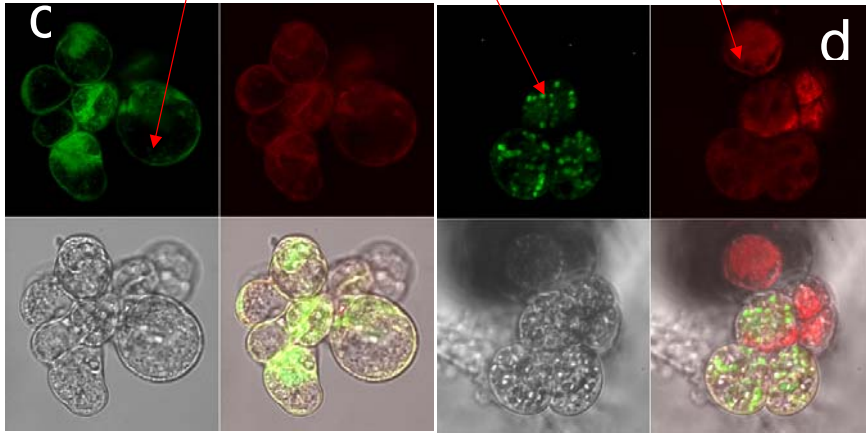
Thin Section Electron Microscopy: Thin section E.M. from WT cells (panel e) and HHS cells (panel f) Arabidopsis cell lines. Note the high degree of vesiculation near the plasma membrane and the appearance of fragmented nucleoli in HHS cells. Magnification, 13,000 x. EM micrographs courtesy of Dr P Dominy, University of Glasgow.



Large Central Vacuole

Small Fluorescing Vesicles

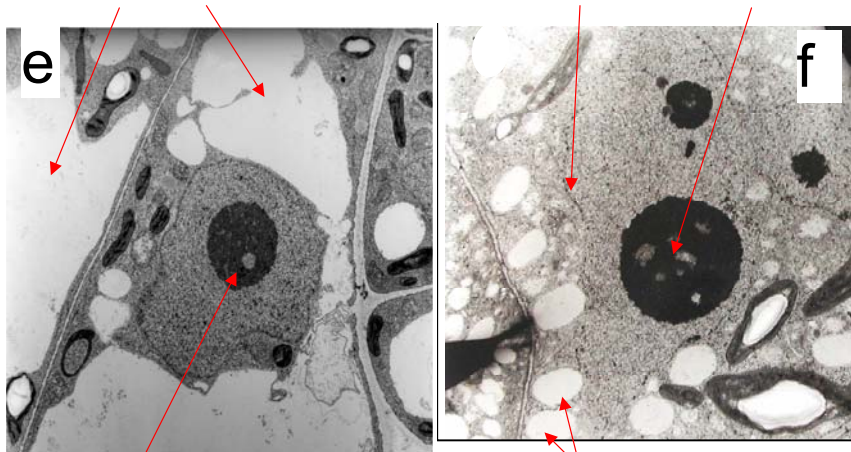
Large Central Vacuole



Large Central Vacuole

Nuclear Envelope

Nucleoli (Fragmented)



Single Nucleolus

Small Vesicles

2.3.2 Comparison of WT and HHS Cell Cultures.

2.3.2.1 Effect of Salinity on the Growth of WT Cells.

Wild type (WT) cells in basic growth media (BGM0_{-0.55}) grew slowly for the first three days in culture (pre-log phase) probably because the cells need some time to adapt to or condition the fresh growth media. After this period growth increased dramatically (log phase, days 3 – 5) and entered the stationary phase by day 7 (see Fig. 2-2). The Relative Growth Rate (RGR) constants (k) and their reciprocals, the Doubling Times (DT), were estimated from the slope of the natural log of the packed cell volumes (ln PCV) *versus* Days in Culture plot (Fig. 2-2 inset) and are also presented in Table 2-2. To assess the effect of NaCl concentration on WT cells, growth was assessed in BGM containing 50 mM NaCl ($\psi_{\text{H}_2\text{O}} = -0.77$ MPa, *i.e.* BGM50_{-0.77}). To separate the effects of ionic stress from water stress, WT cells were also grown in BGM with 0 mM NaCl but adjusted to a $\psi_{\text{H}_2\text{O}}$ of -0.77 MPa (BGM0_{-0.77}) and -1.96 MPa (BGM0_{-1.96}) by the addition of sorbitol (see Table A2-1). From these data RGR and DT were assessed and are presented in Table 2-2.

When grown in BGM0_{-0.55}, WT cells had a doubling time of 2.45 ± 0.23 days, but this increased by to 2.84 ± 0.16 days when grown in BGM50_{-0.77}; clearly salinity decreases growth rate. When WT cells were grown in BGM0_{-0.77} the doubling time increased to 2.53 ± 0.15 (*cf.* BGM0_{-0.55}). Under the experimental conditions used here, WT cells were grown in BGM0_{-0.55} would not grow in BGM0_{-1.96} or in BGM300_{-1.96}. These data suggest that when exposed to 50 mM NaCl the observed slower growth rates of WT cells grown in BGM0_{-0.55} are attributable mainly to ionic stress and not to osmotic stress. WT cells would not grow when exposed to severe desiccation (BGM0_{-1.96})

suggesting osmotic adjustments to regain turgor was not possible under these conditions (Fig. 2.2 and Table 2-2).

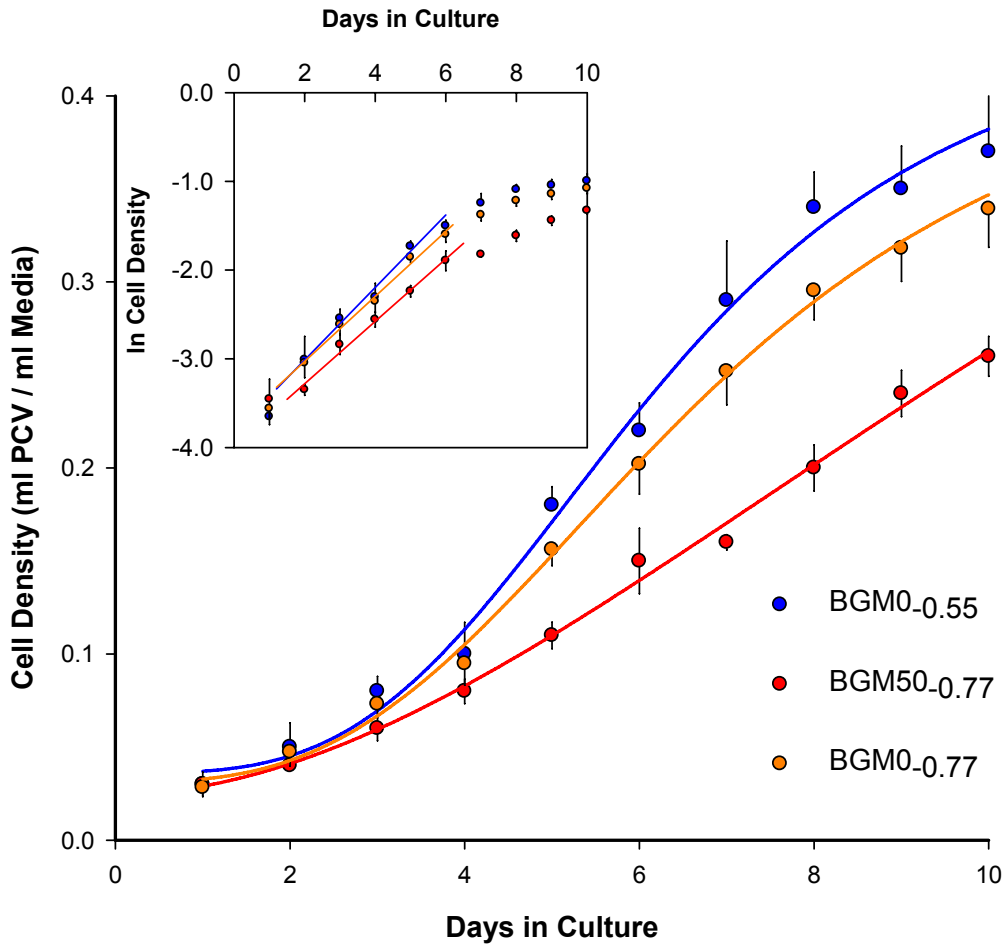


Fig. 2-2 Growth Curves of Wild Type Arabidopsis Cell Suspensions Exposed to Osmotic and Ionic Stress.

Cultures were established as described in Materials and Methods (Section 2.2.1.1) and grown in their respective media (● BGM0-0.55, ● BGM50-0.77, ● BGM0-0.77; see sections 2.2.1 and 2.2.2). Growth was monitored as the Packed Cell Volume (PCV/ml media), as described in Section 2.2.2. Data points are the average and standard errors of three independent replicate cultures. Inset, natural logarithm of PCV *versus* days in culture; the relative growth rates (RGR) and their standard errors were estimated from the initial slopes of each of the three replicate cultures. For details of the media composition, see Table A 2-1.

When HHS cells (grown in BGM300_{-1.96}) were grown in BGM0_{-0.55}, growth rates were always observed to be slower than those of WT cells grown in BGM0_{-0.55} (DT 3.74 ± 0.12 days; Table 2-2 and Fig. 2-3), and like WT cells grown in BGM0_{-0.55} increasing salinity to 50 mM NaCl (BGM50_{-0.77}) impaired growth (DT 5.92 ± 0.39 days). Further, like WT cells grown in BGM0_{-0.55}, only part of this salinity induced impairment can be attributed to water stress as growth in BGM0_{-0.77} was significantly greater than in BGM50_{-0.77} (Table 2-2).

When HHS cells were grown in 300 mM NaCl (BGM300_{-1.96}) doubling time increased to 5.88 ± 0.48 days, but in isotonic, low salt media (BGM0_{-1.96}) the growth rates were even slower (DT of 6.13 ± 0.42 days). These data suggest that the habituation process in HHS cells grown in BGM300_{-1.96} has resulted in slower growth in absence of salt or water stress, but the application of moderate salt stress (50 mM NaCl, $\psi_{\text{H}_2\text{O}}$ of -0.77 MPa) reduces growth rates by both ionic and osmotic effects. Under high saline, dehydrating conditions (300 mM NaCl, $\psi_{\text{H}_2\text{O}}$ of -1.96 MPa), however, HHS cells grown in BGM300_{-1.96} survive well, but their poor growth in isotonic, low salt media (0 mM NaCl, $\psi_{\text{H}_2\text{O}}$ of -0.55 MPa) suggests that at this low water potential Na^+ and / or Cl^- are required as an intracellular solute to regain turgor for expansion-induced growth. Presumably, these ions are stored in the vacuoles of the cell, to reduce their toxic effects on metabolism.

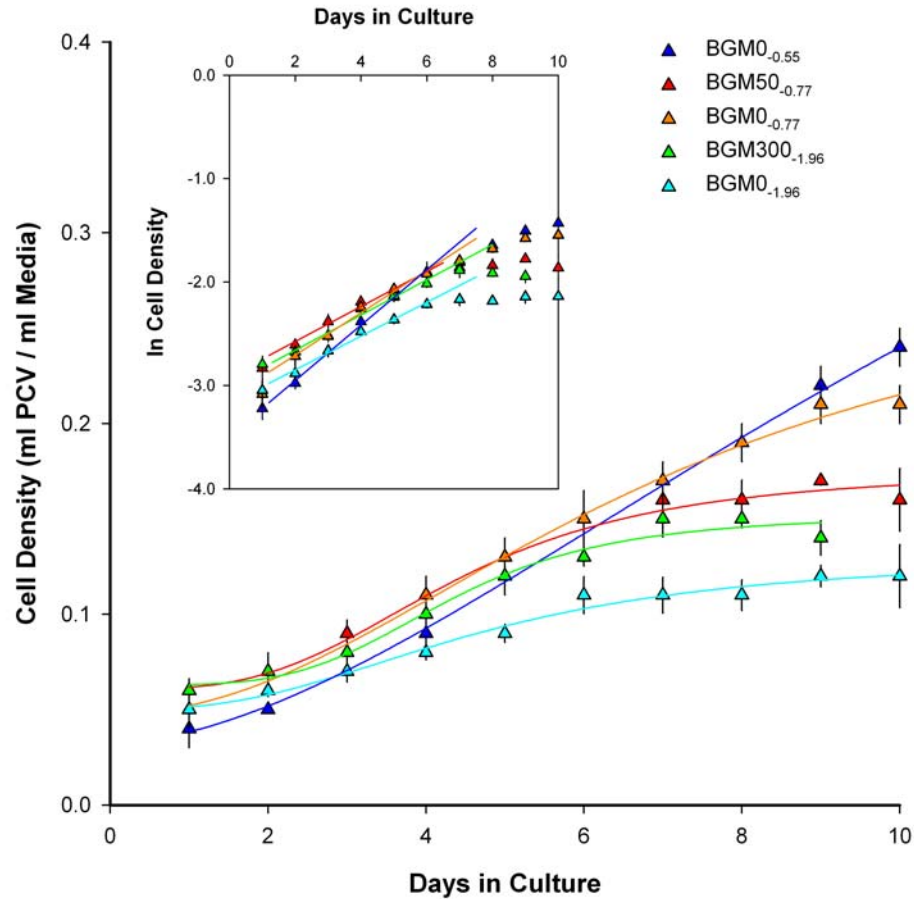


Fig. 2-3 Growth Curves of HHS Arabidopsis Cell Suspensions Exposed to Osmotic and Ionic Stress.

Cultures were established as described in Material and Methods (Section 2.2.1.1) and grown in their respective media (▲ BGM0_{-0.55}, ▲ BGM0_{-0.77}, ▲ BGM50_{-0.77}, ▲ BGM300_{-1.96}, and ▲ BGM0_{-1.96}; see sections 2.2.1 and 2.2.2). Growth was monitored as the Packed Cell Volume (PCV/ml media), as described in Section 2.2.2. Data points are the average and standard errors of three independent replicate cultures. Inset, natural logarithm of PCV *versus* days in culture; the relative growth rates (RGR) and their standard errors were estimated from the initial slopes of each of the three replicate cultures. For details of the media composition, see Table A 2-1.

Table 2-2 The Relative Growth Rates and Doubling Times of Wild Type and HHS Arabidopsis Cell Suspension Cultures Exposed to Osmotic and Ionic Stress.

The Relative Growth Rates (RGR) and their associated standard errors were estimated from the plots presented in Figs. 2-2 and 2-3. Doubling Times (DT) are calculated as $0.693 (\ln 2)/RGRs$; dns = ‘did not survive’. For details of the composition of the media, see Table A 2-1. Analysis of variance tests were performed on these data and comparison between treatments means were made using Turkey tests. Treatment means with different Roman characters shows significant differences within a cell line (WT or HHS). Treatment means with different Greek characters show significant differences between cell lines (WT vs HHS). Bold characters are significant at $p < 0.001$.

Growth Media	WT		HHS	
	DT (Days)	RGR (Day ⁻¹)	DT (Days)	RGR (Day ⁻¹)
BGM0 _{-0.55}	1.70 ± 0.18	0.408 abα ± 0.043	2.60 ± 0.09	0.267 cβ ± 0.009
BGM50 _{-0.77}	1.97 ± 0.12	0.352 aγ ± 0.021	4.10 ± 0.29	0.169 dε ± 0.012
BGM0 _{-0.77}	1.75 ± 0.09	0.395 bδ ± 0.021	3.38 ± 0.21	0.205 eζ ± 0.013
BGM300 _{-1.96}	dns	0	4.08 ± 0.36	0.170 d ± 0.015
BGM0 _{-1.96}	dns	0	4.25 ± 0.31	0.163 d ± 0.012

2.3.2.2 *Effect of Salinity on the Ion Content of WT and HHS Cells.*

In this study Inductively Coupled Plasma Optical Emission Spectroscopy (ICP-OES) was used to profile tissue ion content. ICP-OES is powerful and relatively new technique for measuring several elements at the same time with low detection limits (parts per billion) over a large dynamic range. Liquid organic or aqueous samples in dilute acids are fed into ICP-OES through an argon gas nebulizer. The fine spray is then fed into the ‘torch’ which consists of microwave source that is tuned (coupled) to the sample resulting in intense heating (*ca.* 6000°C). The extreme temperatures of the torch strips all of the electrons from the elements in the sample to produce plasma, and as the plasma nuclei subsequently cool they regain their electrons and emit photons at wavelengths that are characteristic of each element. The spectrophotometer collects the emitted light which is passed to a Fresnel prism that disperses the emission onto a silicon detector array thereby allowing an instantaneous and simultaneous measurement of several ions in a single sample. By using a set of multi-element standards, calibration curves of detector signal *versus* ion concentration can be constructed for each target element, and subsequently used to determine the unknown levels in samples. For most cations, ICP-OES has a good dynamic range and low detection limits. For instance, K can be detected from at least 0.003 up to 30 mg/l (ppm). Samples were prepared from Arabidopsis cell suspensions and the levels of tissue macronutrients (*e.g.* K, Ca, Mg, P, S, and Na) as well as micronutrients (*e.g.* B and Fe) were measured.

The ion content of WT and HHS cells grown in BGM0_{0.55} were similar and not presented. More interesting is a comparison of the ion content of these cell lines exposed to salinity stress (Fig. 2-4). The initial reading over the first few days of growth showed large variances, presumably due to the low tissue biomass during these early phases of growth. During the log phase of growth (days 3-6), however, a clear pattern of

difference emerged. Only minor differences in the levels of K^+ were observed between WT cells grown in BGM50_{0.77} and HHS cells grown in BGM50_{0.77} (Fig. 2-4 panel a), whereas Na^+ levels were nearly 3 times higher in WT cells grown in BGM50_{0.77} (~5 cf ~15 mg/g D Wt; Fig. 2-4 panel b).

As a consequence the K^+/Na^+ ratio of HHS cells grown in BGM50_{0.77} or _{-1.96} were 3 to 4 times greater than WT cells grown in BGM50_{0.77} or _{-1.96} during this period (Fig. 2-4 panel c). Increasing the level of dehydration of WT cells grown in BGM50_{-1.96} and HHS cells grown in BGM50_{-1.96} exposed to 50 mM NaCl by the addition of sorbitol (*i.e.* growth in BGM50_{-1.96}) had little effect on cell K^+ or Na^+ levels (Fig. 2-4a and b). These results suggest that when exposed to saline media HHS cells can maintain lower levels of intracellular Na^+ resulting in higher intracellular K^+/Na^+ ratios (Fig. 2-4 panel c). There is no evidence to suggest that HHS cells are better at acquiring K^+ than WT cells when exposed to salt stress. The intracellular levels of Ca, S, and P were also assessed in WT and HHS cells (Fig.2-4 panels d, e, and f) but no major differences were observed. Also the intracellular levels of Mn, Mg, Fe, and B were measured but no major differences was observed and the data are not presented.

In conclusion, relatively low levels of salt stress (50 mM NaCl) produce a significant decrease in the growth rate of WT cells grown in BGM0_{0.55} Arabidopsis cells probably due to the accumulation of high intracellular Na^+ levels. In contrast, HHS cells grown in BGM0_{-1.96} cells do not grow as well as WT BGM0_{0.55} cells in the absence of salt stress; increasing salinity to 50 and 300 mM NaCl impairs growth rate but these cells can maintain low intracellular levels of Na^+ which may account for their survival.

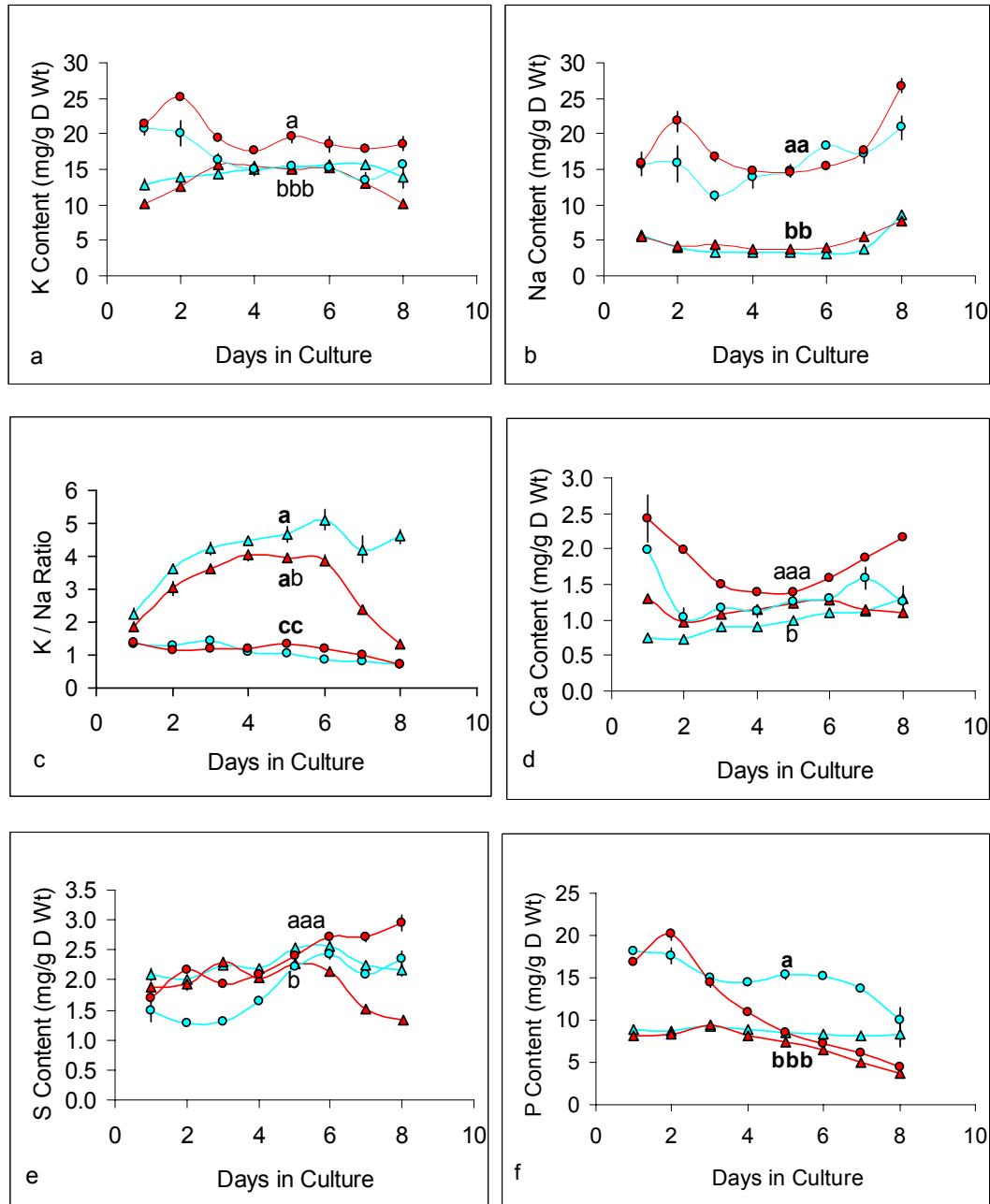


Fig. 2-4 Ion Content of WT and HHS *Arabidopsis* Cell Cultures.

Samples were harvested daily from WT (●) or HHS (▲) cells grown in BGM50.0.77 or WT (●) or HHS (▲) cells grown in BGM50.1.96 (see sections 2.2.1 and 2.2.2). Ion content was measured using a Perkin Elmer Optima 4300 series Inductively Coupled Plasma-Optical Emission Spectrometer (ICP-OES). Averages and SEs of three independent cultures are presented. Two factor analysis of variance (linear model) was performed on the data with Bonferroni pair-wise tests between treatment means. Different Roman characters signify significant differences ($p < 0.05$, 0.01 or 0.001) between treatment means at Day 5 (mid log phase of growth; bold character ($p < 0.001$), normal face ($p < 0.01$, italics ($p < 0.05$)).

2.3.3 The Effects of Salt-Shock on the Growth and Ion Content of HHS Cells.

2.3.3.1 Growth Rates of Salt-Shock HHS Cells.

In section 2.3.2 comparisons were made between WT and HHS cells on the effects of relatively low NaCl concentration (*i.e.* 50 mM NaCl) on growth rate and ion content. These comparisons are possible only under conditions of low ionic stress as WT cells grown in BGM0_{0.55} do not survive above 80 mM NaCl.

To assess the effect of high levels of salinity on the growth of HHS cells grown in BGM300_{-1.96}, a series of experiments were conducted where HHS cells grown in BGM300_{-1.96} were exposed to a salt ‘up-shock’ (50 mM to 300 mM NaCl) and a salt ‘down-shock’ (300 mM to 50 mM NaCl). To separate the effects of ionic and osmotic stress, all media were adjusted to the same water potential ($\psi_{\text{H}_2\text{O}}$, -1.96 MPa) by the addition of sorbitol. HHS cells grown in BGM300_{-1.96} were placed in fresh BGM300_{-1.96} media and grown to mid log phase (day 6); these cells were then used to seed fresh media containing 50 mM NaCl (BGM50_{-1.96}; a high- to- low salt ‘down-shock’) and 300 mM NaCl (BGM300_{-1.96}). These cultures were grown through to their stationary phase and growth was assessed daily. At day 6 (mid log phase) some of the salt down shock (HL) cells were used to seed fresh media containing 300 mM NaCl (BGM300_{-1.96}; a low-to High (HLH) salt ‘up-shock), and these were also grown to the stationary phase whilst growth was assessed daily (see Fig. 3-1). The results from these experiments are presented in Fig. 2-5 and summarized in Table 2-3.

These data suggest that salt down-shock (300-to-50 mM NaCl, HL cells in BGM50_{-1.96}) does not greatly affect the growth rate of HHS cells (10% decrease), whereas salt up-shock (50-to-300 mM NaCl, HLH cells in BGM300_{-1.96}) impairs growth by ~25%. These results are somewhat surprising in that a salt down-shock did not result in an increase in growth rate; however, as expected, a salt up-shock did impair growth. One

explanation for these observations is that HHS cells in BGM300_{-1.96} were still adjusting to the low salt stress conditions during the first 3-5 days after transfer and so growth rates had not accelerated. However, by day 6-7 the cells had adjusted enough so that the imposition of acute stress upon transfer to high salt (50-to-300 mM NaCl) did result in slower growth. Further experiments were conducted to establish the time required for HHS cells in BGM300_{-1.96} to 'adapt' to different salt regimes. In these experiments the growth rates of HHS cells in BGM300_{-1.96} were transferred to 50 mM NaCl (HL cells in BGM50_{-1.96}) and monitored for 14 days (*i.e.* two sub cultures), but growth rates were not significantly different after the first (1-7 days) and second (7-14 days) sub-culture (data not presented).

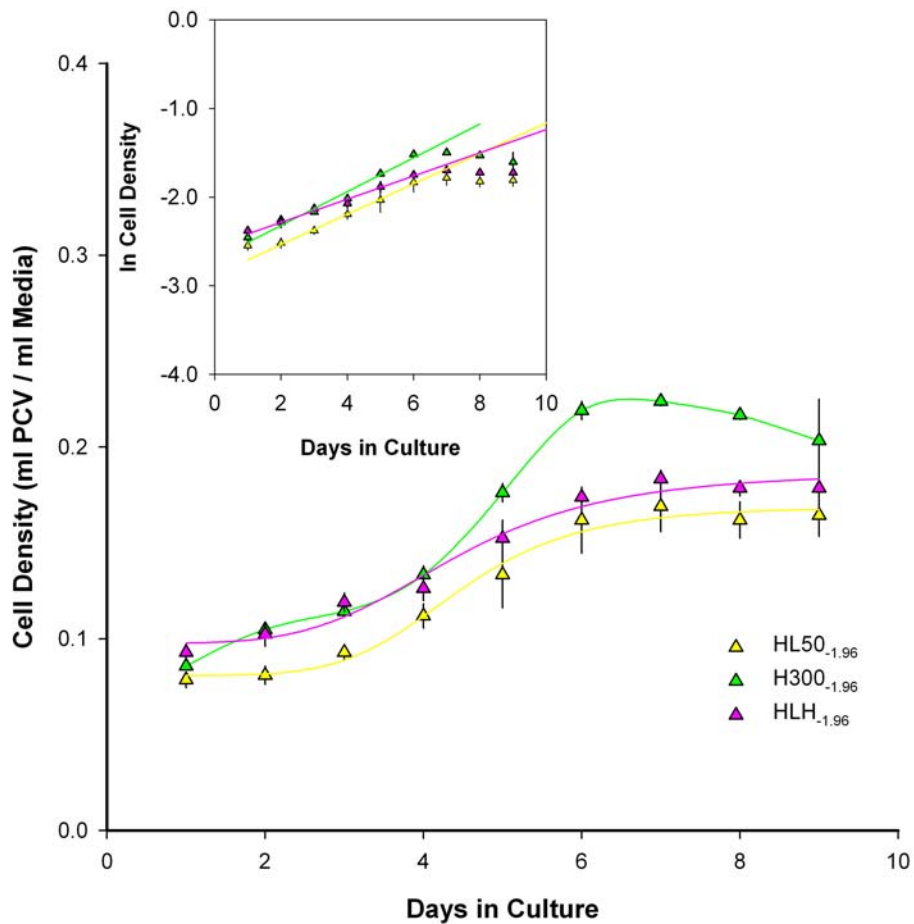


Fig. 2-5 Growth Rates of HHS Cell Suspension Cultures Exposed to Ionic Stress.

▲ HL50_{-1.96}, salt down-shock (Cells shifted from BGM300_{-1.96} to BGM50_{-1.96}):

▲ HLH_{-1.96}, salt up-shock (HL Cells shifted from BGM50_{-1.96} to BGM300_{-1.96}):

▲ H300_{-1.96}, cells grown in BGM300_{-1.96} (see section 2.2.1 and 2.2.2 for details).

Growth of cell cultures was estimated by removing aliquots and packed cell volume was measured (see Section 2.2.2). Each data point represents the average and standard error of single reading from three independent cultures. The average and standard errors of the doubling times and RGR constant are presented in Table 2-3.

Table 2-3 The Relative Growth Rates and Doubling Times of HHS Arabidopsis Cell Suspension Cultures Exposed to Ionic Stress.

The Relative Growth Rates (RGR) and their associated standard errors were estimated from the plots presented in Fig. 2-5. Doubling Times (DT) are calculated as $0.693 (\ln 2)/RGRs$. Analysis of variance tests were performed on these data and comparison between treatments means were made using Turkey tests. Treatment means with different Roman characters shows significant differences between cell lines (HL, H and HLH). Bold characters are significant at $p < 0.001$. For details of the composition of the media, see Table A 2-1.

Growth Media	HHS	
	DT (Days)	RGR (Day ⁻¹)
BGM50 _{-1.96} (HL)	4.03 ± 0.14	0.172 b ± 0.006
BGM300 _{-1.96} (H)	3.63 ± 0.40	0.191 a ± 0.021
BGM300 _{-1.96} (HLH)	5.29 ± 0.40	0.131 c ± 0.010

Media supplemented with 3% sucrose and the pH adjusted to 5.8 using 0.2 M KOH.

2.3.3.2 Ion Content of Salt Shocked HHS Cells.

Figure 2.6 present the effects of salt-shock on the ion content of HHS cells grown in BGM300_{-1.96}. The intracellular levels of K⁺ were not greatly different when HHS cells in BGM300_{-1.96} were exposed to 50 mM or 300 mM NaCl, with concentrations maintained at approximately 10 mg K⁺/g D Wt throughout the culture growth (Fig. 2-6a).

In contrast, intracellular Na⁺ levels were three -to- five times higher (*ca.* 4-5 mg Na⁺/g D Wt) in HHS cells grown in 300 mM NaCl compared with HHS cells grown in 50 mM NaCl (*ca.* 1 mg Na⁺/g D Wt).

These differences in cell Na⁺ levels resulted in significantly lower K⁺/Na⁺ ratios for HHS cells grown in 300 mM NaCl (*ca.* 2 *versus* 10). Measurements on cell Ca²⁺ levels (Fig. 2-6d) proved to be difficult to assess reliably, and it is unclear why this was so. These data, however, do not provide any evidence that Ca²⁺ levels in cells grown in 50 and 300 mM NaCl are significantly different.

The intracellular levels of P (Fig. 2-6f) and Mg (Fig. 2-6e), and Mn, Fe, B (data not presented), were also measured but no major differences between HHS cells grown at 50 and 300 mM NaCl were observed.

In conclusion, transfer of HHS cells from 300 to 50 mM NaCl results in a small decrease in growth rate (Fig 2-5 and Table 2.3) and a concomitant rapid decrease in intracellular Na⁺ content (Fig. 2-6b). During this salt down shock cell K⁺ levels remain unchanged and the K⁺/Na⁺ ratio increases accordingly (Fig. 2-6c). It is concluded that HHS cells are adapted to growth in saline media due to their ability to maintain low levels of intracellular Na⁺; no evidence was found for adaptations to their ability to acquire K⁺ in saline conditions. When HHS cells are grown near their limit of salt tolerance (300 mM NaCl), their ability to maintain low cellular Na⁺ levels becomes

compromised. At this stage, it is unclear whether HHS cells have adapted mechanisms that better discriminate against Na^+ acquisition, or improved Na^+ efflux. Further experiments will be required to resolve this question.

2.3.4 Assessment of Growth Limitation in WT and HHS Cell Cultures.

One of the questions arising from the growth experiments on HHS cells grown in BGM300-1.96 and WT cells grown in BGM0-0.55 presented in Section (2.3.2 and 2.3.3) is why the WT appear to attain greater cell densities at stationary phase (*cf* Fig. 2-2 *versus* 2-3 and 2-5). Impairing growth rates will delay the time taken to reach the stationary phase but it does not necessarily follow that final cell density will be affected. One explanation for the observed differences in the final cell densities of these cultures is that HHS cells in BGM300-1.96 run out of essential resource and this affected biomass accumulation. Another possibility is that HHS cells in BGM300-1.96 excreted some factor into the growth media that affected growth; if this was the case, this compound was not toxic as cells remained viable for up to a month without sub-culturing.

Investigations were undertaken to try to establish why biomass accumulation in HHS cells in BGM300-1.96 was lower than from WT cells in BGM0-0.55. These measurements included assessment of media sugar levels, nutrient ion content, pH, and nitric oxide (Carimi *et al.*, 2005). Figure 2-7 shows the levels of sucrose and its products from extracellular invertase action (glucose and fructose) remaining in the media during the culture growth phase. In all cases, at least 50% of the initial sucrose remained in solution by Day 7, when cultures were near their stationary phase. In addition the amount of reducing sugars (glucose plus fructose) was also significant up to Day 7. These results suggest that growth arrest was not attributable to exhaustion of the sugar supply.

The levels of the major nutrient ions remaining in the media are presented in Fig. 2-8. levels of K, Ca, Mn, and B remained constant throughout the growth period and were approximately equivalent for HHS cells in BGM300_{-1.96} and WT cells in BGM0_{-0.55}. The levels of P and S declined rapidly, with culture age, however, in both HHS cells in BGM300_{-1.96} and WT cells in BGM0_{-0.55}. It is conceivable that the growth of both HHS cells in BGM300_{-1.96} and WT cells in BGM0_{-0.55} was limited in part by the availability of free P or S, but there is no strong evidence to suggest the lower biomass of HHS cells in BGM300_{-1.96} at stationary phase was attributable to the depletion of these two nutrient ions in solution.

Figure 2.9 presents the pH of the media from HHS cells in BGM300_{-1.96} and WT cells in BGM0_{-0.55} during culture growth. Just prior to inoculation, all media were adjusted to pH 5.8. The results from this experiment suggests that whilst culture pH did drift with age, there were no dramatic differences between the pH of the media of HHS cells in BGM300_{-1.96} and WT cells in BGM0_{-0.55} that could account for the differences in final culture cell densities.

Recently reports have appeared to suggest the levels of nitric oxide (NO) in Arabidopsis cell cultures increase with time and this eventually impair growth (Carimi *et al.*, 2005). Aliquots were removed, therefore, from actively growing cultures and NO levels determined using the NO-sensitive fluorescent dye, diaminofluorescein diacetate (DAF-2DA).

When NO levels in WT cells in BGM0_{-0.55} and BGM50_{-0.77} were assessed, no evidence was found for an increase with culture age even if they were left for up to 18 days (Fig. 2-10 and 2-11). Similarly NO levels in HHS cells in BGM300_{-1.96} were grown in BGM0_{-0.55} and BGM50_{-0.77} did not increase significantly with culture age (Fig. 2-12)

although the basal levels appeared to be greater than those of WT cells in BGM0_{-0.55} cells.

Figure 2-13 presents images of DAF-2DA stained HHS cells grown in BGM300_{-1.96}; again, the levels of NO do not appear to change with culture age but basal level are higher than those of WT cultures (Fig. 2-10 and 2-11). It is conceivable, therefore, that HHS cells grown in BGM300_{-1.96} generate higher levels of endogenous NO that partially suppresses cell growth but also confers salinity tolerance

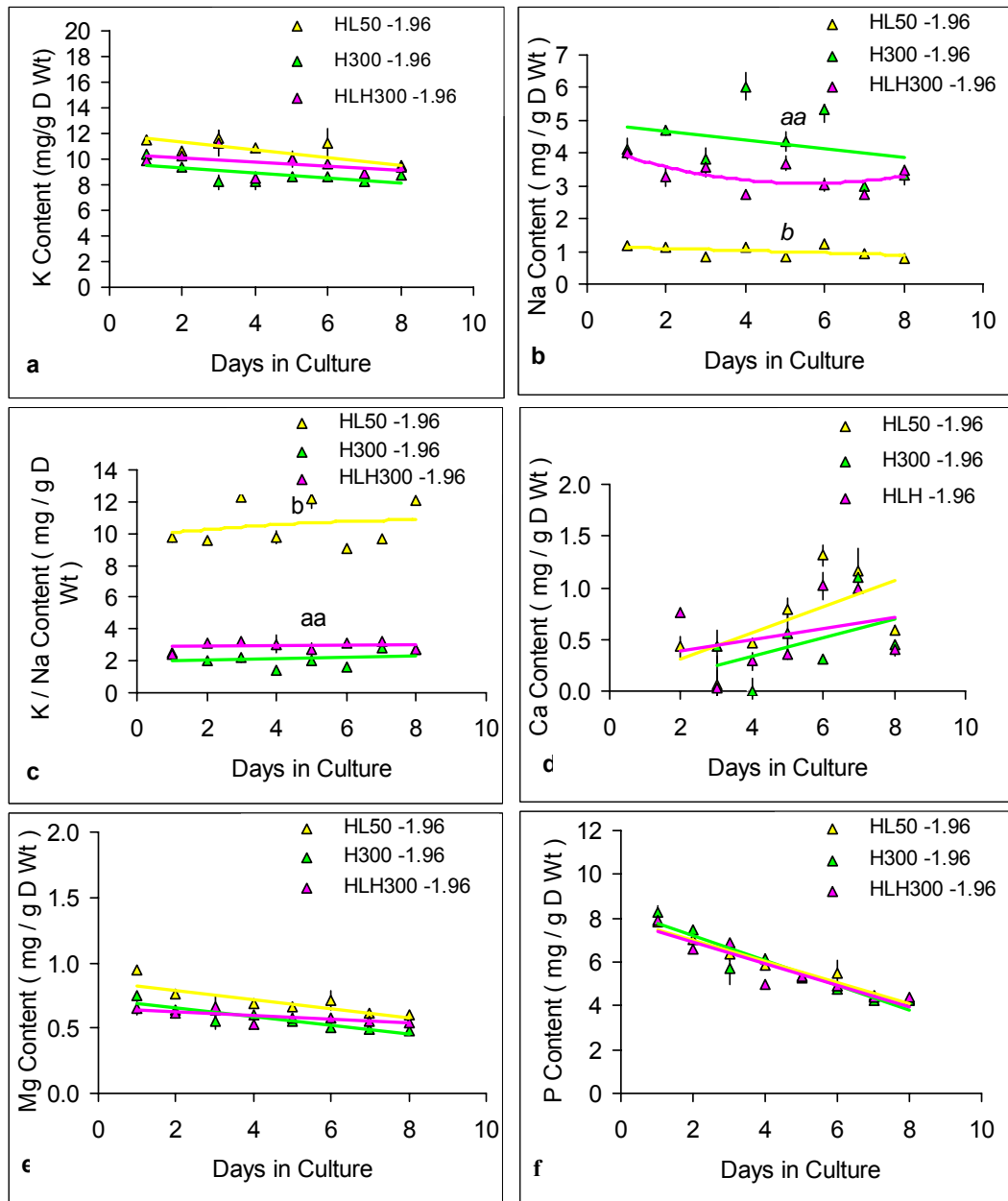


Fig. 2-6 Ion Content of HHS *Arabidopsis* Cell Cultures.

▲ HL50_{-1.96}, salt down-shock (Cells shifted from BGM300_{-1.96} to BGM50_{-1.96}):
 ▲ HLH_{-1.96}, salt up-shock (HL Cells shifted from BGM50_{-1.96} to BGM300_{-1.96}):
 ▲ H300_{-1.96}, cells grown in BGM300_{-1.96} (see section 2.2.1 and 2.2.2 for details).
 Samples were harvested daily from salt stressed cells (HL50_{-1.96}, HLH_{-1.96}, H300_{-1.96}). Minerals content was measured using a Perkin Elmer Optima 4300 series Inductively Coupled Plasma-Optical Emission Spectrometer (ICP-OES). Averages and SEs of three independent cultures are presented. Two factor analysis of variance (linear model) was performed on the data with Bonferroni pair-wise tests between treatment means. Different Roman characters signify significant differences ($p < 0.05$, 0.01 or 0.001) between treatment means at Day 5 (mid log phase of growth; bold character ($p < 0.001$), normal face ($p < 0.01$), italics ($p < 0.05$)).

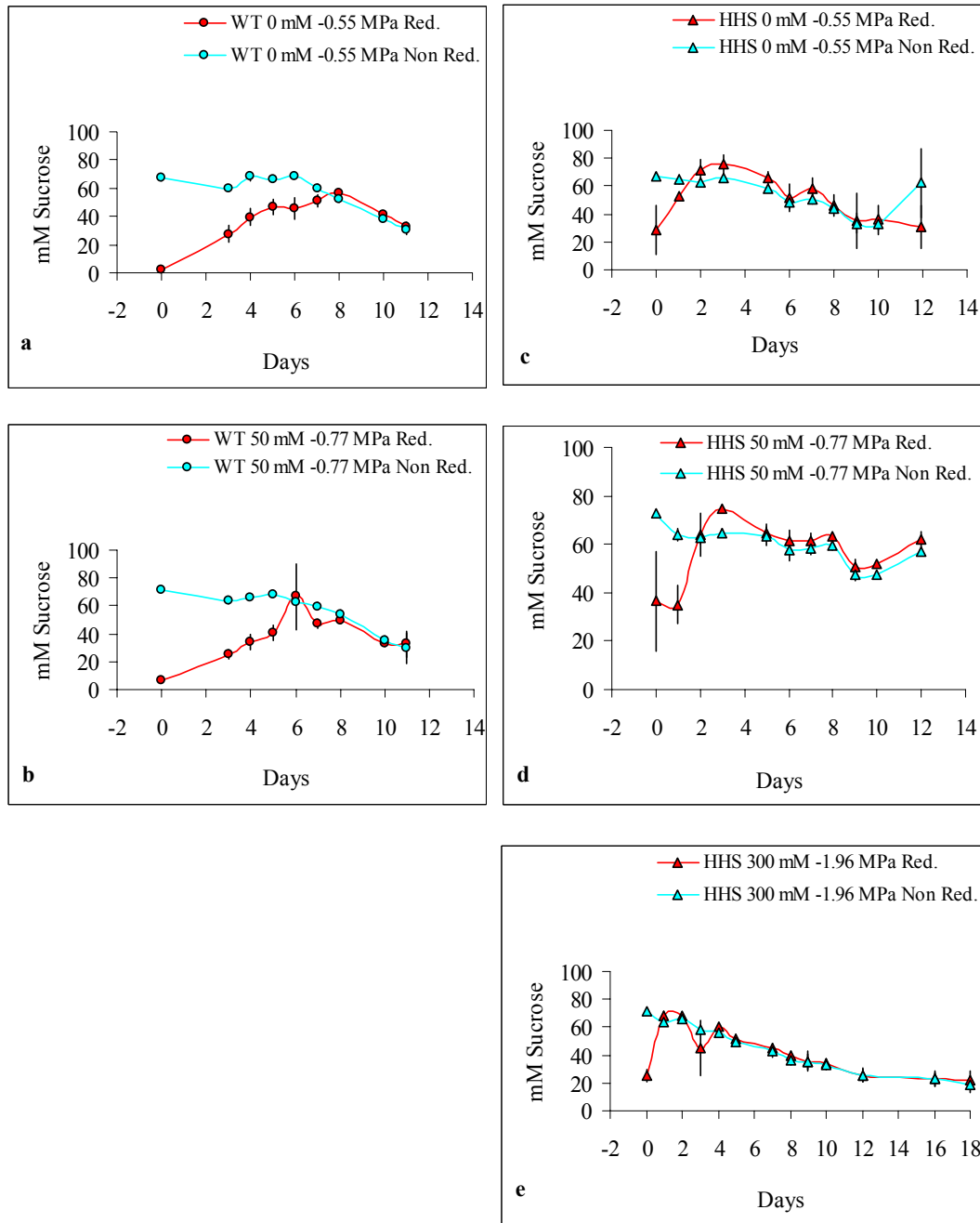


Fig. 2-7 Sucrose Content of Basic Growth Media for *Arabidopsis* Cell Cultures. Samples were harvested daily from WT cells in BGM0.0.55 (circles) and HHS cells in BGM300.1.96 (triangles) growth media to measure the reducing sugar ● ▲ (glucose plus fructose) and non reducing sucrose ● ▲ (glucose and fructose) for ● ▲ WT cells in BGM0.0.55 and ● ▲ WT cells in BGM50.0.77 or ▲ ▲ HHS cells in BGM0.0.55 or in BGM50.0.77 or in BGM300.1.96. Sugar content was measured using a Perkin Elmer Lambda 800 series UV/VIS Spectrometer. Averages and SEs of three independent experiments are presented.

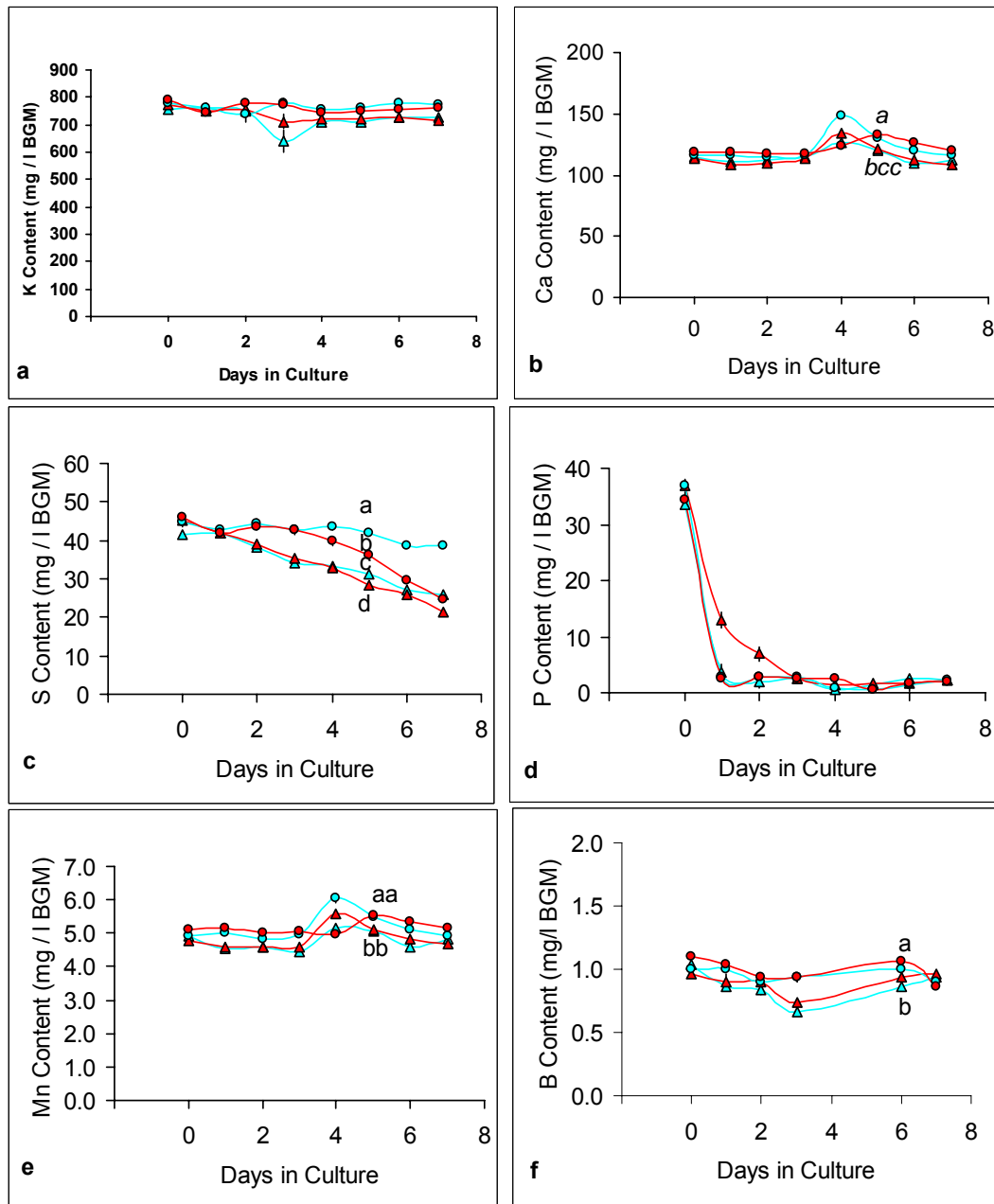


Fig. 2-8 Ion Content of Basic Growth Media for *Arabidopsis* Cell Cultures.

Samples were harvested daily from WT cells (circles) or HHS cells (triangles) in BGM50-0.77 (● and ▲) or BGM50-1.96 (● and ▲); see section 2.2.1 and 2.2.2. Ion content was measured using a Perkin Elmer Optima 4300 series Inductively Coupled Plasma-Optical Emission Spectrometer (ICP-OES). Averages and SEs of three independent cultures are presented. Two factor analysis of variance (linear model) was performed on the data with Bonferroni pair-wise tests between treatment means. Different Roman characters signify significant differences ($p < 0.05$, 0.01 or 0.001) between treatment means at Day 5 (mid log phase of growth; bold character ($p < 0.001$), normal face ($p < 0.01$), italics ($p < 0.05$)).

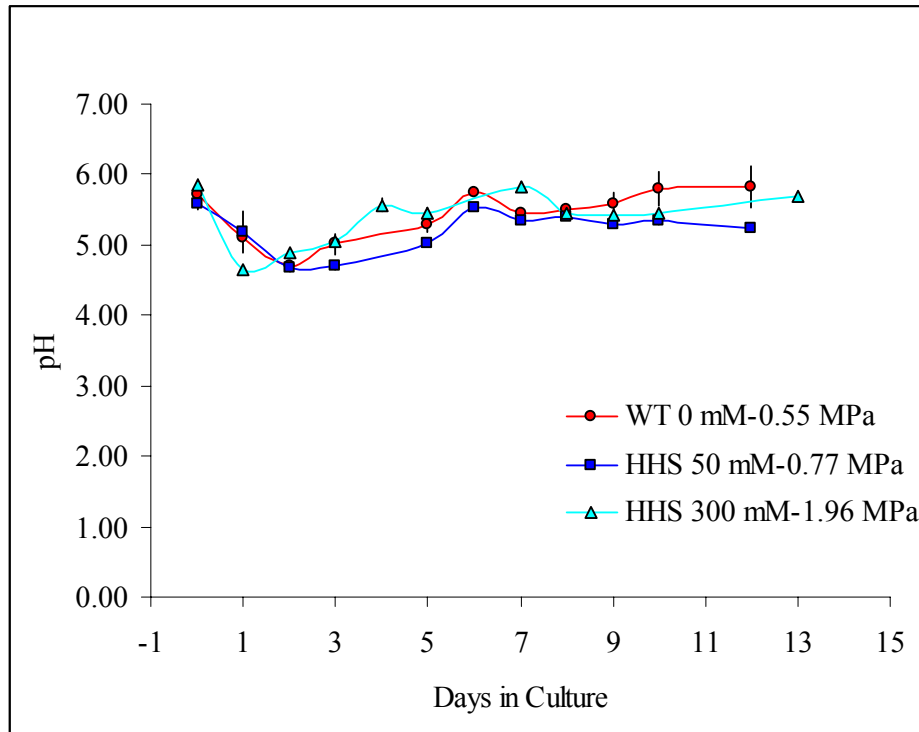


Fig. 2-9 pH measurement of Basic Growth Media for WT and HHS *Arabidopsis thaliana* Cell Cultures.

Samples were harvested daily from WT cells in BGM_{0.55} (●), HHS cells in BGM_{50.0.77} (■) and HHS cell in BGM_{300.1.96} (▲) and the pH was measured using pH meter 3320 JENWAY. Averages and SEs of three independent experiments are presented.

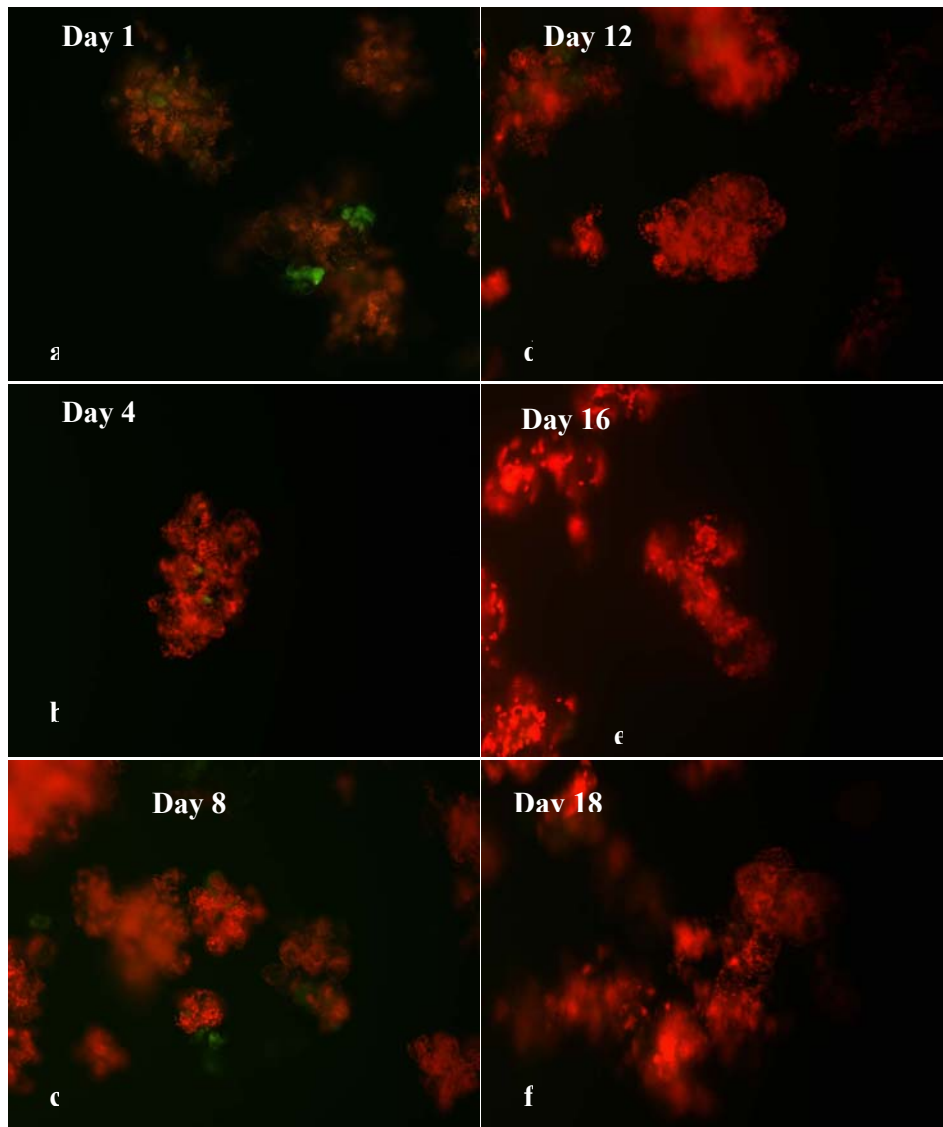


Fig. 2-10 DAF-2DA Stained WT *Arabidopsis thaliana* Cell Suspension Cultures in 0 mM NaCl (BGM0_{0.55}).

DAF-2DA (4,5-diaminofluorescein diacetate) is a nitric oxide (NO) sensitive fluorescein dye.

Cultures were grown for up to 18 days in Basic Growth Media (BGM0_{0.55}; see section 2.2.1) and aliquots were removed and stained with the cell-permeable NO-sensitive dye DAF-2DA (see section 2.3.4) . Red fluorescence is autofluorescence from the sample. Green fluorescence indicates the presence of NO.

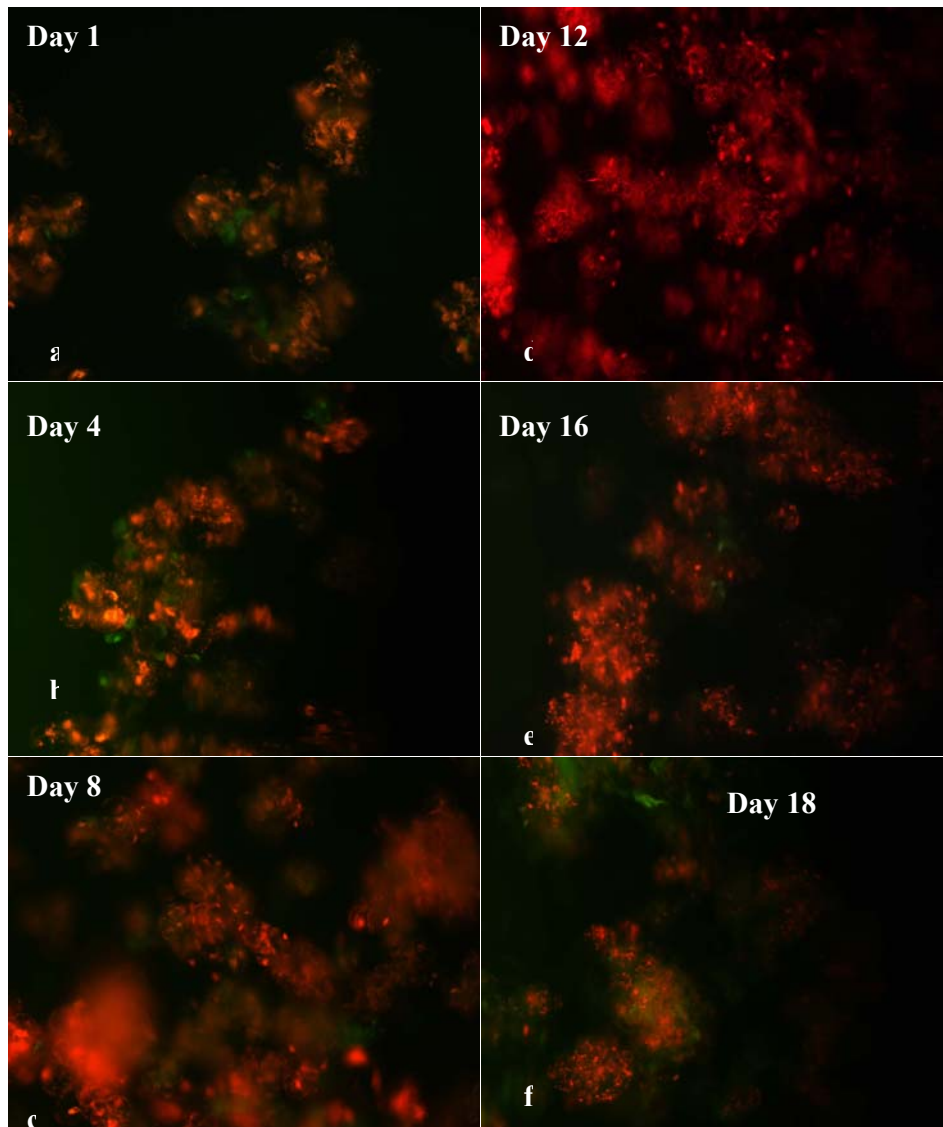


Fig. 2-11 DAF-2DA Stained WT *Arabidopsis thaliana* Cell Suspension Cultures in 50 mM NaCl.

DAF-2DA (4,5-diaminofluorescein diacetate) is a nitric oxide (NO) sensitive fluorescein dye.

Cultures were grown for up to 18 days in Basic Growth Media supplied with 50 mM NaCl (BGM50_{0.77}) and aliquots were removed and stained with the cell-permeable NO-fluorescent sensitive dye DAF-2DA (see section 2.2.1 and 2.3.4). Red fluorescence is autofluorescence shows red, green fluorescence indicates the presence of NO (see section 2.3.4).

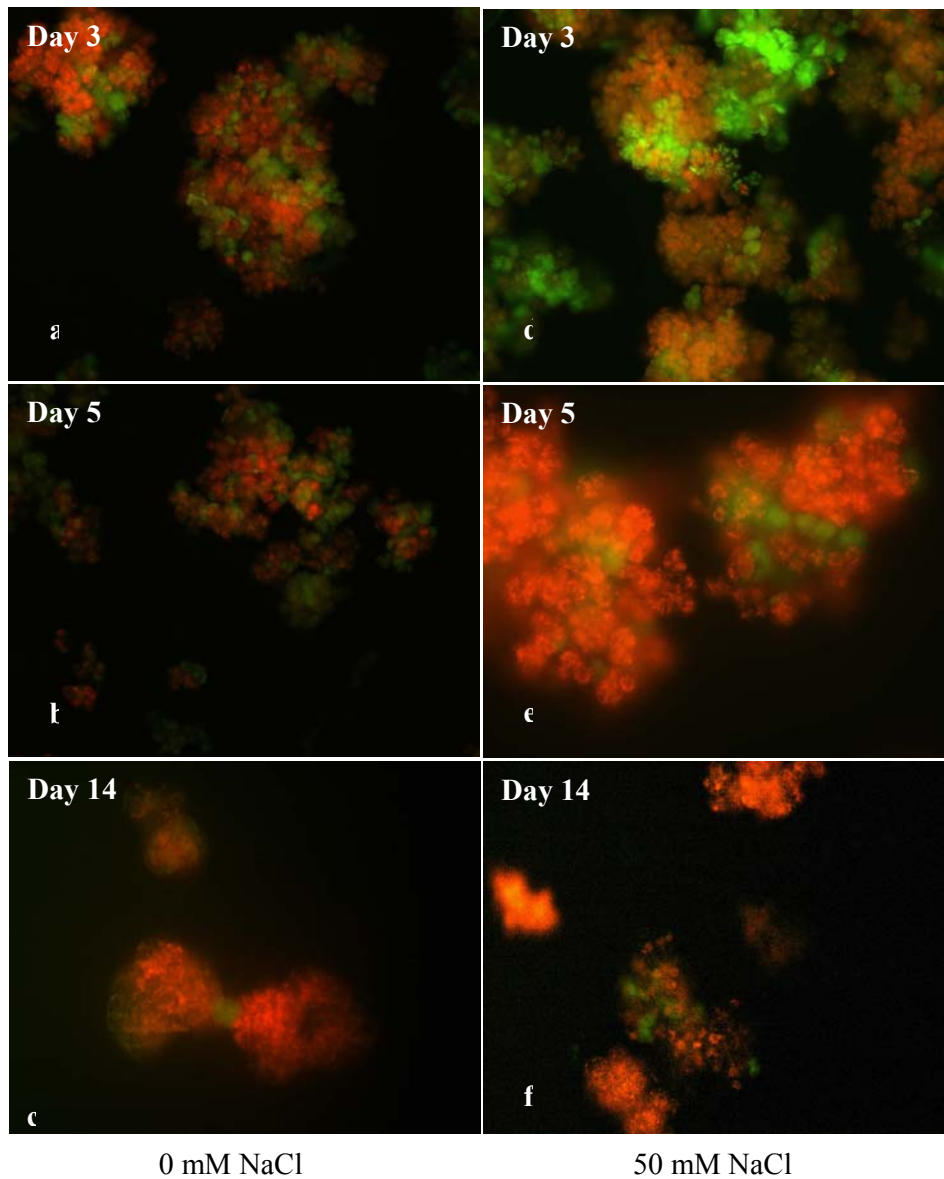


Fig. 2-12 DAF-2DA Stained HHS *Arabidopsis thaliana* Cell Suspension Cultures.

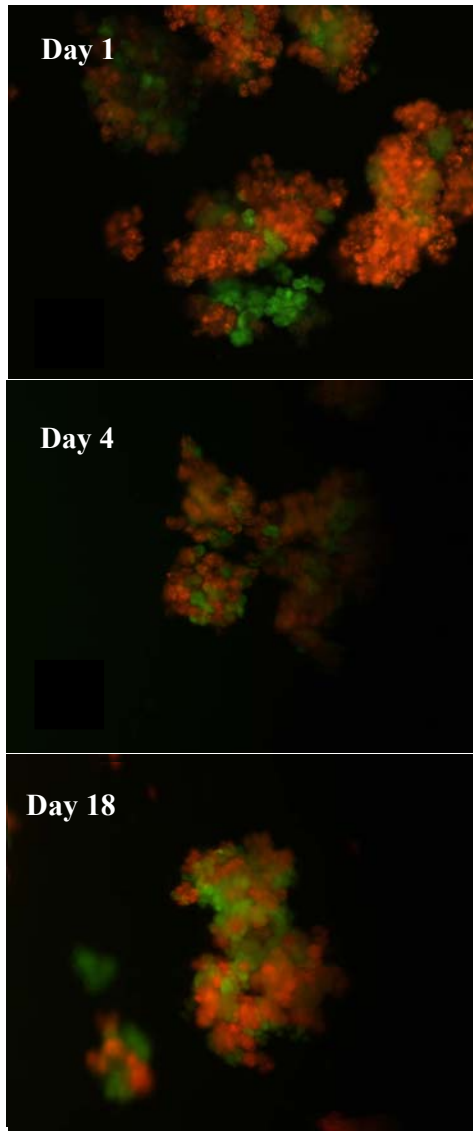
DAF-2DA (4,5-diaminofluorescein diacetate) is a nitric oxide (NO) sensitive fluorescein dye.

Cultures were grown for up to 14 days in Basic Growth Media (BGM_{0.55}, left panel a,

b and c) and cells were grown in Basic Growth Media supplied with 50 mM NaCl

(BGM_{50.77}) (right panel d, e and f). Aliquots were removed and stained with the cell-permeable NO-fluorescent sensitive dye DAF-2DA (see section 2.3.4). Red

fluorescence is autofluorescence shows red, green fluorescence indicates the presence of NO.



300 mM NaCl

Fig. 2-13 DAF-2DA Stained HHS *Arabidopsis thaliana* Cell Suspension Cultures.in 300 NaCl.

DAF-2DA (4,5-diaminofluorescein diacetate) is a nitric oxide (NO) sensitive fluorescein dye.

The Culture was grown for 18 days in Basic Growth Media supplied with 300 mM NaCl (BGM300_{-1,96}; (see section 2.2.2). Aliquots were removed and stained with the cell-permeable NO-fluorescent sensitive dye DAF-2DA (see section 2.3.4). Red fluorescence is autofluorescence shows red, green fluorescence indicates the presence of NO.

2.4 Discussion.

Salinity limits the growth and yield of crop plants. Salt stress results from a number of harmful cellular processes including Na^+ and Cl^- toxicity, the impairment of mineral nutrition, modification of the water status of plant tissues, and secondary stresses such as an oxidative stress linked to the production of toxic reactive oxygen intermediates. Since salt tolerance is a complex trait involving several interacting factors, there is an increasing interest in studying the physiological behaviour of halotolerant plant cells and tissues in order to identify and better understand salt tolerance mechanisms.

In this chapter, plant cell cultures were used to investigate mechanisms involved in plant salt tolerance. Plant cell cultures offer a major advantage for investigating salt tolerance as the complexities of higher levels of tissue organisation are not present. To survive in high salinity, unlike the intact root system of a plant, each cell in the culture must be expressing the required traits for salt tolerance and so important proteins and genes involved in tolerance should be enriched. The plant cell lines investigated in this study included wild type *Arabidopsis* (salt sensitive), HHS *Arabidopsis* (salt tolerant).

The development of the HHS cell line suggests that *Arabidopsis* cells have the genetic potential to tolerate high levels of salinity, and perhaps it is the inability of intact plants to coordinate the expression of the appropriate genes in the appropriate tissues that limits the plants ability to grow in the presence of NaCl.

When WT and HHS cells were incubated with fluorescein diacetate (FDA) and Lyso TrackerTM the dyes moved rapidly into small vacuoles/vesicles that appear in the cytoplasm of the latter but not the former. These vesicular bodies were less prevalent in the wild type *Arabidopsis* cells. The mechanism(s) that accumulate these dyes in the vesicles is not known. In many of these vesicles both the anionic dye Lyso Tracker and the cationic dye fluorescein co-localized suggesting an active transport process.

However in some cases, vesicles clearly fluoresced red only (Lysotracker accumulation) or green only (fluorescein accumulation), and this suggests that there is some separation of function within the vesicle population. The co-localization of both dyes in some vesicles suggests the dyes maybe treated as xenobiotics and are conjugated in the cytoplasm with glutathione and transported into the vesicles by ATP-binding cassette (ABC) transporters (Theodoulou, 2000).

Regardless of the mechanisms of dye sequestration, the presence of large numbers of these vesicles in salt-resistant cell lines is an interesting and novel observation and may reflect a key strategy for survival in high salinity. Whether they are involved in cellular detoxification or in vesicle trafficking (exocytosis), is unclear, but during a four hour tracking period using a confocal microscope, no vesicle movement was detected. It appears therefore, these vesicles/vacuoles act merely as a store for intracellular electrolyte.

When WT cells were grown in BGM0_{0.55} they had a doubling time of 2.45 ± 0.23 days, but this increased by to 2.84 ± 0.16 days when grown in BGM50_{0.77}; clearly salinity decreases growth rate. When WT cells were grown in BGM0_{0.77} the doubling time increased (by only ~3%) to 2.53 ± 0.15 (*cf.* BGM0_{0.55}). Under the experimental conditions used here, WT cells would not grow in BGM0_{1.96} or in BGM300_{1.96}. These data suggest that when exposed to 50 mM NaCl the observed slower growth rates of WT cells are attributable mainly to ionic stress and not to the loss of cell turgor. WT cells would not grow when exposed to severe desiccation (BGM0_{1.96}) suggesting osmotic adjustments to regain turgor was not possible under these conditions (Fig. 2-2 and Table 2-2).

On the other hand when HHS cells were grown in 300 mM NaCl (BGM300_{1.96}) growth slowed to 64% of controls (BGM0_{0.55}), but in isotonic, low salt media (BGM0_{1.96}) the

growth rates were even slower ~60% of controls. These data suggest that the habituation process in HHS cells has resulted in slower growth in the absence of salt or water stress, but the application of moderate salt stress (50 mM NaCl, $\psi_{\text{H}_2\text{O}}$ of -0.77 MPa) reduces growth rates by both ionic and osmotic effects. Under high saline, dehydrating conditions (300 mM NaCl, $\psi_{\text{H}_2\text{O}}$ of -1.96 MPa), however, HHS cells survive well, but their poor growth in isotonic, low salt media (0 mM NaCl, $\psi_{\text{H}_2\text{O}}$ of -1.96 MPa) suggest that at this low water potential Na^+ and / or Cl^- are required as an intracellular solute to regain turgor for expansion-induced growth. Presumably, these ions are stored in the vacuoles of the cell, to reduce their toxic effects on metabolism.

Sodium chloride can exert its toxic effect on plants by interfering with the uptake of other nutrient ions, especially K^+ , leading to nutrient ion deficiency. The ion content (K, Na, S, P, Mn, Mg, Fe and Ca) of Arabidopsis HHS (salt tolerant) and WT (salt sensitive) cells was assessed in 50 mM NaCl, but only Na^+ levels differed between the two lines. The levels of K, Ca, S, and P were found not to be significantly different. Phosphate levels declined with culture age in both cell lines and in the media. However, even at stationary phase intracellular phosphate levels were 50% of those at day 1 (Fig. 2-6f) and were probably sufficient to maintain growth whereas extracellular phosphate levels were almost undetectable (Fig. 2-8f). It is conceivable that the growth of both above cultures were limited in part by the availability of free P, but more work is needed to clarify the role of P in these cultures.

At all times the K^+/Na^+ ratio measured in HHS cell was higher than salt stressed wild type cells. Most interestingly, the HHS cells contained considerably less Na than the salt stressed wild type cells, suggesting that the HHS cell lines have mechanisms for minimizing Na^+ content that are not present in the wild type cells. These may be mechanisms that reduce Na^+ uptake or increase Na^+ efflux.

Further experiments are required using radio active tracers ($^{22}\text{Na}^+$) to resolve how HHS cells maintain low intracellular Na^+ levels.

The lower final biomass of HHS cells at stationary phase does not appear to arise from the depletion of the energy (sugar) source, nutrient ions, or pH shift in the media. One difference between WT and HHS cells that could account for the different biomass at stationary phase was the cellular levels of NO. Nitric oxide has been reported to suppress cell growth and eventually cause cell death (Carimi *et al.*, 2005), but it has also been implicated in salinity tolerance (Maathuis and Sanders, 2001; Price, 2005; Zhang *et al.*, 2006; Zhao *et al.*, 2004). It is conceivable, therefore, that HHS cells generate higher levels of endogenous NO that partially suppresses cell growth but also confers salinity tolerance.

Chapter 3: Comparison the Proteome of Salt Tolerant and Salt Sensitive Arabidopsis Cell Lines.

3.1 Introduction.

3.1.1 Expression Profiling.

By studying the changes in protein and transcript abundance that results from exposure of plants to any treatment, it is possible to gain an insight into the processes that become stressed, and the stress responses that are activated. One of the challenges for these kinds of studies is to differentiate between the effect of stress (pathology) from the stress response (attempts to ameliorate stress).

DNA micro-arrays have become established as the routine method for exploring global transcription patterns in eukaryotes. Although the first application of DNA micro-arrays was to study the pattern of gene expression (de Saizieu *et al.*, 1998; Schena *et al.*, 1995), other uses have been found. For example hybridisation-based assays for mutation detection (Chee *et al.*, 1996; Hacia *et al.*, 1998), polymorphism analysis (Wang *et al.*, 1998), mapping (Sapolsky and Lipshutz, 1996), evolutionary studies (Hacia *et al.*, 1998), and other applications have been documented (Cheung *et al.*, 1998; Shoemaker *et al.*, 1996). In general the applications of DNA micro-arrays fall into two categories: (1) Genomic studies: (2) Gene expression studies.

The advantages of using DNA micro-arrays are that it allows gene expression to be studied on a massive scale, and that the procedures are relatively simple compared with protein profiling. However, DNA micro-arrays also have disadvantages; changes in transcription abundance does not always result in a change in protein abundance: the quality of data generated is highly dependent on the design of the micro-arrays: subtle modifications in protein structure can have profound effects on cell metabolism and these are rarely reflected in changes at the transcript level. An argument could be made,

therefore, that studies on changes in protein profile will be more revealing than studies on transcript profile. Furthermore, protein profiling gives not only information the relative amounts (abundance) of proteins, but also indicates post-translational modification that could affect specific processes. Moreover, studies at the protein level can be extended to provide information on the interaction of proteins with each other and with other molecules of different types. The disadvantages, however, are the complexity of the protein samples in the extracts, and the time and expense involved with the analysis.

3.1.2 General Aspects of Proteomics

A large-scale study of proteins and their properties (such as post-translational modification, expression levels, and interaction with other molecules) to gain a global view of cellular processes at the protein level are termed “proteomics” (Abbott, 1999). Although transcriptional analyses are relatively quick and inexpensive, transcript abundance does not necessarily indicate protein abundance because of post-translational modification (PTM) of proteins, splicing, and RNA editing (Graveley, 2001).

The study of gene expression using microarrays allows for whole cell profiling of the transcriptional response to a certain stimulus. However, because of the numerous levels of possible gene expression control, the transcriptional profile does not always provide précis representation of the cellular protein expression. For example, it has been estimated that each protein encoded by human genome can exist in five or more isoforms due to post-translational modification (PTM) and each of these protein isoforms may have different biological activities in cellular metabolism (Cash, 2002). PTM of proteins is important for biological process, for example in cellular signalling where the phosphorylation state of a protein can induce either activation or inactivation of signalling cascade. Also poor levels of correlation exist between mRNA and protein

levels (generally less than 0.5) due to different degradation rate of individual mRNA and proteins (Gygi *et al.*, 1999; Le Roch *et al.*, 2004). Furthermore, even in one of the simplest self-replicating organism, *Mycoplasma genitalium*, there are 24% more proteins than genes (Teichmann *et al.*, 1998). In humans it has been estimated that there are at least three times as many protein species as there are genes (Abbott, 1999).

To analyse the proteome of cell, three key processes are involved. First, the proteins in the sample have to be separated into a large number of sub-samples to reduce the complexity for analysis. Second, the abundance of each protein within the sample has to be assessed. Finally, the identity of each protein has to be established.

Separation is usually achieved by two dimensional gel electrophoresis (2-DE) or liquid chromatography (2D-LC), and protein identification by mass spectrometry (MS). Protein abundance is usually determined after separation, but in some cases it can be determined by MS.

In this study, a proteome analysis of HHS cells exposed to salinity was assessed using a 2D-gel electrophoresis/MS method called Differential Gel Electrophoresis, or DiGE. A brief description of the method follows.

3.1.3 Two-Dimensional Electrophoresis.

Two-Dimensional Electrophoresis (2-DE) was introduced by O'Farrell (O'Farrell, 1975). In general 2-DE separate proteins firstly by charge using isoelectric focussing (IEF) and secondly by molecular mass using sodium dodecyl sulphate-polyacrylamide gel electrophoresis (SDS-PAGE). Two dimensional Electrophoresis has the ability to separate and profile thousands of proteins (Wu *et al.*, 2002). In brief, samples (*e.g.* cells, tissue extract) are solubilized either chemically and/or mechanically, and proteins are denatured into their polypeptide subunits. The solubilisation methods have to be compatible with the IEF step and should not introduce modifications to proteins that

could affect MS (Chambers *et al.*, 2000). The extract should be incubated with nucleases to remove DNA or RNA that could interfere with protein migration during electrophoresis. Isoelectric focusing (IEF) separates the mixture based on the protein isoelectric point (pI). Proteins are amphoteric molecules, having positive, negative or zero charge depending on the pH of suspension buffer. The pI is the pH at which the protein carries no net electric charge.

When 2-DE was first introduced proteins were separated in the first dimension using polyacrylamide gels contains a mixture of hundreds of carrier ampholytes (CA) when placed in an electric field the CA separate proteins according to their pI and induce a continuous pH gradient. The disadvantage using CA is that the pH gradients produced were unstable and proteins could diffuse across the gradient.

3.1.3.1 First Dimension Immobilized pH Gradient Gels.

In recent years the introduction of immobilised pH gradient (IPG) to replace the CA technique has improved the resolution of separation and reproducibility of 2-DE (Gorg *et al.*, 2000). A pH gradient is generated by the co-polymerisation of 6 to 8 well-defined chemicals (the immobilines) combined with an acrylamide matrix fixed to a plastic-backed strip. An immobilised pH gradient is produced by covalently incorporating a gradient of small basic and acidic buffering peptides (desired pH range is between 3-11) into a polyacrylamide gel at the time it is cast. The advantages of IPG are increasing loading capacity and reproducibility compared with CA system. The resolution can be adjusted further by changing the range of the pH gradient (*e.g.* to look specifically at basic proteins [pH 7-11] or acidic proteins [pH 3-4]). High protein loads are essential if less abundant proteins components are to be identified using mass spectrometry (Molloy, 2000). Disadvantages of IGPs are poor representation of hydrophobic and

membrane proteins in the 2-DE gels as the method relies on solubilisation in aqueous buffers.

3.1.3.2 Second Dimension SDS-PAGE.

The second stage of 2-DE is to separate proteins based on molecular weight using SDS-PAGE (sodium dodecyl sulphate-polyacrylamide gel electrophoresis). The isoelectrically focussed proteins on the IPG strip are applied to the top of a polyacrylamide gel and the polypeptides then migrate in an electric current into the second dimension gel and are separated on the basis of molecular size. Individual proteins are then visualised with an appropriate stain (*e.g.* coomassie blue or silver dye). Several thousand spots may be resolved on single 2-DE gel and initial choice of sample solubilisation conditions and pH range of gel strip used for the first dimension will determine which particular subset of proteins from the proteome are profiled.

The main obstacles in visualisation of total cell or tissue extracted proteins are the highly dynamic range and chemical diversity of proteins reflected in their range of molecular weights, pIs, and solubility. Even though, 2-DE is a powerful technique to profile thousands of proteins from a single sample, there are still some limitations and these included: (1) difficulties in gel reproducibility: (2) limited range of detection (*e.g.* proteins > 100 thousand Daltons and pI values > 9 or < 4; Yanagida, 2002b): (3) Poor staining of some proteins: (4) under representation of hydrophobic proteins: (5) Failure to detect low abundance proteins that may play a key role in cell function (Abbott, 1999).

3.1.4 Mass Spectrometry.

Protein identification by mass spectrometry (MS) is a high throughput method which can provide extremely accurate measurements of the mass of molecules. The data generated can be used to search protein and translated nucleotide databases directly to

identify a protein. Mass spectrometers consist of three essential parts: (1) an ionisation source that converts molecules into gas phase ions: (2) a mass separator that separates the ion anylates based on their mass/charge (m/z) ratio, and (3) an ion detector that detects the ions resolved by the mass separator.

Essentially, there are two types of MS used for protein identification, Matrix Assisted Laser Desorption Ionisation Time of Flight (MALDI-TOF), which is useful for identifying proteins from organisms with sequenced genomes, and Electro Spray Ionisation tandem MS (ESI-MS/MS). In both cases, the instrument can analyse only small peptide fragments (2000-300 Da), and so the protein samples have to be fragmented. In the case of MALDI-TOF this is achieved by peptide digestion; with a tandem MS, fragmentation can be accomplished in the instrument.

3.1.4.1 MALDI-TOF.

MALDI-TOF is an MS technique that is used to calculate the mass of an ionised peptide, and the result is then compared with a library of peptide masses for identification. The method is restricted therefore, to organisms with significant protein data bases. The molecules to be ionised are dried in an energy absorbing crystalline matrix and a laser pulse is then used to exciting the matrix and generate ions which are evaporated. The ions are then swept into an evacuated tube and accelerated by an electromagnetic field, before colliding with a detector positioned at the far end wall. The 'time of flight' of the ion, from laser pulse ionization to end wall collision, is accurately measured and will be a function of the mass/charge ratio (m/z) of the ion. MALDI-TOF is a quick and reliable method of protein identification that relies on comparing peptide mass fingerprints from analysis digested protein to computer generated theoretical fingerprint profiles from protein or translated cDNA databases. Matched proteins are sorted according to algorithms that take into account protein

properties such as species of origin and expected mass range, sequence coverage, and mass accuracy, to calculate the probability of a correct identification.

3.1.4.2 Tandem MS.

As stated by Wu and co-workers (Wu *et al.*, 2002) tandem MS (MS/MS) can perform two stage mass analysis of ions. Electro-spray ionization MS/MS (ESI-MS/MS) can be coupled to different types of mass analyser such as, an ion trap, TOF, or quadrupole. The samples are introduced to the mass spectrometer as a liquid. Every peptide analysed is subjected to further fragmentation to give partial information about the peptide sequence. In a collision cell the fragmentation take place and the molecular masses of the resultant fragment ions are compared with the theoretical masses of fragments from each protein sequence in the databases. This technique will adequately identify protein fragments and is particularly applicable to short sequence data such as those of expression sequence tags (ESTs) (Yanagida, 2002a). MS/MS can provide actual sequence data and can identify large proteins. A good strategy that is often adopted is to first analyse all samples initially by MALDI-TOF MS as it is rapid. Then for proteins that cannot identified by this method, (due to low amounts or to the presence of several proteins in the spot, or if the protein is not present in any of the public domain databases) tandem MS can be used.

The identification of proteins from MS data is simplified by the use of specialised software that compares actual peptide mass fingerprinting data or peptide fragmentation data with theoretical patterns generated from databases.

Post-Translational Modification (PTM) of proteins has a profound effect on protein function and so the identification of PTMs is an important goal of proteomics. Phosphorylation, glycosylation, ubiquitination, sumoylation, sulphonylation, palmitoylation, and ADP ribosylation are all examples of PTM that can affect protein

function. Such modifications are vital for the correct functioning of many proteins. Even though PTMs are determined to some extent by the protein amino acids, it is not currently possible to predict reliably which modifications occur for any particular protein (Cash, 2002). MALDI-TOF can identify when a protein is phosphorylated (Palzkill, 2002) as the expected fragment sizes with and without a phosphate can be calculated. More commonly tandem MS is used to investigate PTMs by searching against theoretical PTM databases.

3.1.4.3 Quantitative Proteomics.

Quantitative proteomics is a very important and necessary to evaluate differences between protein abundance in two samples. There are several quantitative proteomic techniques used. These include: SILAC (Stable Isotope Labelling by Amino acids in cell Culture) which allows for the differential *in vivo* incorporation of a stable isotope (e.g. $^{14}\text{N}/^{15}\text{N}$ or $^{12}\text{C}/^{13}\text{C}$) into two samples which are subsequently pooled for MS based quantitative proteomics. The resolved individual proteins, which consist of sample from both treatments, are then fed into the tandem MS and the relative abundance from each treatment assessed by the ratio of the isotope signatures.

Another method is Isotope-Coded Affinity Tags (ICAT) technique. In this approach, two cysteines in samples of interest are labelled with the thiol reagent $^1\text{H}_4\text{NiCNHS}$ (light isotope containing hydrogen) and $^2\text{H}_4\text{NiCNHS}$ (heavy isotope containing deuterium) respectively. The samples are then pooled and resolved into their individual polypeptides. MS analysis of the combined digest then provides information on the expression levels of those proteins by comparison of $^1\text{H}_4/{}^2\text{H}_4$ ratios of individual peptides.

Another commonly used method is Difference Gel Electrophoresis (DiGE). Two samples of interest are labelled with different fluorophores (CyDyes), mixed together,

and run on the same gel. The ratio of fluorescent signal intensity of matching spots between samples is determined (Unlu *et al.*, 1997). For protein identification by MS, spots are selected and then excised from a preparative gel.

Jiang and co-workers (Jiang *et al.*, 2005) compared the DiGE and ICAT techniques and found that DIGE could separate proteins in certain low molecular mass ranges and also identified cysteine-free proteins that were not detected by ICAT analysis, whereas ICAT analysis quantifies the sum of the protein species of one gene product while DiGE quantifies at the level of resolved domains and protein localisation. The web site of the Human Protein Reference Database (HPRD) (www.hprd.org) gives information on protein domain architecture, interaction networks, posttranslational modification, and disease association for each protein in the human proteome. There is also web site on gene ontology project (<http://www.geneontology>) which is a collaborative effort to address the need for consistent descriptions of gene products in different databases.

3.1.5 Integration of Genomic, Proteomics, and Bio-Informatics.

To understand the complex behaviour of a biological system several approaches are needed, and future studies will involve a mix of genomics, proteomics, bioinformatics and maybe other new technologies and methods (Russell, 2002).

Le Naour and co-workers (Le Naour *et al.*, 2001) combined oligonucleotide microarray and proteomic approaches to reveal genes associated with dendritical cell differentiation and maturation and this then allowed analysis of posttranslational modification (PTM) of specific proteins as part of these processes. Novel genes and proteins were identified in this study, but the conclusion was that the proteomics part of the study was paramount as it provided information that was unavailable at the RNA level (Le Naour *et al.*, 2001). Therefore genomic studies in combination with proteomic analyses of

host-pathogen interactions are essential to fully understand virulence and pathogenesis mechanisms (Zhang *et al.*, 2005).

3.2 Materials and Methods.

3.2.1 Plant Material.

Wild type (WT cells grown in BGM0_{0.55}) and Habituated to High Salt (HHS cells grown in BGM300_{-1.96}) cell lines were established, maintained and grown as described in Materials and Methods (Chapter 2 Section 2.2.1).

3.2.2 Reagents and Apparatus.

All equipment for 2-DE (*e.g.* IPGphor, DALT 6 & 12 gel tanks, Typhoon 9400 gel scanner, etc.) were supplied by Amersham Biosciences, Little Chalfont, Buckinghamshire. In addition, Immobiline gel strips, all buffers, reagents and dyes were also supplied by Amersham Biosciences apart from the following: phenol, pH sticks, polyacrylamide and bis-acrylamide, and TEMED (Sigma); lysine and sucrose (Fisher); Sypro Ruby (Bio-Rad); lint-free wipes (Canford Audio Kimwipes).

3.2.3 Experiment Setup.

The starter cultures for these experiments were HHS cells that had been sub-cultured every seven days into Basic Growth Media supplemented with 300 mM NaCl (BGM300, solute potential of -1.96 MPa; see Materials and Methods, Chapter 2.2). These cultures had been maintained in this growth media for several months before the experiment commenced. Ten ml aliquots of media (containing approximately 3 ml of cells) were removed after 6 days (log phase grow period) and transferred under sterile conditions into 80 ml of BGM300_{-1.96} in 250 ml conical flasks; these were then sealed with a sterile cotton wool bung and an aluminium foil cover taped in place. Twelve replicate flasks were prepared and placed in an illuminated orbital shaker (see Section

3.2.1 for details). After a further 6 days, 4 flasks were randomly selected and the cells harvested and stored -20°C for subsequent protein extraction; the remaining 8 flasks were used to seed 8 fresh cultures containing BGM50_{-1.96} (Basic Growth Media supplemented with 50 mM NaCl and 398 mM sorbitol; solute potential -1.96 MPa). These cultures were returned to the orbital shakers, and after a further 6 days 4 flasks were randomly selected and the cells harvested and stored at -20°C for subsequent protein extraction; the remaining 4 cultures were used to seed 4 fresh flasks containing 80 ml BGM300. After a further 6-day growth period the cells from these 4 flasks were also harvested and stored at -20°C . This procedure produced 4 replicate samples of log phase cells grown in isotonic conditions (-1.96 MPa) and exposed to each of the following ionic conditions (see Fig 3.1 for a diagrammatic representation), cells grown in 300 mM NaCl (1); cells grown in 300 mM NaCl and shifted to 50 mM NaCl (2, representing a ‘salt down-shock’), cells transferred up from 50 mM to 300 mM (3, representing a ‘salt up-shock’).

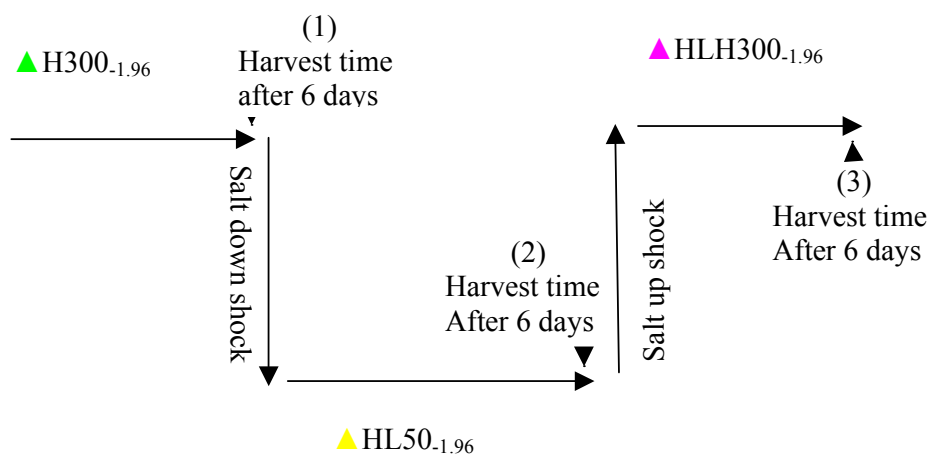


Fig. 3-1 Schematic Diagram of the Three Different Growth Conditions of HHS Cells Used for Proteome Analysis.

▲ H300.1.96, cells grown in BGM300.1.96:

▲ HL50.1.96, salt down-shock (Cells shifted from BGM300.1.96 to BGM50 + Sor.-1.96):

▲ HLH300.1.96, salt up-shock (HL Cells shifted from BGM50.1.96 to BGM300.1.96):

Samples were harvested at mid-log phase of growth (6 days) and used for analysis or to seed fresh cultures, (see section 2.2.1, 2.2.2, and 3.2.4 for details).

3.2.4 Sample Preparation.

3.2.4.1 Harvesting Arabidopsis Cells.

The cells were harvested by transferring to 50 ml falcon tubes and allowing them to settle for 5 minutes. The supernatant was discarded and the pellet washed with 50 ml of the appropriate isotonic ice cold BGM media, inverted gently several times to re-suspend the cells, and again allowed to settle. The pellets were then placed on a Whatman filter (47 mm Glass micro-fibre filter cat # 1821-047), and dried with a vacuum pump for approximately 20 seconds. The samples were then scrapped off the filters with a spatula into 50 ml Falcon tubes and stored at -20 C° until required.

3.2.4.2 Protein Extraction.

Approximately 500 mg of Arabidopsis cells were ground in liquid nitrogen using a mortar and pestle, and the powder transferred to 50 ml Falcon tubes. In a fume hood 2.5 ml of extraction buffer (0.1 M Tris pH 8.4, 20 mM KCl, 10 mM EDTA, 40% (w/v) sucrose) and 2.5 ml of Tris pH 8.8 buffered phenol TE (Sigma # p-4557) per sample were added, the tubes gently inverted to re-suspend the pellet, and then left gently shaking (~2 rpm.) at 4°C for 30 minutes. After incubation, the samples were centrifuged for 15 min at 4400 g (4 °C), and the upper phenol phase carefully removed with a short Pasteur pipette. Another 2.5 ml phenol was added to the tube, the content shaken vigorously, and a second extraction performed, as described above. The two phenol phases were pooled and protein precipitated overnight at -20°C by the addition of 5 volume of cold 0.1 M ammonium acetate in methanol. The protein samples were then collected by centrifugation, as described above, and the pellets were resuspended with a plastic staker in 1.5 ml cold ammonium acetate/methanol, and sonicated at 0°C for 15 minutes using a water bath sonicator, Grant Ultrasonic Bath XB2 (Grant Instruments,

Cambridge Ltd.). This washing procedure was repeated a further three times; the first two washes were in ammonium acetate/methanol, the second two washes in cold 80% acetone. Pellets were stored in 80% acetone at -20°C until required.

3.2.5 Determination of Protein Concentration.

The samples were centrifuged for 15 min at 4400 g (4°C) and the supernatant decanted; pellets were partially dried using a vacuum desiccators for half hour at room temperature. Approximately 30 mg of sample pellet was weighed in a 1.5 ml Eppendorf tube and resuspended in 600 µl of IEF buffer A (7 M urea, 2 M thiourea, 4% (w/v) CHAPS, 30 mM Tris-HCl, pH 8.5) using a plastic inoculation loop followed by a sonicating water bath for 10 minutes at 0°C (Grant XBZ Ultrasonic Bath). The samples were then centrifuged at 13,400 g for 5 minutes at room temperature, and the supernatant removed to clean Eppendorf tubes. Three µl of samples was removed for protein quantification using the 2D-Quant-kit (Amersham Biosciences, catalog # 80-6483-56); the manufacturer's protocols were followed throughout and Bovine Serum Albumin (BSA) was used as protein standards.

3.2.6 CyDye Labelling of Proteins.

The stored protein samples were thawed and protein extracted and quantified as described in (Sections 3.2.4.2 and 3.2.5 respectively).

3.2.6.1 Minimal Labelling.

For optimal CyDye labelling the pH of samples must be alkaline (pH 8-9). Samples were tested on pH strips (Sigma # P 4536) but the pH was always found to lie between pH 8-9. Adjustments can be made, however, by adding 1.0 or 0.1 M NaOH, or 1.0 or 0.1 M HCl. Aliquots of the twelve protein samples (in IEF Buffer) containing 50 µg protein were placed in 500 µl Eppendorf tubes and placed on ice in the dark for 30

minutes with 1 μ l (400 pmoles/ μ l) of the appropriate Cy3 or Cy 5 dye. In addition, a Pooled Standard Sample was prepared by placing 25 μ g of each of the 12 samples in a 500 μ l Eppendorf tube (a total of 300 μ g protein), and labelled for 30 minutes with 1 μ l Cy 2 dye (400 pmoles/ μ l). After the incubation period, the reactions (Fig. 3-2) were stopped by the addition of 1 μ l of 10 mM lysine. IEF Loading Sample was then prepared for each of the six gels by mixing together 50 μ g of a Cy 3 labelled sample, 50 μ g of a Cy 5 labelled sample, and 50 μ g of the Cy 2 labelled Pooled Sample (*i.e.* 150 μ g total protein per gel). The volumes of each of these six IEF Loading Samples (\sim 150 μ l) were made up to 350 μ l using 150 μ l IEF Buffer B (7M urea, 2M thiourea, 2% (w/v) Amido Sulfo betaine (ASB-14), 1% (v/v) IPG buffer (pH 6-11 or 4-7), 2.4% (v/v) DeStreak) and 50 μ l of Rehydration Buffer (7M urea, 2M thiourea, 1% (w/v) ASB-14, 2% (w/v) CHAPS, 0.002 % bromophenol blue, 0.28 % (w/v) DTT, 0.5% (v/v) IPG Buffer, 1.2% (v/v) DeStreak). For both buffers, IPG Buffer and DeStreak were added just prior to use. A scheme for the design of this experiment is presented in Table A.3-1 (see Appendix).

3.2.6.2 1st Dimension Separation by Isoelectric Focussing.

Each IEF Loading Sample mixture was then pipetted along the bottom of an 18 cm ceramic IEF strip holder, and then a single dehydrated pre-cast IPG strip was placed gel face down onto the sample mixture. Two ml of cover fluid was then carefully layered on top of the IPG strip to prevent evaporation. The strip holder plastic cover was then replaced and positioned on the IPGphor platform (Amersham Bioscience, Amersham, UK). The following program was used for isoelectric focussing 20°C, 50 UA/strip: Step 1 (Rehydration), 30 Volts for 13 hours: Step 2, 500 Volts for 1 hour: Step 3, 1000 Volts for 1 hour: Step 4, 8,000 Volts for 13 hours or until 60,000 Volt-hours was exceeded: Step 5 (if necessary), 100 Volts for 9 hours or until 60,000 Volt-hours was exceeded.

After electro-focussing, the strips were removed using clean forceps, and placed into an equilibration tube, the plastic back should be in contact with the side of the tube with 10 ml of equilibration Buffer, 25% (v/v) 4x Resolving gel buffer, 6 M Urea, 30% (v/v) Glycerol, 2% (w/v) Sodium dodecyl sulphate (SDS), 0.002% (v/v) Bromophenol blue. The 4x resolving gel buffer, 1.5 M Tris base and HCl pH 8.8. The strips were first equilibrated with 0.5% (w/v) DTT for 15 minutes, followed by a 15 minute wash in 4.5% (w/v) iodoacetamide. The IPG strips were then ready for the 2nd dimension separation.

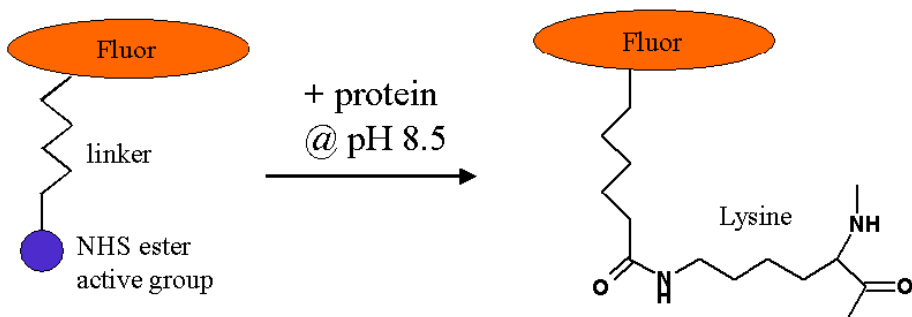


Fig. 3-2 Schematic diagram of CyDye protein labeling reaction.

CyDye fluors containing N-hydroxysuccinimide (NHS) ester active group covalently bound to lysine residues of the protein via an amide linkage (Amersham Ettan User Manual).

3.2.6.3 2nd Dimension SDS Page Gel.

3.2.6.3.1 Preparation of Large Format Gels.

As pre-cast plastic backed gels are incompatible with DiGE due to the plastic backing fluorescing during scanning, these gels were poured manually.

3.2.6.3.1.1 Preparation of Gel Plates.

Plates were soaked in 10 % SDS to remove old bounded acrylamide. Back plates should not be immersed for more than an hour as it ruins the gel spacers over time. A soft sponge was used to wipe the acrylamide off carefully to avoid scratches which show up in gel scans. Then the plates were dried off and checked for any bits of acrylamide were missed and these removed with the soft side of the sponge until the plates were completely clean. The plates were rinsed in tap water followed by distilled water, dried with lint-free (Kim Wipes, Canford Audio # 55-179) and finished off with the Reusable lint-free wipes (Wypall wipes # 55-186).

In the fume hood the back plates were laid flat and 1 ml of bind-silane mix (80% (v/v) Ethanol, 0.2% (v/v) Glacial acetic acid, 0.01% (v/v) Bind-silane (Plus One Amersham), 18% ddH₂O) was pipetted onto each back plate and spreaded over the plate using a Kim Wipe lint free tissue and then was rubbed in until completely dry using a new tissue to ensure there were no streaks. The plates were put in the plate rack in the fume hood to dry for at least half an hour, with the bind-silane faces towards each other to prevent bind-silane evaporating onto the outside face of the back plates which can cause problems when casting.

Before assembling the cast, a little dH₂O was squirted onto each bind-silane surface and wiped until completely dry and smear-free making sure there were no dust particles or streaks. This step removes excess bind-silane and the ethanol that was present in the bind-silane mixture. Reference fluoresce markers were applied, not too near to edges

but not so far into the gel that it will interfere with the spot pattern (see Fig. 3-3). Then the plates were assembled, making sure the bottom of the front and back plates were levelled and that the spacers had been well sealed. The cassettes were placed in the caster starting with a separator sheet and then a gel cassette; a separator was placed between each cassette. When assembled the plates in the gel caster should not be sealed too tightly as this affects the quality of the gel.

3.2.6.3.1.2 Gel Casting.

Large format (20 cm x 26 cm) 12.5% acrylamide gels were cast with, 41.7% (v/v) acrylamide stock solution (30% (w/v) 37.5:1 acrylamide: bis-acrylamide, N,N-methylene-bis-acrylamide from Sigma # D-89555), 25% (v/v) 4x resolving buffer, 1% (v/v) SDS 10% stock, 1% (v/v) of APS (Ammonium Pyrosulphate) 10% stock, 0.00138% (v/v) of TEMED (N,N,N',N'-tetramethylethylenediamine) 10% stock, 31.2% ddH₂O. Seventy five ml per gel plus extra 100 ml were used to fill caster spaces. The acrylamide, resolving buffer and water were filtered (Nalgene reusable bottle top filter holders catalogue # 320-2533, with 0.22 µm Millipore, Durapore membrane filter catalogue # GVWP04700) then degassed using desiccator and vacuum pump in a cold room for at least an hour. Afterward SDS, TEMED and APS were added in this order with a few seconds of gently stirring between each addition.

The gel filling channel at the back of the Dalt 6 gel caste was not used as manual pouring was quicker and prevented premature polymerization (<10s). The final level was ~1 cm from the top of the front plate. Each gel was overlaid immediately with 2 ml of 30% of isopropanol and the gels were left overnight to polymerise.

After overnight polymerization the gels were removed from the caster, rinsed thoroughly with water followed by distilled water. Gels were also checked for bubbles within the gel matrix. The tops of acceptable gels were rinsed with distilled water and

were racked up side down to prevent the top surface from drying out. Gels that were not used immediately were wrapped in Cling film with approximately 5 ml of storage solution (25% (v/v) 4x resolving gel buffer, 0.1% (v/v) SDS) and kept in fridge.

Separation in the second dimension is based on protein molecular mass. The proteins had previously been separated according to their pI during IEF, in an immobilised pH gradient set onto a polyacrylamide gel strip. After the focusing was completed the strips were equilibrated, which prepares the proteins for the second dimension separation, (See Section 3.2.6.2).

The equilibrated Immobiline pH gradient strips were removed from the equilibration tubes with clean forceps, rinsed briefly with electrophoresis SDS-running buffer and placed on top of a pre-poured 12.5% SDS-PAGE gel. Once the strip was put in the place making sure no bubbles were trapped, then it was sealed with 0.5% agrose on top for more details (See Section 3.2.6.3.2).

3.2.6.3.2 Running the Second Dimension Gel.

Isoelectric focusing (IEF) strips were rinsed briefly in electrophoresis SDS-running buffer (25 mM tris-base, 192 mM glycine; and 0.1% (w/v) SDS). The top of the gel and the top back plates were wetted with electrophoresis running buffer and the IEF strips placed on the top of the SDS-PAGE, with the plastic back towards the back plate and an anode towards the left hand side of the gel. The strip was slid down along the back plate using a 1 mm plastic spacer taking care not to disrupt the gel matrix.

The strip was pushed down until one end of the strip is in contact with the SDS gel and then worked into place until it was flush. Care was taken to ensure contact with the gel and that no bubbles were trapped between the gels. The strip was sealed by pipetting agrose sealing solution on top, 100% (v/v) of electrophoresis running buffer , 0.5%

(w/v) agarose NA (Normal melting agarose; Plus One Amersham), and 0.002% (v/v) bromophenol blue (BPB).

When all gels were sealed (~1 min) the lower chamber of Dalt 6 tank was filled with 1x SDS-running buffer to the appropriate level. Then the upper buffer chamber was pushed into place over the gels and filled with 2x SDS-running buffer. A funnel was used to add more 1x SDS-running buffer until the both chamber solutions were levelled. The circulating cooler was set at 21°C and started to run. Then the lid of Dalt 6 tank was placed on. There are two phases to run the electrophoresis, first slow entry phase where proteins are transferred from the strip to the gel; this was achieved using a power of 2.5 W per gel for 30 min. The second was the separating phase, and the power applied depends on the length of time the gel is run. A fast daytime run was done at 18 W per gel and took 3.5 and 4 hrs for a full set of six gels. An overnight run was done at 3 W per gel. Fast runs give better resolution and produce higher temperature. The running limits were set at maximum voltage 600 V and max current 400 mA, the cooling circulator to 21°C as mentioned above. The run was stopped when the bromophenol blue run off the bottom of the gels.

3.2.7 Gel Scanning.

When the second dimension run was finished, the gels and platen were inspected and if the surface of the plates were contaminated, they were washed using distilled water and dried with lint-free cloths. If the platen needed more thorough cleaning then 70% (v/v) ethanol followed by ddH₂O was used, if further cleaning was needed 10% hydrogen peroxide was used). The gels were then scanned while still between the two low fluorescence glass plates using the settings in Table 3-1, which are recommended by Amersham in the Ettan DiGE user manual. The Image Quant V 5.2 and Typhoon

Variable Mode 9400 were used for cropping the images and scanning the gels respectively.

The Typhoon 9400 scanner and Image Quant software scan three CyDye channels (wave lengths) on each gel (see Table 3-1). For each channel the photomultiplier detector (PMT) voltage was initially set at 550 V and prescans of the gel taken; the PMT voltage was manually adjusted until the spot with the maximum intensity was ~80,000 counts. The PMT voltage for this channel was then noted and used subsequently for the same channels on all gels. A final gel scan was then undertaken and the emission of the spot with the highest intensity usually rose to ~100,000 counts. This process was repeated for all channels. The output for each gel scan will be 4 gel images (see Fig. 3-3).

3.2.8 Sypro Orange Staining.

For spot picking and to detect total protein present on the preparative gel, the total protein stain (with 380 µg total protein loaded) Sypro Orange. was used. When 1st and 2nd dimension are finished as described in sections 3.2.6.2 and 3.2.6.3.2 respectively.

The gel was fixed in 7% (v/v) acetic acid, 10% (v/v) methanol for 1:30 hr, then washed briefly (~2 min) in 7% (v/v) acetic acid. The gel was stained with Sypro Orange, 1:10,000 in 7% acetic acid for ~1:30 hr. the gel then was washed briefly in 7% acetic acid and scanned using green laser Cy 3 (532 nm, 580 BP, excitation band-pass filter 30) see Table 3-1.

Table 3-1 The Appropriate Laser and Wavelength Settings for Each Dye Scan.

Typhoon 9400 imager was used for scanning 2-DE .

Fluorophore	Emission Filter(nm)	Laser and wavelength
Cy2	520 BP 40	Blue2 (488)
Cy3	580 BP 30	Green (532)
Cy5	670 BP 30	Red (633)
Sypro Ruby	610 BP 30	Blue1 (457)
Sypro Orange	580 BP 30	Green (532)

3.2.9 Spot Excision, Digestion, and Preparation for MS.

The Ettan Spot Handling Work Station 2.1 (Amersham Biosciences) was used to excise protein spots from 2D gels and digest the proteins using Trypsin (Procine sequencing Grade Modified Trypsin, Promega, Cat. # V3021) to cleave at the carboxylic acid group of lysine and arginine. The work station was also used to spot peptides and matrix (α -cyano-4-hydroxy-cinnamic acid, Amersham or Sigma-Aldrich) on the MALDI target grids. The protocol used in the workstation is as follows.

3.2.9.1 Spot Excision.

Spot excision was performed with a picking head of 1.4 mm diameter. The gel plug was removed using a 40 μ l aliquot and expelled from the picking head into a 96-well microplate using a 150 μ l aliquot of distilled water. Finally the excess water was removed from the microplate using 200 μ l aliquot.

3.2.9.2 Trypsin Digestion of Protein Samples.

The gel plug preparation was performed by washing twice with 100 μ l 50 mM ammonium bicarbonate in 50% (v/v) methanol, each time incubating at room temperature for 30 minutes before aspiration. The solution was then removed and the gel plug dehydrated by the addition of 100 μ l of 75% acetonitrile (ACN) for 10 minutes at room temperature. After aspiration, the gel plug was allowed to air-dry for 22 minutes.

The protein in the gel plugs was then digested by the addition of 10 μ l digester solution (10 μ g ml⁻¹ trypsin in 20 mM ammonium bicarbonate, NH₄HCO₃) and incubated at 37°C for 4 hours. After trypsin treatment the resulting peptides were extracted from the gel plugs by 60 μ l of peptide elution buffer (50% (v/v) acetonitrile (ACN) / 0.1% (v/v) TFA (trifluoroacetic acid) treatment for 20 minutes at room temperature. Aliquots of 80

μl were then removed from each sample well and dispensed into a clean second 96-well plate. The gel plug was then treated again with 40 μl aliquot of 50% (v/v) ACN/0.1 (v/v) TFA for another 20 minutes at room temperature and the aspirated samples pooled. After the processing of the final sample the second microplate was dried for 90 minutes to allow complete drying of the peptides. The dried peptide spots were resolubilized in 3 μl spotter solution (50% (v/v) ACN/0.5% (v/v) TFA). Of each tryptic digest, 0.3 μl was mixed with 0.3 μl matrix solution (α -cyano-4-hydroxy cinnamic acid (90% saturated in 50% (v/v) ACN, 0.5% (v/v) TFA)). The dissolved peptides were then spotted onto the target MALDI plate.

3.2.10 Mass Spectrometry.

3.2.10.1 MALDI-TOF.

The Voyager DE PRO MALDI-TOF from PerSeptive Biosciences (Voyager) was used to conduct matrix assisted laser desorption ionisation, time-of-flight mass-spectrometry (MALDI-TOF-MS). The Voyager consists of several main parts namely; the target, a laser, an accelerating source, a low mass gate, a guide wire, reflector, and multi-channel plate detector. Here, briefly are the function of each of these parts and the parameters that were used to operate them. The peptide and matrix were spotted on to target, which was then loaded into Voyager. The laser intensity was optimised to give the greatest signal-to-noise ratio and 200 shots per spectrum were acquired. During each shot that was fired at the spot to be analysed and after a short delay of 200 ns the desorbed ions were accelerated through two grids of 15,200 V (76%) and 20,000 V (100%).

These two grids create a non-linear field that ensures equal kinetic energy is given to every ion, no matter what its starting position in the field. The low mass gate is a deflector timed to deflect the smaller ions, below a mass of 750 Da, using an electric

field, thus only ions of 750 Da or more are allowed to travel along the flight tube. Along the centre of the flight tube there is a wire, set at 10 V (0.05%), so that it attracts the ions into the centre of the flight tube instead of travelling towards the side. The reflector or mirror is a set of grids and rings at a total voltage of 22,400 V (ratio 1.12 of 20,000 V) that reflects and focuses the ions back down the flight-tube, thus giving the ions longer flight and the system more resolution. Finally a multi-channel plate (MCP) detector senses voltage changes induced by individual ions. The relative mass of the ions is calculated from the time of flight and calibrated against three trypsin fragment peaks (842.5100 Da, 1045.5642 Da and 2211.104 Da. Masses between 800 and 3500 were recorded. Three spectra, each from a different place on the spot were accumulated to create the final spectrum. An automatic acquisition was attempted using a spiral search, rejecting any spectra with a signal to noise ratio of less than 10. Acquisition was absorbed for any spots yielding 5 consecutive rejected spectra.

3.3 Analyses of Gel Images.

3.3.1 Preparation of Gel Imaging.

To perform analytical scan, a 100 μm pixel size was selected for quantitative scans. When all the gels were scanned each gel image was cropped in Image Quant (V 5.2). Landmarks' were used to cut gels to a similar size and any blank area at the top or bottom of the gel were cropped. Gels that were used for protein spot picking the reference markers were included in the cropped image. The cropped images were saved onto a CD for analysis by DeCyder software.

3.3.2 Spot Detection, Spot Matching and Generation of a Spot Map Using the Decyder V 5.01 DIA Module.

After image cropping, gel pair images were analyzed by the DeCyder V 5.01 Differential In-gel Analysis (DIA) Module. This module automatically identifies spots,

performs background subtractions, generates estimates of spot intensity (protein abundance), and allows manual editing of the processed data. The main output from this module is a 'Spot Map', a template containing information on the relative position of each spot that can be used to identify matching spots on all gel image pairs; this then allows between-gel spot matching.

A typical screen output from the DIA module is shown in Fig. A 3-3 (appendix). The screen is divided into four quadrants; the upper left shows the gel pair images and the upper right presents basic information on the number of spots matched between the two images, estimates of their abundance, *etc.* For the example shown, 2143 spots were matched between the two images. The DIA module calculates the Log_{10} Volume Ratio, which is the log of a standardized abundance ratio (secondary/primary image); values of +0.301 represent a doubling and -0.301 a halving of spot intensity. A graphical representation is also provided in the upper right quadrant showing spots with significantly different (2 standard deviations) intensities; blue representing an increase and red a decrease in the secondary image compared with the primary image. For the example shown in Fig. A 3-3 (appendix), ~76% of spots are unchanged, whilst 11% show a decrease (red) and ~13% an increase in the secondary image. Another feature of the DIA module is manual editing of the processed data. If spot boundaries differ between the two images, or if spots appear in only one image (a possible artifact), the software alerts the user thereby allowing manual corrections to be applied.

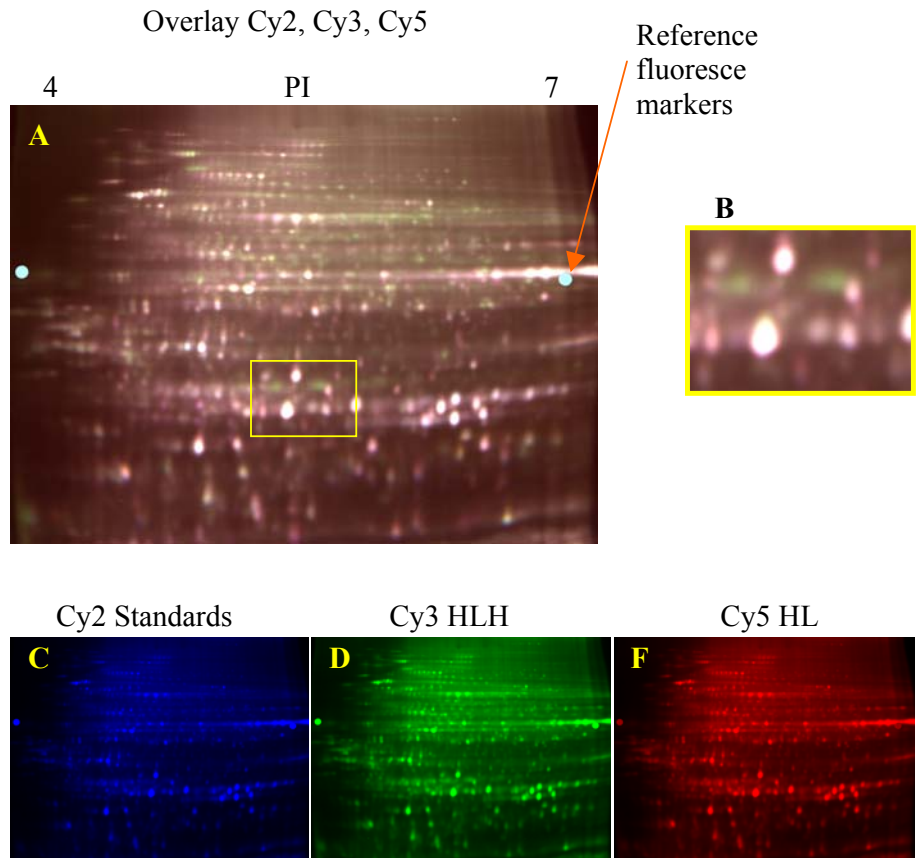


Fig. 3-3 Images from a 2-D analysis showing two different samples plus the pooled Sample Image.

Equal amounts (50 μ g) of salt up shock D (HLH300-1.96, salt up-shock, HL Cells shifted from BGM50-1.96 to BGM300-1.96, Cy3), salt down shock F (HL50-1.96, cells shifted from BGM300-1.96 to BGM50-1.96, Cy5), and Pool of 12 samples labeled with Cy2 C. Panel A shows the merged image for three Cy images. B, magnification of selected spot area; note the three different types of spot (green, red and white).

Samples were harvested at mid-log phase of growth (6 days) from three different salt stressed cells (H300-1.96, HL50-1.96, HLH-1.96, and used for protein analysis (see section 2.2.1, 2.2.2, and 3.2.4 for details).

3.3.3 Between-Gel Spot Matching, Determination of Protein Abundance, and Statistical Analysis Using the DeCyder V5.01 BVA Module.

The Spot Map output from the DIA module was then used to spot match across all gels using the Batch Processor Module. Gel images from all gels were cropped using Image Quant V 5.2 software, and then processed by the Batch Processor, and the output fed to the Biological Variation Analysis (BVA) module. It is an automated process and does not introduce any further processing and analyzing to the spot map data. All of the gel images in the experiment to be matched were loaded into the processor and the number of spots detected entered. The processor then links each Cy3 and Cy5 spot on a gel to the corresponding Cy2 spot on the same gel. The output file is in *xml* format ready for use in the BVA module.

The BVA module performs spot matching between gels and allows quantitative comparison of protein expression across multiple gels. The software processes the gel image pairs (Cy3 and Cy5), and one gel image is assigned a Master Gel Image status, and all other CyDye images are then matched to the Master image; in this way common protein spots are identified across all gels. The raw output from the BVA Module consists of four panels Fig A 3-4 (appendix), and data can be viewed in one of four tabular forms; the Spot Map Table (SP), the Match Table (MT), the Protein Table (PT), and the Appearance Table (AT).

The spot Match Table was used to set up spot matching for matching and statistical analysis. then consulted to identify protein spots that were not found on all gels. Each of these inconsistencies were examined by consulting Image View. In practice, many of these spots arise from particles of dust in the gels.

Spot Map Table Fig A 3-4 (appendix) was used to set up spot matching for matching and statistical analysis. The table lists all data related to the spot maps in the experiment

imported from DIA Fig A 3-4 (Appendix), including which group each gel belongs to, the number of spots detected on the gel and the number of spots matched to the master gel. The Match Table Fig A 3-5 (Appendix) was used for the processes associated with inter gel matching. To aid the matching algorithm, a few spots were matched manually, a process called land-marking, and the automated matching algorithm were carried out which matched all spots maps in the workspace. The Protein Table Fig A 3-6 (Appendix) demonstrates and processes data associated with the protein identified across the gels. Every row of the table corresponds to one protein spot that may be present in several Spot Maps. The Graph View at the top right shows the average ratio trend of the volume of this spot in the 6 gel sets in salt shock cells experiment. The Appearance Table (see Fig A 3-7 Appendix) was used to show data associated with a single selected spot across gels.

3.3.4 BVA Protein Table.

From the experiment set of 6 gels (18 images), the DeCyder module BVA (Biological Variance Analysis) generates a Protein Table that reports a number of important parameters. These include a unique spot identity number, or Master Number, confirmation that the protein appears on all images (19, the 18 sample gel images plus the Prep-Gel, an indication of statistical confidence that abundance changes are consistent (T-test and ANOVA), and confirmation that the protein spot has been selected or not for sequencing Fig A 3-6 (Appendix). From the Protein Table proteins that showed a high ANOVA probability of differential abundance were selected ('Picked') for further analysis. The DeCyder BVA module also provides the facility to view any of the sample images, or any of the individual protein spots on the gels. Fig A 3-6 (Appendix) shows two images of protein 917 on two gels where the abundance of this protein changes. The BVA module also provides a pseudo 3-D image of protein

abundance, as well as a graph from the ANOVA analysis showing how the abundance of this protein varies across the 12 samples Fig A 3-6 (Appendix).

The Prep-gel was then loaded into the Amersham Robot Spot Handling Workstation 2.1 'Picker', and from the Spot Pick List in the Protein Table, the corresponding proteins were excised from the Prep-Gel and placed into 96-well plates. The co-ordinates of each protein are determined from the positioning of the reference spot markers. When all selected protein spots had been excised, 10 µl of a Trypsin digestion medium was added to digest the protein; incubation was carried out for 4 hours at 37 °C. After completion, the samples were air dried at ambient conditions. The mass of extracted peptides were carried out by MALDI-TOF (The Voyager DePro from Perseptive Biosciences (Voyager)). The resulting peptide fingerprint was searched against the NCBI database restricted to plants using program MASCOT (Modular Approach to Software Construction Operation and Test) software version 2.1 (<http://www.matrixscience.com>). Proteins that were not unambiguously identified by MALDI TOF were subjected to *de novo* protein sequencing methods using an electrospray ionization tandem mass spectrometer (ESI-MS/MS System; Applied Biosystems/MDS Sciex, API QSTAR® Pulsar and running MASCOT V 2.1).

From the pH range 6-11 Immobililine gels, 38 spots were selected for sequencing. Of these, the identity of only 17 were established with any degree of certainty Table A 3-2 (Appendix) From the pH range 4-7 Immobililine gels, 48 spots were selected for sequencing.

3.3.5 Results.

The DeCyder version 5.01 software threshold detection limit was set to identify approximately 2,500 protein spots on the 2D-gels. Further quantitative analysis revealed the abundance of 86 proteins that differed significantly between the salt treatments ($p <$

0.05). Of these 86 proteins, 45 were found to be up-regulated in high salt Table A 3-2 (Appendix), and 9 were down-regulated Table A 3-3 (Appendix). The remaining 32 spots showed consistent salt-induced changes but were unrelated to NaCl concentration Table A 3-4 (appendix). Twelve were found to be down regulated where cells were shifted from 300 to 50 mM NaCl, and further down regulated when shifted back from 50 to 300 mM NaCl. Twenty proteins showed the opposite response; they were up regulated when shifted from 300 to 50 mM NaCl, and further up regulated when shifted back to 300 mM.

3.3.6 Spot Picking, MS and Protein Identification.

The use of minimal labeling procedure creates two populations (labeled and non labeled) for each protein in a lysate. For every protein spot on 2-DE gel, the labeled species will be slightly shifted from the unlabeled due to the single dye molecule that was added. This phenomenon is more marked for smaller than larger molecular weight proteins. When protein was picked using the centre of the spot detected from the CyDye flour fluorescent image (*i.e.* labeled protein), this may not correspond to the area of highest protein concentration. To solve this problem the total protein was visualized by post-staining using Sypro Orange dye and the position of spots for picking based on this new image.

This will maximize the amount of protein available for MS. However it means that another matching analysis is needed between the master gel and the preparative gel. The preparative gel contains large amount of protein (380 µg in total) representing all the samples in the study. The gel was used to pick spots for MS analysis. All spots present on the preparative gel were detected using the DIA module, then was loaded into the BVA module and the 'proteins of interest' ($P < 0.05$) from the CyDye labeled master gel matched to the preparative gel. Eighty six protein spots were matched to the preparative

gel. Of these 86 proteins, 45 were found to be up-regulated in high salt (H) Table A 3-2 (Appendix), 9 were down regulated Table A 3-3 (Appendix). The remaining 32 spots showed consistent salt induced changes not related to salt shock treatments Table A 3-4 (Appendix).

Spots of interest were picked from preparative gels using the Amersham Ettan Spot Handling WorkStation 2.1. Protein spots were digested using trypsin, mixed with α -cyano-4-hydroxy cinnamic acid (α CHCA) matrix and plated onto MALDI targets. All spots were analyzed by MALDI-TOF and some spots which not identified by MALDI were then analyzed by MS/MS.

The MS spectra were searched using the MASCOT search engine. All MALDI and MS/MS (Application Program Interface, API Q star) identified proteins with MOWSE (molecular weight search) score >40 ($P<0.05$) were significant hits.

In salt shock experiment protein identification were gained from 86 spots using MS or MS/MS. Many of these spots contained mixtures of proteins. Therefore, the actual number of proteins species identified from 86 was 133. Often several isoforms of the same protein were detected on the same gel. The expression of the modulated proteins was up-regulated, down-regulated or modulated. Modulated means that the protein was identified as both up and down regulated and its expression in high salt cells is not clear cut. Of the 86 identified proteins, 9 were down regulated, 45 were up regulated and 32 were modulated due to salt down shock or up shock treatment. Figure A 3-1(Appendix) shows a MASCOT search result for protein spot ID 566 against the NCBI (National Center for Biotechnology Information) *Arabidopsis thaliana* database. The protein was identified as 2-oxoglutarate dehydrogenase E2 subunit and was up regulated in high salt treatments. The protein has significant MALDI score of 106 and $P<0.05$.

Many of the spots identified using tandem MS turned out to be a mixture of proteins. Figure A 3-2 (Appendix) is the MASCOT result page of a MS/MS search. Ten proteins were identified from this one spot (spot ID 897) on the high salt gel. The mitochondrial F1 ATP synthase beta subunit has the highest score (445) therefore it is likely that this protein is contributing to the abundance change seen between the different salt shock treatments, mixed spots may potentially cause problems in determining which proteins are up or down regulated in abundance in different salt shock cell treatment, as it is not always possible to determine which protein or proteins in the mixed spot are responsible for the change in abundance. There some ways to get around this problem including identification of all the proteins present in the mixed spots followed by fractionation of the sample or fractionation of the gel (*e.g.* using narrow pH ranges) to allow for increased spot resolution. This will allow for accurate quantitation of individual protein spots. However this technique is not very practical and as yet, no one has attempted this approach. The problem of mixed spots has not received much attention in the literature. The output of the protein profiling according to the protein abundance was classified to three main categories, these are Up-regulated, Down-regulated, Modulated proteins.

3.3.7 Salt Stress Up-Regulated Proteins.

For clarity, the peptides in Table A 3-2 (Appendix) has been sorted into six functional groups; these are Transport, Signalling, Metabolism, Stress-Related, Senescence/Autophagy, and DNA/RNA binding proteins. Proteins that have not been unambiguously identified (MASCOT Score <40) are listed at the end of Table A 3-2 (Appendix).

Table A 3-2 (Appendix) presents a description of the 45 proteins that show elevated abundance in high salt. Each of these proteins was analyzed by MALDI-TOF mass spectrometry using the MASCOT (version 2.1) software for 17 of the 45 peptides, with

MALDI MASCOT score values ranging from 40 to 645. Of the remaining 28 unidentified peptides, *de novo* protein sequencing was undertaken on 12 proteins using a Q Star tandem mass spectrometer and MASCOT (version 2.1) software. The criteria for selecting these 12 proteins for identification was based on their fold change in abundance and the ANOVA statistical probability (p-value) that these observed changes were not random events. Ideally, all of these proteins should have been sequenced, but this was cost-prohibitive.

Compared with the levels at 50 mM NaCl high salt induced an increase of just a few percent (*e. g.* spot ID 1715 and 330) to nearly a 4-fold change (*e. g.* spot ID 586 and 731); it is emphasized, however, that in all cases, these changes were consistent across four completely independent replicates.

3.3.8 Salt Stress Down-Regulated Proteins.

Table A 3-3 (Appendix) presents a description of the 9 proteins that showed lower abundance in high salt. Each of these proteins was analyzed by MALDI-TOF mass spectrometry using the MASCOT (version 2.1) software for 4 of the 9 peptides, with MALDI MASCOT score values were 80,74, 67 and 60. The remaining 5 unidentified peptides, *de novo* protein sequencing was undertaken on them using a Q Star tandem mass spectrometer and MASCOT (version 2.1) software. Of the 5 protein spot, 18 proteins were identified from these mixed spot (see Section 3.3.6). Criteria for selecting these 5 proteins for identification was based on their fold change in abundance and the ANOVA statistical probability (p-value) that these observed changes were not random events.

3.3.9 Salt Stress Modulated Proteins (up and down-regulated).

Table A 3-4 (appendix) presents a description of the 32 proteins that showed either an increase or decrease in abundance when exposed to a salt shock, regardless of whether it

was an up or down shock. Each of these proteins was analyzed by MALDI-TOF mass spectrometry using the MASCOT (version 2.1) software. Nine of the 32 peptides were unambiguously identified from MALDI-TOF analysis and the remaining 23 unidentified peptides, were subjected to *de novo* protein sequencing using a Q Star tandem mass spectrometer and MASCOT (version 2.1) software (for more details see Table A 3-4, Appendix).

3.4 Discussion.

The aim of the work reported in this chapter was to identify proteins in *Arabidopsis* cells that may be involved in salt tolerance. To achieve this an *Arabidopsis* HHS (Habituated to High Salt) culture grows in 300 mM NaCl was used. Comparison of proteomic profiles were not feasible with WT cells lines because cell cultures were very different, even in absence of NaCl stress. Consequently, it is difficult to identify proteins involved in salt stress against a background of many changes. Moreover, an Affymatrix 8000 gene microarray experiment by our group showed over 800 changes in transcript occurred when WT (0 mM NaCl) cells were compared with HHS (300 mM NaCl). The ultimate goal was to identify protein spots in the 2-D gels that change in abundance in a way that correlates with salt stress. Therefore, proteins were extracted from salt up and salt down shocked *Arabidopsis* HHS cells in their mid-log phase of growth (6 days), and were subsequently analyzed using 2D DiGE. Several hundred spots were identified whose volume (abundance) changed significantly ($P < 0.05$) and reproducibly in the salt stressed cells. Of these spots, 86 were selected on statistical criteria for protein sequencing by MS.

These sequenced proteins fell into three categories as follows: (1) forty-five were found to be up-regulated in high salt: (2) nine were down-regulated in high salt: and (3) thirty two showed consistent salt-induced changes on salt shock, but it was immaterial whether it was a salt up or down shock. Twelve of the later were found to be down regulated 6 days after transfer from 300 to 50 mM NaCl, and further down regulated six days after transfer back to 300 mM. Twenty proteins showed the opposite response; these were up regulated six days after transfer from 300 to 50 mM NaCl, and further up regulated six days after transfer back to 300 mM NaCl. These proteins probably

represent general stress responses that arise when ever the cells are stressed and not related to salt stress *per se*.

3.4.1 Up-Regulated Proteins.

The forty-five up-regulated proteins Table A 3-2 (Appendix) can be broadly classed according to their function. These classes were Transport (5 proteins), Signalling (6 proteins), Stress-related (1 protein), DNA/RNA binding (4 proteins), Metabolism (10 proteins). The identify of the remaining proteins were ambiguous with MALDI/Q star MASCOT scores of <40; further work will be required to determine the function of these proteins.

3.4.1.1 Transport proteins.

Of particular interest in this group of up-regulated proteins are the two voltage-dependent anion-selective channels. Although these two proteins were identified at two different locations on the gel (Spot ID 917 and 979), *de-novo* protein sequencing by the Q-star MS identified the protein product arose from the same gene (At5g15090). According to the entries on the TAIR database, this gene encodes a 29.2 KDa mitochondrial membrane anion channel that is involved in oxidative stress (Sweetlove *et al.*, 2002). It is unclear what this anion channel conducts, or why it responds to NaCl stress. One possibility is that it conducts Cl⁻ across the mitochondrial membrane, but it is unlikely that Cl⁻ influx into the mitochondria will be a useful strategy in salt tolerant plant cells. Another possibility is that under stress conditions, mitochondrial activity is impaired by salt-induced inhibition of an essential anion transport process. Thus, to alleviate the stress, the abundance of the inhibited anion channel is increased.

It is well established that the steady state mitochondrial inner membrane potential for driving ATP biosynthesis ($\Delta\psi$) is regulated at around -200 mV and controlled by cation influx and anion efflux transporters. It is conceivable that in HHS cells, respiration rate

increases dramatically and $\Delta\psi$ increases to high levels (> -200 mV), and to dissipate this high potential, the density of these anion transporters increase. Another possibility is that these transporters are involved in ion homeostasis in the mitochondria, not associated with the bioenergetics of respiration. These channels could, therefore, be involved in Cl^- efflux from the mitochondria into cytoplasm.

The appearance of two separate spots on the gel encoded by the gene At5g15090 suggests the proteins were modified in some way. It is conceivable that one of the products has a different phosphorylation pattern, or some other post-translational modification. Alternatively, it is possible that the two proteins are splice variants. Further work will be required to resolve this.

Another up-regulated protein of interest was spot ID 940 (Table A 3-2, Appendix). The TAIR database reports the gene (At5g67500) encodes a 29.6 KDa mitochondrion membrane porin (Heazlewood *et al.*, 2004). Porins are membrane proteins that act as a pore through which solute can diffuse. Unlike other membrane transport proteins, porins are large enough to allow passive diffusion (*i.e.* they act as channels which are specific to different types of solute). They are prevalent in the outer membrane of the mitochondria and gram-negative bacteria. Porins typically control the diffusion of small metabolites like sugars, ions, and amino acids. The term ‘nucleoporin’ refers to porins facilitating transport through nuclear pores in the nuclear envelope. The outer bacterial membrane protein F (OmpF) porin functions to regulate osmotic potential between the cell and its surroundings. Many factors affect OmpF porin regulation, however, two of the better known are the inner membrane osmosensor, EnvZ and OmpR. In the experiments described here, however, no osmotic stress was imposed by the salt treatments.

A protein identified as PEX14 was up-regulated in high salt stressed cells (spot ID 528, Table A 3-2, Appendix). According to the entries in the TAIR database, the gene At5g62810 encodes a 55.6 KDa protein located in the cytosol and peroxisome that is involved in the peroxin-peroxisomal protein import machinery. This complex constitutes a major peroxisome protein import pathway and is found in all tissues in Arabidopsis, there are some other PEXs that produce severe phenotype change like pex5-knockdown (pex5i) and pex7-knockdown (pex7i). Pex5i and pex7i knockdown lines show reduced levels of germination unless grown on sucrose, implicating a dysfunction in fatty acids mobilization. In addition, mature pex5i knockdown lines appear to have accelerated levels of photorespiration as their growth in normal air (but not CO₂-enriched air) is impaired when compared with WT lines (Nito *et al.*, 2002; Hayashi and Nishimura, 2006; Nito *et al.*, 2007). An up-regulation of pex14 might suppress photorespiration thereby providing more carbon for cell growth.

The question arises why is PEX14 protein up-regulated in the salt-stressed HHS cells? Peroxisomes have three major functions in plants. They are involved in the mobilization of lipid reserves by β -oxidation during germination. They also play a central role in the conversion of glycolate to glycine during photorespiration. Finally, peroxisomes are the site of many de-toxifying oxidation reactions in plants; for example alcohol is reported to be metabolized in the peroxisomes. The resolution of this question will require further investigation.

3.4.1.2 Signalling Proteins.

There were 6 up-regulated proteins that were assigned to the signalling class. Two of these were identified as arising from the same gene (At1g 56340 spot ID 740 and 741). Both of them had high scores (398 MALDI MOWSE score and 371 Q-star MOWSE score for spots 740 and 741 respectively). According to the TAIR database, this gene

encodes a 48.5 KDa mitochondrial membrane protein that is involved in responses to oxidative stress (Heazlewood *et al.*, 2004). The At1g 56340 gene encodes Calreticulin (CRT 1) protein; calreticulin 1 is a high-capacity calcium-binding protein which is present in most tissues and located at the periphery of the endoplasmic (ER) and sarcoplasmic reticulum (SR) membranes. It probably plays a role in the storage of calcium in the lumen of the ER and SR. Calreticulin is a protein of about 400 amino acid residues consisting of three domains, 180 amino acid residue (N-domain): the central domain of ~70 residues (p-domains); that binds calcium with a low-capacity, but a high-affinity: the C-terminal domain which is rich in acidic residues and lysine and binds calcium with a high-capacity but a low-affinity.

Another up-regulated protein is encoded by a 25.3 KDa SNF7 family protein (At2g 06530). This family consists of a group of SNF-7 homologues involved in protein sorting and transport from the endosome to the vacuole/lysosome in eukaryotic cells.

3.4.1.3 Stress Proteins.

One major stress protein (At1g 02920) was up-regulated in high salt with a MASCOT identity score of 107 from MALDI-MS; spot ID 1028. According to the entries on the TAIR database, this gene encodes a 23.6 KDa cytoplasmic Glutathione S-transferase protein belonging to the phi class of GSTs. It has been reported to be involved in toxin catabolism (Wagner *et al.*, 2002), but it is unclear why its abundance increases in response to salt stress.

3.4.1.4 Senescence/Autophagy Proteins.

The product of gene At4g11320 was up-regulated in high salt (MASCOT identity score from Q-star of 486, spot ID number 590). According to the entries on the TAIR database this gene encodes a 40.7 KDa endomembrane protein. The main components of the endomembrane system are endoplasmic reticulum, Golgi bodies, vesicles, cell

membrane and nuclear envelope. Members of the endomembrane system pass materials through the system and then to vesicles (vesicle trafficking). It is involved in the hydrolysis of cysteine linkages in oligopeptides or polypeptides (Tournaire *et al.*, 1996).

3.4.2 Down-Regulated Proteins.

3.4.2.1 *GST proteins (stress proteins).*

Surprisingly the same gene product (At1g02920), which was up-regulated (Spot ID 1028; Table A 3-2 (appendix), was down-regulated (spot ID 1918; Table A 3-3 (appendix) for more details see Section 3.4.1.3. Also spot ID 1945 according to the entries on the TAIR database is a 23.4 KDa cytoplasmic Glutathione S- transferase protein belonging to the phi class of GST. It is involved in toxin catabolism (Frova, 2003). Glutathione transferases (GSTs) are ubiquitous, multifunctional proteins that constitute a large gene family. In some plant species this gene family is comprised of 25–60 members, which can be grouped into six classes on the basis of sequence identity, gene organization, and active site residues in the protein. The Phi and Tau classes are the most represented and are plant specific, while Zeta and Theta GSTs are found also in animals. Despite pronounced sequence and functional diversification, GSTs have maintained a highly conserved three-dimensional structure through evolution. Most GSTs are cytosolic and active as dimers, performing diverse catalytic as well as non-catalytic roles in detoxification of xenobiotics, prevention of oxidative damage, and endogenous metabolism.

3.4.2.2 *Ambiguous Ferritin proteins.*

Two different spot ID (1939 and 1972; MASCOT score 74 and 67 respectively) were reported to encode Ferritin proteins. These proteins are encoded by genes At3g56090 and At5g01600; they are 28.8 and 28.2 KDa proteins respectively and located in chloroplast. They are involved in binding up to 4500 iron atoms, and are expressed in

the leaf, flower and root, but not in the seed (Harrison and Arosio, 1996; Petit *et al.*, 2001).

3.4.3 Modulated (Down & up-regulated) proteins.

3.4.3.1 Transport proteins.

An interesting vacuolar H⁺-ATPase subunit B protein had come up in spot ID 807 (gene At1g76030). According to the entries on the TAIR database, this gene encodes a 54.1 KDa located in cytoplasm, hydrogen-transporting two-sector ATPase complex and involved in ATP biosynthesis, energy coupled proton transport, hydrogen transport and glucose mediated signalling (Cho *et al.*, 2006).

Also a porin family protein (spot ID 1519, gene At3g20000) was identified. According to entries in the TAIR database, this gene encodes a 34.3 KDa protein located in the mitochondrial inner and outer membranes and involved in protein targeting to mitochondrion (Lister *et al.*, 2004).

3.4.3.2 Stress proteins.

Three interesting proteins encoded Heat Shock Protein were identified from the same spot ID (567). The genes were At4g37910, At5g09590 and At1g80030. According to entries in the TAIR database, these genes encode a 73.1, 72.99 and 53.8 KDa protein respectively. They are located in mitochondrial and thylakoid membrane and involved in response to heat stress and virus infection (Sung *et al.*, 2001).

A SHEPHERD (At4g24190) protein was also identified (spot ID 193). According to entries in the TAIR database, this gene encodes a 94.2 KDa protein, located in the endoplasmic reticulum and mitochondrion, and is involved in response to cold, protein folding and secretion, and regulation of meristem development (Klein *et al.*, 2006).

One way to take this work forward would be to use a genetic approach. There are now several collections available of Arabidopsis knockout lines where individual genes have

been deleted. It would be interesting to procure knockout lines for carrying deletions in some of the genes identified from proteomics studies in this chapter and to assess their phenotypes. Also, transgenic lines could be made where some of the sequences identified are over expressed in a wild type background. Together these approaches should help to assess the function of some of these sequences.

Chapter 4: Comparison of Salt Tolerant and Salt Sensitive Barley Lines.

4.1 Introduction.

Barley (*Hordeum vulgare* L.) is a small grain cereal belonging to the Poaceae family (alternative name, Gramineae) and to the Triticeae (alt. Hordeae) tribe. Barley has many different varieties. The most common is *Hordeum vulgare*, which is a six-rowed type of barley that has a spike notched on opposite sides with three spikelets on each notch. At each notch there is a flower or floret that later develops into a kernel. *Hordeum distichum* is a two-rowed type of barley that has central florets producing kernels and it has lateral florets that are sterile. Lastly there is *Hordeum irregulare* which has fertile central florets and different arrangements of sterile and fertile lateral florets. This is the least cultivated species of the three main forms (Berrie, 1977). Barley is a major world crop and is the most important field crop after rice, wheat and maize (Bengtsson, 1992). Barley is an annual grass that has two growing seasons, winter and spring. It does best in the spring in a temperate zone with a 90 day growing season, it can also be found growing in sub-arctic regions, like in Alaska or in Norway, with very short growing seasons (Berrie, 1977). Barley is grown and cultivated widely and extensively in Mediterranean areas, Europe, Ethiopia, Russia, China, India and North America (Harlan, 1995). In Great Britain, barley has been cultivated on a large area of land for considerable period of time and along with wheat still represents one of the major crops. It has been claimed that barley originated from wild barley (*Hordeum spontaneum* C. Koch), that has its centre of origin in the Fertile Crescent of the middle East (Zohary, 1969), with scattered stands over a much wider area from west of Tunisia to east of Afghanistan (Clarke, 1967; Harlan and Zohary, 1966). Barley is known to be one of the

most salt-tolerant crops and can grow in soils with elevated salt contents (Maas and Hoffman, 1977; Shannon, 1984; Gorham, 1992b), there is a high level of variability in tolerance among cultivars (Ayers, 1953; Donovan and Day, 1969; Schaller *et al.*, 1981; Srivastava and Jana, 1984). *H. vulgare* is recognized as being more salt-tolerant than wheat (Bole and Wells, 1979; Heakal *et al.*, 1981; Rawson *et al.*, 1988; Richard *et al.*, 1987). However, the search for reliable salt-tolerant germplasm requires not only quick and accurate methods of screening (Shannon, 1984), but also a correct evaluation of its salt-tolerance.

4.1.1 The Barley Genotype Lines Used in This Study.

Two different genotypes of Barley (*Hordeum vulgare* L.) were used in this study (Zhou 1 and Zhou 85). These were donated by Pro. Guoping Zhang, Agronomy Department, Huajia Chi Campus, Zhejiang University, Hangzhou 310029, China. These lines were identified from a salt-tolerance screen of over 100 varieties that are commercially grown in China and out of these, 16 barley genotypes with different salt tolerance was investigated by Huang and co-workers (Huang *et al.*, 2006). These two genotypes were used to investigate the effect of salt stress on photosynthesis, growth, and ion content (see Fig. 4.1). Hydroponic experiments were carried out to assess how the tolerant (Zhou 1) and salt-sensitive (Zhou 85) lines respond to salt treatments (0, 50, 100, 150 and 200 mM NaCl). When seedlings reached 19 days post germination they were stressed with salt. Seven days (26 days old) after the application of salt, photosynthesis rates were measured in fully expanded fourth leaves using Infra Red Gas Analyzers (IRGAs) see section 4.2.4.1 and basic growth parameters were assessed. At this time, estimates were also made of the water status of the shoot using the pressure chamber method (P.M.S. Instruments, Corvallis, Oregon, USA; (Pardossi *et al.*, 1991), and relative water content. At harvest, various measurements were also made on grain yield.

4.2 Materials and Methods.

4.2.1 Plant Material.

Two hundred Seeds of each barley line were germinated for 6 days in the dark on moist filter paper. One hundred and twenty seedlings were selected for uniformity and then transplanted into aerated hydroponic culture ($\frac{1}{4}$ Hoagland solutions; see Appendix Table A 4-1). The solution pH was adjusted to 5.8 with KOH or HCl and was renewed weekly until the seedling reached the 4th leaf stage, and then replaced every three days. Plants were grown in 2 liter capacity ceramic pots filled with 1.8 liter of $\frac{1}{4}$ strength Hoagland solutions. The medium was aerated (~ 100 ml/min) through small plastic tubes submerged in each pot that connected to an air pump. The plants were grown in controlled environment growth chambers with 14 hr light and 10 hr dark period, with light intensity of $\sim 180 \mu\text{mol m}^{-2} \text{s}^{-1}$ at the bench surface, and 22/18 °C day/night temperature. The relative humidity was held between 60 - 70%. Twenty-six days post germination photosynthesis rates were measured by collecting CO₂ response curves and light response curves (see sections 4.2.4.1.1 and 4.2.4.1.2). On day 37 when floral spike emergence completed, shoot water potential (ψ_{HO_2}) was determined with a pressure chamber (P.M.S. Instruments, Corvallis, Oregon, USA) on the fourth leaf. Roots were briefly washed three times in ice cold 10 mM MgCl₂, and then shoot and root were separated and basic growth parameters were measured. These included shoot and root length, and shoot and root fresh and dry weights (± 0.1 mg). In addition, the ion content of samples was measured by Inductively Coupled Plasma Optical Emission Spectroscopy (ICP-OES) using an Optima 4300 DV (Perkin Elmer Instruments, Beaconsfield, Bucks, UK) see Section 4.2.3.

4.2.2 Experimental Design.

The experiment was laid out as a factorial completely randomized design with four replications, 5 Salt treatments and 2 barley genotypes. Pots were re-randomized weekly to ensure even growth.

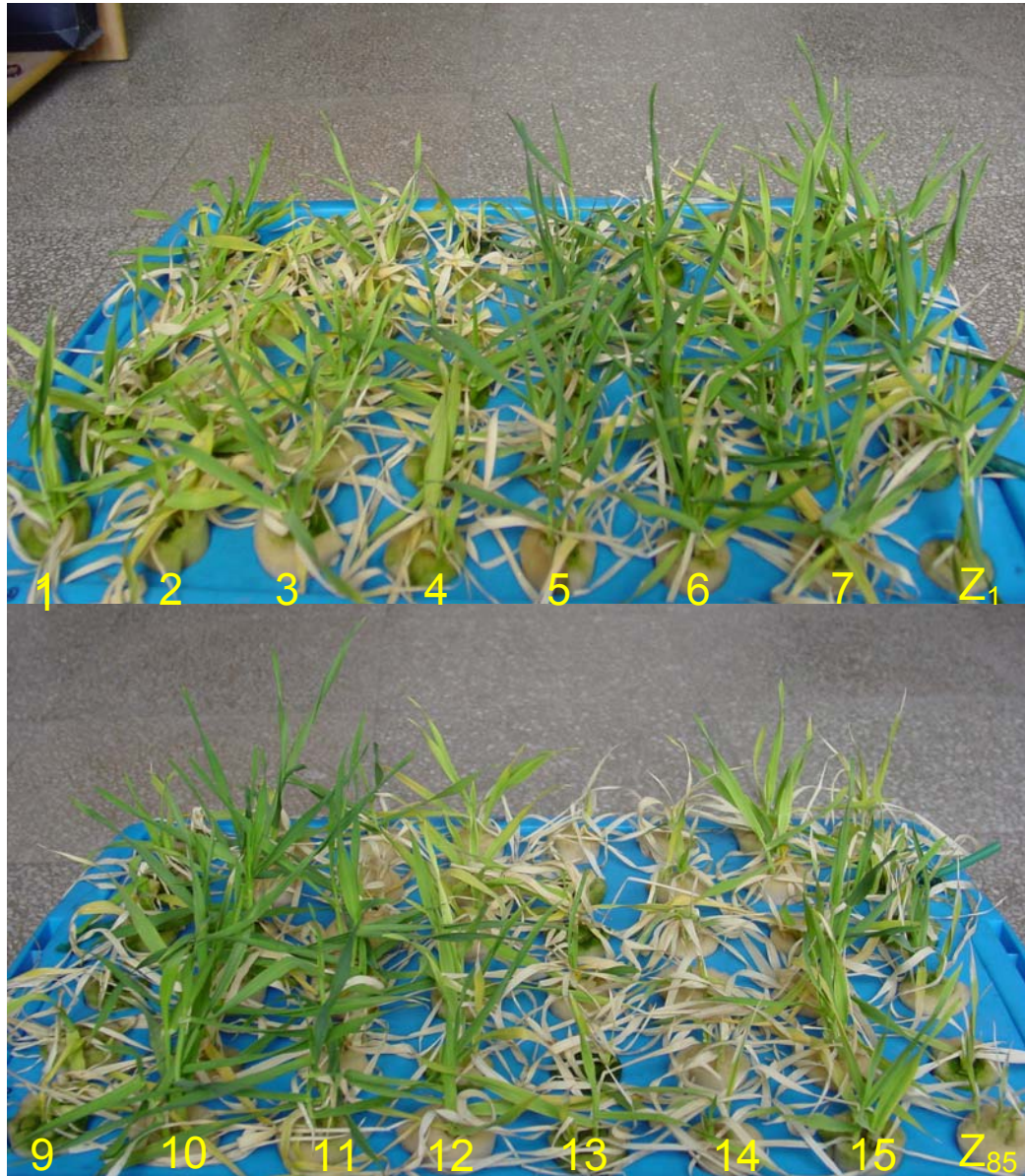


Fig. 4-1 The Effect of Salinity on the Growth of Sixteen Commercial Barley Lines.

The effect of NaCl on the growth of sixteen Chinese barley lines. Plants were germinated in Hoagland's solution and after 6 days transferred to hydroponics ($\frac{1}{4}$ Hoagland's) containing 0 mM or 300 mM NaCl. By day 18 no significant difference was found between the growths of any of the lines at 0 mM NaCl (data not presented), but between genotype differences were apparent when plants were grown in 300 mM NaCl (photograph courtesy of Pro. G. Zhang). Line Zhou 1 (top panel, far right, Z 1, 8) was selected as a salt tolerant line and Zhou 85 (lower panel, far right, Z 85, 16) was selected as a salt-sensitive line (Huang *et al.*, 2006).

4.2.3 Preparation Barley Material for ICP-OES Analysis.

Barley shoot and root were dried in the oven for 7 days at 75°C and ground to a fine powder in liquid nitrogen using a pestle and mortar. The powder was transferred to a pre-weighed 15ml sterile falcon tube, and then reweighed and the dry weight of the samples calculated. Five ml of 10% (v/v) analytical reagent grade nitric acid was added to each tube and left to digest for 7 days on a shaking incubator. Ion content (Na, Fe, K, S, P, B, Mn, Mg and Ca) was measured using Perkin Elmer Inductively Coupled Plasma-Optical Emission Spectrometer (ICP-OES) model optima 4300 DV (Perkin Elmer, Warrington, UK) see Chapter 2 Section 2.2.3.

4.2.4 Photosynthesis.

Photosynthesis and transpiration are two basic processes underpinning crop productivity. Accurate estimations of photosynthesis rate and water consumption is important not only in directing irrigation and improving water use efficiency of field crops, but also in studying the interactions between plants and the atmosphere. Photosynthesis has been intensively studied over the past few decades at all levels, from the chloroplast to the canopy level. Salt tolerance in many plant species is reported to be associated with the ability to exclude Na^+ so that high Na^+ concentrations do not occur in leaves, particularly in the leaf blade (Läuchli, 1984; Munns, 2005). High leaf Na^+ concentrations can cause premature leaf senescence and loss of photosynthetic activity (James *et al.*, 2002), which reduces the rate of carbon assimilation and ultimately grain yield (Husain *et al.*, 2003).

4.2.4.1 Photosynthesis Measurements.

Photosynthesis rates were determined using Infra Red Gas Analyzers (IRGA), *LCpro+* portable photosynthesis system (*LCpro+*, ADC Bioscientific Ltd., Hoddeston, Herts., UK) fitted with a rectangular narrow leaf chamber (window area of 5.8 cm²). The

LCpro+ instruments are fully programmable IRGAs that control ambient temperature, incident light levels, humidity, and CO₂ concentration. These features allow automated measurement of CO₂ response and light response curves (see sections 4.2.4.1.1 and 4.2.4.1.2). A portion of the fully expanded fourth leaf was enclosed in the *LCpro+* ensuring the leaf completely filled the chamber area. The chamber was illuminated with the adjustable *LCpro+* LED unit, and chamber CO₂ (*i.e.* C_{air} or C_a), chamber humidity, and temperature (*i.e.* T_{ch}) were controlled by the *LCpro+* console. In all cases, once sealed in the chamber, each leaf sample was subjected to a CO₂-response experiment followed immediately by a light response experiment. This was possible using the programmable features of the *LCpro+* instrument. The flow rate of air through the chamber was adjusted to 200 μmol s⁻¹ (~ 4.5 ml s⁻¹); the chamber area was 5.8 cm², and the boundary layer resistance set to 0.3 m² s mol⁻¹. Leaf temperature was calculated using the protocols in the *LCpro+* hand book.

Three *LCpro+* instruments were used simultaneously to provide replication (for more details see sections 4.2.4.1.1 and 4.2.4.1.2).

4.2.4.1.1 CO₂ Response Curve.

Carbon uptake is reduced by environmental stresses that lower transpiration rates, triggered by lowering leaf water potential (Kramer and Boyer, 1995). This is particularly so for water stress (Lawlor, 1995) and also for salinity stress (Munns, 1993), which firstly induce the so-called osmotic or water deficit effect of salinity, and thus impairs the ability of plants to take up water. There have been many recent advances in our understanding of the mechanisms by which photosynthesis responds to environmental factors. However, conflicts still arise in the debate on the relative importance of CO₂ diffusive (Cornic, 2000) and metabolic (Tezara *et al.*, 1999) factors

to the overall control of photosynthesis rates even under mild environmental stress (Flexas and Medrano, 2002).

A rapid rate of CO₂ assimilation (A) requires correspondingly large amounts of many components of the chloroplasts, particularly the light harvesting chlorophyll–protein complexes (LHCP), electron transport and NADP⁺-reducing (nicotinamide adenine dinucleotide phosphate) components of thylakoids, and the CO₂ assimilating enzyme ribulose 1-5 biphosphate carboxylase-oxygenase (Rubisco), plus other enzymes of the C₃ cycle for CO₂ assimilation in the stroma.

Only a limited amount of information can be derived directly from an A/C_a curve. But Farquhar *et al.*, 1980 and Farquhar and Sharkey, 1982 have shown how to extract useful photosynthetic parameters by plotting assimilation rate (A) against the CO₂ concentration inside the leaf (C_i). A/C_i plots can be constructed from A/C_a plots using simple calculations (Farquhar *et al.*, 1980). Simply put, the A/C_i plot of a sample represents the CO₂ response when stomatal and boundary layer resistance to CO₂ diffusion have been removed, and thus assimilation rate is limited by the kinetics of the carboxylation processes only; the small ‘mesophyll’ resistance that impairs CO₂ diffusion into the chloroplast from the intra cellular spaces is ignored. At low C_i the A/C_i curve is linear and the slope is an estimate of the carboxylation efficiency (v_{rubisco}), and the intercept estimates photorespiration (Farquhar *et al.* 1980; Fig. 4-3).

A perpendicular extrapolation through the A/C_a and A/C_i plots at ambient CO₂ levels (360 ppmv), therefore, shows the relative impairment that the stomata and boundary layer resistance impose on assimilation rate. Farquhar and co-workers (Farquhar and Sharkey, 1982) have shown the simple parameter L can be used to estimate the importance of stomatal resistance on assimilation (Fig. 4-3).

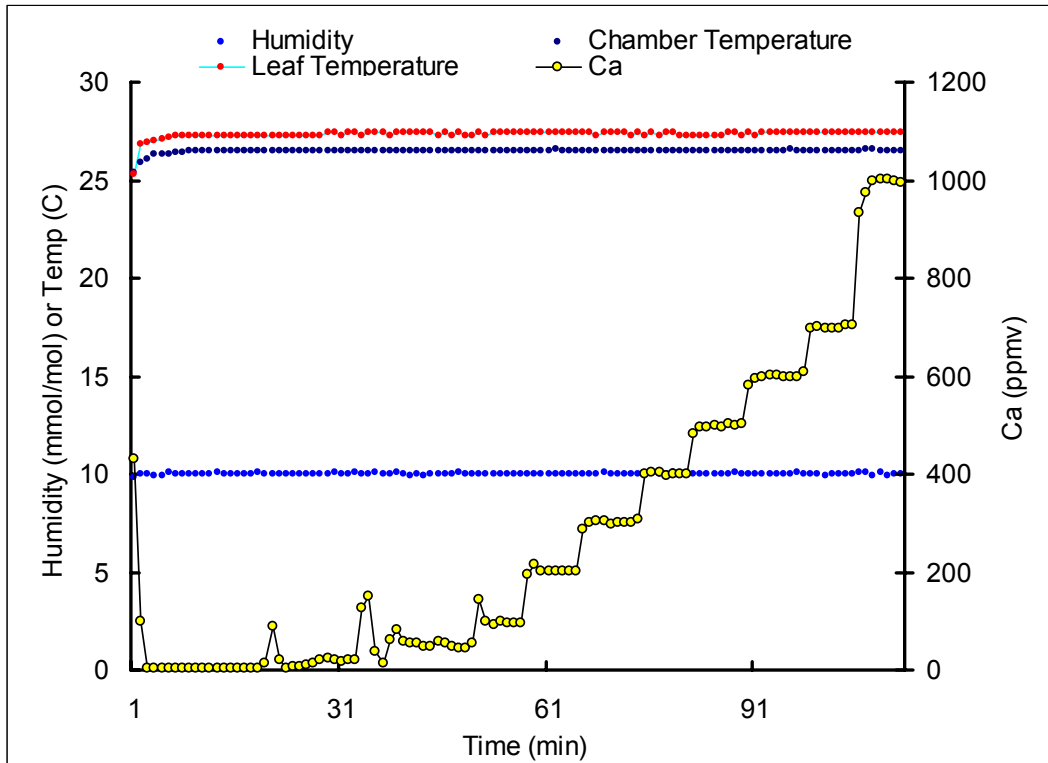


Fig. 4-2 Profile of Leaf Chamber Conditions Used to Collect CO₂- Response Curves.

(●), chamber CO₂ (C_a) controlled by the LCpro+ consol. C_a levels increased incrementally every 15 minutes as follows (0, 10, 20, 50, ppmv). After this period, the C_a levels were increased every 7 minutes (100, 200, 300, 400, 500, 600, 700 and 1000 ppmv).

(●), chamber humidity controlled by the LCpro+ consol and was set to 10 mmol/mol.

(●), chamber temperature controlled by the LCpro+ consol and was set to 25°C.

(●), leaf temperature controlled by the LCpro+ consol and was ~27-28°C.

See Section 4.2.4.1.1 for details. Readings were taken every one minute.

During the course of these experiments light levels were maintained at 487 μmol photons m⁻² s⁻¹ (PPFD) using the LCpro+ light emitting diode unit.

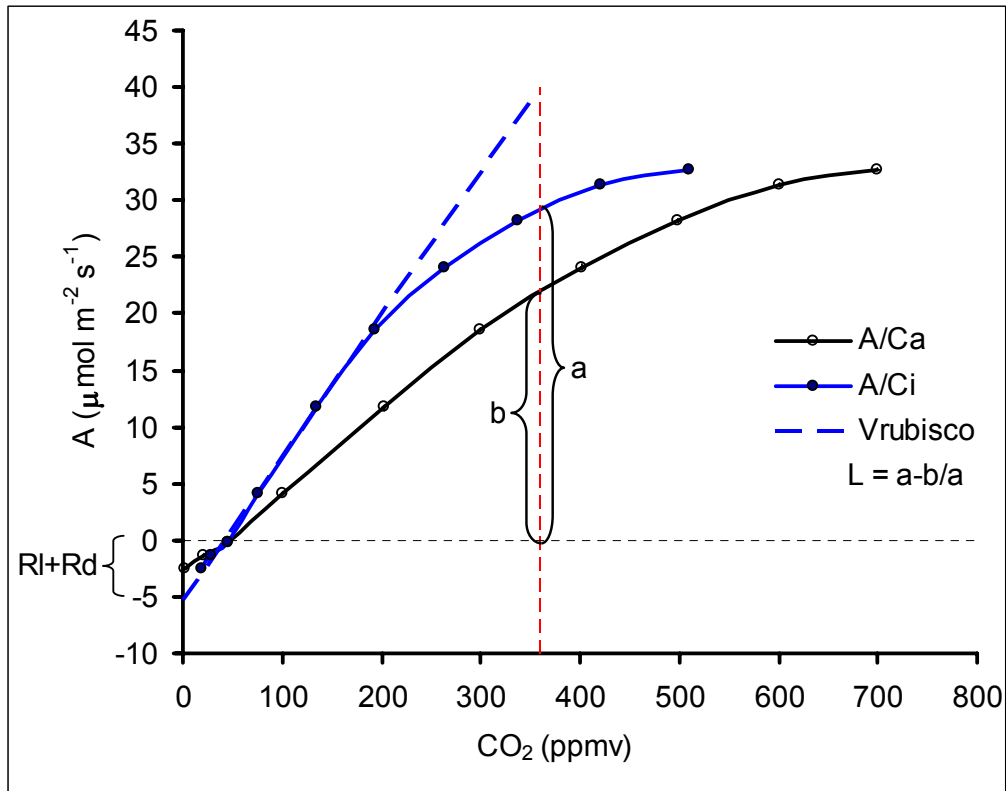


Fig. 4-3 Carbon Dioxide Response Curve (CRC) of a Barley Leaf.

Leaves were carefully sealed in the LCpro+ Narrow Leaf Chamber taking care to avoid damage; leaves were chosen that completely filled the chamber area (5.8 cm²). Samples were dark adapted in conditioned air (0 ppmv CO₂, 10 mmol/mol humidity, and 26°C) for 10 minutes to adapt prior to running the program shown in Fig. 4-2.

Blue solid line (—) is the relationship between net photosynthesis (A_n) and the internal CO₂ concentration (C_i). Black solid line (—) is the relationship between net photosynthesis (A_n) and the air CO₂ concentration (C_a). Blue dashed line (---) V_{rubisco} (carboxylation efficiency) from initial slope of the A/C_i curve. Red vertical dashed line (|) ambient CO₂ (360 ppmv). Extrapolation of the initial slope of the A/C_i curve to the abscissa gives the total respiration rate (photorespiration, R_l , and dark respiration, R_d). The chamber light level was 487 $\mu\text{mol photons m}^{-2} \text{s}^{-1}$ (PPFD). L can be used to estimate the importance of stomatal resistance on assimilation rate. Values of L that tend to zero indicate small stomatal limitation, whilst values that tend to 1 suggest large stomatal control; $L = (a-b)/a$ (see section 4.2.4.1.1 for details). Raw data for both barley lines (Z_1 and Z_{85}) at each level of NaCl (0, 50, 100, 150, and 200 mM) are presented in appendix Figs. A 4-1, 2, 3, 4, and 5). The data above were collected from a Z_1 barley leaf growing in 0 mM NaCl.

In these experiments the *LCpro+* instruments were programmed to collect CO₂ responses using the following protocols. An area of leaf blade from the 4th emergent leaf (fully expanded by day 26) was sealed in the leaf chamber and the data logger started. The sample was illuminated at 487 $\mu\text{mol photons m}^{-2} \text{s}^{-1}$ (PPFD) and exposed to 0 ppmv C_a, 10 mmol/mol humidity for 15 minutes. After this period, the leaf samples had attained steady state and the C_a levels increased incrementally every 15 minutes as follows (0, 10, 20, 50, ppmv). After this period, the C_a levels were increased every 7 minutes (100, 200, 300, 400, 500, 600, 700 and 1000 ppmv). A profile of the chamber conditions is presented in (Fig. 4-2). Values of L that tend to zero indicate small stomatal limitation, whilst values that tend to 1 suggest large stomatal control.

4.2.4.1.2 Light Response Curve.

Photosynthesis or Assimilation rates (A) can be measured as a function of incident light intensity (I or Photosynthetic Photon Flux Density, PPFD). To generate a light response curve (LRC; A versus I), the *LCpro+* was programmed to collect data using the following protocols. Samples were placed in the dark and C_a adjusted to ambient levels (360 ppmv); chamber humidity was set to 10 mmol/mol, and chamber temperature to 25 °C (measured Tch was 27-28 °C). The *LCpro+* data logger was started and the samples left for 10 minutes to dark adapt. After this period the incident light intensity (I) was increased sequentially to provide 10 minutes illumination at each of the following levels (0, 9, 17, 44, 87, 174, 261, 358, 435, 522, 696 and 870 $\mu\text{mol m}^{-2} \text{s}^{-1}$, PPFD). A profile of the chamber conditions used for collect LRC is shown in (Fig. 4-4). Figure 4-5 present a typical light response curve from barley. From this curve several important photosynthetic parameters can be extracted, such as the apparent quantum yield of photosynthesis (α), the maximum photosynthesis rate (A_{max}), the dark respiration rate (Rd), and the convexity term (θ). Linear hyperbolic relationships between A and I are often assumed (Rabinowich, 1951). Alpha (α) is estimated by forcing a linear regression

line through the first few low-light data points (Fig. 4-5). A_{\max} is also estimated by forcing a line parallel to the I axis through a few data points considered to lie on the asymptote (Fig. 4-5). Estimation of both α and A_{\max} by these methods can incur large errors as only a few data points are used. The initial curve may not be truly linear, values of A and I associated with these data points are small (and hence errors of measurement proportionally large). Therefore, an alternative approach that is often used relies on the transformation of the linear hyperbolic data to a linear function (*e.g.* plots of I/A versus I; $\alpha = 1/\text{intercept}$, $A_{\max} = 1/\text{gradient}$). Using this method it is believed that errors are reduced as all of the data points are used for estimating α and A_{\max} .

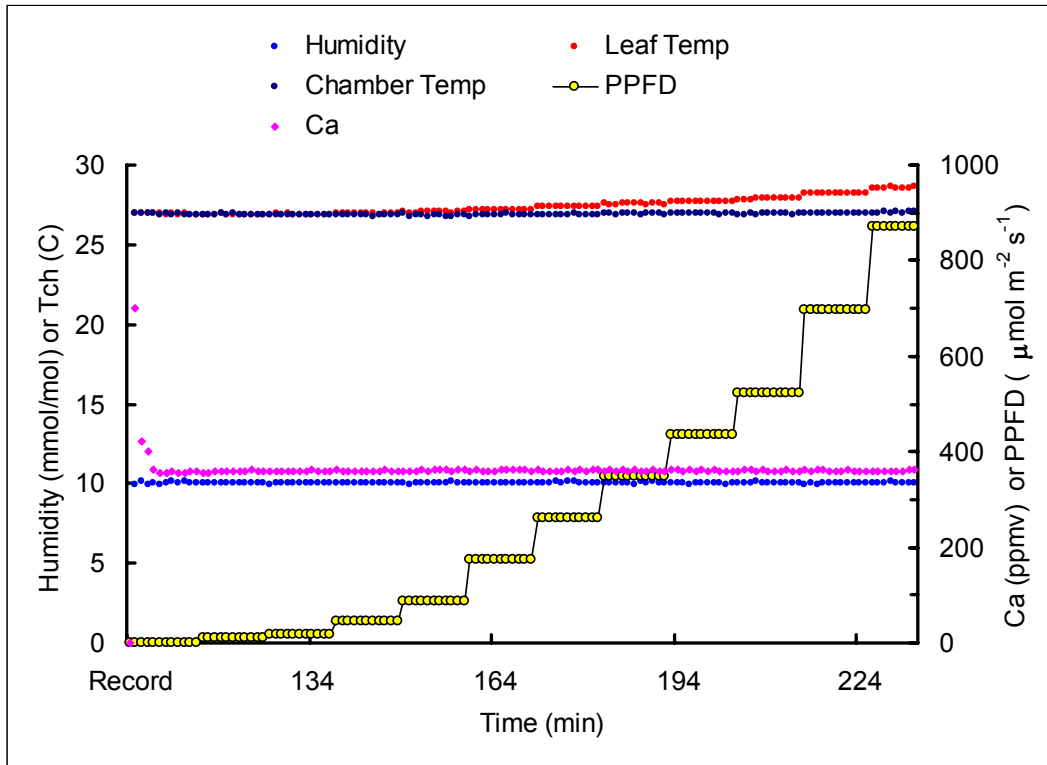


Fig. 4-4 Profile of Leaf Chamber Conditions Used to Collect Light Response Curves.

Leaves were carefully sealed in the LCpro+ Narrow Leaf Chamber taking care to avoid damage; leaves were chosen that completely filled the chamber area (5.8 cm²). Samples were first exposed to a CO₂-response regime (see Fig 4-2 and 4-3). Before being subjected to the light response regime here (Fig 4-5).

(●), chamber incident light intensity (Photosynthetic Photon Flux Density, PPFD). It was increased sequentially to provide 10 minutes illumination at each of the following levels (0, 9, 17, 44, 87, 174, 261, 358, 435, 522, 696 and 870 μmol m⁻² s⁻¹, PPFD).

(●), chamber humidity controlled by the LCpro+ consol was set to 10 mmol/mol.

(●), chamber temperature controlled by the LCpro+ consol and was set to 25°C.

(●), leaf temperature was measured by the LCpro+ consol.

(●), chamber air CO₂ concentration (C_a) was set at ambient (360 ppmv).

See Section 4.2.4.1.2 for details. Readings were taken every one minute. Leaf temperature was calculated using the protocols in the *LCpro+* hand book.

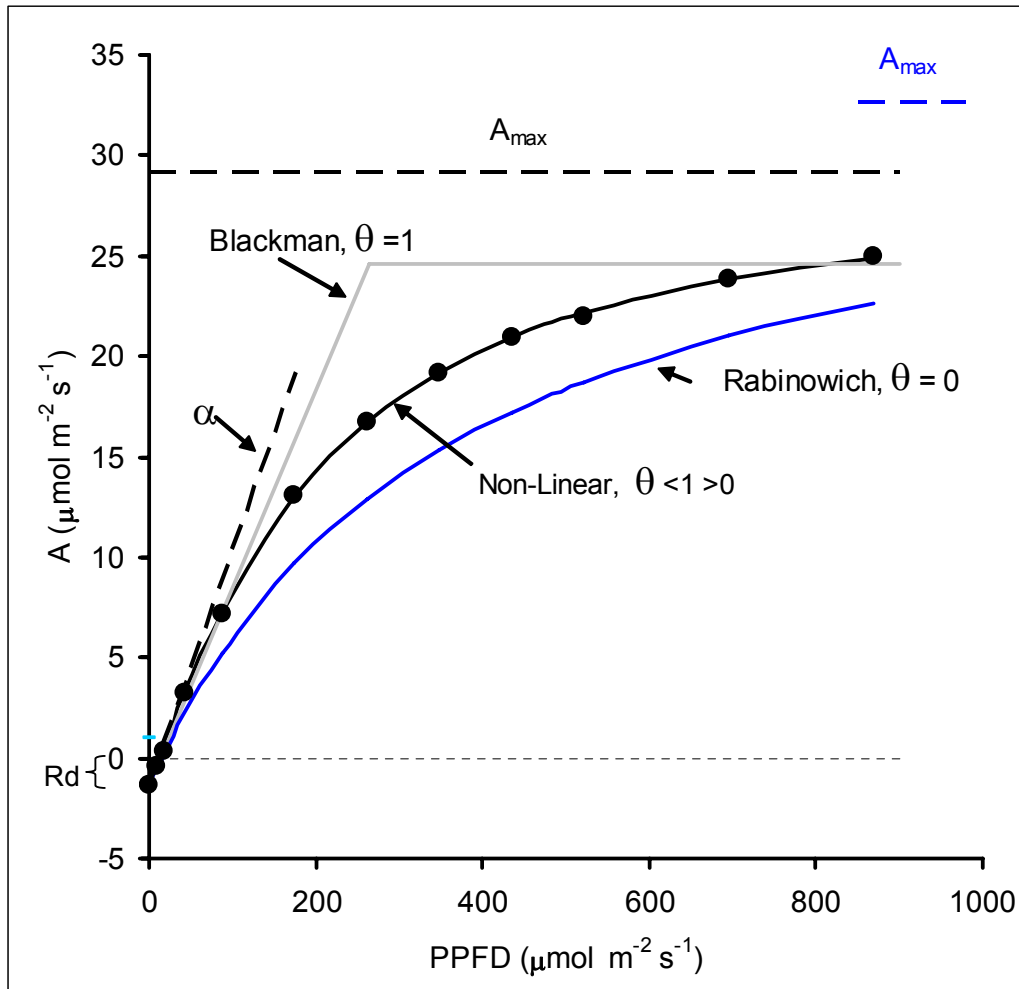


Fig. 4-5 Light Response Curve of Barley Leaf.

Leaves were carefully sealed in the LCpro+ Narrow Leaf Chamber taking care to avoid damage; leaves were chosen that completely filled the chamber area (5.8 cm²). Samples were first exposed to a CO₂-response regime (see Fig 4-2 and 4-3). Before being subjected to the light response regime here.

Carbon dioxide assimilation rate (*A*) *versus* incident Light Intensity (PPFD). A typical response is shown from barley line (Zhou 85), actual data points are shown as sold circles (●). Grey line (—), fitted Blackman response. Blue line (—), fitted hyperbolic response (Rabinowich 1951). Black line (—), fitted non-linear quadratic response (Thornley 1976). The fitted lines were obtained by an iterative method (Excel Solver) for minimization of errors (Akhkha *et al.*, 2001). Estimations of A_{\max} from the three models are color coded. The quantum efficiency, α (---); was estimated from the non-linear model. For full details, see Sections 4.2.4.1.2 and 4.2.4.2.

4.2.4.2 Modeling Photosynthetic Light Response.

Several models have been proposed to describe the photosynthesis light response curve (LRC). In 1905 Blackman derived one of the earliest models which describes a response of photosynthesis which increases linearly with irradiance (light limited) until the CO₂ supply becomes limiting (equation I). This model is inadequate, because the LRC shows no sharp discontinuity between the light limited and CO₂ limited regions (Fig. 4-5). Also, the true value of A_{max} tends to be under-estimated. For these reasons, this simple model is now rarely used.

$$A = A_{\max} \frac{I}{I_s} \text{ when } I < I_s, \text{ and } A = A_{\max} \text{ when } I > I_s. \quad (I)$$

A is the net assimilation rate, I is the light intensity, A_{max} is the maximum assimilation rate under the given conditions, and I_s is the light saturation constant (Blackman, 1905).

4.2.4.2.1 Rectangular Hyperbola Model (Linear).

One popular version of this model was proposed by (Rabinowich, 1951) and describes the relationship between photosynthesis and light in term of a rectangular hyperbola (Fig. 4-5). This model is a linear hyperbolic model and is related to the Michaelis-Menten formulation between the rate of an enzyme-catalyzed reaction (photosynthesis) and the concentration of its substrate (light). Mainly it defines two parameters, A_{max} the maximum (gross or net) photosynthesis rate, and the quantum efficiency (α) as illustrated in Equation (II).

$$A = \frac{A_{\max} \alpha I}{A_{\max} + \alpha I} \quad (II)$$

Where A is the net assimilation rate, I is the light intensity, A_{max} is the maximum assimilation rate under the given conditions, α is the quantum efficiency (initial slope) of the A vs. I plot (Rabinowich, 1951). Figure 4-5 present a best-fit Rabinowich model to observed data from barley. Clearly the model does not describe well the data in this case; α is underestimated, A_{max} is over-estimated, and generally the curve underestimates the observed assimilation rates (Chartier, 1970; Thornley, 1976).

4.2.4.2.2 Non Linear Model.

This model was developed by Thornley (1976) who realized that the LRC was better described using a quadratic model with three parameters, $A_{g_{max}}$, α and θ see equation (III).

$$0 = (A_{max} \alpha I) - (A_{max} + \alpha I)A + \theta A^2 \quad (III)$$

Where A is the gross assimilation rate, and θ is the convexity term. The terms I , A_{max} , and α ; have the same meaning as equation (II). The Convexity term controls the sharpness of transition between the initial slope and the asymptote of the A vs. I plot (Fig. 4-5). When θ is 0 equation (I) degenerates into equation (II), when θ is 1 equation (II) can be simplified to equation (I).

This model combines a simple description of the biochemical reactions in the chloroplasts. Marshall and Biscoe, 1980 have extended this model to include estimates of dark respiration and net photosynthesis assimilation (A_n) rates.

4.2.5 Assessment of Development.

Sixteen plants of each line (Zhou 1 and Zhou 85) were placed in 1 liter pots containing potting compost and thoroughly watered. The pots were then placed in a glasshouse (22°C/18°C day/night temperature) and supplemented with artificial light to provide a 14/10 light and dark respectively of 180 to 250 $\mu\text{mol m}^{-2} \text{s}^{-1}$ PPFD. Plants were watered regularly to ensure 1 cm of standing water in the drip trays. The developmental stage of each individual plant was assessed to the Zadok's Scale (see Fig. A 4-7 and Table A 4-3).

4.2.6 Assessment of Ppd-H1 Flowering Locus.

4.2.6.1 Isolating of Zhou 1 and Zhou 85 Genomic DNA for PCR Analysis.

A modified protocol for the preparation of plant genomic DNA (gDNA) for PCR analysis was used (Edwards *et al.*, 1991). The top two-thirds of a single second emergent leaves of 14 day old barley seedling (leaves were cut ~100 mm from the base, and approximately 170 mm in length and ~13 mm in width) was harvested and grounded to a fine powder under liquid nitrogen using a mortar and pestle. The powder was then transferred into 1.5 ml Eppendorf tube and 400 μl of extraction buffer (200 mM Tris HCl pH 7.5, 250 mM NaCl, 25 mM EDTA, 0.5% SDS) were added and the sample vortexed for 5 seconds. The extracts were then centrifuged at 12,000 g for 30 sec and 300 μl of the supernatant transferred to a fresh Eppendorf tube. The supernatant was mixed with 300 μl isopropanol and left at room temperature for 2 minutes. Following this, the sample was then centrifuged at 12,000 g for 8 minutes, rinsed in 75% ice cold ethanol, and the pellet air dried before dissolving in 100 μl 1xTE buffer (10 mM Tris-HCl pH 8.0, 1 mM EDTA).

The genomic PCR reaction contained 15 μ l 2x ReddyMix (ABgene, AB-0575-DC-LD), 4 μ l template genomic DNA from Zhou 1 or Zhou 85, 2 μ l (50 pmol) of either the control (CF and CR) or test (TF and CR) primers (Table 4-1), and 7 μ l dH₂O.

Amplification was performed in 30 μ l volumes using PCR, MJ Research DYAD, and the conditions were 94°C for 2 min followed by 30 cycles of 94 °C for 1 min, 50°C for 40 sec and 72°C for 90 sec. The resulting PCR products were visualized on 1% agarose gels stained with 1 μ l (10 μ g/ml) ethidium bromide. The gels (11 cm width x 6 cm height x 1 cm thick) were run in TBE buffer (45 mM Tris-borate, 1 mM EDTA) at RT using Embi Tec, RunOne Electrophoresis cell (www.embitec.com). DNA visualized under UV illumination using Bio RAD Gel Doc 2000. The 1 K ladder from Promega was used as marker (Fig. 4-26) (Sambrook and Russell, 2001).

Table 4-1 Primers Used to Amplify SNP 22 of the Ppd-H1 Flowering Gene.

Primer	Sequence	GC Content	Tm	MW	Length bp
HvCF	GAT GAA CAT GAA ACG GG	0.47	50.4	5293	17
HvCR	TAT AGC TAG GTG CGT GGC G	0.58	58.8	5900	19
HvTF	ATG CGA ATG GTG GAT CGG C	0.58	58.8	5909	19

Note: Primers and PCR reactions were designed by Turner *et al*, 2005.

4.3 Results.

4.3.1 Growth Parameters.

4.3.1.1 Shoot and Root length.

The primary shoot length at day 37 of both barley lines, Zhou 1 and Zhou 85, decreased with increasing NaCl concentration in the media (Fig. 4-7a). The primary shoot length was 50% shorter in the Zhou 85 line even at 0 mM NaCl (see Figures 4-6 and 4-7a). Similarly root length decreased from ~55 cm to ~40 cm in both barley lines with increasing salt (from 0 to 200 mM NaCl) in the media, but at all concentrations the roots of Zhou 85 were longer than those of Zhou 1 (Fig. 4-7b).

4.3.1.2 Shoot and Root Fresh Weight.

Shoot fresh weight significantly decreased from ~13 g to ~4 g and also root fresh weight was declined from ~5.5 g to ~1.5 g in both Zhou 85 and Zhou 1 with increasing salt concentration (from 0 to 200 mM NaCl) as shown in Figs. 4-6 and 4-8ab. However, no significant changes between the two lines were observed.

4.3.1.3 Shoot and Root Dry Weight.

Shoot and root dry weights for both lines declined from ~2.2 g to ~0.5 g in Zhou 1 and from ~1.2 g to ~0.5 g in Zhou 85 with increasing salt concentration NaCl (from 0 to 200 mM NaCl) in growth media (see Fig. 4-9ab). The shoot dry weight of line Zhou 1 was significantly greater than that of Zhou 85 at 0 and 50 mM NaCl confirming the observations in Figs. 4-6 and 4-9a.

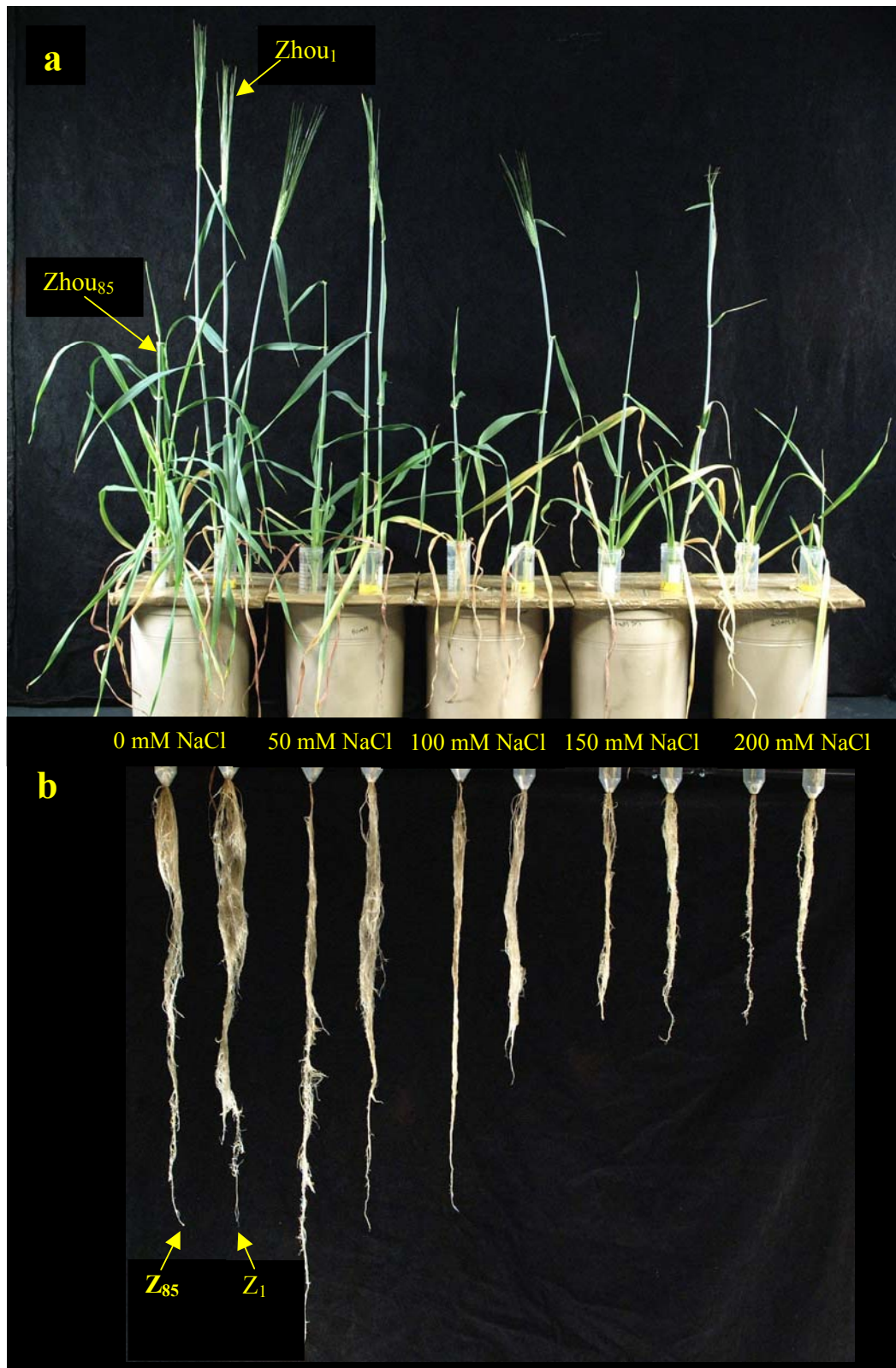
4.3.1.4 Number of Tillers per Plant.

In all treatments (100, 150, 200 mM NaCl) Zhou 85 produced more tillers than Zhou 1, but the number of tillers was decreased from ~3.5 to ~2 tillers for Zhou 85 and from ~2.75 to ~1 for Zhou 1 with increasing salt concentration (from 0 to 200 mM NaCl) (see Fig. 4-10).

Fig. 4-6 Zhou 1 and Zhou 85 Barley Lines Exposed to NaCl.

Plants were germinated and grown for 19 days in ¼- strength Hoagland's solution and then transferred into media containing NaCl (0, 50, 100, 150, and 200 mM NaCl). The plants shown are 37 days old.

Top panel (a), shoot growth. Bottom panel (b) root growth. In all pots, Zhou 85 is on the left and Zhou 1 on the right.



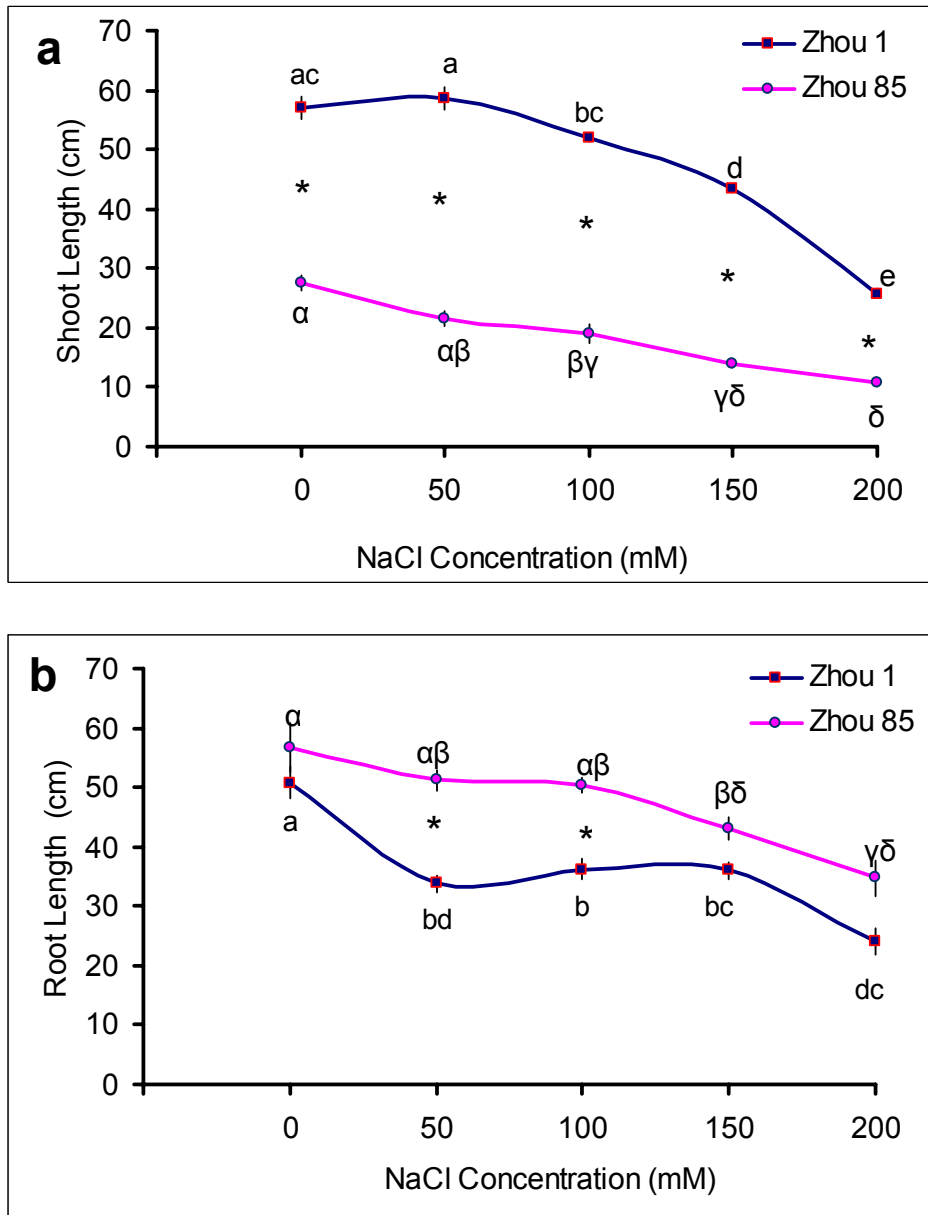


Fig. 4-7 The Effects of Salt Treatments on Primary Shoot and Root Length of Two Barley Lines (Zhou 1 and Zhou 85).

Top panel, shoot length (a); bottom panel, root length (b). ■, Zhou 1; ●, Zhou 85. Each data point presents the mean and standard error of four replicates. Measurements were made 37 days after germination (18 days after salt treatment). See Section 4.2.1 for experimental details. Two factor analysis of variance (linear model) was performed on the data with Bonferroni pair-wise tests between treatment means. Different Roman characters signify significant differences ($p < 0.05$) between Zhou 1 treatment means; Greek characters, significant difference ($p < 0.05$) for Zhou 85 treatment means. Asterisks identify significant differences ($p < 0.05$) between Zhou 1 and Zhou 85 means at each given salt concentration.

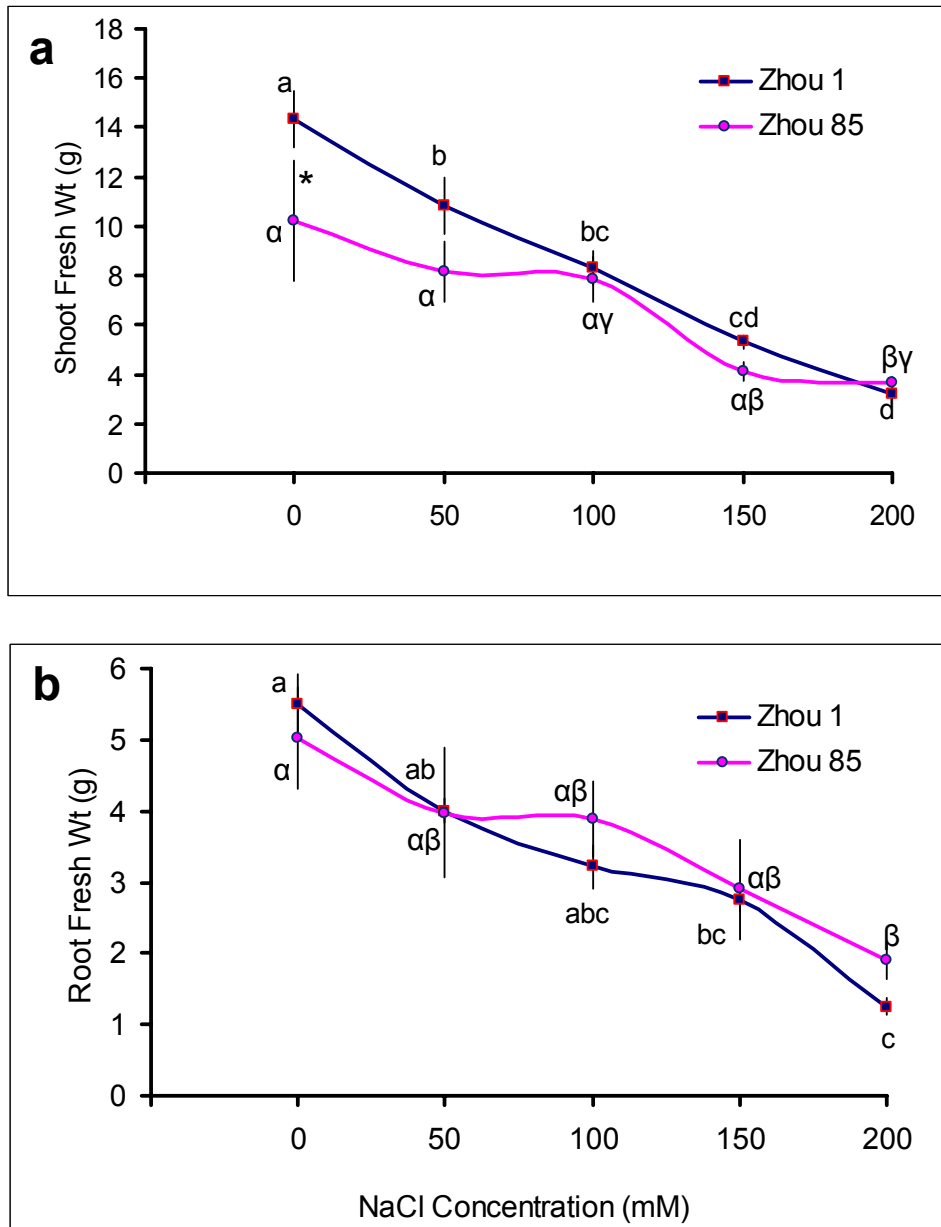


Fig. 4-8 The Effects of Salt Treatments on Shoot and Root Fresh Weight of Two Barley Lines (Zhou 1 and Zhou 85).

Top panel, shoot fresh weight (a); bottom panel, root fresh weight (b). ■, Zhou 1; ●, Zhou 85.

Each data point presents the mean and standard error of four replicates. Measurements were made 37 days after germination (18 days after salt treatment). See section 4.2.1 for experimental details. Two factor analysis of variance (linear model) was performed on the data with Bonferroni pair-wise tests between treatment means. Different Roman characters signify significant differences ($p < 0.05$) between Zhou 1 treatment means; Greek characters, significant difference ($p < 0.05$) for Zhou 85 treatment means. Asterisks identify significant differences ($p < 0.05$) between Zhou 1 and Zhou 85 means at each given salt concentration.

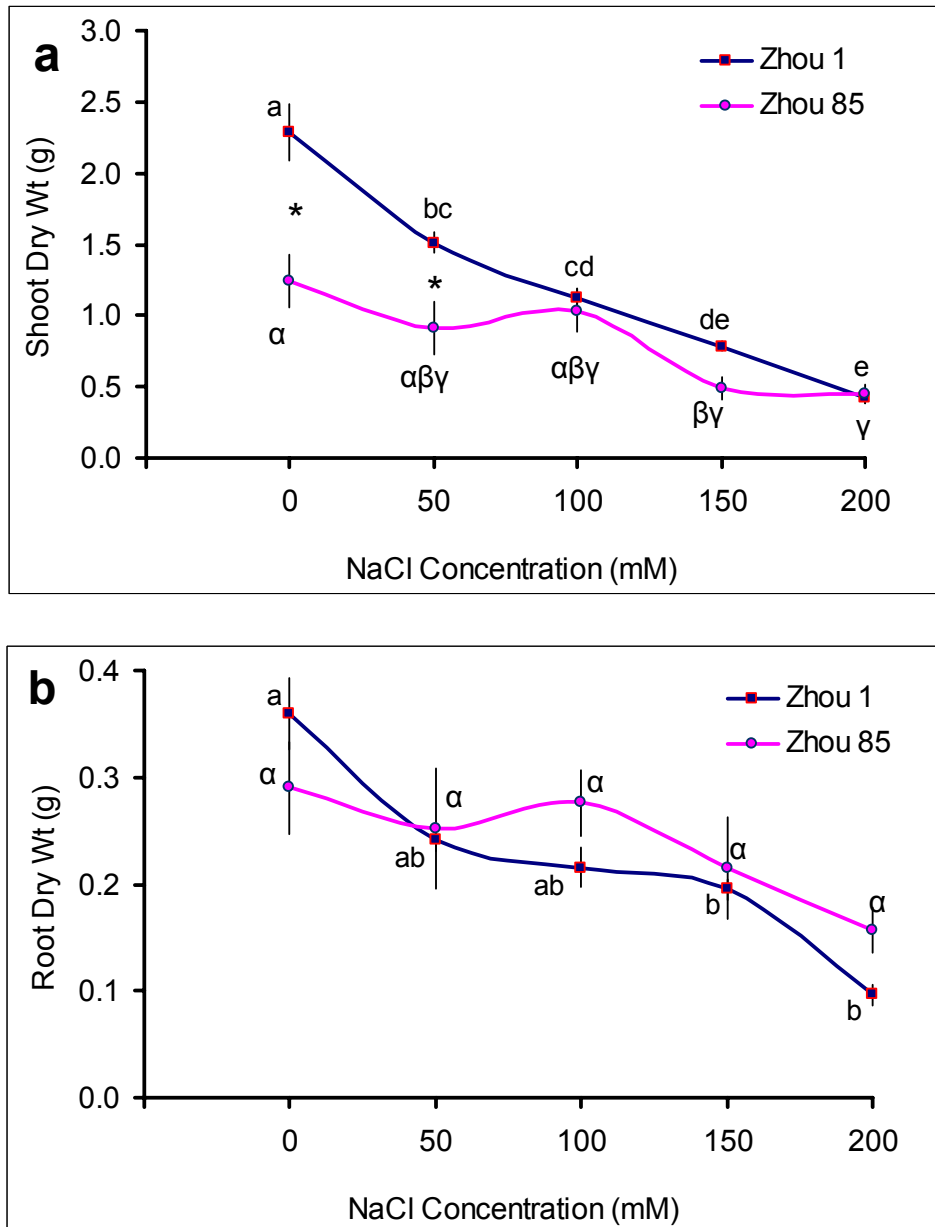


Fig. 4-9 The Effects of Salt Treatments on Shoot and Root Dry Weight of Two Barley Lines (Zhou 1 and Zhou 85).

Top panel, shoot dry weight (a); bottom panel, root dry weight (b). —■—, Zhou 1; —●—, Zhou 85.

Each data point presents the mean and standard error of four replicates. Measurements were made 37 days after germination (18 days after salt treatment). See section 4.2.1 for experimental details. Two factor analysis of variance (linear model) was performed on the data with Bonferroni pair-wise tests between treatment means. Different Roman characters signify significant differences ($p < 0.05$) between Zhou 1 treatment means; Greek characters, significant difference ($p < 0.05$) for Zhou 85 treatment means. Asterisks identify significant differences ($p < 0.05$) between Zhou 1 and Zhou 85 means at each given salt concentration.

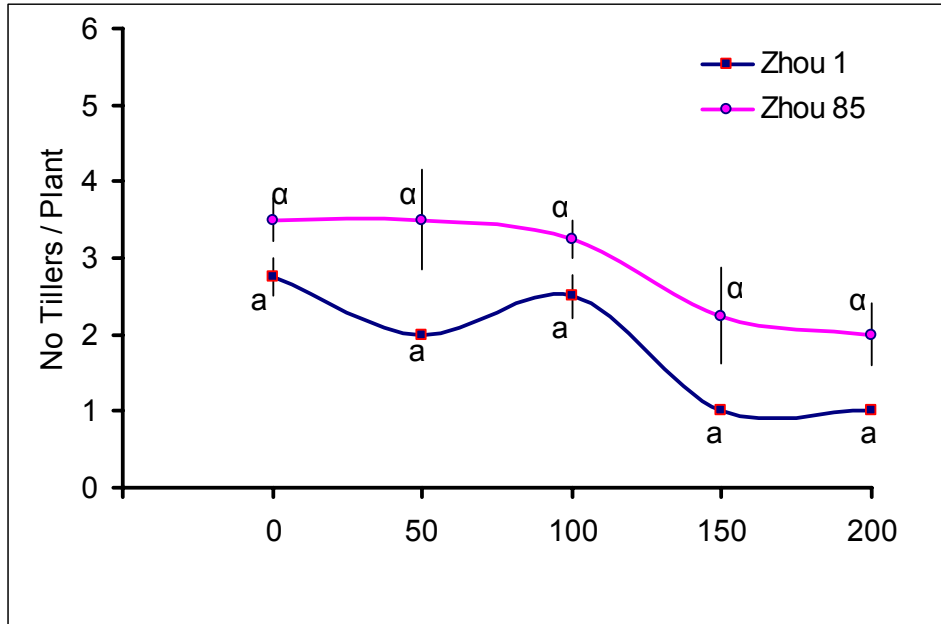


Fig. 4-10 The Effects of Salt Treatments on Number of Tillers of Two Barley Lines(Zhou 1 and Zhou 85).

—■—, Zhou 1; —●—, Zhou 85.

Each data point presents the mean and standard error of four replicates for the number of tillers. Measurements were made 37 days after germination (18 days after salt treatment). See section 4.2.1 for experimental details. For the number of floral spikes per plant, measurements were made at harvest (day 70). Two factor analysis of variance (linear model) was performed on the data with Bonferroni pair-wise tests between treatment means. Different Roman characters signify significant differences ($p < 0.05$) between Zhou 1 treatment means; Greek characters, significant difference ($p < 0.05$) for Zhou 85 treatment means.

4.3.2 Grain Yield.

4.3.2.1 Spikes and Seeds per Plant.

Zhou 85 has significantly fewer spike/plant at 100, 150 and 200mM NaCl. For both lines there was a salt-induced decrease in number of spikes per plant (see Fig. 4-11a). The number of seeds per plant was always greater for Zhou 1 regardless of salt concentration (Fig. 4-11b).

4.3.2.2 Grain Yield and % Grain Yield.

Zhou 85 showed a 40% lower grain yield than Zhou 1 at 0 mM NaCl (Fig. 4-12a). Increased salinity severely reduced grain yield of both lines but Zhou 85 failed to produce any significant yield above 100 mM NaCl, whereas Zhou 1 still managed to produce a small yield at 200 mM NaCl, albeit ~ 5% of the value at 0 mM NaCl. When the relative grain yields are plotted for the two lines (Zhou 85 / Zhou 1) as a function of NaCl concentration, it is clear that Zhou 85 does not yield as well as Zhou1 above 100 mM NaCl (Fig. 4-12b)

4.3.2.3 Thousand Grain Yield.

Thousand Grain Yield is a good parameter used to measure yield. Between two lines there was not significant different observed (see Fig 4-13).

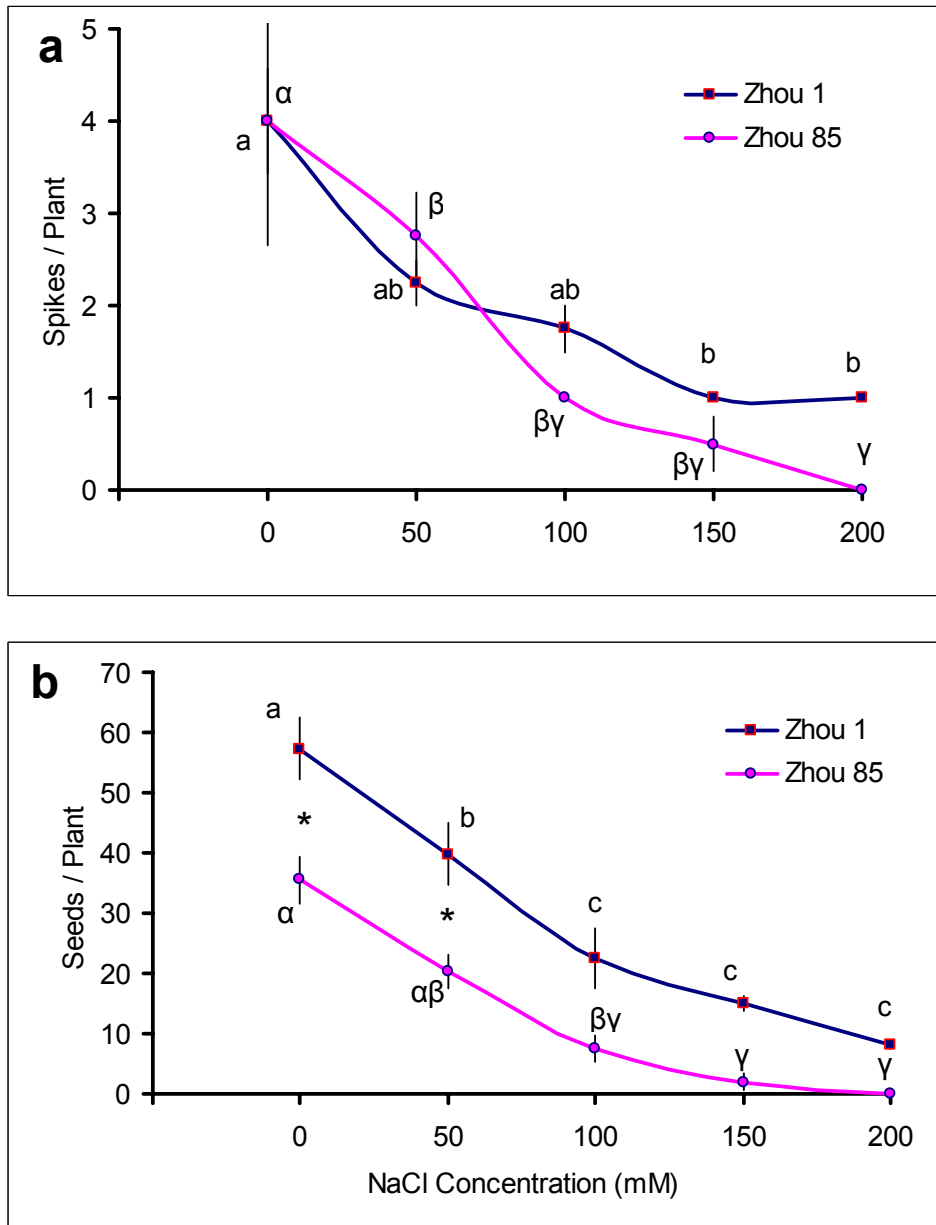


Fig. 4-11 The Effects of Salt Treatments on Spikes and Seeds per Plant of Two Barley Lines (Zhou 1 and Zhou 85).

Top panel, number of spikes per plant (a); bottom panel, number of seeds per plant (b). ■, Zhou 1; ● Zhou 85.

Note that Z 1 had managed to produce one spike and ~10 seeds (seeds not tested for viability). Each data point presents the mean and standard error of four replicates. Measurements were made at harvest, day 70 (52 days after salt treatment). See Section 4.2.1 for experimental details. Two factor analysis of variance (linear model) was performed on the data with Bonferroni pair-wise tests between treatment means. Different Roman characters signify significant differences ($p < 0.05$) between Zhou 1 treatment means; Greek characters, significant difference ($p < 0.05$) for Zhou 85 treatment means. Asterisks identify significant differences ($p < 0.05$) between Zhou 1 and Zhou 85 means at each given salt concentration.

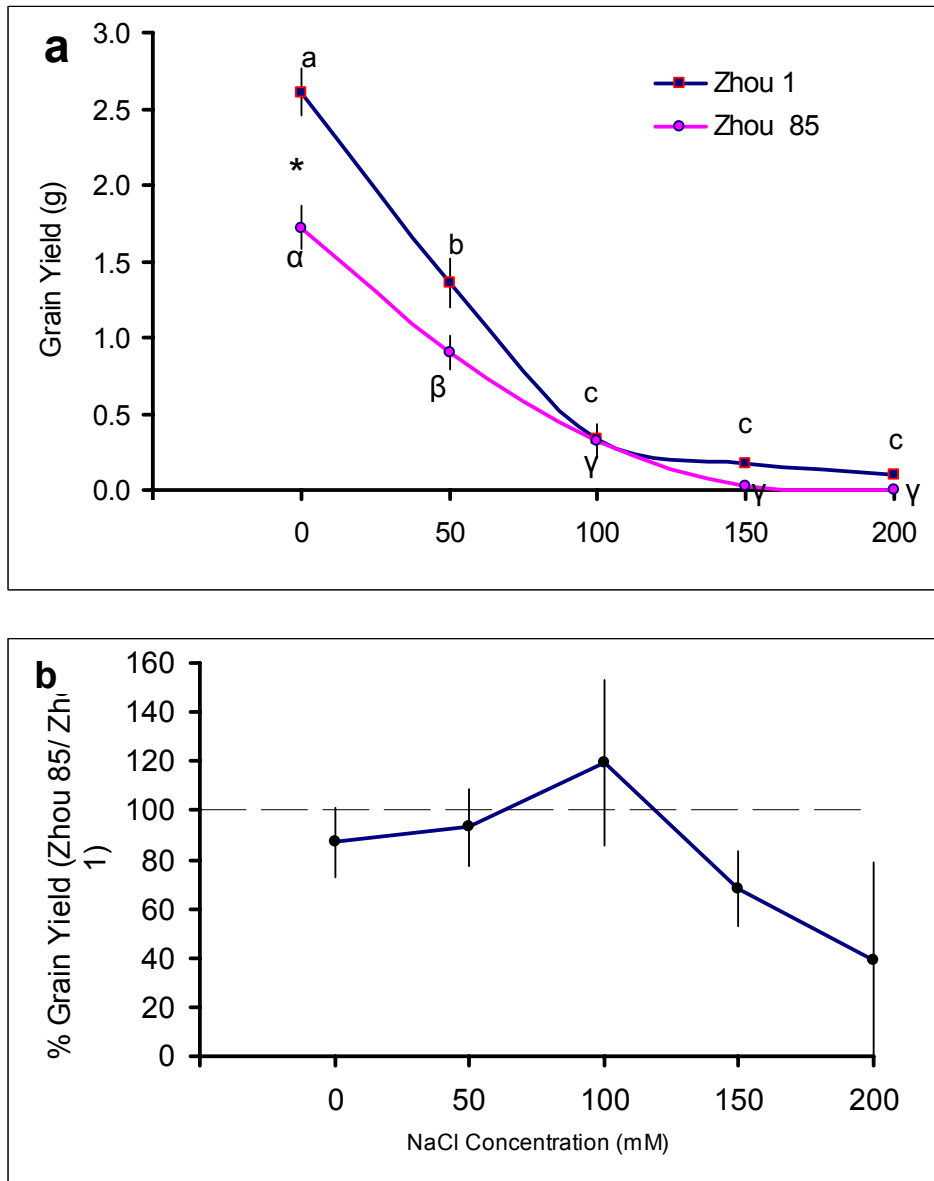


Fig. 4-12 The effects of salt treatments on the Grain Yield and % Grain Yields of two barley lines.

Top panel, Grain Yield (a); bottom panel, Relative Grain Yield (b), calculated as yield of Zhou 85/yield of Zhou 1. values for Zhou 85 and Zhou 1 yield were ranked before relative yield averages and standard errors were calculated. ■, Zhou 1; ●, Zhou 85; ●, Zhou 85/Zhou 1 Relative Grain yield.

Each data point presents the mean and standard error of four replicates. Measurements were made at harvest (day 70). See Section 4.2.1 for experimental details. Two factor analysis of variance (linear model) was performed on the data with Bonferroni pairwise tests between treatment means. Different Roman characters signify significant differences ($p < 0.05$) between Zhou 1 treatment means; Greek characters, significant difference ($p < 0.05$) for Zhou 85 treatment means. Asterisks identify significant differences ($p < 0.05$) between Zhou 1 and Zhou 85 means at each given salt concentration.

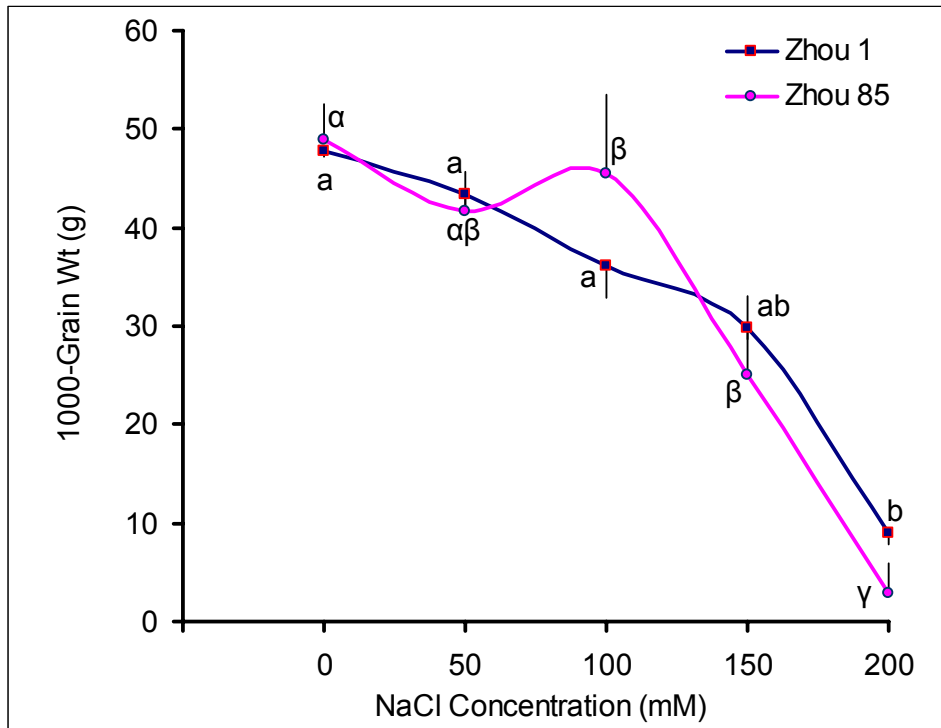


Fig. 4-13 The Effects of Salt Treatments on 1000-Grain Weight (g) of Two Barley Lines.

■, Zhou 1; ●, Zhou. 85.

Each data point presents the mean and standard error of four replicates. Measurements were made at harvest (day 70). See Section 4.2.1 for experimental details. Two factor analysis of variance (linear model) was performed on the data with Bonferroni pair-wise tests between treatment means. Different Roman characters signify significant differences ($p < 0.05$) between Zhou 1 treatment means; Greek characters, significant difference ($p < 0.05$) for Zhou 85 treatment means.

4.3.3 Plant Water Status.

4.3.3.1 *Relative Water Content and Water Potential.*

The water status of plants can be estimated from their relative water content (RWC) or their water potential (ψ_{H_2O}). The RWC is simply estimated as the ratio of the hydration state of the treated plant compared with control plants ($RWC = ([g\ H_2O/g\ D\ Wt]^{treated} / [g\ H_2O/g\ D\ Wt]^{control}) \times 100\%$).

Measurements of shoot RWC showed that Zhou 1 retains control level hydration state up to 100 mM external NaCl levels, whereas Zhou 85 shows a steady decline from 0 mM NaCl (Fig. 4-14a). Measurements of plant water status (ψ_{H_2O}) using a pressure chamber did not follow the same pattern as RWC measurements (Fig. 4-14b). Increasing NaCl concentration produced a significant decrease in ψ_{H_2O} , and there was some evidence that, unlike Zhou 85, Zhou 1 maintains shoot ψ_{H_2O} at control levels up to 100 mM NaCl. The values for ψ_{H_2O} were consistently low, however, in the range of -1.0 to -2.5 MPa. Under control conditions, shoot water potentials of -0.5 to -1.0 MPa are expected; the values observed (>-1.0 MPa) are usually considered to be indicative of moderate desiccation. Similar values for ψ_{H_2O} were obtained for both experiments (February and June 2005). Further subsequence measurements of barley plants growing in soil and in hydroponics have generated values consistently within this range (-1.0 to -2.0 range).

4.3.3.2 *Water Use Efficiency (WUE).*

From simultaneous measurements on carbon assimilation and transpiration the water use efficiency (WUE) can be calculated. These measurements express the moles of carbon dioxide fixed for each mole of water lost by transpiration. Drought tolerant plants may show improved stomatal responses when exposed to dehydrating conditions, and therefore lose less water. The WUE of both lines increased from 0.27% to 0.33% as external NaCl increased from 0 to 100 mM, suggesting that over this range stomatal

conductance declined, thereby reducing transpiration, but assimilation did not change. The experiments performed here, however, suggest no significant difference in the WUE of Zhou 1 and Zhou 85 (Fig. 4-15).

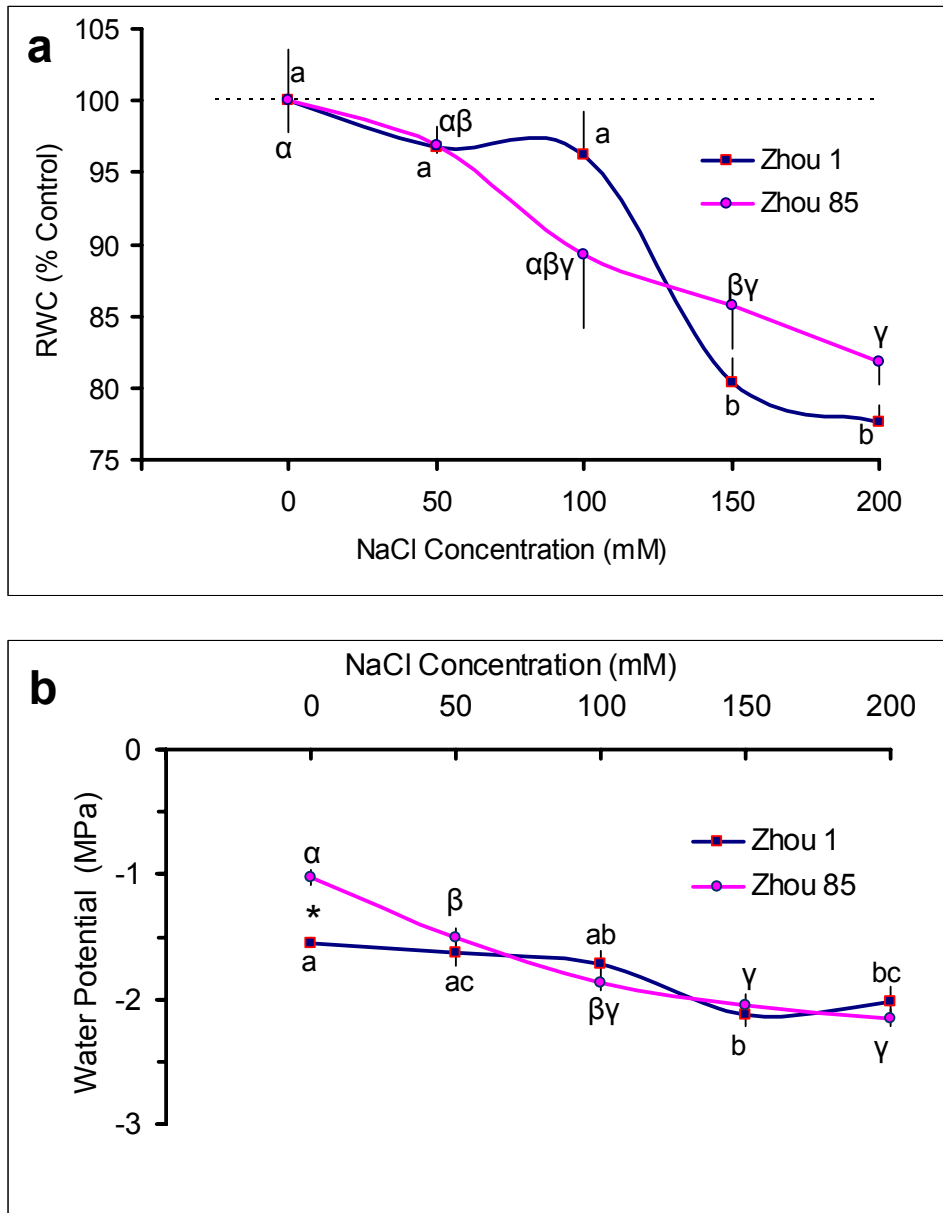


Fig. 4-14 The Effects of Salt Treatments on Relative Water Content (RWC) and Water Potential (ψ_{H_2O}) of Two Barley Lines.

Top panel, shoot Relative Water Content (a) see section 4.3.3.1 for details and bottom panel, Water Potential (b). ■, Zhou 1; ●, Zhou 85.

Each data point presents the mean and standard error of four replicates. Measurements were made 26 days after germination (7 days after salt treatment) on fully expanded 4th emergent leaves, see Section 4.2.1. Two factor analysis of variance (linear model) was performed on the data with Bonferroni pair-wise tests between treatment means. Different Roman characters signify significant differences ($p < 0.05$) between Zhou 1 treatment means; Greek characters, significant difference ($p < 0.05$) for Zhou 85 treatment means. Asterisks identify significant differences ($p < 0.05$) between Zhou 1 and Zhou 85 means at each given salt concentration.

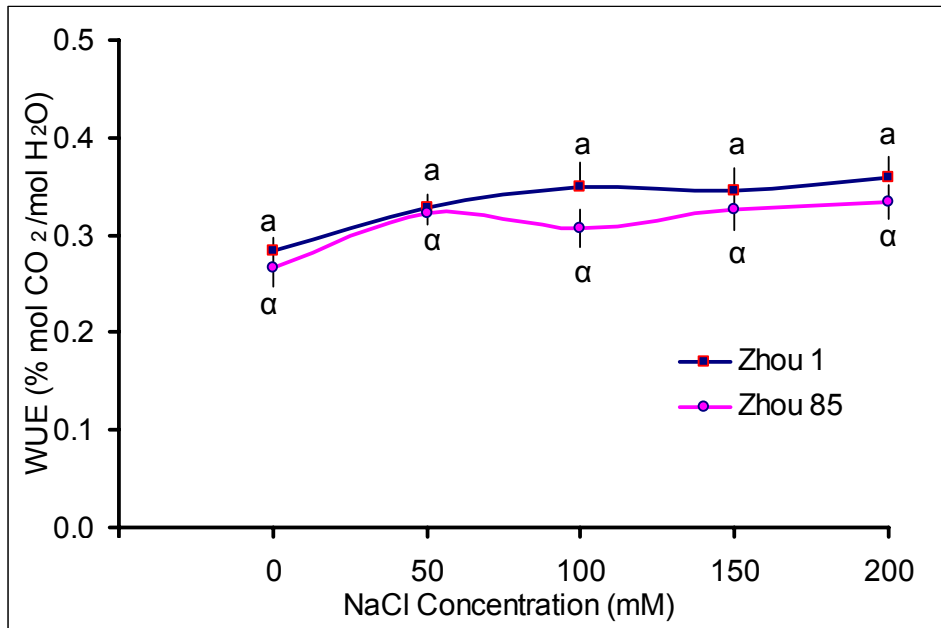


Fig. 4-15 The Effect of Salt Treatment on the Water Use Efficiency of Two Barley Lines.

■, Zhou 1; ●, Zhou 85.

Each data point presents the mean and standard error of four replicates. Measurements were made 26 days after germination (7 days after salt treatment) on fully extended 4th emergent leaves. See section 4.2.1 for experimental details. These data were taken from steady transpiration rates (E) *versus* light intensity (I) and assimilation rates (A) *versus* I curves at 180 $\mu\text{mol m}^{-2} \text{s}^{-1}$ PPFD (see Section 4.2.4.1.2). Two factor analysis of variance (linear model) was performed on the data with Bonferroni pair-wise tests between treatment means. Different Roman characters signify significant differences ($p < 0.05$) between Zhou 1 treatment means; Greek characters, significant difference ($p < 0.05$) for Zhou 85 treatment means. Asterisks identify significant differences ($p < 0.05$) between Zhou 1 and Zhou 85 means at each given salt concentration.

4.3.4 Ion Content Assessment.

Nutrient ion profile of shoot and root tissues were determined by an Inductively Coupled Plasma-Optical Emission Spectrometer; see Chapter 2 and 4, Sections 2.2.3 and 4.2.3 respectively. Data were collected for the following elements: K, Na, Ca, P, S, Mg, Mn, Fe, and B. No major differences were observed for any of the micronutrients and therefore only data for K, Na and Ca will be presented.

4.3.4.1 K⁺ Content of Barley Shoot and Root.

Increasing NaCl concentration to 50 mM produced a 30-50% decline in shoot K⁺ levels, but at higher concentrations the levels maintained at ~15 mg/g D Wt (Zhou 1) and 28 mg/g D Wt (Zhou 85; Fig. 4-16a). In contrast, in both lines root K⁺ levels did not change over the 0-50 mM NaCl range, but above this root K⁺ concentration steadily declined (Fig. 4-16b). The data presented here suggest line Zhou 85 partitions proportionately more K⁺ in the shoot than Zhou 1.

4.3.4.2 Na⁺ Content of Barley Shoot and Root.

Increasing external NaCl concentration from 0 to 200 mM NaCl produced a ten-fold increase in shoot Na⁺ levels (Fig. 4-17a). The data show that shoot Na⁺ levels increase sharply when external NaCl is increased to 50 mM NaCl, but that between 50 and 150 mM both lines then appear to adopt a strategy that maintains shoot Na⁺ levels at ~30 mg/g D Wt. Beyond 150 mM external NaCl concentrations, this mechanism may break down as shoot Na⁺ levels begin to rise again. No major differences were observed between the two lines with respect to the response of shoot Na⁺ levels to salinity.

Root Na⁺ levels in both lines increased with salinity up to 100 mM; at higher NaCl concentrations, root Na⁺ levels did not change markedly (Fig. 4-17b).

4.3.4.3 K^+/Na^+ Ratio of Barley Shoot and Root.

The relationship between tissue Na^+ and K^+ content can be revealed by plotting K/Na ratio as a function of external salinity (Fig. 4-18). A large decline (from ~ 8 to ~ 1) in the shoot ratio was observed when external NaCl was increased from 0 to 50 mM NaCl. In the shoot the ratio was maintained at ~ 0.5 - 1.0 at all higher concentrations. It appears that line Zhou 85 maintains a significantly higher K^+/Na^+ ratio than Zhou 1 at all concentrations except at 0 mM (Fig. 4-18a). Root K^+/Na^+ levels showed a progressive decline in both lines as external NaCl was increased to 100 mM NaCl (from ~ 1.5 to ~ 0.4); at higher concentration root K^+/Na^+ ratio did not change dramatically. The data show that over the 50 to 150 mM NaCl range, Zhou 1 maintains a significantly higher K^+/Na^+ ratio than Zhou 85 (Fig. 4-18b).

4.3.4.4 Ca^{+2} Content of Barley Shoot and Root.

Measurements were also made on shoot and root Ca^{+2} content. Increasing external NaCl concentration from 0 to 50 mM produced a large decline in both shoot and root Ca^{+2} levels, but no further decrease was observed at higher concentrations. No clear differences were observed between the two lines at any external NaCl concentration (Fig. 4-19a and b).

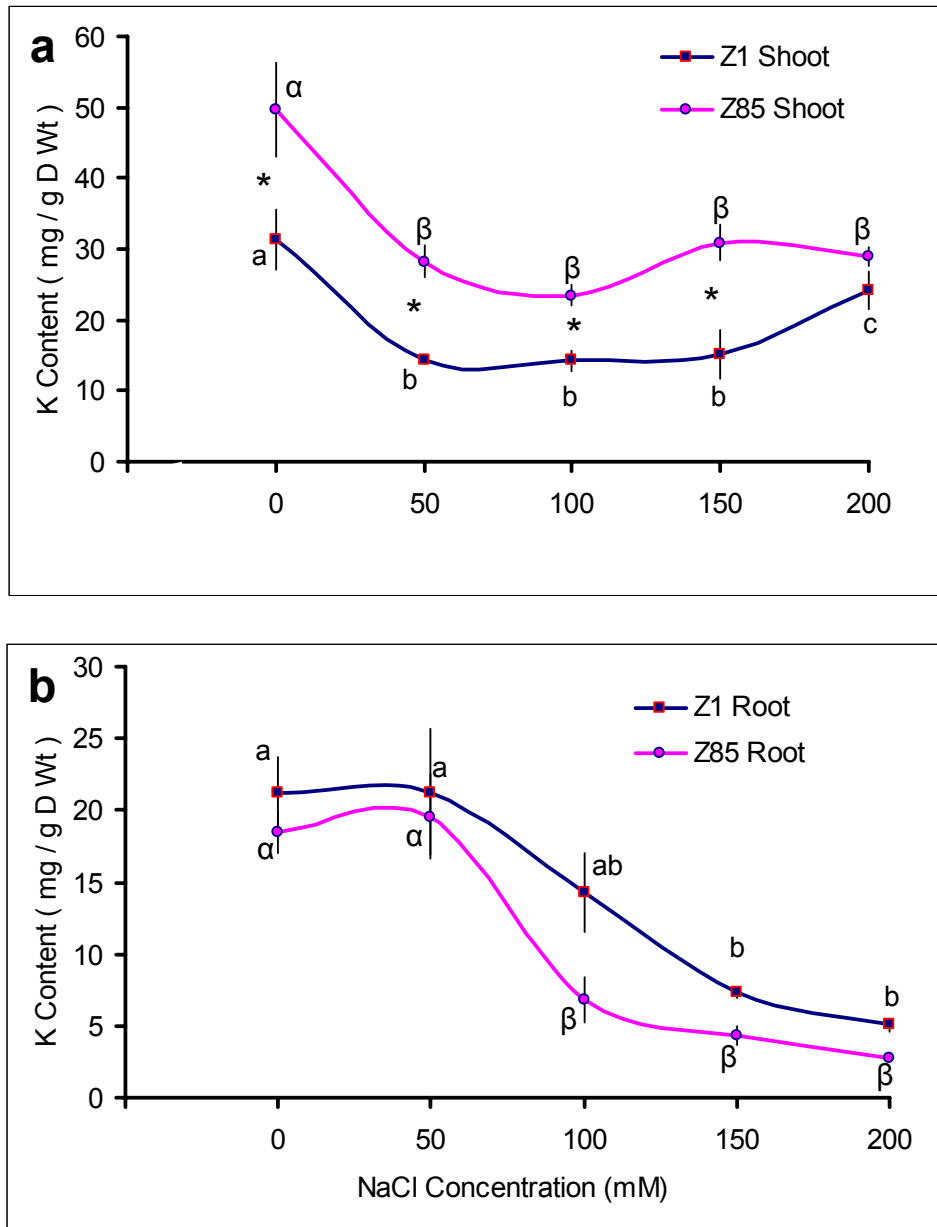


Fig. 4-16 K Content of Salt Stressed Barley Shoots and Roots.

Top panel, Shoot K⁺ Content (a) and bottom panel, Root K⁺ Content (b). ■, Zhou 1; ●, Zhou 85.

Samples were harvested at day 37 after germination (18 days after NaCl treatment) and prepared as described in Chapter 2 and 4 in Sections 2.2.3 and 4.2.3 respectively. The data points are the Averages and SEs of four independent samples. Two factor analysis of variance (linear model) was performed on the data with Bonferroni pair-wise tests between treatment means. Different Roman characters signify significant differences ($p < 0.05$) between Zhou 1 treatment means; Greek characters, significant difference ($p < 0.05$) for Zhou 85 treatment means. Asterisks identify significant differences ($p < 0.05$) between Zhou 1 and Zhou 85 means at each given salt concentration.

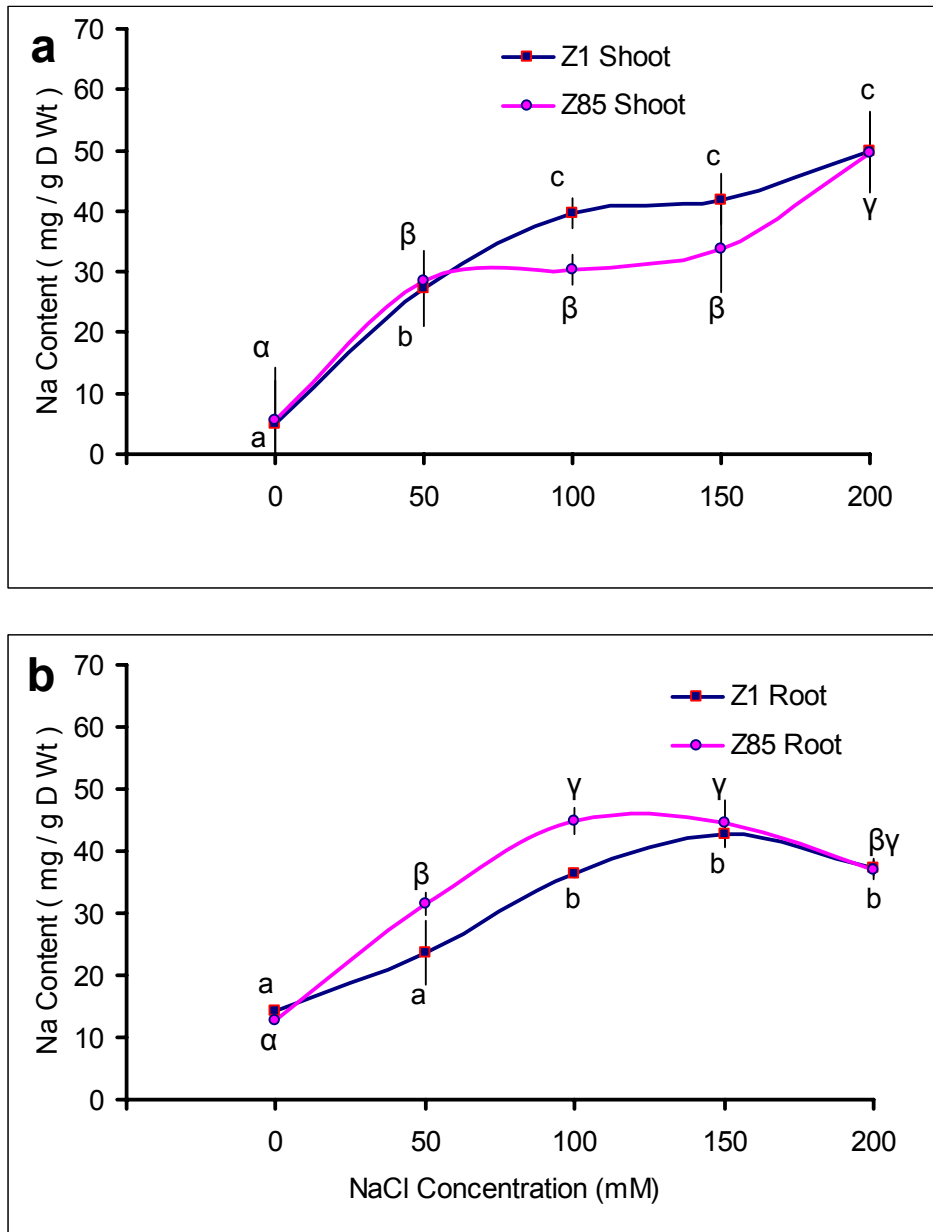


Fig. 4-17 Na Content of Salt Stressed Barley Shoot and Root.

Top panel, Shoot Na^+ Content (a) and bottom panel, Root Na^+ Content (b). \blacksquare , Zhou 1; \bullet , Zhou 85.

Samples were harvested and prepared as described in Chapter 2 and 4 in Sections 2.2.3 and 4.2.3 respectively. The data points are the Averages and SEs of four independent samples. Two factor analysis of variance (linear model) was performed on the data with Bonferroni pair-wise tests between treatment means. Different Roman characters signify significant differences ($p < 0.05$) between Zhou 1 treatment means; Greek characters, significant difference ($p < 0.05$) for Zhou 85 treatment means.

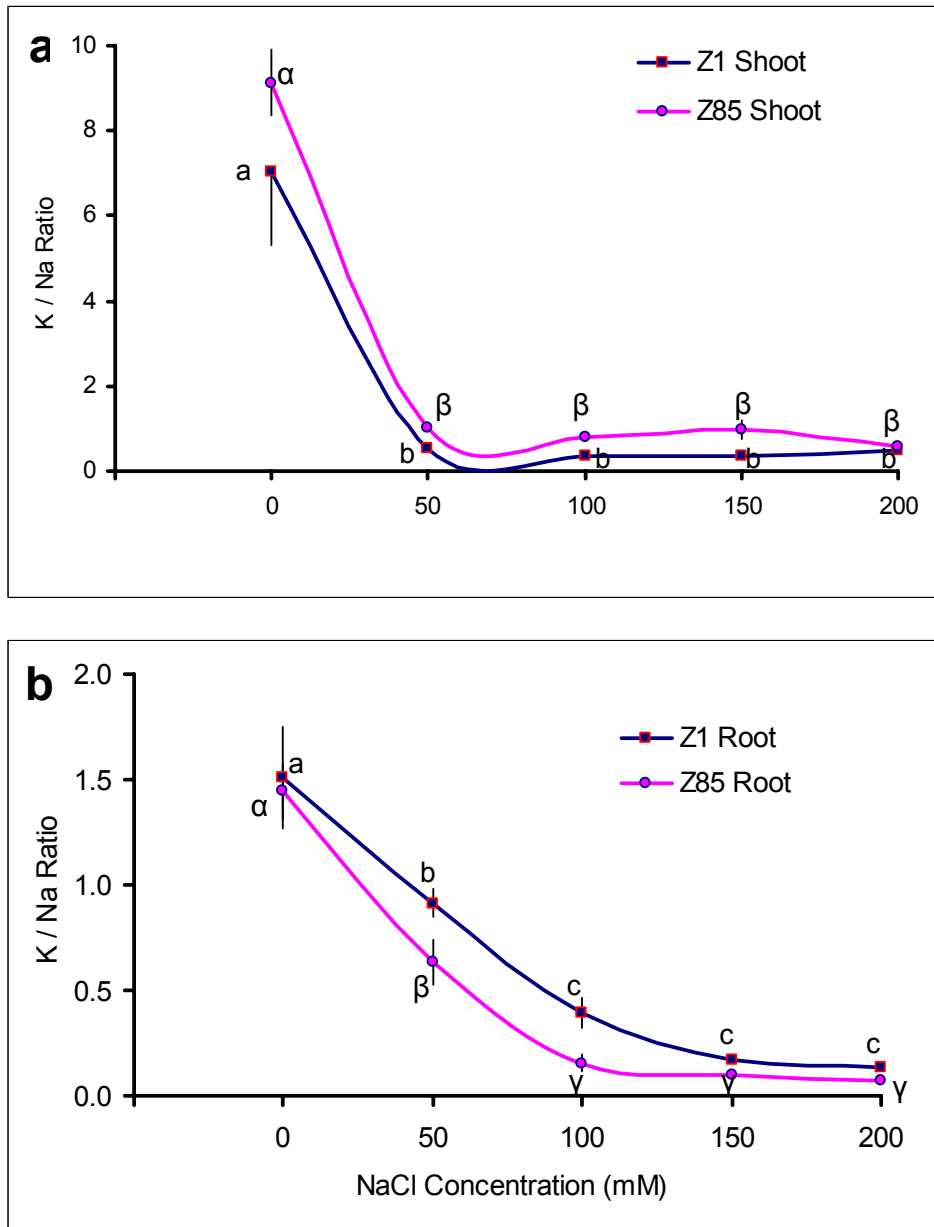


Fig. 4-18 K⁺/Na⁺ Ratios of Salt Stressed Barley Shoot and Root Tissue.

Top panel, Shoot K⁺/Na⁺ Ratio (a) and bottom panel, Root K⁺/Na⁺ Ratio (b). ■, Zhou 1; ●, Zhou 85.

Samples were harvested and prepared as described in Chapter 2 and 4 in Sections 2.2.3 and 4.2.3 respectively. The data points are the Averages and SEs of four independent samples. Two factor analysis of variance (linear model) was performed on the data with Bonferroni pair-wise tests between treatment means. Different Roman characters signify significant differences ($p < 0.05$) between Zhou 1 treatment means; Greek characters, significant difference ($p < 0.05$) for Zhou 85 treatment means.

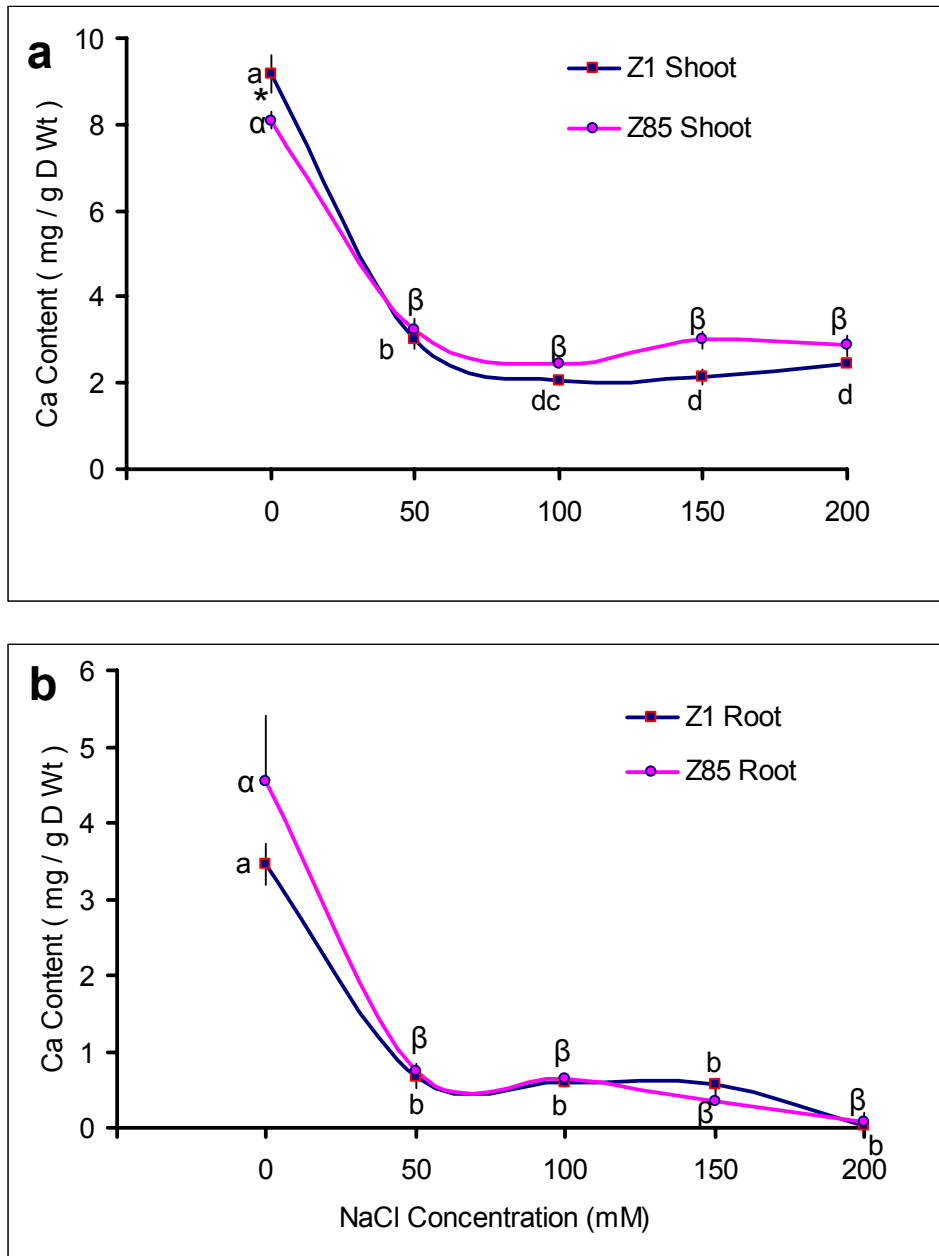


Fig. 4-19 Calcium Content of Salt Stressed Barley Shoot and Root.

Top panel, Shoot Ca⁺² Content (a) and bottom panel, Root Ca⁺² Content (b). ■, Zhou 1; ●, Zhou 85.

Samples were harvested and prepared as described in Chapter 2 and 4 in Sections 2.2.3 and 4.2.3 respectively. The data points are the Averages and SEs of four independent samples. Two factor analysis of variance (linear model) was performed on the data with Bonferroni pair-wise tests between treatment means. Different Roman characters signify significant differences ($p < 0.05$) between Zhou 1 treatment means; Greek characters, significant difference ($p < 0.05$) for Zhou 85 treatment means. Asterisks identify significant differences ($p < 0.05$) between Zhou 1 and Zhou 85 means at each given salt concentration.

4.3.5 Photosynthesis Measurements.

4.3.5.1 Photosynthesis Rates.

Several important parameters relating to the efficiency of the photosynthesis can be derived from the CO₂ and Light Response Curves (see Section 4.2.4).

4.3.5.1.1 A_{max} and Alpha (α).

The effect of salinity on the light-saturated maximum assimilation rate (A_{max}) obtained at 360 (ppmv) CO₂ for Zhou 1 and Zhou 85 are presented in Fig. 4-20a. These data indicate A_{max} values are maintained at near control levels (~25-30 μmol CO₂ m⁻² s⁻¹); only when exposed to salt levels above 150 mM NaCl does A_{max} decline significantly. No major differences in A_{max} were observed between the two lines.

The quantum efficiency (α) of both lines decreased with increasing salinity, from ~0.090 at 0 mM NaCl to ~0.075 at 200 mM NaCl. These data indicate the capacity of leaves to capture and process light energy is not severely impaired by the concentrations of salinity used here, and that no major differences were observed between the two lines (see Fig. 4-20b).

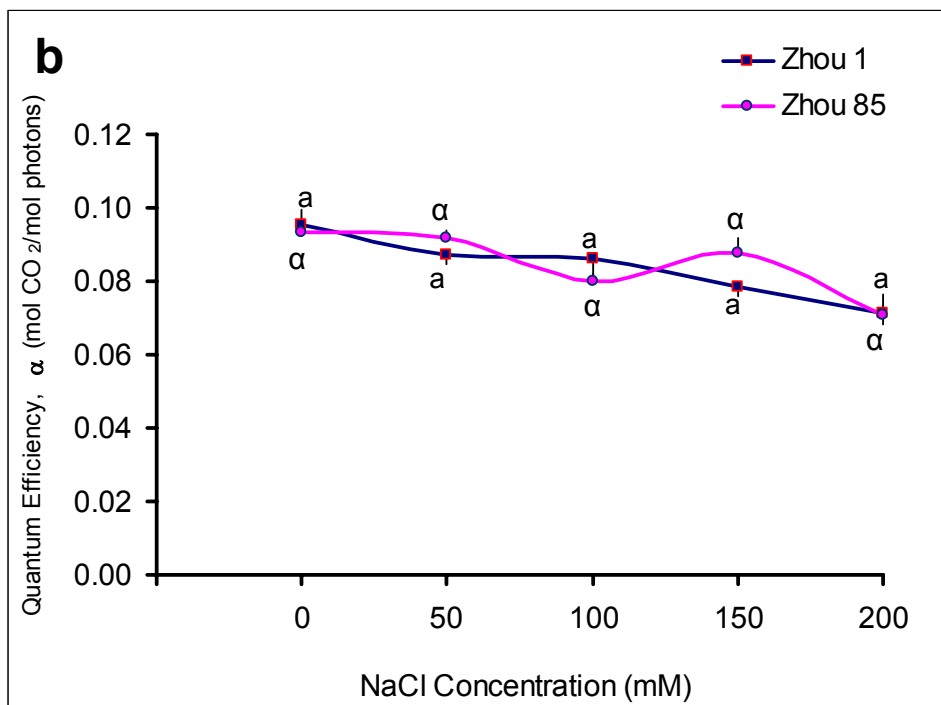
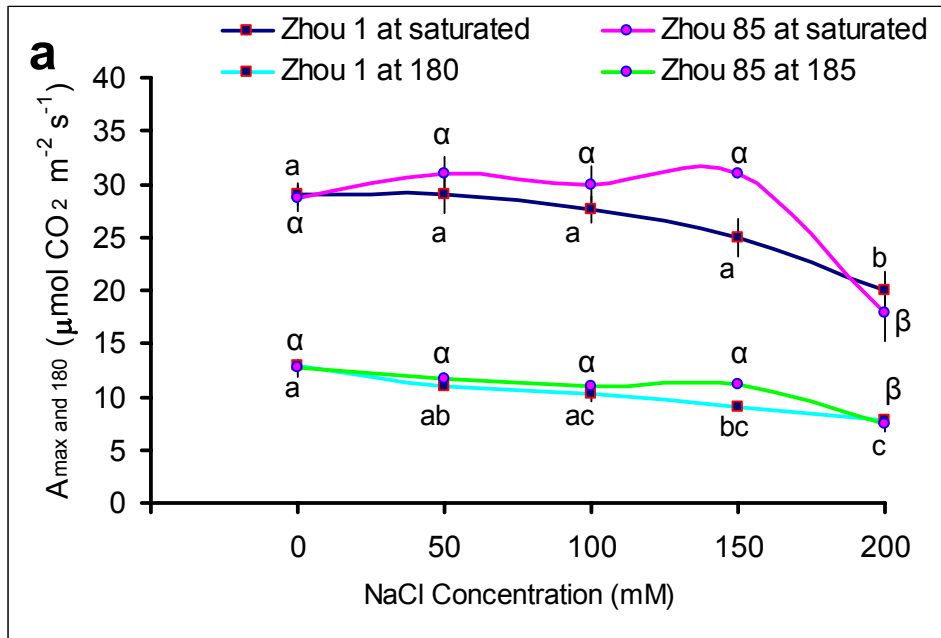
Fig. 4-20 The Effects of Salt Treatments on CO₂ Assimilation and Quantum Efficiency, α of Two Barley Lines.

Top panel (a), \blacksquare Zhou 1 light saturated assimilation rate (A_{\max} , saturated): \blacksquare Zhou 1 assimilation rate at growth room light levels ($180 \mu\text{mol m}^{-2} \text{s}^{-1}$ PAR). \bullet Zhou 85 light saturated assimilation rate: \bullet Zhou 85 assimilation rate at $180 \mu\text{mol m}^{-2} \text{s}^{-1}$ PAR.

Bottom panel (b). Zhou 1 (\blacksquare) and Zhou 85 (\bullet) quantum efficiency.

Other chamber conditions were; C_a , 360 ppmv; chamber temperature ($\sim 26^\circ\text{C}$); humidity, 10 mmol/mol; flow rate, 200 mmol s^{-1} .

Each data point presents the mean and standard error of four replicates. Measurements were made 26 days after germination (7 days after salt treatment) on fully expanded 4th emergent leaves. Assimilation rates and α values were determined from light response curves, as described in Section 4.2.4.1.2. Two factor analysis of variance (linear model) was performed on the data with Bonferroni pair-wise tests between treatment means. Different Roman characters signify significant differences ($p < 0.05$) between Zhou 1 treatment means; Greek characters, significant difference ($p < 0.05$) for Zhou 85 treatment means.



4.3.5.1.2 Photorespiration (Rl) and Dark Respiration (Rd).

For both barley lines photorespiration (Rl) values remained constant at ~ -4.5 ($\mu\text{mol CO}_2 \text{ m}^{-2} \text{ s}^{-1}$) with increasing salinity up to 100 mM NaCl and then decreased to ~ -3.0 ($\mu\text{mol CO}_2 \text{ m}^{-2} \text{ s}^{-1}$) see Fig. 4-21a. Dark respiration increased progressively with increasing NaCl concentration, from values of ~ -1.0 ($\mu\text{mol CO}_2 \text{ m}^{-2} \text{ s}^{-1}$) at 0 mM to ~ -2.0 ($\mu\text{mol CO}_2 \text{ m}^{-2} \text{ s}^{-1}$) at 200 mM NaCl see Fig. 4-21b. No major differences were observed between the two lines either Rl or Rd.

4.3.5.1.3 V_{rubisco} .

The efficiency of the C3 cycle *in vivo* can be estimated from the parameter V_{rubisco} ; as rubisco is usually the rate limiting step in the C3 cycle, the values of V_{rubisco} are routinely used to estimate the kinetic properties of rubisco *in vivo* (Yeo *et al.*, 1994).

Increasing NaCl concentration up to 100 mM had no major effect on V_{rubisco} although it appears to decline over this concentration range. For both lines values of ~ 0.12 mol $\text{CO}_2 \text{ m}^{-2} \text{ s}^{-1}$ were recorded and these declined to ~ 0.10 mol $\text{CO}_2 \text{ m}^{-2} \text{ s}^{-1}$ at 200 mM NaCl (see Fig. 4-22). The conclusion is that for both lines high levels of salinity at the roots do not result in an impairment line of the kinetics of the carboxylation processes in the chloroplast.

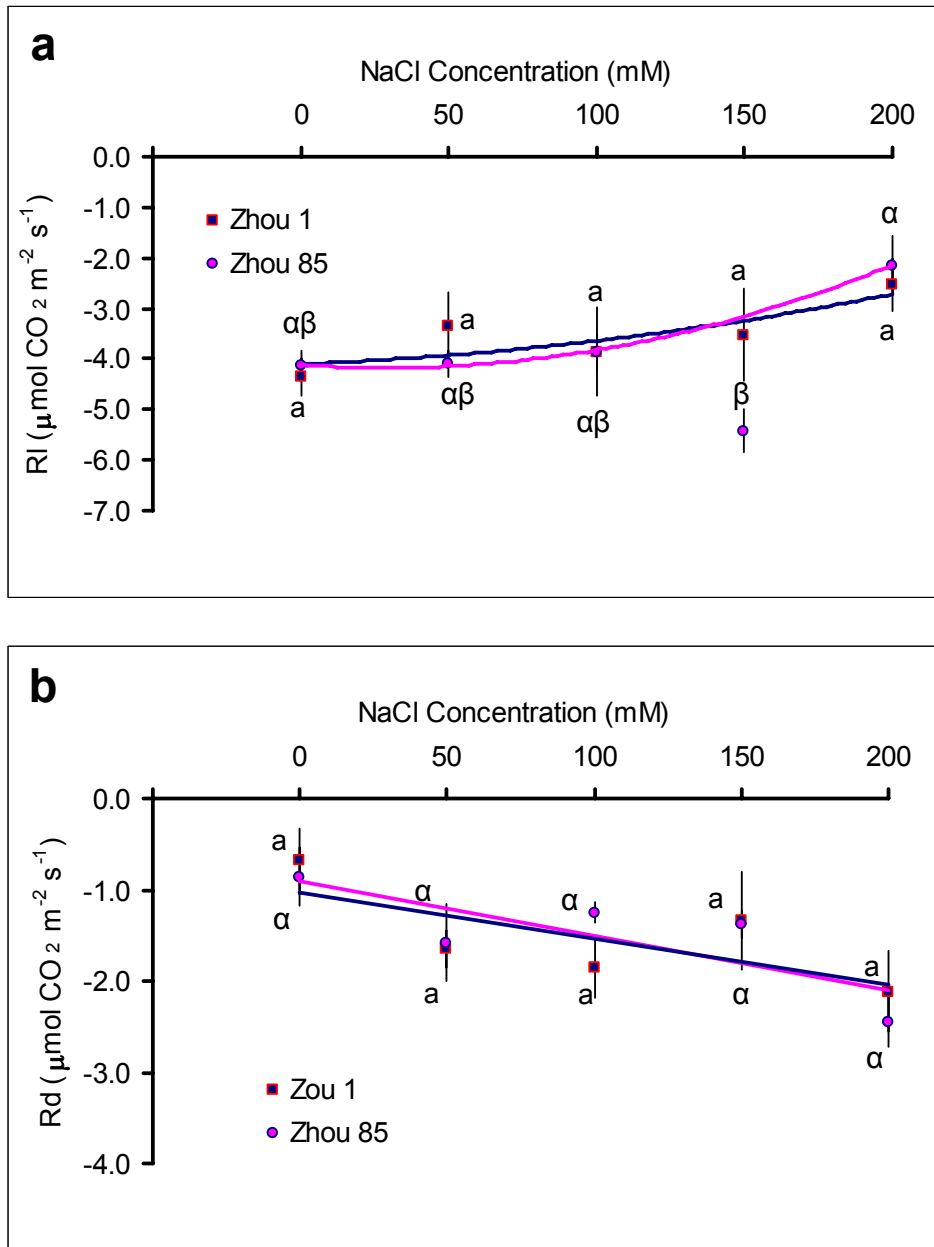


Fig. 4-21 The Effects of Salt Treatments on Photorespiration, RI and Dark Respiration, Rd of Two Barley Lines.

Top panel, photorespiration (a); bottom panel, dark respiration (b). ■, Zhou 1; ●, Zhou 85.

Each data point presents the mean and standard error of four replicates. Measurements were made 26 days after germination (7 days after salt treatment). Values of total respiration (RI + Rd) were estimated from CO₂ response curves (see Section 4.2.4.1.1) and values of Rd from light response curves (see Section 4.2.4.1.2). RI was then determined by difference. Two factor analysis of variance (linear model) was performed on the data with Bonferroni pair-wise tests between treatment means. Different Roman characters signify significant differences ($p < 0.05$) between Zhou 1 treatment means; Greek characters, significant difference ($p < 0.05$) for Zhou 85 treatment means.

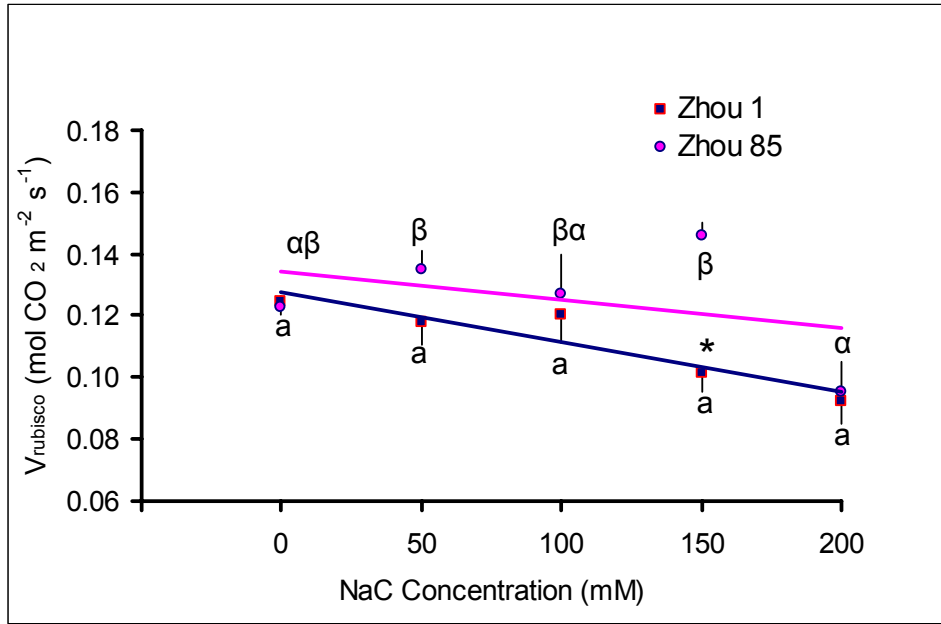


Fig. 4-22 The Effect of Salt Treatments on V_{rubisco} of Two Barley Lines.

V_{rubisco} for Zhou 1 (■) and Zhou 85 (●).

Each data point presents the mean and standard error of four replicates. Measurements were made 26 days after germination (7 days after salt treatment). See section 4.2.4.1.1 for experimental details. V_{rubisco} was determined from the initial slope of the A/C_i response curve (Fig. 4-3). Two factor analysis of variance (linear model) was performed on the data with Bonferroni pair-wise tests between treatment means. Different Roman characters signify significant differences ($p < 0.05$) between Zhou 1 treatment means; Greek characters, significant difference ($p < 0.05$) for Zhou 85 treatment means. Asterisks identify significant differences ($p < 0.05$) between Zhou 1 and Zhou 85 means at each given salt concentration.

4.3.5.2 *Carbon Dioxide Supply.*

Net photosynthesis rate can be affected by the efficiency of light capture, the efficiency of photosynthetic electron transport, the kinetic properties of the C3 cycle and respiration, and by the supply of CO₂ to the chloroplast (see Section 4.2.4.1). In this section the effect of salinity on CO₂ supply to the chloroplast is considered.

4.3.5.2.1 *Stomatal Conductance (gs) and Stomatal Control of Photosynthesis (L).*

Stomatal conductance (**gs**) decreased rapidly in both lines (from ~0.5 to ~0.25 mol m⁻² s⁻¹) as external NaCl increased from 0 to 50 mM NaCl (Fig. 4.23a). Higher salt concentrations produced only a minor decrease in both lines. No significant differences in **gs** were observed between the two lines.

A large reduction in **gs** might be expected to cause a reduction in Assimilation rate, but this is not observed when A_{max} values are considered (Fig. 4-20a); over the 0 – 50 mM NaCl range A_{max} does not change for either line. One explanation for this observation is that at high stomatal conductance (above 0.3 mol m⁻² s⁻¹), it is the kinetic properties of the C3 cycle that limits Assimilation, not the supply of CO₂ to the chloroplast. This hypothesis can be tested by studying changes in the parameter L with external NaCl concentrations. The parameter L is a measure of the relative importance of **gs** on Assimilation rate; values near 0 suggest a minimal effect, values near 1, a major dominant effect (see Section 4.2.4.1.1 for full discussion).

Figure 4-23b presents the response of the parameter L to increasing NaCl concentration. Generally, L increases (from 0.23 to 0.35) over the 0 to 200 mM NaCl concentration range, suggesting increased stomatal limitation on Assimilation rate as external salinity increases.

The plot of Assimilation versus stomatal conductance (*A versus gs*) shows sharp discontinuity at **gs** values of ~0.3 mol m⁻² s⁻¹ confirming the observation that only when

g_s is lower than $0.3 \text{ mol m}^{-2} \text{ s}^{-1}$, is photosynthesis impaired significantly by the CO_2 supply to the chloroplast (Fig. 4-24).

From the light response curves, another parameter, theta (θ), can be determined that is reported to reflect the relative contribution of CO_2 supply and C3 cycle kinetics to Assimilation rate (see Section 4.2.4.1.2). Values of θ approaching 1 are reported to reflect strong limitation through reduced CO_2 supply, whilst values approaching 0 are believed to show limitations impaired at the enzyme level (Akhkha *et al.*, 2001; Thornley, 1976). In the experiments reported here θ remained at values of ~ 0.5 regardless of external NaCl concentration of barley line see Appendix (Fig. A 4-6). The observation that θ did not vary with g_s suggests that θ is not related to the relative limitations on assimilation rate, but may reflect developmental changes in leaf architecture (Leverenze, 1987; Leverenze, 1988; Ogren, 1993; Ogren and Evans, 1993; Terashima and Saeki, 1983).

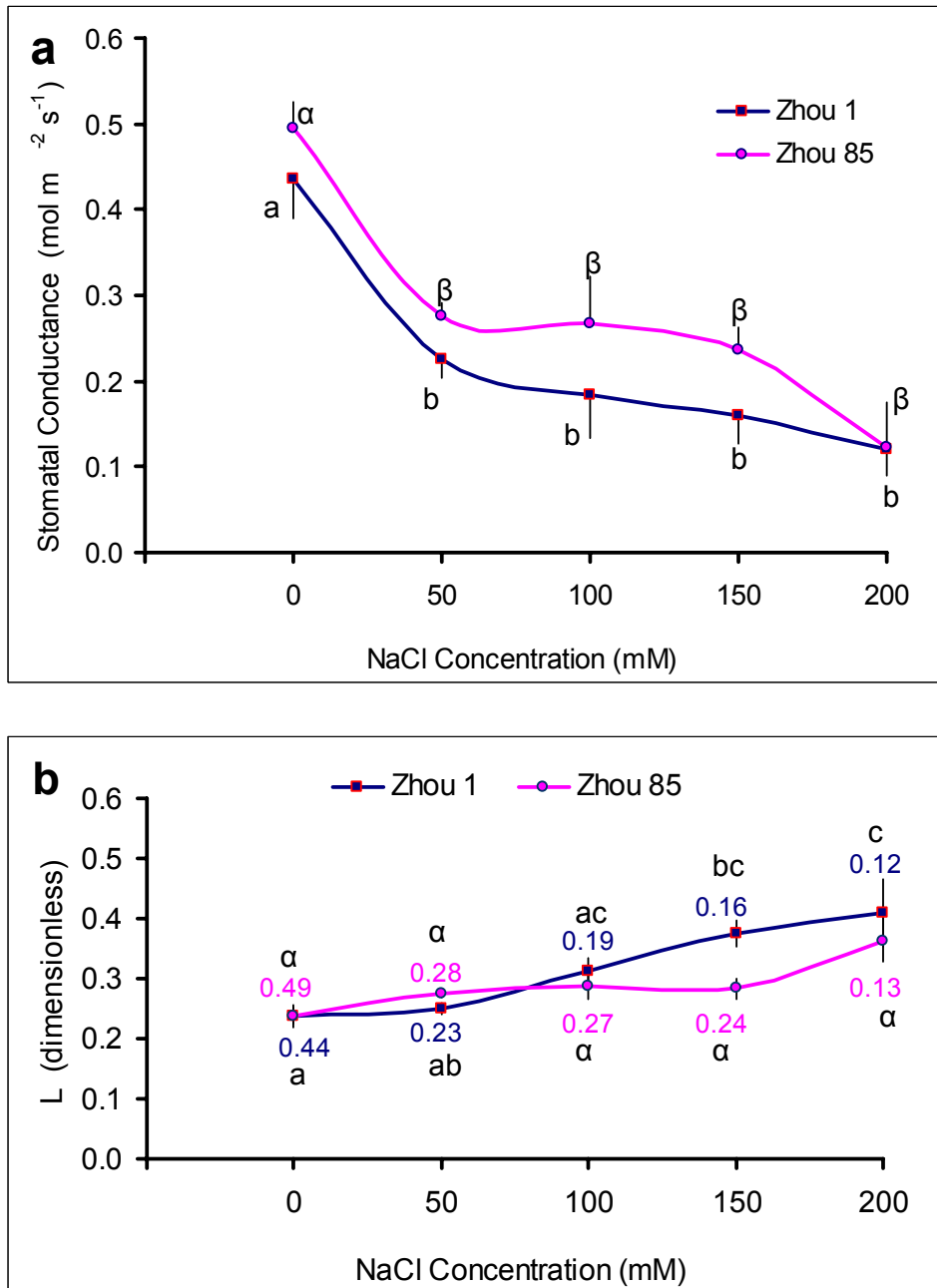


Fig. 4-23 The Effects of Salt Treatments on Stomatal Conductance, (g_s) and Stomatal Control of Photosynthesis, (L) of Two Barley Lines.

Top panel, stomatal conductance, g_s (a); bottom panel, stomatal control of photosynthesis, L (b). ■, Zhou 1 ● Zhou 85.

Each data point presents the mean and standard error of four replicates. Measurements were made 26 days after germination (7 days after salt treatment) on fully expanded 4th emergent leaves. See section 4.2.4.1 for experimental details. Average values for L are presented (panel b). Two factor analysis of variance (linear model) was performed on the data with Bonferroni pair-wise tests between treatment means. Different Roman characters signify significant differences ($p < 0.05$) between Zhou 1 treatment means; Greek characters, significant difference ($p < 0.05$) for Zhou 85 treatment means.

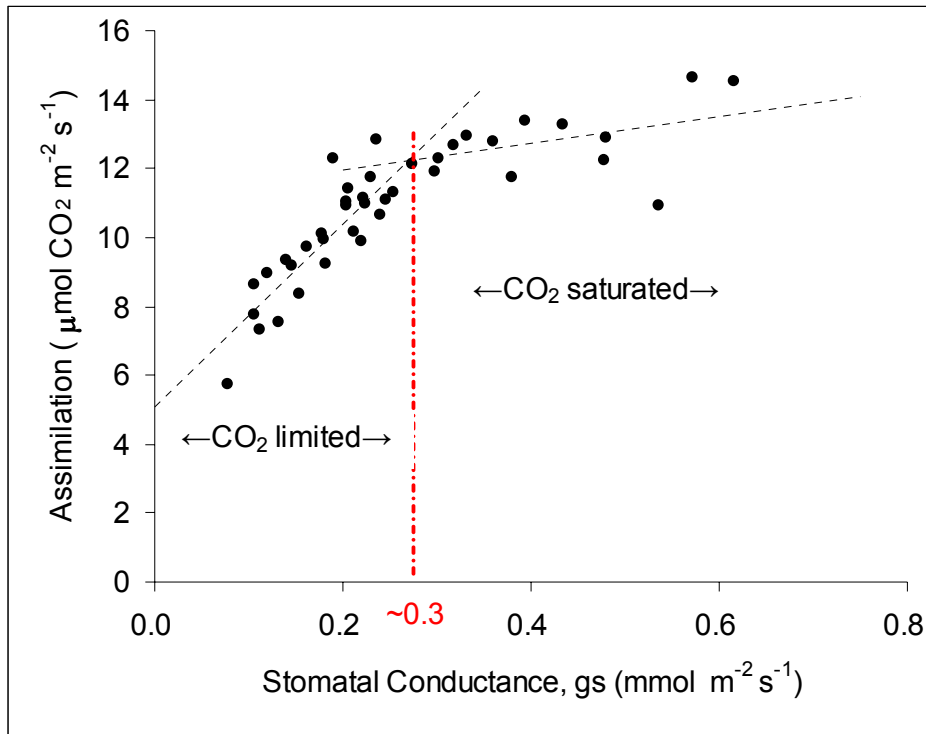


Fig. 4-24 Assimilation rate (A) Versus Stomatal Conductance (gs) of two barley lines.

Assimilation rates (A) were plotted against the corresponding values for stomatal conductance (gs); both values were estimated from light response curves at $180 \mu\text{mol m}^{-2} \text{s}^{-1}$ light intensity, the level at plant height in the growth room (see section 4.2.4.1.2 for experimental details). No differences were found between lines Zhou 1 and Zhou 85 and so data (●) were pooled. Linear regression lines (---) were fitted to the data to emphasize the apparent disjunction at the gs value of $0.3 \text{ mmol m}^{-2} \text{s}^{-1}$ (|). At gs values below $0.3 \text{ mmol m}^{-2} \text{s}^{-1}$, A appears to be linear dependant on gs; above this value A appears to be largely independent of gs.

4.3.6 Development Measurements.

The observation reported in Section 4.3.1 and 4.3.2 suggest that line Zhou 1 undergoes the transition from vegetative growth to reproductive growth earlier than Zhou 85, and this may reduce the exposure time of the reproductive structures to salinity, resulting in improved yields. To establish the developmental delay between Zhou 1 and Zhou 85, sixteen plants of each line were placed in soil, germinated and grown to maturity in a glass house as described in Section 4.2.5. At least every second day their development was assessed using the Zadoks' Scale (Zadoks *et al.*, 1974). The Zadoks' scale extends from 0 (dry seed), through germination (1-9), seedling growth (10-19), tillering (20-29), stem elongation (30-39), booting (40-49), inflorescence emergence (50-59), anthesis (60-69), milk stage (70-77), and ripening (80-99); see Appendix (Fig. A 4-2 and Table A 4-2). Once individual plant scores were allocated at each day, the average delay in development (in days) was calculated and plotted (Fig. 4-25). It is clear that in the absence of NaCl, Zhou 1 enters the reproductive phase of the life cycle (day 39, anthesis) approximately 6 days earlier than Zhou 85, and by the milk stage (day 44) is fully a week ahead of Zhou 85. The implication is that ten days of exposure to high salinity (day 19-29) does not result in a sufficient level of stress to prevent the development of the gametes or embryo. However, the longer periods of exposure (up to 17 days), as experienced by Zhou 85 before anthesis, may result in sufficient shoot stress that severely impair seed development.

4.3.7 Assessment of Ppd-H1 Flowering Locus.

Commercially grown barley is available as winter barley (delayed flowering) and spring barley (early flowering) lines. The locus controlling flowering in barley has been known for many years and named the photoperiod-H1 locus (Ppd-H1) but other loci (e.g. VRN 1-3) in cereals have also been implicated (Yan *et al.*, 2004; Yan *et al.*, 2003). Early

flowering lines carry a dominant allele, Ppd-H1, whilst delayed flowering lines carry a recessive allele ppd-H1. The identify of the Ppd-H1 gene was revealed by positional cloning and found to encode a 'Pseudo-Response' regulator protein with homology to the Arabidopsis clock gene CONTANS (CO) (Turner *et al.*, 2005). Further extensive Single Nucleotide Polymorphism (SNP) analysis with an extensive collection of early and delayed flowering lines identified SNP 22, a G to T (glycine to tryptophan) substitution (Turner *et al.*, 2005) as the critical SNP causing the observed difference in flowering time.

To assess whether the observed delayed flowering in Zhou 85 line was attributable to a similar substitution, PCR primers were designed to amplify this region of barley genomic DNA. The test interval containing the putative SNP 22 variant was amplified using test primers (HvTF; ATG CGA ATG GTG GAT CGG C and HvCR; TAT AGC TAG GTG CGT GGC G) and the 506 bp PCR product digested with BstU 1 restriction site (ppd-H1) whereas the dominant allele (Ppd-H1) is cut to produce a 432 and 74 bp product. Figure 4-26 shows the digested and undigested PCR products for Zhou 1 and Zhou 85; clearly, in both cases the 506 bp PCR fragment has been restricted indicating both Zhou 1 and Zhou 85 contain the Ppd-H1 (early flowering allele).

It is well established that the barley locus Ppd-H1 has a profound influence on flowering in cereals. Dominant forms of the locus (Ppd-H1) flower early, and is associated with spring barley. In contrast, homozygous lines carrying the recessive ppd-H1 locus, require a longer period to flower and constitute the winter barleys (Turner *et al.*, 2005; Laurie *et al.*, 1995).

In conclusion, it appears the delayed flowering response of Zhou 85 is not associated with the Ppd-H1 locus.

Fig. 4-25 Comparison of the Rate of Development of Zhou 1 and Zhou 85 Barley Lines.

Plants were germinated and grown in soil as described in Section 4.2.5. The development of both lines was scored according to the Zadok's scale (see Appendix Fig. A 4-7 and Table A 4-3). The development of Zhou 85 compared with Zhou 1 is presented (n=16 plants) for each line.

Panel (a), modal Zadok's score (n=16) for Zhou 1 and Zhou 85. note, early and late development are in phase, but reproductive development in Zhou 1 up to one week earlier than in Zhou 85. panel (b), Days Zhou 85 Developmental Delay. Zhou 1 and Zhou 85 plants were randomly ascribed an index number (1-16) at germination and for each Z 85/Z 1 pair the time difference (days) for Z 85 (*cf* Z 1) to enter each of the Zadoks stages (1-99) was determined. From these values, the average delay (in days) was calculated. Plants were not treated with NaCl, but in the experiments reported in Sections 4.3.1 to 4.3.5, exposure was given at Day 19 (orange arrow). Significant developmental stages are presented as Tillering (1), Inflorescence Emergence (2), Anthesis (3), and Kernel Hardening (4). See Appendix Table A 4-2 for raw data.

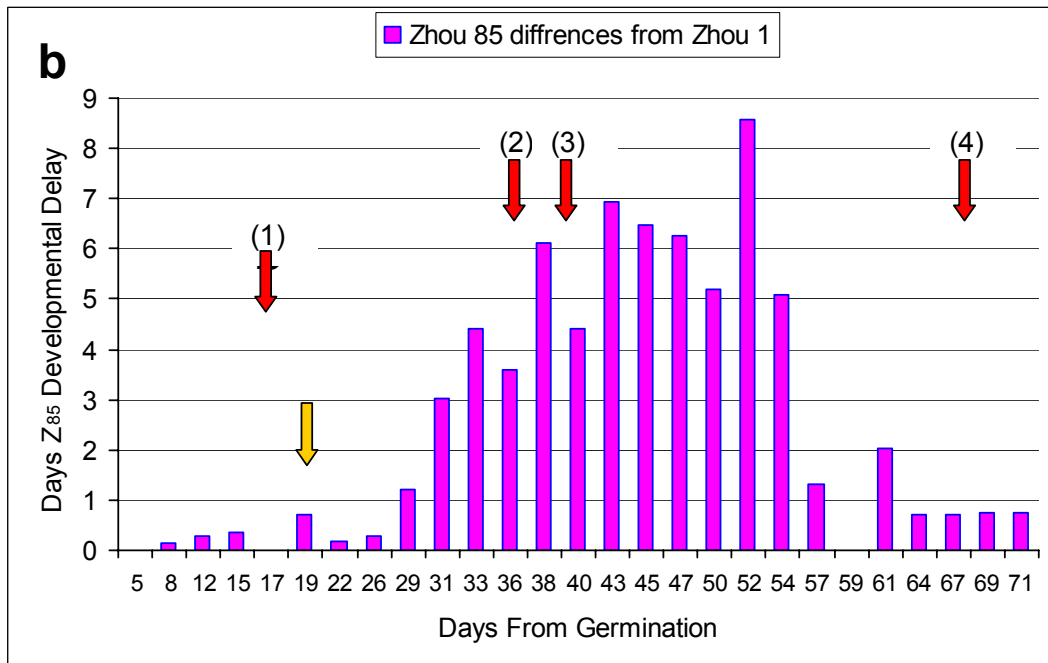
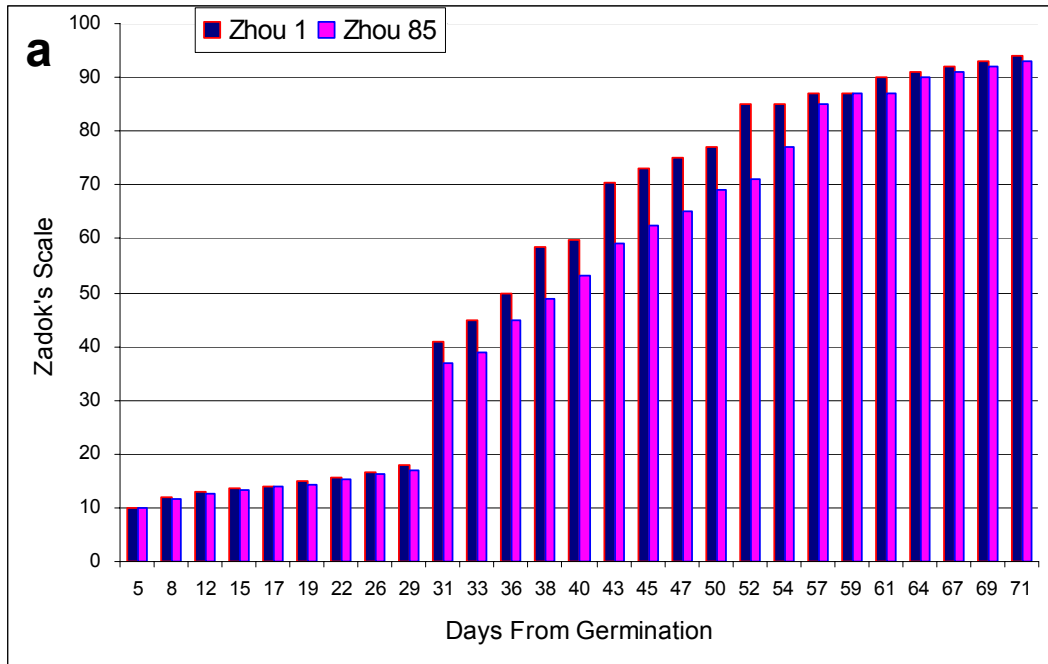
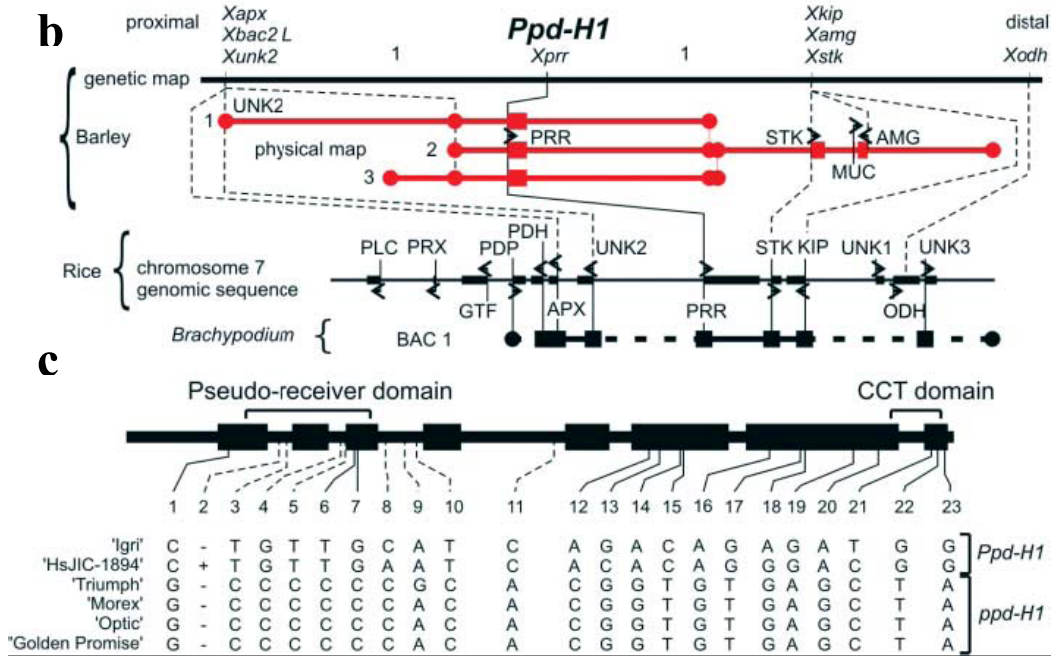
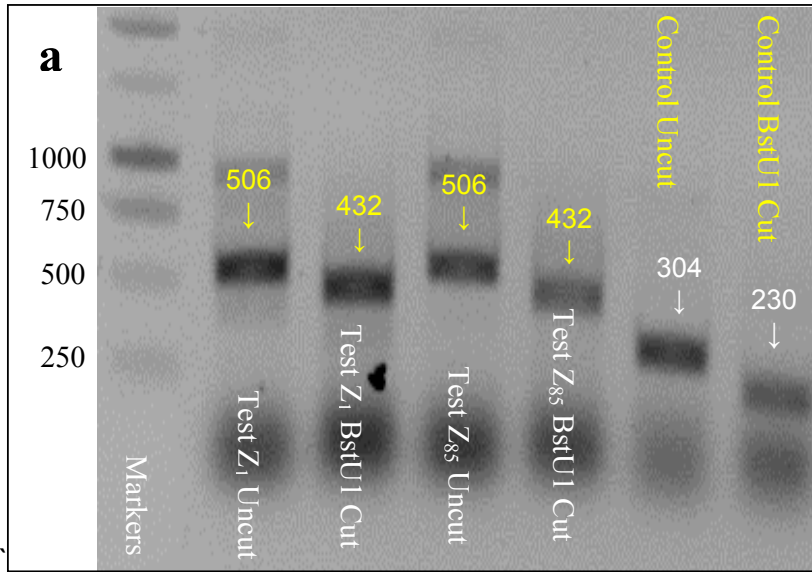


Fig. 4-26 Genotyping Zhou 1 and Zhou 85 Barley Lines for the Early Flowering Locus Ppd-H1.

Panel (a); PCR for Ppd-H1 (dominant) and ppd-H1 (recessive) alleles of the early flowering locus in barley. PCR primers were used that amplifies a 506 bp product containing SNP 22 (a G/T substitution giving rise to a Glycine/ Tyrosine substitution). Restriction digests of this 506 bp fragment with BstU1 will generate a 432 bp fragment if the Ppd-H1 locus is present, but remains uncut if the ppb-H1 it appears that both the Zhou 1 and Zhou 85 506 bp PCR fragment (lanes 2 and 4) are cut on BstU1 treatment (lane 3 and 5), and therefore both lines carry the dominant early flowering locus, Ppd-H1. Lane 1, molecular weight markers: lanes 6 and 7 controls for BstU1 activity.

Panel (b), schematic diagram showing location of Ppd-H1 locus on barley chromosome 3 taken from (Turner *et al.*, 2005).

Panel (c), schematic diagram showing all 23 SNPs between early (Ppd-H1) and late (ppd-H1) flowering lines of barley. SNP 22 has been identified as that associated with the Ppd-H1 locus (Turner *et al.*, 2005).



4.3.8 Discussion.

In this chapter the claim that barley line Zhou 1 is more salt tolerant than Zhou 85 was investigated. Other groups (Pro. Zhang, G, Zhejiang University, China; Fig. 4-1), suggested this was so, and therefore experiments were designed and undertaken to establish the effects of salinity on a number of parameters in these two lines. These parameters included those relating to vegetative growth, yield, water status, ionic status, assimilation and respiration rates, and stomatal function. The results are summarized below.

Clear and significant differences between the two lines were observed in the development of the shoot and root. At the time of measurement (day 37) line Zhou 1 was significantly taller than Zhou 85 (Fig. 4-7a), and at low external NaCl concentrations attained more fresh (Fig. 4-8) and dry weight (Fig. 4-9).

Interestingly, the longer shoots of Zhou 1 were accompanied by shorter roots (Fig. 4-7a) although no difference in root biomass was observed (Fig. 4-8b and 4-9b). Zhou 1 produces fewer tillers than Zhou 85, a feature that was retained at all external NaCl concentrations (Fig. 4-10). Taken together, these results suggest that at the time of measurement (day 37) line Zhou 1 had diverted more of its resource away from producing tillers and put more into flower development (Fig. 4-6). The question that should now be addressed is whether this strategy affects yield.

Measurements on yield parameters suggested Zhou 1 does yield better than Zhou 85 at all external NaCl concentrations, but particularly above 100 mM NaCl (Fig. 4-12a and b). Line Zhou 85 failed to produce seed at 150 mM NaCl and above; in contrast, although the yields of Zhou 1 in 200 mM NaCl were only ~8% of those at 0 mM NaCl, seed was produced (viability of the seeds was not tested). Other yield parameters indicated that in high salinity Zhou 1 produced larger seed (Fig. 4-13), and more seed

per plant (Fig. 4-11), the latter arising from the ability of Zhou 1 to produce 1 floral spike per plant. The conclusions are that the early transition of Zhou 1 into flowering may be responsible for partly offsetting the salinity-induced losses in or experienced by Zhou 85 (Fig. 4-12b).

It is conceivable the modest improvement in yield observed with line Zhou 1 is attributable to the early floral development. Gamete and/or embryo development may be very sensitive to high salinity, and so early development before the levels of salinity in the developing flower become toxic may offer a significant advantage.

Chapter 5: General Discussion

At the outset of this study the intention was to compare and contrast the response of salt-sensitive and salt-tolerant cell cultures of higher plants to high salinity. It was hoped that this approach would identify cellular processes that contribute to salt tolerance in whole plants. For this purpose two cell suspension cultures of *Arabidopsis thaliana* were available; one was salt-sensitive (WT) and would not survive above 80 mM NaCl, the other was salt-tolerant (HHS) and survives in up to 380 mM NaCl. These two cell lines should allow an investigation into potential salt tolerance mechanisms in cells from the glycophyte *Arabidopsis thaliana*. To determine whether the mechanisms identified in the HHS cells are typical of those found in the cells of halophytes, cell suspension cultures were also prepared from the leaves of the dicots sugar beet (*Beta vulgaris*) and *Atriplex halimus*, and from the monocots *Distichlis spicata* (all halotolerant) and rice (*Oryza sativa*). It was hoped that physiological, biochemical, and molecular comparisons between these cell lines would provide a consensus view on salt tolerance mechanisms in higher plants, at least at the cellular level.

Unfortunately, although these cell lines were produced, continuous failures of the growth facilities were encountered over a period of eighteen months and this prevented completion of these experiments. Consequently, only a full set of experiments for comparisons between WT and HHS cells from *Arabidopsis thaliana* are presented. To augment these experiments on cell suspension cultures, a whole plant study was undertaken to investigate salt tolerance mechanisms in barley (*Hordeum vulgare*). Two varieties of spring barley that are widely grown in China were donated by Professor Guoping Zhang (University of Zhejiang, China) that are reported to differ in their

sensitivity to NaCl. The origin of these two lines is unclear; they may have originated from European lineages that have been selected and bred mainly for malting quality, or from Tibetan (Asian) lineages that have been selected for stress tolerance, or they may be hybrids of European and Asian lines. These two spring barley lines were grown in hydroponic solutions containing a range of NaCl concentrations, and their performance assessed at the physiological and biochemical level.

5.1 Assessment of the Halotolerance of WT and HHS *Arabidopsis thaliana* Cell Suspension Cultures.

The growth rates of WT cell cultures were impaired by increasing levels of NaCl in the culture medium. The doubling time of cultures containing 50 mM NaCl was reduced to 75% of that of controls (0 mM NaCl) and growth ceased completely if NaCl concentrations were raised above 80 mM NaCl. It appears this salinity-induced suppression of growth is mainly attributable to ionic effects as growth in isotonic media containing low (0 mM) NaCl (*i.e.* BGM0_{0.77}) suppressed growth to only 96% of controls. In contrast, the growth of HHS cells in 0 mM NaCl (BGM0_{0.55}) was consistently slower than that of WT cells (~65%). The growth rates of HHS cells in 300 mM NaCl were approximately the same as those in 50 mM NaCl. All of this decrease appears to have arisen from osmotic stress as a similar decline was observed in low salt isotonic media (BGM0_{1.96}). When grown in 50 mM NaCl a similar decline (~60% of control) in growth rates were observed but only approximately half of this was attributable to osmotic stress. It appears that moderate levels of salinity stress (50 mM NaCl) induces ionic and osmotic stress, but growth reduction in severe stress (300 mM NaCl) may be mainly attributable to osmotic stress.

From these results it can be concluded that relatively low levels of NaCl (*i.e.* 50 mM) impairs the growth of WT *Arabidopsis* cells mainly by the toxic effects of Na⁺ and/or

Cl⁻. This conclusion is supported by measurements of the ion content of cells during their growth phase. Intracellular Na⁺ levels were approximately five times higher in WT cells than HHS cells when they were grown in identical cultures of 50 mM NaCl.

Halotolerance of higher plant cells has been attributed to any one or combination of three physiological strategies: the ability to prevent the accumulation in the cytoplasm of toxic levels of Na⁺ and Cl⁻; the ability to acquire and maintain normal levels of nutrient ions when exposed to saline media; the ability to offset the dehydrating effects of the external saline media.

Taken together the results from the experiments on cell suspension cultures suggest that the sensitivity of WT Arabidopsis cells to salinity is largely attributable to their inability to prevent the accumulation of toxic intracellular levels of Na⁺ (and possibly Cl⁻). In contrast, HHS cells prevent this accumulation and are therefore able to survive media containing much higher levels of NaCl (up to 380 mM). No evidence was found to support the contention that HHS cells are better adapted than WT cells at acquiring or maintaining nutrient ions when exposed to salinity. Some evidence was found to suggest that in moderately low levels of salinity (50 mM NaCl) the growth of both WT and HHS cells is impaired partly by osmotic effects, but any conclusions should be treated with caution. First, dehydration of cells is likely to increase intracellular concentrations of ions in the cytoplasm so growth impairment may be caused directly by ionic effects that arise indirectly from water loss from the cell. Second, in the experiments reported here, the osmotic stress induced by shifting cells from media containing 0 mM to 50 mM NaCl is trivial. The solute potential (Ψ_s , here, at atmospheric pressure, equivalent to the water potential, Ψ_{H_2O}) of BGM0_{-0.55} is -0.55 MPa and that of BGM50_{-0.77} is -0.77 MPa. These values compare favorably with the range of Ψ_{H_2O} of the shoots of well hydrated plants growing in soils with high field

capacities (typically -0.7 to -1.2 MPa); most plants begin to show signs of wilting (loss of turgor pressure, Ψ_p) only when shoot Ψ_{H_2O} fall below -1.2 MPa.

Unfortunately, it was not possible to measure the components of the Ψ_{H_2O} (*i.e.* Ψ_s and Ψ_p) of WT and HHS cells in different conditions, but it is possible to speculate on what these might be. If the cells were not capable of osmoregulation, in BGM50_{-0.77} they would adopt the Ψ_{H_2O} of the growth media (*i.e.* -0.77 MPa). Typical values for shoot cell Ψ_s is in the range -1.5 to -2.5; therefore, without any attempt to osmoregulate Ψ_p values of at least 0.73 and 1.73 MPa would be expected ($0.73 = -1.5 + 0.77$, and $1.73 = -2.5 + 0.77$), and these are well within the range of turgor pressures found in well-hydrated plant cells and of sufficient magnitude to support cell expansion. If we now superimpose the effect of osmoregulation on this situation (*i.e.* a decrease in cell Ψ_s through the acquisition of compatible and incompatible solutes), even greater turgor pressures and/ or higher (less negative) cell water potentials would occur further decreasing the effect of any osmotic stress. Both the experimental evidence from these results, and theoretical considerations, therefore, strongly indicate that it is only the ionic component that impairs the growth of WT Arabidopsis cells in culture. Following the same reasoning, it seems likely that the inability of Arabidopsis plants to grow in media containing physiologically significant levels of nutrient ions supplemented with 100 mM NaCl is attributable entirely to the ionic component of the salinity stress as even without the beneficial effects of osmoregulation, tissue water potentials and turgor pressures of < -0.6 MPa and ~0.9 MPa, respectively, would arise (assuming a cell Ψ_s of -1.5MPa)¹. On this basis salt concentrations of 200 mM NaCl would at worst reduce Ψ_{H_2O} to -1.0 MPa and Ψ_p to 0.5 MPa, again levels that are consistently

¹ Conversion from Concentration to Pressure units using the Vant Hoff relationship, $P = (n/v) R T$ with $R = 8.314 \cdot 10^{-3} \text{ MPa M}^{-1} \cdot \text{K}^{-1}$. The osMolar concentration of physiologically significant growth media plus 100 mM NaCl is taken as 0.25 osM.

found in well-watered plants. Perhaps a research focus on manipulating cellular components associated with osmoregulation to offset salt stress in glycophytes is not of the highest priority.

There is clear evidence that HHS cells maintain low intracellular levels of Na^+ when compared with WT cells. This observation also supports the contention that osmoregulation is not a critical response for the survival of Arabidopsis cells at low levels of NaCl (*i.e.* 50 mM); if it were, one would expect the halotolerant HHS cells to take up and sequester more Na^+ in their vacuoles than WT cells in an attempt to regain turgor (osmoregulate) and this does not appear to be the case. Instead, it is WT cells that accumulate high levels of Na^+ , and presumably they cannot sequester it all in their vacuoles, hence cellular metabolism is compromised and growth and survival are affected. At this stage it is not clear whether HHS cells maintain low intracellular levels of Na^+ by showing reduced rates of Na^+ uptake, increased rates of Na^+ efflux, or both. To address this question the kinetics of Na^+ exchange between both cell lines and the growth media will have to be determined. These investigations are currently underway using $^{22}\text{Na}^+$ uptake and efflux experiments by our group.

One of the interesting morphological differences between HHS and WT Arabidopsis cells was the appearance of a large number of small vacuoles / vesicles in the halotolerant line when they were exposed to a salt stress. These vesicles / vacuoles were greatly reduced in number in WT cells although a few did appear when cells were shifted to 50 mM NaCl. In HHS cells it was noted that the number of these vesicles appeared to increase when cells were given a shock, by either transferring them from higher to lower salinity, or *vice versa*. The steady state number of vesicles, however, always seemed greater when growth conditions were harshest. Cell lines from the halophytes sugar beet and *Atriplex halimus* were established in this study, and these

cell lines also appeared to show an enhanced level of vesicle proliferation when exposed to salt stress although the evidence for this is anecdotal. It might be that intracellular vesicle proliferation is a general response of halotolerant plant cells to salinity stress, a property that is not well developed in the cells of glycophytes. Further experiments using a range of plants and confocal imaging techniques will be required to confirm this observation.

It is unclear what function these intracellular vesicles perform. Although there was a proliferation of these vesicles in HHS cells grown in 50 mM NaCl, the accompanying low levels of intracellular Na⁺ suggest that they do not accumulate large quantities of this ion, at least not at this external NaCl concentration. It is conceivable, however, that as external levels of Na⁺ rise (> 100 mM) the damaging effect of increased Na⁺ influx is offset by rapid sequestration into these vesicles. From a kinetic perspective, sequestration of Na⁺ into intracellular vesicles/vacuoles would be achieved more rapidly with a large number of small vacuoles than a single large central vacuole as this would offer a larger membrane surface area-to-volume ratio. Once fully loaded with Na⁺ these vesicles / vacuoles may migrate to the central vacuole or plasma membrane and eject their contents. Alternatively, they may be static organelles that are Na⁺ stores. The dynamics of these vesicles was studied in HHS cells for up to 5 hours using confocal imaging, but no evidence was found for trafficking, and their function, therefore, is not clear. One approach that could determine the function of these vesicles would be to attempt to fractionate the cells and purify the population of vesicles. This would allow biochemical analysis of the vesicles with respect to their associated enzyme activities and protein content and from this information their function might be inferred.

5.2 Proteome Analysis of Arabidopsis HHS Cell Suspension Cultures Exposed to Salt Shock.

A proteome approach was used in this study to identify Arabidopsis sequences that might confer halotolerance upon HHS cells. Previously others in our laboratory had used Affymetrix DNA microarray chips to assess the transcriptome profile of WT and HHS cells. In their first experiments over 10% of the transcripts changed significantly when the profiles of cells grown in BGM0_{0.55} and BGM50_{0.77} were compared. In an attempt to reduce these changes to a manageable level, the subsequent microarray experiments were conducted under isotonic conditions (*i.e.* BGM0_{0.77} and BGM50_{0.77}).

Over one hundred proteins were identified by DiGE to change their abundance upon salt shock. Due to the high cost of protein sequencing, eighty-six were selected for identification by mass spectrometry. Approximately half of these were up regulated in high salt, nine were down regulated in high salt, and thirty two showed a consistent change (either up or down regulation only) regardless of whether they were exposed to a high or low salt shock. There is a general consensus that the regulation of ion balance is the major physiological trait for the attainment of halotolerance in plants. The precise regulation of ion content in salt stressed cells and tissues will prevent the accumulation of toxic levels of Na⁺ and Cl⁻, allow normal levels of nutrient ions to occur, and enable osmoregulation for the development of an appropriate turgor pressure.

The 2-dimensional DiGE proteome analysis of salt-shock HHS cells did not identify any difference in the abundance of major ion transporters of the plasma membrane or tonoplast that might account for improved halotolerance by Na⁺ and/or Cl⁻ export from the cytoplasm. There are several reasons that might explain this deficiency. First, it is

well known that DiGE is not particularly well suited to resolving hydrophobic proteins residing in membranes. Although several transporters associated with organelle membranes were detected, separation of hydrophobic proteins is reported to be more efficient using 2-dimensional liquid chromatography methods; these facilities were not available at Glasgow University at the time. Second, it is not at all clear that Na⁺ (or Cl⁻) flux through transporters on the plasma membrane (*e.g.* AtSOS-1) or tonoplast (*e.g.* AtNHX1) is ever near the V_{max} for these transporters, as it is only if this is the case that increasing the density of transporters will increase flux. To view this another way, the rate of transport is dependent upon the driving force and the conductance pathway. The driving force for coupled Na⁺ and/or Cl⁻ efflux from the cytoplasm is supplied by the pH and ion gradients, and the membrane proteins across the respective membrane. Therefore, if efflux is limited by the driving force, increasing the number of ion transporters will have no effect on cytoplasmic ion concentration. Indeed work by Gaxiola and colleagues showed that halotolerance was improved only if the vacuolar Na⁺/H⁺ antiporter AtNHX1 and an energizing H⁺ pump (AtPPIase) were co-expressed (Gaxiola *et al.*, 1999). Further, it is clear that the activity of all transporters (channels, carriers, and pumps) are subject to regulation through a variety of means (oligomerization, phosphorylation, ubiquitination/sumoylation, 14-3-3 protein binding, *etc.*) and it follows that manipulating these regulatory processes is perhaps more likely to confer a benefit than altering the abundance of the transporters *per se*.

It was anticipated that the proteome analysis of salt-shocked HHS cells would identify proteins that are involved with halotolerance. From the lists of consistent changes, however no clear picture has emerged on what cellular and metabolic processes may be associated with salt tolerance. None-the-less, significant and reproducible changes in

over one-hundred proteins were catalogued and it remains to be established whether these changes have a biological meaning.

Experiments were undertaken in our laboratory to determine the changes in transcript profile of HHS cells salt-shock under similar conditions (Dr. J. Price, University of Glasgow), but the recorded changes from Arabidopsis gene chip analysis were not consistent with those reported here from proteome profiling. There are several possibilities to explain this discrepancy. First, it is clear that changes in transcriptional activity are not always reflected by commensurate changes in protein abundance. Second, as already mentioned, hydrophobic proteins not well resolved by 2-dimensional DiGE. Another possibility is that both transcript and proteome provide a reliable assessment of stress-induced changes in cell responses to salinity, but as these experiments were not performed in parallel, temporal changes in the cell cultures generated spurious artifacts. On reflection, it will be more useful to perform these experiments on the same cultures, and in addition, attempt to resolve changes in the metabolome of these cells. If these experiments were undertaken in parallel on the same samples a better understanding of the general applicability of transcriptome, proteome, and metabolome profiling of plant tissues should emerge. In addition, it may be possible to establish which cellular processes are damaged by salt stress, and which are involved in the amelioration of stress.

5.3 Comparison of Salt Stress in Two Barley Lines.

The overall conclusion from the experiments on the barley lines is that Zhou-1 is marginally more salt-tolerant than Zhou-85, but neither can be considered salt-tolerant. For most growth and yield parameters, Zhou-1 was less affected by increasing salinity than Zhou-85 but neither line yielded well when grown in concentration above 100 mM

NaCl. Zhou-1 appears to establish a higher K^+ shoot/root ratio than Zhou-85, but Na^+ levels in root and shoots were similar for both lines.

None of the instantaneous photosynthetic parameters measured showed a major decline that paralleled the decline in growth or yield parameters. Assimilation rates measured at growth cabinet light levels ($180 \mu\text{mol m}^{-2} \text{s}^{-1}$) declined only 40% and V_{Rubisco} (a measure of the apparent V_{max} of the C3 cycle) declined only 20%, whereas shoot dry weight decreased by 60-80%. These photosynthetic parameters, however, were measured on living green tissues and are expressed on a unit leaf area basis. They do not, therefore, reflect the cumulative effect of salt stress on the proportion of living green tissues that contribute to plant growth. It is recommended that some attention is paid to estimating the amount of living and dead tissues in further studies. The results presented here do not show major effects of salinity on many photosynthetic parameters expressed on a per unit leaf area basis but this does not preclude the possibility that the amount of living, photosynthetically active material differed between the lines with the application of salt stress.

Perhaps the most interesting observations on these two barley lines was the relatively small level of dehydration imposed by salinity. After seven days exposure to salinity (up to 200 mM NaCl) shoot tissues did not appear to lose more than 20% of their tissue water. Growth and yields were severely impaired when plants were exposed to 100 mM NaCl and this produced only a ~10% loss of shoot water content in both lines. The question arises, is this loss of water large enough to account for direct effects on growth and yield or are these losses attributable to ionic stress?

As shoot RWC decreases from 100% (0 mM NaCl) to 80% (200 mM NaCl) several important physiological processes change. First the water potential ($\psi_{\text{H}_2\text{O}}$) of the tissue declines (becomes more negative) and this is considered to impair metabolism.

However, in this study estimates in the apparent V_{\max} of the C3 (Calvin) cycle enzymes (V_{Rubisco}), a value dependent on the activities of many enzymes, showed no change up to 100 mM NaCl (RWC of 90%), and only relative small changes above this concentration (RWC of 80%). Second, turgor pressure will decline in parallel with tissue water loss and this will result in a decline stomatal conductance (**gs**), and therefore an impairment in CO₂ uptake and transpiration. For both barley lines it appears that only when **gs** declines below a critical value ($\sim 0.30 \text{ mol m}^{-2} \text{ s}^{-1}$) is Assimilation affected (Fig. 4-24). For both lines this occurs when plants are exposed to concentrations of 50 mM NaCl and above (Fig. 4-24 and Fig. 4-23a), commensurate with a tissue RWC of 95% and a $\Psi_{\text{H}_2\text{O}}$ -1.5 MPa (Fig. 4-14). Taken together, these two observations suggest that the dehydration imposed on leaves by exposure of their roots to NaCl solutions does not directly affect metabolism though a decrease in water concentration, but stomatal conductance is affected. The decrease in **gs** does not affect Assimilation rate greatly, but does significantly reduces transpiration rate and evaporation cooling. In the temperature controlled, low light growth rooms used in this study, reducing evaporative cooling may have no consequence, but for plants growing in the field where light levels (heat loads) are much higher, this may not be so.

5.4 General Summary.

The effect of high salinity on salt-tolerant and salt-sensitive Arabidopsis cells, and on barley plants are reported to arise through three stress factors. The toxic effects of Na⁺ (and Cl⁻) on intracellular metabolism: the impairment of normal nutrient ion acquisition: osmotic effects (dehydration) that impairs metabolism, reduces CO₂ assimilation, and decreases transpiration.

The result of experiments reported here do not support the notion that osmotic effects are responsible for growth impairment. In salt-stressed cells nutrient ion content

appeared to be normal although in whole barley plants shoot K^+ did decline with increasing salinity and it is not certain whether this affected plant performance. Intracellular Na^+ levels appear to correlate well with necrosis and growth impairment and do not appear to be involved in an osmotic response to salinity. The main conclusion from this study is that for glycophytes that do not complete a full life cycle above 100 mM NaCl (which includes all of the world's major crops), it is the ionic component of salinity stress that impairs growth and yield. Further research on salinity stress in crops should focus on understanding the processes that control ionic balance rather than osmoregulation.

One way to take this work forward would be to use a genetic approach. There are now several collections available of Arabidopsis knockout lines where individual genes have been deleted. It would be interesting to procure knockout lines for carrying deletions in some of the genes identified from the proteomics studies presented in this thesis and to assess their phenotypes. Also, transgenic lines could be made where some of the sequences identified are over expressed in a wild type background. Together these approaches should help to assess the function of some of these sequences.

Appendix.

Table A 2-1 Linsmaier & Skoog Basal Medium (MSMO) is Components.

Source <http://www.phytotechlab.com/TABSTYLE/webdocs/MediaFormulations.pdf>

Component	formula	FW	mg.l ⁻¹
Potassium Iodide	KI	166.003	0.83
Potassium Nitrate	KNO ₃	101.11	1900
Potassium Phosphate, Monobasic	KH ₂ PO ₄	136.09	170
Ammonium Nitrate	NH ₄ NO ₃	80.04	1650
Calcium Chloride, Anhydrous	CaCl ₂	110.98	332.2
Magnesium Sulfate, Anhydrous	MgSO ₄	120.36	180.7
Myo-Inositol	C ₆ H ₁₂ O ₆	180.2	100
Na ₂ EDTA.2H ₂ O)	C ₁₀ H ₁₄ O ₈ N ₂ Na ₂ .2H ₂ O	372.24	37.26
Ferrous Sulfate.7H ₂ O	FeSO ₄ *7H ₂ O	278.02	27.8
Manganese Sulfate.H ₂ O	MnSO ₄ *H ₂ O	169	16.9
Zinc Sulfate.7H ₂ O	ZnSO ₄ *7H ₂ O	287.54	8.6
Boric Acid	H ₃ BO ₃	61.83	6.2
Thiamine.HCl	C ₁₀ H ₁₆ N ₂ O ₃ S	337.3	0.4
Cobalt Chloride.6H ₂ O	CoCl ₂ .6H ₂ O	237.93	0.025
Cupric Sulfate.5H ₂ O	CuSO ₄ *5H ₂ O	249.68	0.025
Molybdic Acid (Sodium Salt).2H ₂ O	H ₂ MoO ₄ *2H ₂ O	241.9	0.25
Grams of powder to prepare 1L			4.43

Table A 3-1 Experimental Design of 2-D DiGE.

Six experimental gels run, each contains two different samples labeled CyDye3 and CyDye5 plus CyDye2 labeled pooled. There are 12 samples with three different populations and four replications each. H (cells grown at 300 mM NaCl), HL (cells shifted down from 300 to 50 mM NaCl) and HLH (cells shifted up from 50 to 300 mM NaCl).

Gel Number	Label	Group ID	Group Description
1	Cy2	Standard	Pool of all 12 samples
1	Cy3	H	High salt (300mM)
1	Cy5	HL	Down shock (300 → 50 mM)
2	Cy2	Standard	Pool of all 12 samples
2	Cy3	H	Down shock (300 → 50 mM)
2	Cy5	HLH	Up shock (50 → 300mM)
3	Cy2	Standard	Pool of all 12 samples
3	Cy3	HL	High salt (300mM)
3	Cy5	H	Up shock (50 → 300mM)
4	Cy2	Standard	Pool of all 12 samples
4	Cy3	HLH	High salt (300mM)
4	Cy5	H	Up shock (50 → 300mM)
5	Cy2	Standard	Pool of all 12 samples
5	Cy3	HLH	High salt (300mM)
5	Cy5	HL	Down shock (300 → 50 mM)
6	Cy2	Standard	Pool of all 12 samples
6	Cy3	HL	Down shock (300 → 50 mM)
6	Cy5	HLH	Up shock (50 → 300mM)

Table A 3-2 Up-regulated Proteins in HHS *Arabidopsis* Cells Grown in High Salt.

Spot ID, arbitrary protein spot identification number assigned by DeCyder software. Protein ID, the unique AGI gene identification number for sequenced protein. MALDI Score, confidence of correct protein identification by MASCOT (V 2.1) software from MALDI-ToF sequencing. Q-Star Score, confidence of correct protein identification by MASCOT (V 2.1) software from electrospray/tandem MS sequencing. Description, AGI entry for protein function. Down Shock Fold Change, fold higher levels of protein in 6 day-old cultures of HHS cells grown at 300 mM NaCl compared with those in 6 day-old cultures grown in isotonic media at 50 mM NaCl. Up Shock Fold Change, fold increase in proteins in HHS cells after transfer from isotonic media containing 50 mM NaCl to 300 mM NaCl; in both cases protein was harvested from 6 day-old cultures.

Spot ID	Protein ID	MALDI Score	Q Star Score	Description	Down Shock Fold Change (300→50)	Up Shock Fold Change (50→300)	P	PI	Mr
Transport									
917	At5g15090		596	Voltage-dependent anion-selective channel protein hsr2.	3.268	3.521	0.000	8.6789	29211
979	At5g15090		322	Voltage-dependent anion-selective channel protein.	2.366	2.455	0.001	8.6789	29211
528	At5g62810		285	PEX14 (peroxin - peroxisomal protein import and peroxisome biogenesis. PEX14 - membrane associated, protein import).	1.390	1.150	0.000	5.7727	55595
330	At5g11710	645		Clathrin binding protein-like (clathrin: molecular scaffold that drives formation of transport vesicles).	1.070	1.280	0.002	4.6975	60634

Spot ID	Protein ID	MALDI Score	Q Star Score	Description	Down Shock Fold Change (300→50)	Up Shock Fold Change (50→300)	P	PI	Mr
940	At5g67500	200		Porin / VDAC Mitochondria outer membrane.	1.991	2.451	0.001	9.3022	29595
Signalling									
740	At1g56340	398		Calreticulin 1 (CRT1) (ubiquitous ER Ca ²⁺ binding lectin-like chaperone).	1.560	2.800	0.000	4.2038	48527
	At2g19480	77		Nucleosome assembly protein (NAP).	1.560	2.800	0.000	4.0584	43543
741	At1g56340		317	Calreticulin 1 (CRT1) (ubiquitous ER Ca ²⁺ binding lectin-like chaperone).	1.150	2.850	0.000	4.2038	48527
1715	At3g52570		276	Expressed protein, contains interpro enter IPR000379.	1.040	1.270	0.003	6.5235	37527
	At2g06530		173	SNF7 family protein (This family consists of a group of SNF-7 homologues involved in protein sorting and transport from the endosome to the vacuole/lysosome in eukaryotic cells.	1.040	1.270	0.003	5.287	25293
891	At5g57050	41		Protein phosphatase 2C (abscisic acid-insensitive) (ABI2).	1.588	1.796	0.000	6.2578	46307

Spot ID	Protein ID	MALDI Score	Q Star Score	Description	Down Shock Fold Change (300→50)	Up Shock Fold Change (50→300)	P	PI	Mr
829	At1g66340	41		ETR1, Chain A, of Arabidopsis Ethylene Receptor.	1.540	1.665	0.036	7.8274	82567
922	At1g66340	40		Ethylene receptor 1 (ETR1).	2.055	2.105	0.006	7.8274	82567
Stress									
1028	At1g02920	107		Glutathione S-transferase.	2.649	2.159	0.006	6.6102	23580
Senescence / Autophagy									
590	At4g11320		486	Similarity to cysteine proteinase.	1.622	2.184	0.039	5.6606	40711
928	At2g32730	42		26S proteasome regulatory subunit.	1.660	1.469	0.010	5.0475	108978
DNA / RNA Binding Proteins									
598	At5g47210	68		Nuclear RNA binding protein.	2.034	2.399	0.027	9.3527	38000
622	At5g47201	86		Nuclear RNA binding protein.	1.961	2.366	0.016	9.3527	38000
609	At5g47210	77		Nuclear RNA binding protein.	1.926	2.173	0.010	9.3527	38000
1097	At4g16830		269	Nuclear antigen homolog (Hyaluronan / mRNA binding protein (pfam pf04774).	1.320	1.450	0.007	8.6278	37468
	At1g65930		122	Isocitrate dehydrogenase, putative / NADP+ isocitrate dehydrogenase, putative (TCA cycle).	1.320	1.450	0.007	6.5224	45747

Spot ID	Protein ID	MALDI Score	Q Star Score	Description	Down Shock Fold Change (300→ 50)	Up Shock Fold Change (50 → 300)	P	PI	Mr
Metabolism									
731	At1g13440		897	Glyceraldehyde 3-phosphate dehydrogenase, cytosolic.	3.676	3.669	0.000	7.2154	36914
765	At1g13440		483	Glyceraldehyde 3-phosphate dehydrogenase NAD binding domain.	1.640	1.610	0.004	7.2154	36914
729	At3g04120		318	Cytosolic glyceraldehyde-3-phosphate dehydrogenase; responds to ROS signals during stress.	2.841	2.717	0.000	7.1467	36915
	At3g15000		231	Expressed protein, similar to DAG protein.	2.841	2.717	0.000	9.6063	42870
	At2g20360		176	Expressed protein.	2.841	2.717	0.000	9.6501	43936
	At1g53260		79	Similar to expressed protein (TAIR: At3g15000).	2.841	2.717	0.000	9.6249	30114
869	At5g40770	126		Prohibitin.	2.111	1.969	0.001	7.8895	30400
566	At5g55070	106		2- oxoglutrute dehydrogenase E2 subunit	2.147	2.579	0.000	9.6694	50134.0

Spot ID	Protein ID	MALDI Score	Q Star Score	Description	Down Shock Fold Change (300→50)	Up Shock Fold Change (50→300)	P	PI	Mr
Metabolism/ cont.									
650	At5g43960		167	Rubisco subunit binding-protein alpha subunit, chloroplast.	1.320	1.090	0.001	4.6451	50123
	At2g28000		104	Rubisco subunit binding-protein alpha subunit, chloroplast / 60 kda chaperonin alpha subunit / CPN-60 (groel) alpha rubisco folding.	1.320	1.090	0.001	4.8154	62073
1917	At3g55440		106	Triose-phosphate isomerase (EC 5.3.1.1), cytosolic [imported] (Glycolysis / Gluconeogenesis, Inositol.	1.440	1.020	0.043	5.1668	27169
	At1g44790		80	Chac-like family protein (The chac protein is thought to be associated with the putative chaa Ca ²⁺ /H ⁺ cation transport protein in.	1.440	1.020	0.043	4.9621	22229
1146	At4g03950	42		Glucose-6-phosphate/phosphate translocator.	1.630	2.143	0.002	10.1134	30603
548	At2g46040	44		ELM2 domain-containing protein.	2.012	2.138	0.003	7.5964	63315
903	At1g62810	42		Copper amine oxidase.	1.753	2.118	0.013	6.3891	80139
Ambiguous Function									
952	At1g66340	39		Ethylene receptor 1 (ETR1)	2.056	2.175	0.005	7.8274	82567

Spot ID	Protein ID	MALDI Score	Q Star Score	Description	Down Shock Fold Change (300→50)	Up Shock Fold Change (50→300)	P	PI	Mr
Ambiguous Function/ cont.									
1029	At1g55480	38		Expressed protein.	2.139	1.981	0.001	8.3697	37410
879	At3g55290	37		Short-chain dehydrogenase/reductase (SDR) family protein.	1.933	2.130	0.029	8.3682	30204
1026	At5g46150	32		LEM3 (ligand-effect modulator 3).	2.317	1.989	0.034	9.6623	39546
1038	At3g60880	37		Dihydrodipico-linate synthase 1 (DHDPS1).	1.705	1.927	0.000	6.9578	40465
1016	At2g33570	36		Expressed protein.	1.695	1.874	0.072	9.1097	56865
1132	At3g27530	35		Vesicle tethering family protein.	1.262	1.730	0.066	4.5774	101836
1140	At3g51070	35		Dehydration-responsive protein-related.	2.175	1.691	0.019	5.2092	101445
661	At3g27430	34		20S proteasome beta subunit B (PBB1).	1.521	1.598	0.010	8.9501	28812
	At5g40580	34		20S proteasome beta subunit B (PBB1).	1.521	1.598	0.010	7.2026	29617
133	At1g29710	39		Pentotricopeptide (PPR).	1.184	1.499	0.040	6.77	53814
1278	At3g27430	36		20S proteasome beta subunit B (PBB1).	1.193	1.472	0.003	8.9501	28812

Spot ID	Protein ID	MALDI Score	Q Star Score	Description	Down Shock Fold Change (300→ 50)	Up Shock Fold Change (50 → 300)	P	PI	Mr
Ambiguous Function/ cont.									
586	At1g69170	38		Squamosa promoter-binding protein-like6 (SPL6).	3.987	1.499	0.040	7.7384	45953
526	At4g23160	37		Protein kinase family protein.	2.430	1.472	0.003	7.1501	141387
726	At5g28750	37		Thylakoid assembly protein.	2.889	3.601	0.000	9.8186	15713
888	At2g28680	36		Cupin family protein.	2.424	2.714	0.002	6.6805	38465
576	At2g26210	22		Ankyrin repeat family protein.	2.480	2.892	0.000	5.8252	20324
715	At2g22640	20		WAVE protein.	2.392	3.211	0.000	5.8265	9481

Table A 3-3 Down-regulated Proteins in HHS *Arabidopsis* Cells Grown in High Salt.

Spot ID, arbitrary protein spot identification number assigned by DeCyder software. Protein ID, the unique AGI gene identification number for sequenced protein. MALDI Score, confidence of correct protein identification by MASCOT (v 2.1) software from MALDI-ToF sequencing. Q-Star Score, confidence of correct protein identification by MASCOT (v 2.1) software from electrospray/tandem MS sequencing. Description, AGI entry for protein function. Down Shock Fold Change, fold higher levels of protein in 6 day-old cultures of HHS cells grown at 300 mM NaCl compared with those in 6 day-old cultures grown in isotonic media at 50 mM NaCl. Up Shock Fold Change, fold increase in proteins in HHS cells after transfer from isotonic media containing 50 mM NaCl to 300 mM NaCl; in both cases protein was harvested from 6 day-old cultures.

Spot ID	Protein ID	MALDI Score	Q Star Score	Description	Down Shock Fold Change (300→50)	Up Shock Fold Change (50→300)	P	PI	Mr
Stress									
1918	At1g02920		165	Glutathione S-transferase(GST) bits or putative Arabidopsis has 48 GST genes.GST11.	0.952	0.735	0.011	6.6102	23598
	At2g02930		142	GST16	0.952	0.735	0.011	6.7317	24121
	At4g02520		137	GST2.	0.952	0.735	0.011	6.315	24129
	At2g30860		102	ATGSTF9.	0.952	0.735	0.011	6.6378	24146
1945	At1g75270		187	GSH dependent dehydroascorbate reductase, putative (Ascorbate and aldarate metabolism, Glutamate metabolism, Glutathione metabolism).	0.990	0.813	0.014	6.0387	23407
	At4g02520		178	GST2.	0.990	0.813	0.014	6.3150	24129
	At1g02920		156	GST11; supported by cDNA G 443697.	0.990	0.813	0.014	6.6102	23598
Spot	Protein ID	MALDI	Q Star	Description	Down Shock	Up Shock	P	PI	Mr

ID		Score	Score		Fold Change (300→ 50)	Fold Change (50 → 300)			
DNA / RNA Binding Proteins									
1523	At1g09760	60		U2 small nuclear ribonucleoprotein A, putative (snRNPs are involved in RNA synthesis, processing, transportation, translation and degradation).	0.926	0.840	0.014	5.8558	28042
Metabolism									
1582	At1g75280		571	Isoflavone reductase, putative (biosynthesis of phytoalexin medicarpin, fungicide).	0.885	0.943	0.012	5.7348	33737
	At2g05990		186	Enoyl-ACP reductase (Fatty acid biosynthesis (path 1)).	0.885	0.943	0.012	9.3608	41214
1475	At1g74020		536	Strictosidine synthase (Terpenoid biosynthesis Indole and ipecac alkaloid biosynthesis).	0.714	0.885	0.000	5.4345	35293
1920	At4g10340		217	Chlorophyll A-B binding protein CP26, chloroplast / light-harvesting complex II protein 5 / LHCIIC (LHCB5).	0.704	0.840	0.000	6.2942	30157
	At3g55440		161	Triose-phosphate isomerase.	0.704	0.840	0.000	5.1668	27169
	At3g10410		149	Serine carboxypeptidase III, putative all of these serine carboxypeptidase-like (SCPL) metabolism is unknown).	0.704	0.840	0.000	5.0271	57302
	At5g01600		136	Ferritin 1 (FER1) (4 ferritin genes in arabidopsis – atfer1 involved in response to excess iron, expressed in veg tissue, not seeds. Iron homeostasis).	0.704	0.840	0.000	6.0408	28178
Spot	Protein ID	MALDI	Q Star	Description	Down Shock	Up Shock	P	PI	Mr

ID		Score	Score		Fold Change (300→ 50)	Fold Change (50 → 300)			
Metabolism/ cont.									
1367	At3g04120	80		Glyceraldehyde-3-phosphate dehydrogenase, cytosolic (GAPC) / NAD-dependent glyceraldehyde-3-phospha (Glycolysis / Gluconeogenesis.).	0.847	0.952	0.002	7.1467	36915
Ambiguous Function									
1939	At3g56090	74		Ferritin, putative	0.667	0.763	0.000	5.6186	28837
1972	At5g01600	67		Ferritin 1 (FER1).	0.521	0.671	0.000	6.0408	28178

Table A 3-4 Modulated (Down & Up-regulated) Proteins in HHS *Arabidopsis* Cells Grown in High Salt.

Spot ID, arbitrary protein spot identification number assigned by DeCyder software. Protein ID, the unique AGI gene identification number for sequenced protein. MALDI Score, confidence of correct protein identification by MASCOT (v 2.1) software from MALDI-ToF sequencing. Q-Star Score, confidence of correct protein identification by MASCOT (v 2.1) software from electrospray / tandem MS sequencing. Description, AGI entry for protein function. Down Shock Fold Change, fold higher levels of protein in 6 day-old cultures of HHS cells grown at 300 mM NaCl compared with those in 6 day-old cultures grown in isotonic media at 50 mM NaCl. Up Shock Fold Change, fold increase in proteins in HHS cells after transfer from isotonic media containing 50 mM NaCl to 300 mM NaCl; in both cases protein was harvested from 6 day-old cultures.

Spot ID	Protein ID	MALDI Score	Q Star Score	Description	Down Shock Fold Change (300→50)	Up Shock Fold Change (50→300)	P	PI	Mr
Transport									
1822	At3g23400		124	Plastid-lipid associated protein (fibrillin).	1.150	0.735	0.002	5.903	30455
	At3g58010		105	Expressed protein.	1.150	0.735	0.002	5.0774	34091
	At2g37410		82	Inner mitochondrial membrane protein importer (TIM17).	1.150	0.735	0.002	4.985	25571
807	At1g76030		815	Vacuolar H ⁺ -ATPase subunit B.	1.030	0.901	0.004	4.7287	54108
	At5g55220		72	Trigger factor-like protein (chaperone).	1.030	0.901	0.004	4.9767	61734

Spot ID	Protein ID	MALDI Score	Q Star Score	Description	Down Shock Fold Change (300→50)	Up Shock Fold Change (50→300)	P	PI	Mr
Transporters / cont.									
1519	At3g20000		221	Porin family protein (ubiquitous eukaryote voltage-gated diffusion pore).	0.901	1.140	0.001	6.8102	34250
	At1g53240		128	Mitochondrial NAD-dependent malate dehydrogenase.	0.901	1.140	0.001	8.5824	35805
897	At5g08670		445	Mitochondrial F1 ATP synthase beta-subunit.	0.917	1.040	0.006	6.5979	59672
	At5g08690		445	Mitochondrial F1 ATP synthase beta subunit.	0.917	1.040	0.006	6.5979	59714
	At5g08680		445	Mitochondrial F1 ATP synthase beta subunit.	0.917	1.040	0.006	6.4527	59860
	At2g36530		167	Enolase 2-phosphoglycerate dehydratase.	0.917	1.040	0.006	5.5147	47720
	AtCg00480		142	Chloroplast ATP synthase CF1 beta chain.	0.917	1.040	0.006	5.1528	53935
	AtCg00490		119	RUBISCO large subunit.	0.917	1.040	0.006	6.2395	52956
	At3g48000		78	Mitochondrial aldehyde dehydrogenase (ALDH2) (detoxification of acetaldehyde).	0.917	1.040	0.006	7.5221	58589
842	At5g17010	41		Sugar transporter family protein.	0.939	1.556	0.052	6.7421	53539

Spot ID	Protein ID	MALDI Score	Q Star Score	Description	Down Shock Fold Change (300→50)	Up Shock Fold Change (50→300)	P	PI	Mr
Signalling									
1432	At1g35720	80		Annexin 1 (ANN1); Ca ²⁺ -dependent phospholipid binding protein, involved in cytoskeletal interactions, phospholipase inhibition, intracellular signalling, anticoagulation, and membrane fusion).	0.935	1.090	0.002	5.0181	36204
Stress									
567	At5g42270		661	FtsH metalloprotease, putative (Filamentation temperature sensitive H).	1.300	0.901	0.000	5.1291	75233
	At4g37910		538	heat shock protein 70, mitochondrial, putative	1.300	0.901	0.000	5.2535	73076
	At5g09590		538	Heat shock protein 70 / HSP70 (HSC70-5).	1.300	0.901	0.000	5.4467	72991
	At1g78900		432	Vacuolar H ⁺ ATPase alpha subunit.	1.300	0.901	0.000	4.8641	68813
2062	At4g11600		291	Phospholipid-hydroperoxide glutathione peroxidase.	1.110	0.787	0.021	9.8566	25584
1133	At5g03630	152		Monodehydroascorbate reductase, putative (K ⁺ transport).	1.100	0.820	0.002	4.9701	47480

Spot ID	Protein ID	MALDI Score	Q Star Score	Description	Down Shock Fold Change (300→ 50)	Up Shock Fold Change (50 → 300)	P	PI	Mr
Stress/ cont.									
1936	At1g02920		176	GST11.	1.110	0.775	0.007	6.6102	23598
	At1g20225		130	Contains domain of protein-disulfide isomerase [Posttranslational modification, protein turnover, chaperones].	1.110	0.775	0.007	7.1423	26052
	At4g02520		121	GST2.	1.110	0.775	0.007	6.315	24129
	At2g30860		108	ATGSTF7.	1.110	0.775	0.007	6.6378	24146
193	At4g24190	258		SHEPHERD (ER-resident HSP90-like protein possibly required for folding CLV (clavata) proteins).	0.909	1.570	0.000	4.6612	94205
941	At1g80030		124	DNAJ heat shock protein, putative.	0.893	1.210	0.005	7.6466	53821
1018	At1g63940	121		Monodehydroascorbate reductase, putative (K ⁺ transport).	0.800	1.250	0.005	7.5265	52502

Spot ID	Protein ID	MALDI Score	Q Star Score	Description	Down Shock Fold Change (300→50)	Up Shock Fold Change (50→300)	P	PI	Mr
Senescence / Autophagy									
973	At1g11910		245	Aspartyl protease (senescence, stress responses, programmed cell death and reproduction).	1.190	0.794	0.002	5.2041	54614
1615	At3g27310		114	Contains UBX domain. Domain present in ubiquitin-regulatory proteins).	1.040	0.909	0.047	6.7016	28502
	At1g65260		103	Poss: PspA/IM30 family protein (PspA - phage shock protein A - transcription factor).	1.040	0.909	0.047	9.7025	36393
DNA / RNA Binding Proteins									
1387	At4g17720		317	RNA recognition motif (RRM)-containing protein.	1.030	0.781	0.004	5.902	33548
	At1g07750		117	Cupin family protein (functionally diverse enzyme superfamily with barrel structure).	1.030	0.0.781	0.004	6.0615	38311
619	At1g15340		552	5' Methyl-CpG-binding domain-(transcriptional repression).	0.935	1.180	0.007	4.336	42358
618	At1g15340		387	5' Methyl-CpG-binding domain-(transcriptional repression).	0.893	1.200	0.010	4.336	42358
	At2g15860		176	Expressed protein.	0.893	1.200	0.010	4.3778	55575

Spot ID	Protein ID	MALDI Score	Q Star Score	Description	Down Shock Fold Change (300→50)	Up Shock Fold Change (50→300)	P	PI	Mr
Metabolism									
1422	At1g13440		149	Cytosolic Glyceraldehyde-3-phosphate dehydrogenase.	1.100	0.787	0.004	7.2154	36914
	At2g01140		91	Fructose-bisphosphate aldolase, putative.	1.100	0.787	0.004	8.2763	42327
	At1g12900		76	Chloroplast Glyceraldehyde 3-phosphate dehydrogenase.	1.100	0.787	0.004	8.2028	42847
1123	At5g55070		392	Mitochondrial 2-oxoglutarate dehydrogenase E2 subunit.	0.901	1.110	0.000	9.6694	50134
	At3g52880		140	Monodehydroascorbate reductase, putative (Ascorbate and aldarate metabolism).	0.901	1.110	0.000	6.8015	46487
924	At3g03250		654	UTP--glucose-1-phosphate uridylyltransferase, putative / UDP-glucose pyrophosphorylase, putative.	0.709	1.470	0.001	5.9815	51739
1685	At5g54770		252	Thiazole biosynthetic enzyme, chloroplast (ARA6) (THI1) (THI4)thiamin (vitB1).	0.787	1.080	0.001	6.1651	36665
	At5g24490		77	30S ribosomal protein, putative.	0.787	1.080	0.001	6.7427	34857

Spot ID	Protein ID	MALDI Score	Q Star Score	Description	Down Shock Fold Change (300→50)	Up Shock Fold Change (50→300)	P	PI	Mr
Metabolism/ cont.									
1261	At2g20420		172	Succinyl-CoA ligase beta subunit (TCA cycle).	0.709	1.250	0.001	6.6863	45346
	At2g39730		101	RuBisCO activase .	0.709	1.140	0.001	5.9289	51982
	At4g13360		68	Enoyl-CoA hydratase/isomerase (Fatty acid metabolism).	0.709	1.140	0.001	6.639	46251
376	At2g38040	755		Acetyl co-enzyme A carboxylase carboxyltransferase alpha subunit (Fatty acid and phospholipid metabolism).	0.926	1.170	0.002	5.5794	85307
1383	At3g55800	418		Chloroplast Sedoheptulose-1,7-bisphosphatase, (Carbon fixation).	0.714	1.420	0.002	6.5221	42415
	At1g62380	140		Putative ACC oxidase, (Final step in ethylene biosynthesis)	0.714	1.420	0.002	4.7436	36183
602	At1g70730		648	Putative cytoplasmic Phosphoglucomutase, / glucose phosphomutase.	0.909	1.110	0.003	5.5658	63482
	At5g60980		68	Nuclear transport factor 2 (NTF2) with RNA recognition motif (RRM).	0.909	1.110	0.003	5.8109	49416
1511	At3g47520		217	Chloroplast Malate Dehydrogenase [NAD].	0.800	1.280	0.004	8.8111	42406
874	AtCg00490	74		RuBisCO large subunit.	0.847	1.240	0.000	6.2395	52956

Spot ID	Protein ID	MALDI Score	Q Star Score	Description	Down Shock Fold Change (300→ 50)	Up Shock Fold Change (50 → 300)	P	PI	Mr
Metabolism/ cont.									
925	At3g03250		67	UTP--glucose-1-phosphate uridylyltransferase, putative / UDP-glucose pyrophosphorylase, putative (Pentose and glucuronate interconversions, Galactose metabolism, Starch and sucrose metabolism, Nucleotide sugars metabolism).	0.862	1.310	0.002	5.9815	51739
Ambiguous Function									
1990	At4g01050		144	Hydroxyproline-rich glycoprotein family protein (HRGPs are known as constituents of extracellular matrix of HPs – seem to function as structural barriers in defense responses).	1.090	0.806	0.021	4.9351	49387
1882	At3g55440	74		Triose-phosphate isomerase (EC 5.3.1.1), cytosolic [imported].	1.000	0.870	0.006	5.1668	27169
1806	At3g58010		415	Expressed protein (PAP_fibrillin domain.)	0.901	1.050	0.003	5.0774	34091
	At4g37200		244	Thioredoxin family protein.	0.901	1.050	0.003	5.0364	28745
	At1g64520		237	26S proteasome subunit RPN12 (Protein degradation).	0.901	1.050	0.003	4.538	30706
	At3g07410		116	Ras-related GTP-binding family protein (Vesicle trafficking, signalling, salt stress.	0.901	1.050	0.003	4.4622	24320

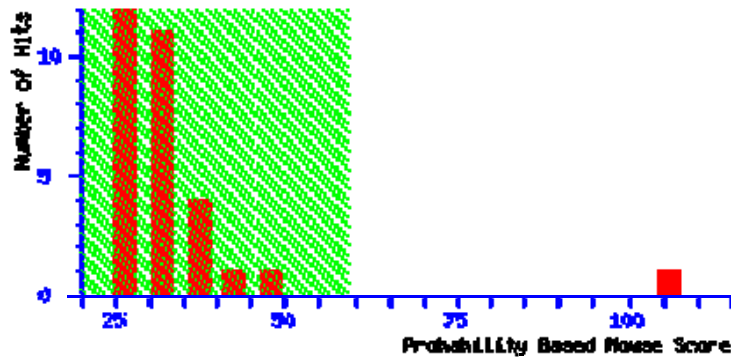
MATRIX SCIENCE Mascot Search Results

User : Attumi
 Email : 0108932a@student.gla.ac.uk
 Search title : poonam 55029 - 08-04-05-plate 2_54_0001.dat
 Database : NCBIInr 20050416 (2440425 sequences; 825931499 residues)
 Taxonomy : Arabidopsis thaliana (thale cress) (49672 sequences)
 Timestamp : 21 Apr 2005 at 09:45:40 GMT
 Top Score : 106 for [gi|22136096](#), 2-oxoglutarate dehydrogenase E2 subunit [Arabidopsis thaliana]

Probability Based Mowse Score

Ions score is $-10 \cdot \log(P)$, where P is the probability that the observed match is a random event.

Protein scores greater than 59 are significant ($p < 0.05$).



Concise Protein Summary Report

Format As [Help](#)

Significance threshold $p <$ Max. number of hits

- [gi|22136096](#) - Mass: 50273- Score: **106-**
 Expect: 1.2e-06- Queries matched: 11
 2-oxoglutarate dehydrogenase E2 subunit [Arabidopsis thaliana]

Fig. A 3-1MASCOT Protein Identity Output.

This protein was identified as 2-oxoglutarate dehydrogenase E2 subunit and was up regulated in high salt *Arabidopsis thaliana* cells. The protein identification has significant. Score of 106, ($p < 0.05$).

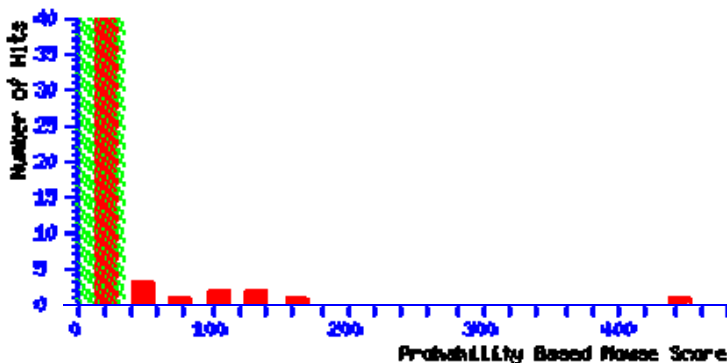
MATRIX SCIENCE Mascot Search Results

User : Attumi
 Email : 0108932a@student..gla.ac.uk
 Search title : h4
 MS data file : C:\Attumi\May 04 MSMS\10_07_04 Attumi Plate 11450.wiff
 Database : NCBIInr 20040612 (1846720 sequences; 611532004 residues)
 Taxonomy : Arabidopsis thaliana (thale cress) (49702 sequences)
 Timestamp : 12 Jul 2004 at 14:09:25 GMT

Significant hits: [gi|17939849](#) mitochondrial F1 ATP synthase beta subunit [Arabidopsis thaliana]
[gi|15227987](#) enolase [Arabidopsis thaliana]
[gi|7525040](#) ATP synthase CF1 beta chain [Arabidopsis thaliana]
[gi|15809970](#) At2g36530/F1O11.16 [Arabidopsis thaliana]
[gi|1944432](#) ribulosebiphosphate carboxylase [Arabidopsis thaliana]
[gi|15226092](#) ATP synthase alpha chain, mitochondrial, putative [Arabidopsis thaliana]
[gi|15228319](#) aldehyde dehydrogenase (ALDH2) [Arabidopsis thaliana]
[gi|18399468](#) polygalacturonase, putative / pectinase, putative [Arabidopsis thaliana]
[gi|18399468](#) expressed protein [Arabidopsis thaliana]
[gi|7525018](#) ATPase alpha subunit [Arabidopsis thaliana]

Probability Based Mowse Score

Ions score is $-10 \cdot \log(P)$, where P is the probability that the observed match is a random event. Individual ions scores > 35 indicate identity or extensive homology ($p < 0.05$). Protein scores are derived from ions scores as a non-probabilistic basis for ranking protein hits.



Concise Protein Summary Report

Format As	Concise Protein Summary	Help
Significance threshold p<	0.05	Max. number of hits
		20
<input type="button" value="Re-Search All"/>		

Fig. A 3-2 MASCOT Result Page of a Mixed Spot.

Ten different proteins were identified using tandem MS from one spot on the 2-DE gel.

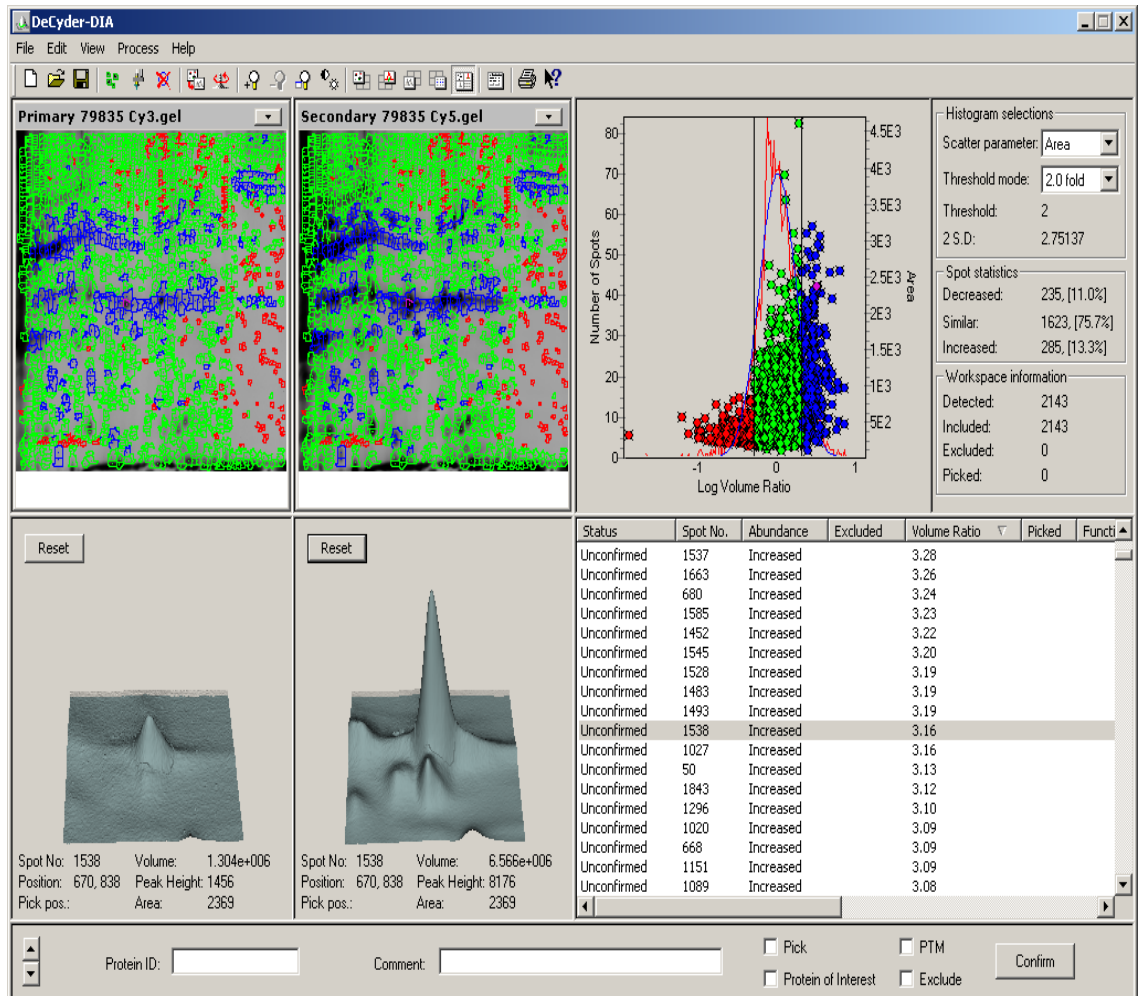


Fig. A 3-3 Example of DeCyder DIA Screen Print.

The DIA window has four sections. Upper left is the Image View that shows both the primary (Cy3, salt down shock cells (HL) and secondary (Cy5, salt up shock cells (HLH) gel images. Spots shown in red are down regulated in HL cells; spots shown in blue are up regulated salt HLH. Spots shown in green are similar. Upper right is the Histogram View, which displays data associated with all detected spots in the primary and secondary images. The left y axis displays the spot frequency. The red curve represents the frequency distribution of the log volume ratio. The blue curve represents a normalized model frequency fitted to the spot ratio so that the modal peak is zero. The right y axis represents the scatter parameter selected in the histogram selection box (right of the histogram). A plotted single data point on the histogram represents an individual protein spot. At the bottom left is the 3D view of a selected spot on the primary and secondary image. Bottom right is the Table View that displays data associated with selected co-detected spots, including volume ratio and whether the spot volume is increased / decreased or unchanged.

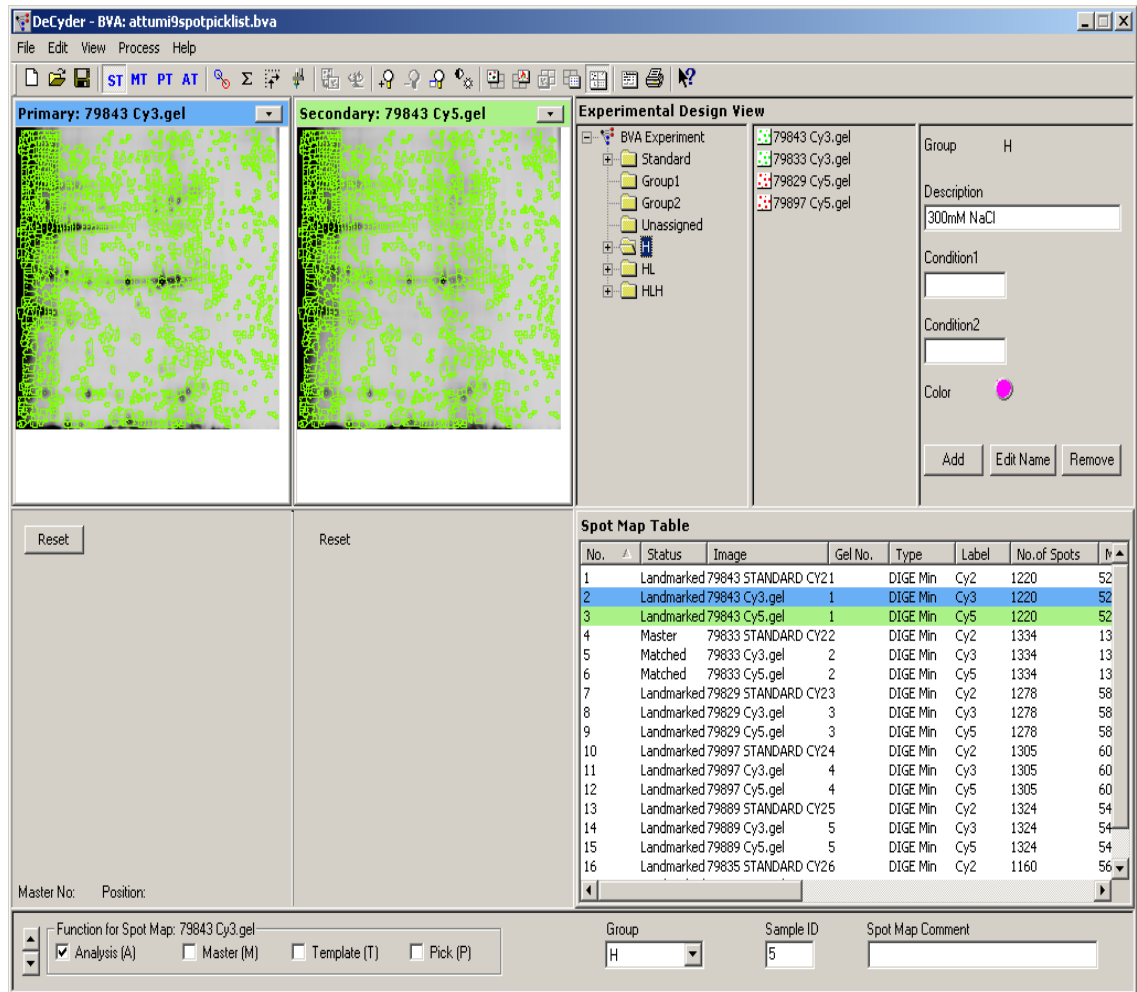


Fig. A 3-4 Screen-Print of the BVA Analysis Software in the Spot Map Table Mode Used to Analyze the Salt Shock Experiment.

The Screen is split into four sections. The upper left is the image view that demonstrates a high salt Cy3 labeled image on the left and the corresponding salt down shock Cy5 labeled image on the right. The spots detected by the DIA/Batch Processor module are shown in green. The second section of the screen top right contains information on all of the groups and gels in the experiment, including the group type and which CyDye they are labeled with. The bottom right section is the Table View which contains more details about all of the gels in the experiment, including the number of image, gel number, type of labeling, CyDye label, the number of spots detected on the gel, the number of spots matched to the master, which gel has been assigned master status (M) and which group the gel belongs to; salt down shock (HL), salt up shock (HLH), High salt (H) or standard. The Cy2 labeled standard gel was assigned master status in salt shock experiment.

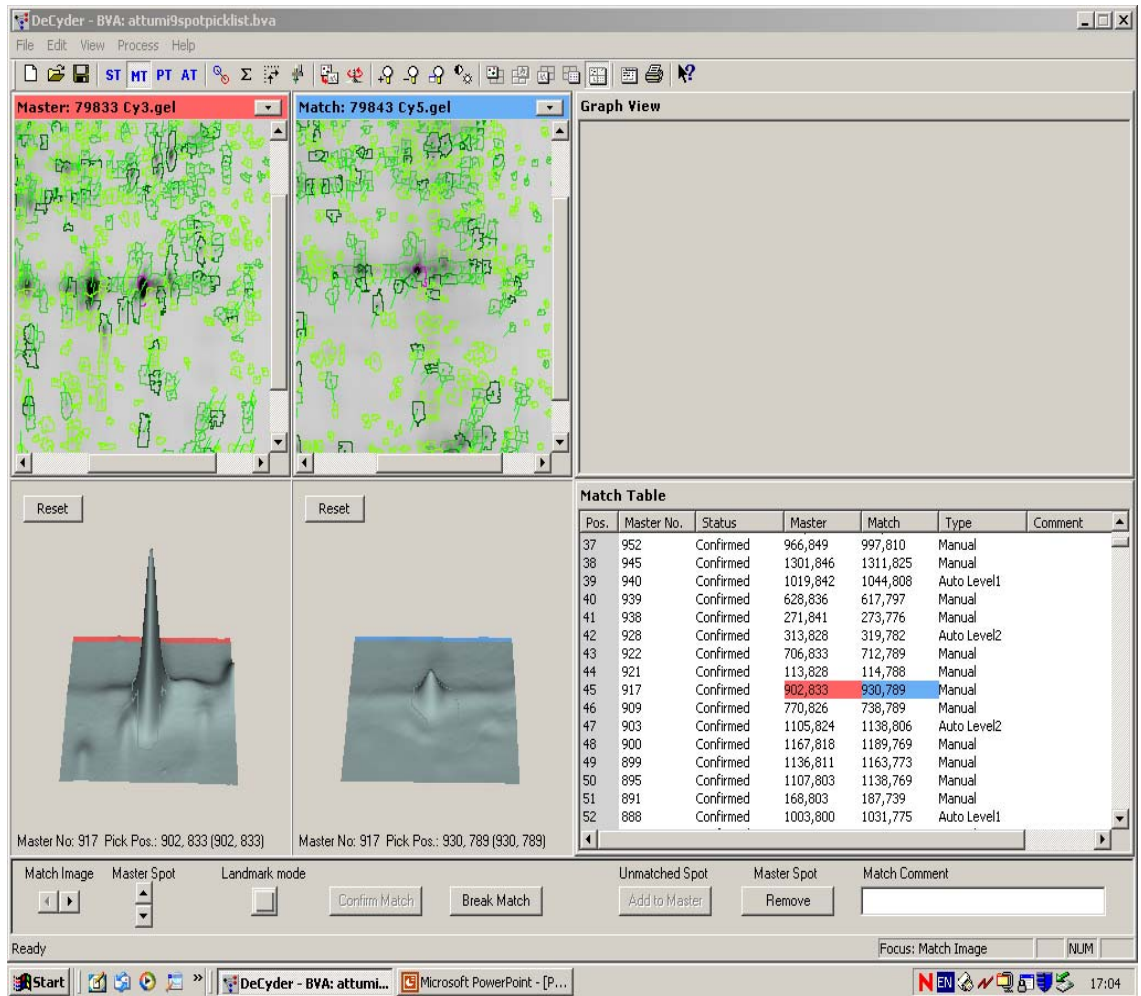


Fig. A 3-5 Screen-Print of the BVA Analysis Software in the Match Table Mode.

This mode gives lists of all data associated with inner-gel matching in salt shock experiment. This figure displays spot number 917 matched between two gel images from different two gels (High salt (H) Cy3 on the left and salt down shock (HL) Cy5 on the right). The image View can be magnified to show the area of interest of gel in details. Bottom left is 3D View showing the abundance of the matched protein in the two images from gel 2 on the left and gel 1 on the right.

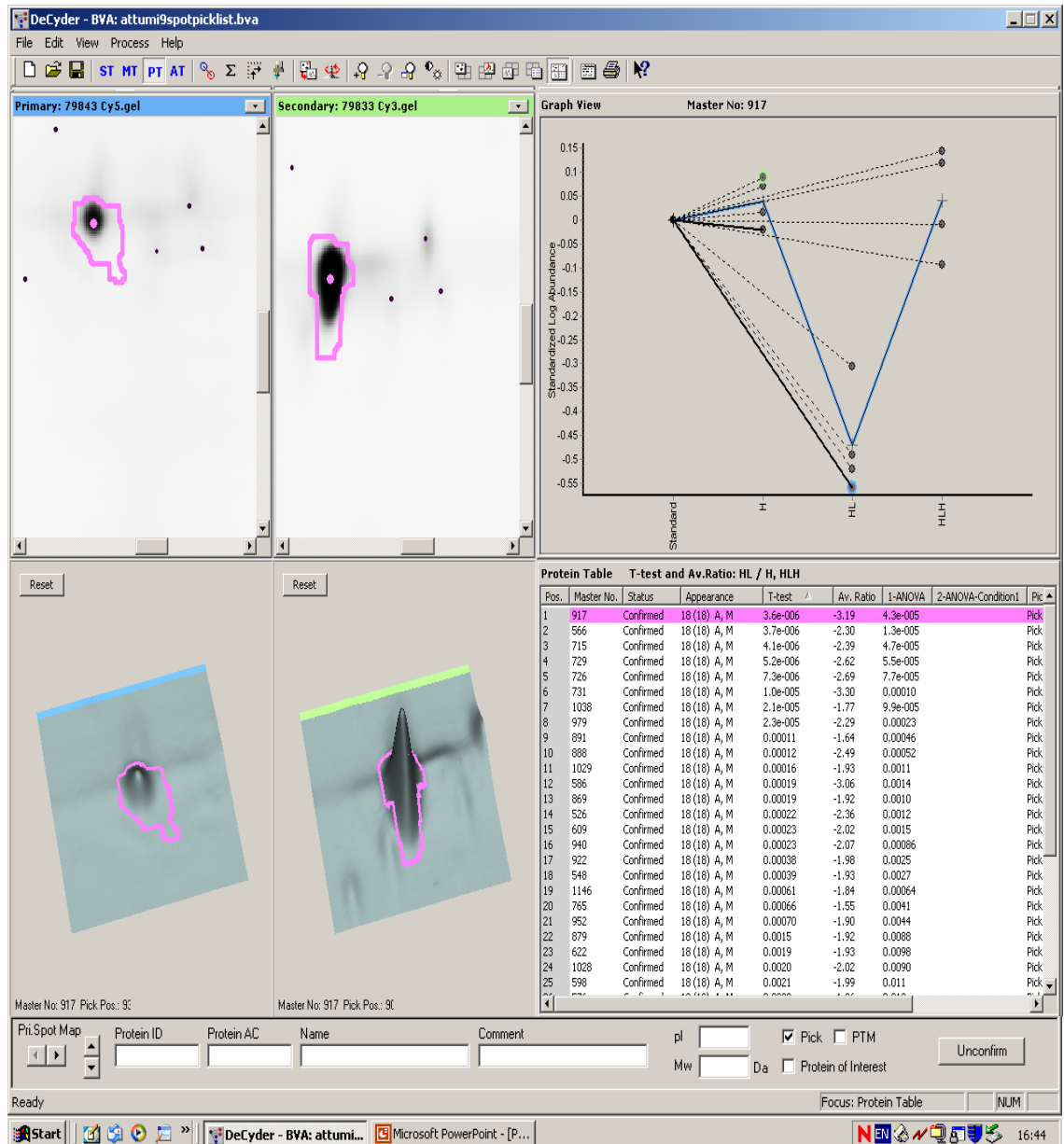


Fig. A 3-6 Screen-Print of the BVA Analysis Software in the Protein Table Mode.

The protein match table shows spot specific information including the serial number, master number of the spot, the status of the spot (confirmed or unconfirmed), how many gel images the spot has been detected in, the (t-test and ANOVA) values and the average ratio of spot volume. This screenshot shows spot number 917 from gel number 1. The graph in the top right section illustrates that the volume of this spot is consistently higher in *Arabidopsis thaliana* high salt cells than salt down shock cells (as measured by standardized log abundance).

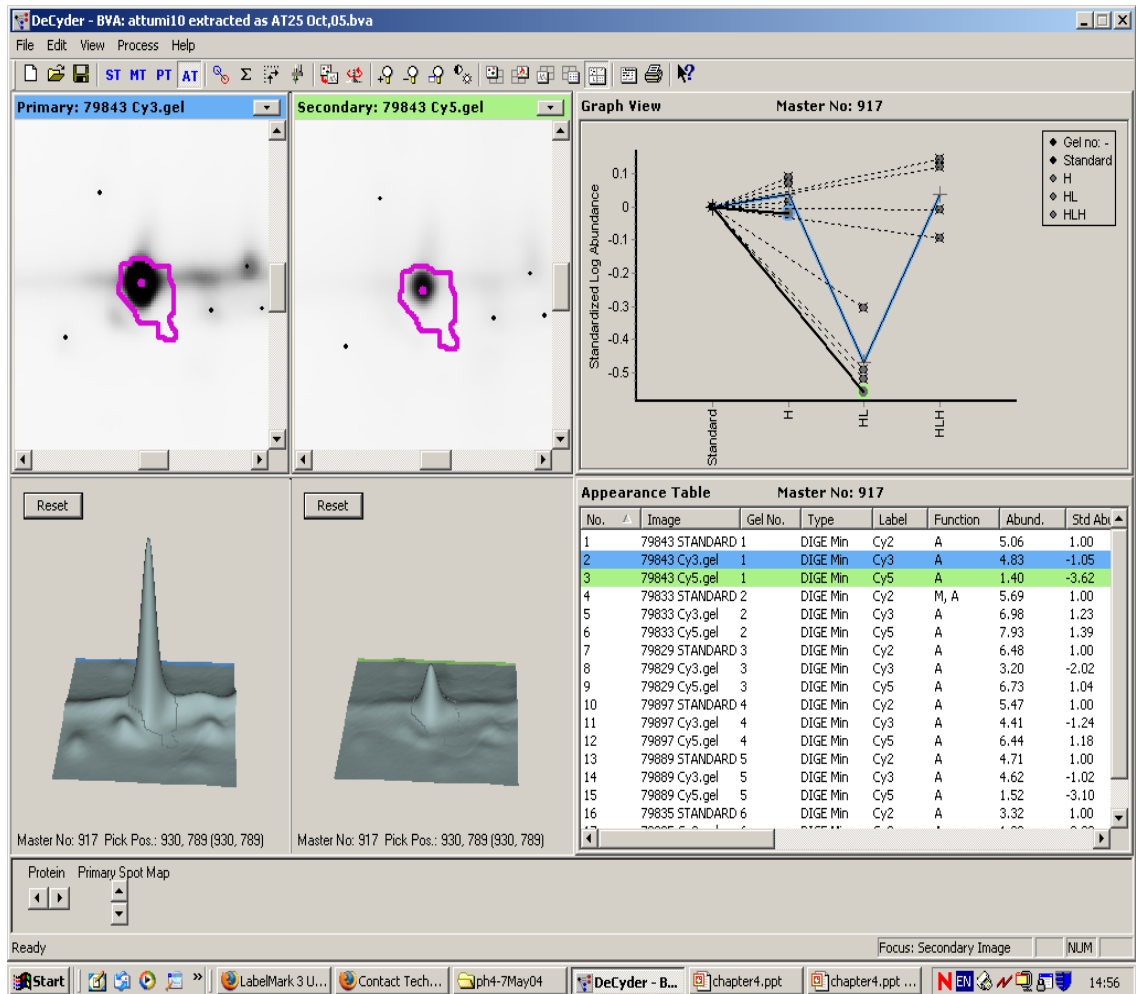


Fig. A 3-7 Screen-Print of the BVA Analysis Software in the Appearance Table Mode.

This table is used to show and process data associated with a single protein spot identified across the gels. Here we can see master spot number 917 which is present on all 19 gel images (18 CyDye images and the one SYPRO Orange stained preparative gel image) in salt shock experiment. The table view contains information about this one particular spot including the volume and abundance in all images.

Table A 4-1 Composition of 1/4 Strength Hoagland's Nutrient Solution (SHNS)

Ingredients.

Source (Hoagland and Arnon, 1950). *Applied concentration.

<http://bbc.botany.utoronto.ca/efp/cgi-bin/efpWeb.cgi>

Macronutrient Compound's name	Formula and Stock solution	1/4 SHNS to use*, ml/l	
Mono-potassium phosphate	1 M K H ₂ PO ₄ (fw 136.09)	0.25	
Potassium nitrate	1 M K NO ₃ (fw 101.11)	1.25	
Calcium nitrate	1 M Ca (NO ₃) ₂ (fw 236.2)	1.25	
Magnesium sulphate	1 M Mg SO ₄ x 7H ₂ O	0.5	
Micronutrient Compound's name	Formula	g/l	1/4 SHNS to use*
Boric acid	H ₃ BO ₃ (fw 61.83)	2.86	0.25 ml/l
Manganese chloride-4 hydrate	MnCl ₂ x 4H ₂ O (fw 197.9)	1.81
Zinc sulphate - 7 hydrate	ZnSO ₄ x 7H ₂ O (fw 287.5)	0.22
Cupric sulphate 5 hydrate	CuSO ₄ x 5H ₂ O (fw 249.7)	0.08
Sodium molybdate	Na ₂ MoO ₄ x 2H ₂ O (fw 241.9)	0.12
FeNa-EDTA, ferric monosodium Ethylenediaminetetra acetic acid	Fe Na EDTA (fw 367.05)	42.5 mM

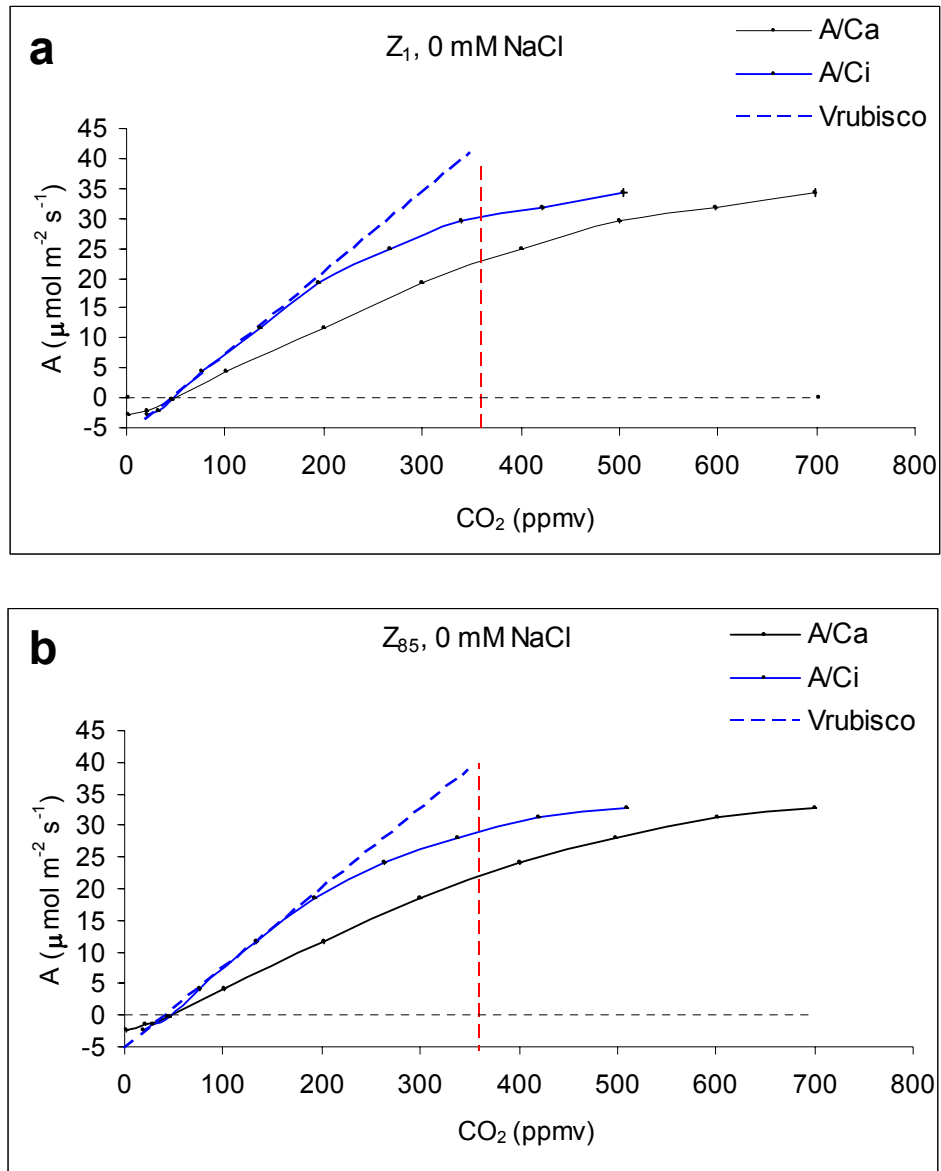


Fig. A 4- 1 Raw Data of Carbon Dioxide Response Curve (CRC) of Barley Leaves (Control, 0 mM NaCl).

Upper panel (a) shows Zhou 1 CRC and lower panel (b) shows Zhou 85 CRC.

Blue solid line (—) the relationship between net photosynthesis (A_n) and the internal CO_2 concentration (C_i). Black solid line (—) the relationship between net photosynthesis (A_n) and the air CO_2 concentration (C_a). Blue dashed line (---) V_{rubisco} (carboxylation efficiency) from initial slope of the A/C_i curve. Red vertical dashed line (|) ambient CO_2 (360 ppmv). The chamber light level was $487 \mu\text{mol photons m}^{-2} \text{s}^{-1}$ (PPFD).

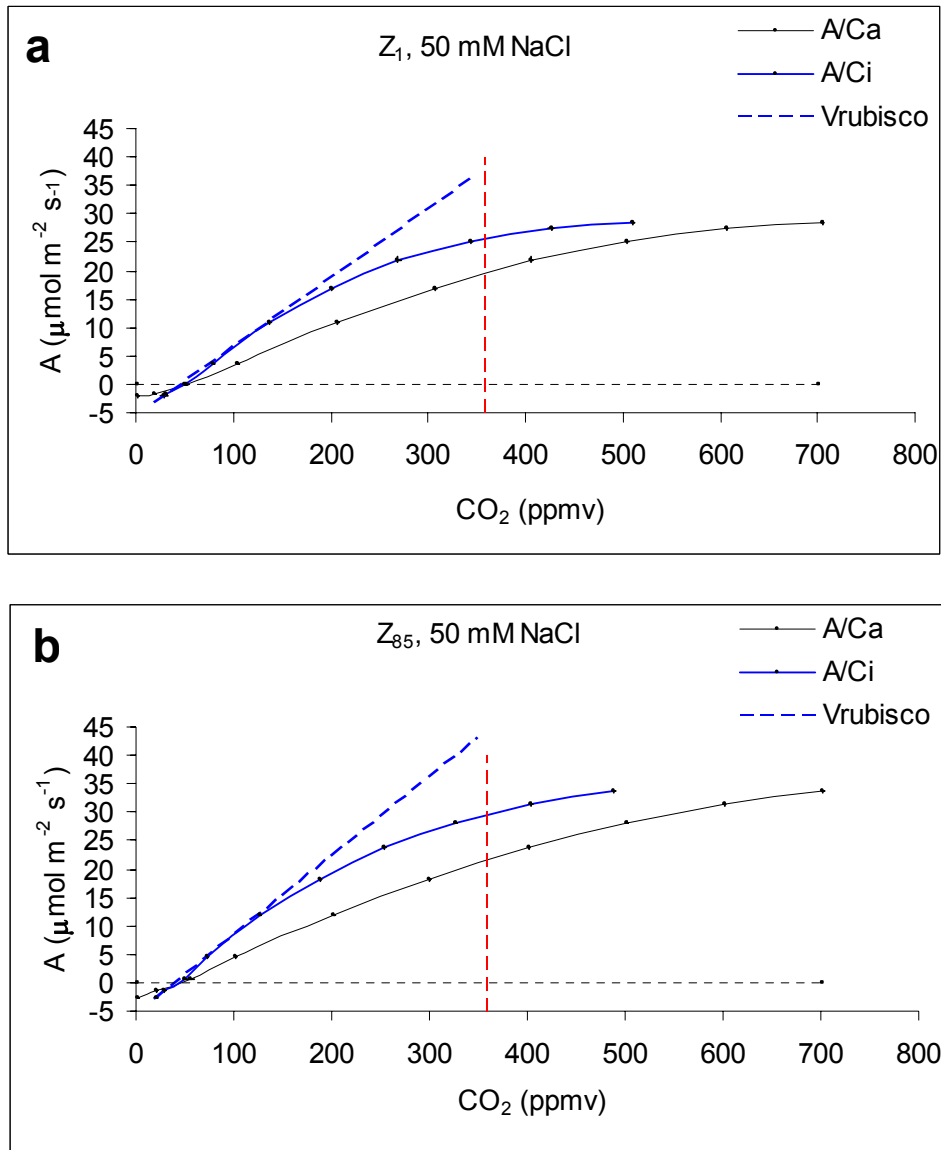


Fig. A 4- 2 Raw Data of Carbon Dioxide Response Curve (CRC) of Barley Leaves treated with (50 mM NaCl).

Upper panel (a) shows Zhou 1 CRC and lower panel (b) shows Zhou 85 CRC.

Blue solid line (—) the relationship between net photosynthesis (A_n) and the internal CO_2 concentration (C_i). Black solid line (—) the relationship between net photosynthesis (A_n) and the air CO_2 concentration (C_a). Blue dashed line (---) V_{rubisco} (carboxylation efficiency) from initial slope of the A/C_i curve. Red vertical dashed line (|) ambient CO_2 (360 ppmv). The chamber light level was $487 \mu\text{mol photons m}^{-2} \text{s}^{-1}$ (PPFD).

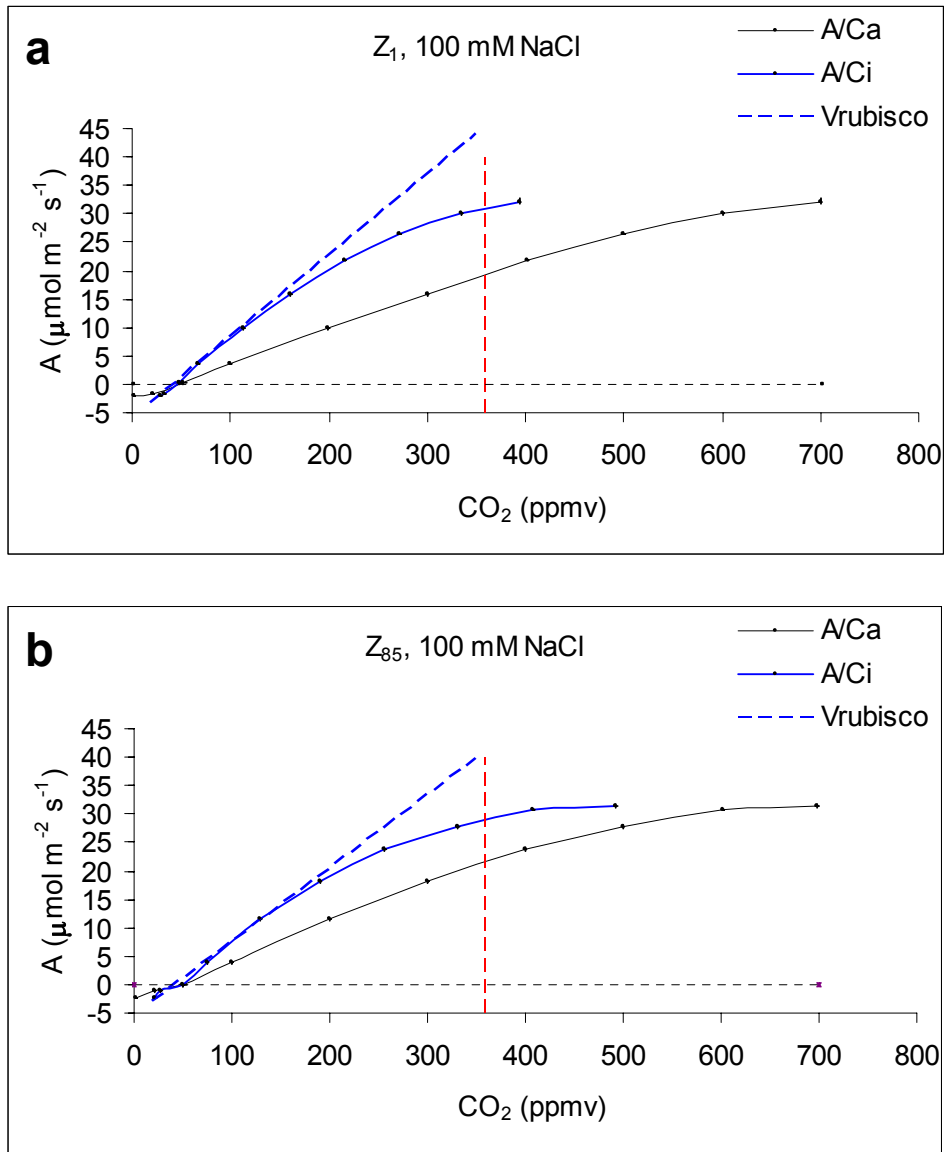


Fig. A 4- 3 Raw Data of Carbon Dioxide Response Curve (CRC) of Barley Leaf treated with (100 mM NaCl).

Upper panel (a) shows Zhou 1 CRC and lower panel (b) shows Zhou 85 CRC.

Blue solid line (—) the relationship between net photosynthesis (A_n) and the internal CO_2 concentration (C_i). Black solid line (—) the relationship between net photosynthesis (A_n) and the air CO_2 concentration (C_a). Blue dashed line (---) V_{rubisco} (carboxylation efficiency) from initial slope of the A/C_i curve. Red vertical dashed line (|) ambient CO_2 (360 ppmv). The chamber light level was $487 \mu\text{mol photons m}^{-2} \text{s}^{-1}$ (PPFD).

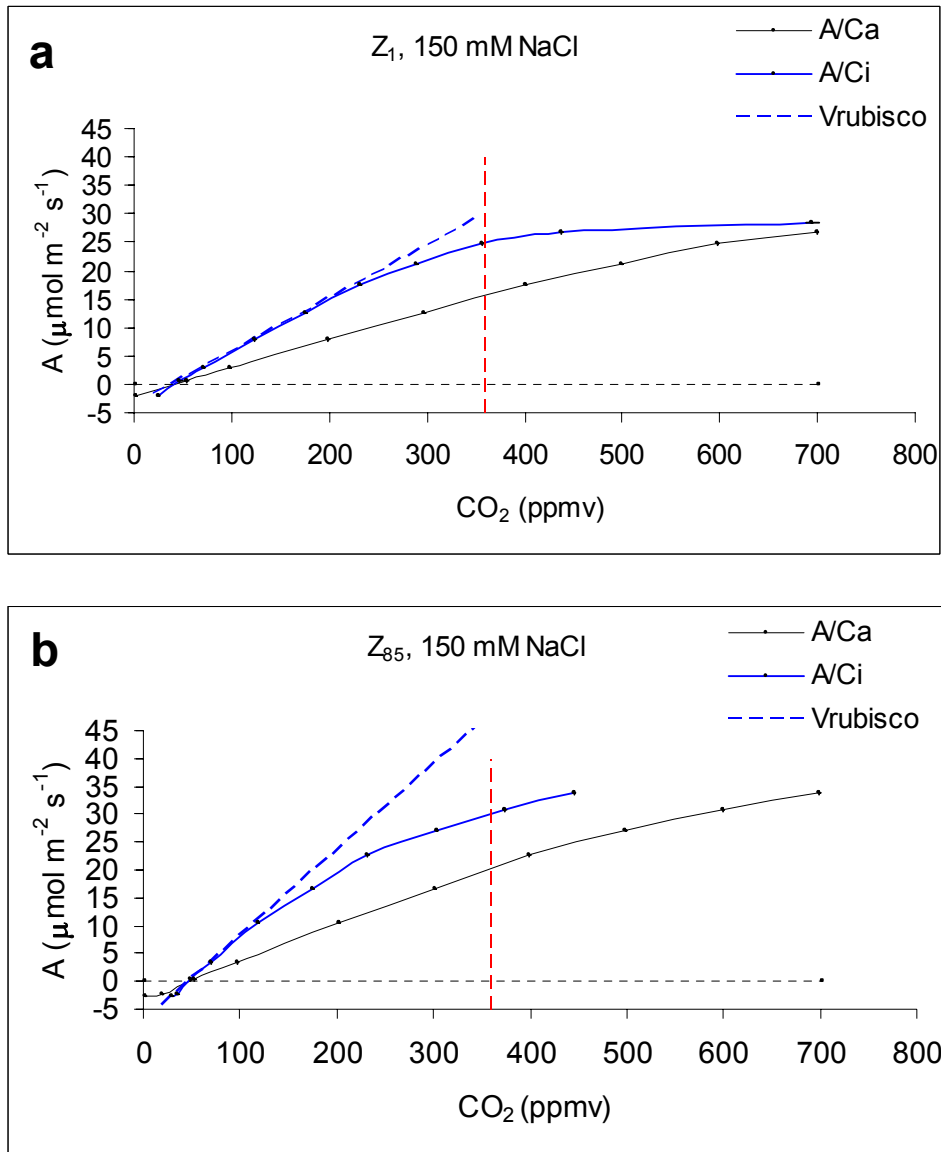


Fig. A 4- 4 Raw Data of Carbon Dioxide Response Curve (CRC) of Barley Leaf treated with (150 mM NaCl).

Upper panel (a) shows Zhou 1 CRC and lower panel (b) shows Zhou 85 CRC.

Blue solid line (—) the relationship between net photosynthesis (A_n) and the internal CO_2 concentration (C_i). Black solid line (—) the relationship between net photosynthesis (A_n) and the air CO_2 concentration (C_a). Blue dashed line (---) V_{rubisco} (carboxylation efficiency) from initial slope of the A/C_i curve. Red vertical dashed line (|) ambient CO_2 (360 ppmv). The chamber light level was $487 \mu\text{mol photons m}^{-2} \text{s}^{-1}$ (PPFD).

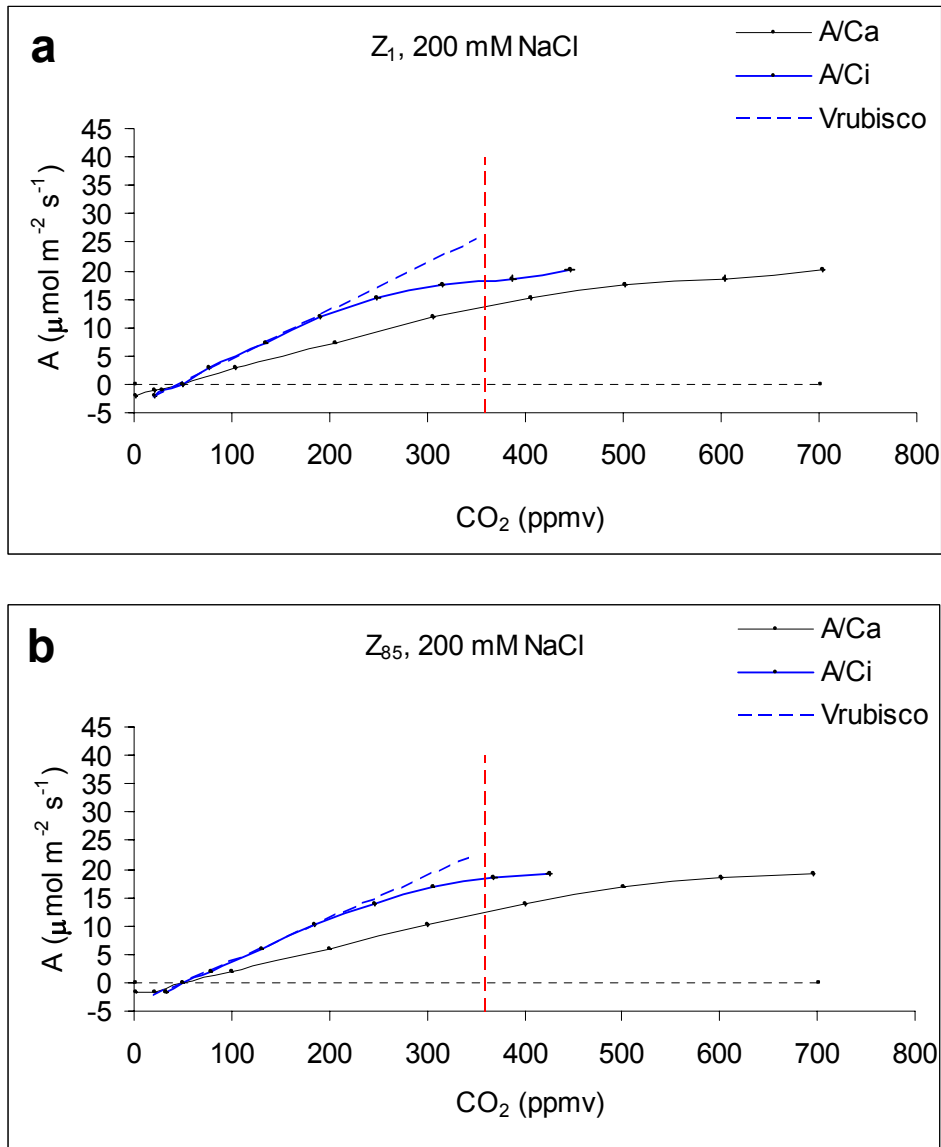


Fig. A 4- 5 Raw Data of Carbon Dioxide Response Curve (CRC) of Barley Leaf treated with (200 mM NaCl).

Upper panel (a) shows Zhou 1 CRC and lower panel (b) shows Zhou 85 CRC.

Blue solid line (—) the relationship between net photosynthesis (A_n) and the internal CO_2 concentration (C_i). Black solid line (—) the relationship between net photosynthesis (A_n) and the air CO_2 concentration (C_a). Blue dashed line (---) V_{rubisco} (carboxylation efficiency) from initial slope of the A/C_i curve. Red vertical dashed line (|) ambient CO_2 (360 ppmv). The chamber light level was $487 \mu\text{mol photons m}^{-2} \text{s}^{-1}$ (PPFD).

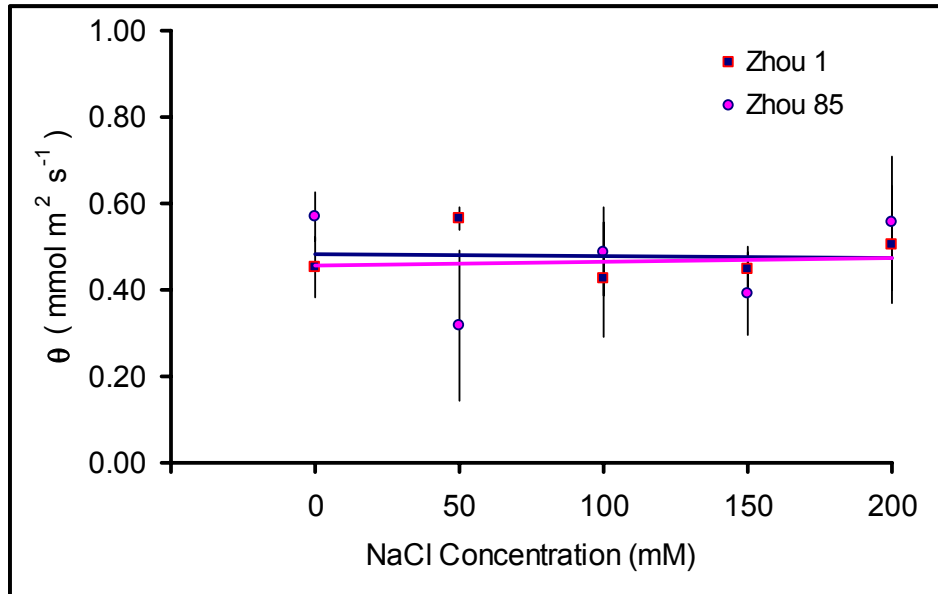


Fig. A 4-6 The Effects of Salt Treatments on Theta (θ) of two barley lines.

■, Zhou 1; ●, Zhou. 85

Each data point presents the mean and standard error of four replicates. Measurements were made 26 days after germination (7 days after salt treatment). Two factor analysis of variance (linear model) was performed on the data with Bonferroni pair-wise tests between treatment means. No significant differences ($p < 0.05$) were found between Zhou 1 and Zhou 85 treatment means.

Table A 4-2 Raw Data of Two Barley Lines Development According to Zadok's Scale.

	Z_1		Z_{85}		Z_{85} Development Day	
day	Average (n=16)	St Error	Average (n=16)	St Error	Average	Days Delay
5	10.00	0.00	10.00	0.00	5.00	0.00
8	11.94	0.14	11.75	0.26	7.87	0.13
12	13.00	0.00	12.69	0.28	11.71	0.29
15	13.75	0.26	13.44	0.30	14.66	0.34
17	14.00	0.00	14.00	0.00	17.00	0.00
19	14.94	0.14	14.38	0.29	18.28	0.72
22	15.50	0.30	15.38	0.29	21.82	0.18
26	16.56	0.30	16.38	0.29	25.71	0.29
29	17.81	0.23	17.06	0.14	27.78	1.22
31	41.00	0.00	37.00	0.00	27.98	3.02
33	45.00	0.00	39.00	0.00	28.60	4.40
36	50.00	0.00	45.00	0.00	32.40	3.60
38	58.38	1.44	49.00	0.00	31.90	6.10
40	59.94	0.14	53.31	2.34	35.58	4.42
43	70.38	0.29	59.00	0.00	36.05	6.95
45	73.00	0.84	62.50	1.49	38.53	6.47
47	75.00	0.00	65.00	0.00	40.73	6.27
50	77.00	0.00	69.00	0.00	44.81	5.19
52	85.00	0.00	71.00	0.00	43.44	8.56
54	85.00	0.00	77.00	0.00	48.92	5.08
57	87.00	0.00	85.00	0.00	55.69	1.31
59	87.00	0.00	87.00	0.00	59.00	0.00
61	90.00	0.00	87.00	0.00	58.97	2.03
64	91.00	0.00	90.00	0.00	63.30	0.70
67	92.00	0.00	91.00	0.00	66.27	0.73
69	93.00	0.00	92.00	0.00	68.26	0.74
71	94.00	0.00	93.00	0.00	70.24	0.76

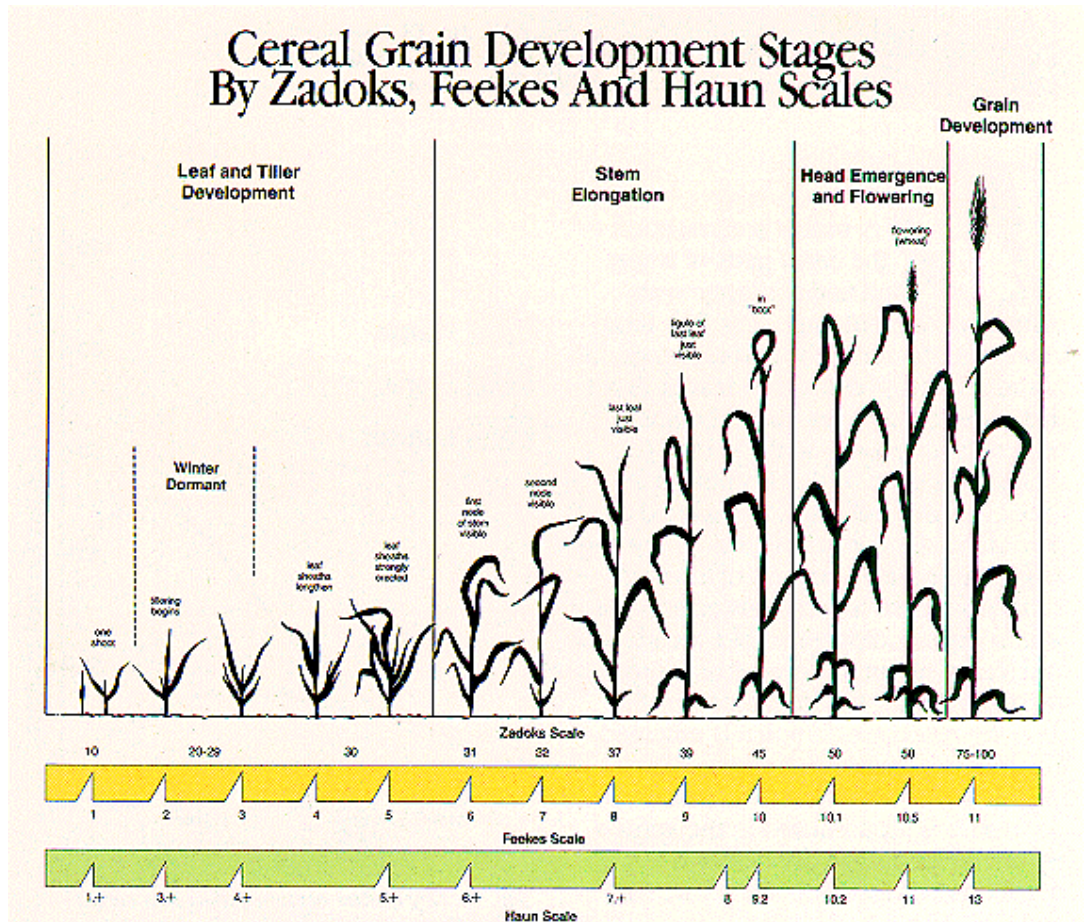


Fig. A 4-7 Cereal grain development stages by Zadoks, Feekes and Haun codes.

Source: http://plantsci.missouri.edu/cropsys/growth.html#Field_staging_form

Table A 4-3 Cereal Grain Development Stages by Zadoks, Feekes and Haun.

Source: http://plantsci.missouri.edu/cropsys/growth.html#Field_staging_form

Zadoks Scale	Feekes Scale	Haun Scale	Description
<hr/>			
<u>Germination</u>			
00	-	-	Dry Seed
01	-	-	Start of imbibition
03	-	-	Imbibition complete
05	-	-	Radicle emerged from seed
07	-	-	Coleoptile emerged from seed
09	-	0.0	Leaf just at coleoptile tip
<u>Seedling Growth</u>			
10	1	-	First leaf through coleoptile
11	-	1.0	First leaf extended
12	-	1.+	Second leaf extending
13	-	2.+	Third leaf extending
14	-	3.+	Fourth leaf extending
15	-	4.+	Fifth leaf extending
16	-	5.+	Sixth leaf extending
17	-	6.+	Seventh leaf extending
18	-	7.+	Eighth leaf extending
19	-	-	Nine or more leaves extended
<u>Tillering</u>			
20	-	-	Main shoot only
21	2	-	Main shoot and one tiller
22	-	-	Main shoot and two tillers
23	-	-	Main shoot and three tillers
24	-	-	Main shoot and four tillers
25	-	-	Main shoot and five tillers
26	3	-	Main shoot and six tillers

27	-	-	Main shoot and seven tillers
28	-	-	Main shoot and eight tillers
29	-	-	Main shoot and nine tillers

Stem Elongation

30	4-5	-	Pseudo stem erection
31	6	-	First node detectable
32	7	-	Second node detectable
33	-	-	Third node detectable
34	-	-	Fourth node detectable
35	-	-	Fifth node detectable
36	-	-	Sixth node detectable
37	8	-	Flag leaf just visible
39	9	-	Flag leaf ligule/collar just visible

Booting

40	-	-	---
41	-	8-9	Flag leaf sheath extending
45	10	9.2	Boot just swollen
47	-	-	Flag leaf sheath opening
49	-	10.1	First awns visible

Inflorescence Emergence

50	10.1	10.2	First spikelet of inflorescence visible
53	10.2	-	1/4 of inflorescence emerged
55	10.3	10.5	1/2 of inflorescence emerged
57	10.4	10.7	3/4 of inflorescence emerged
59	10.5	11.0	Emergence of inflorescence completed

Anthesis

60	10.51	11.4	Beginning of anthesis
65	-	11.5	Anthesis 1/2 completed

69 - 11.6 Anthesis completed

Milk Development

70 - - ---

71 10.54 12.1 Kernel watery-ripe

73 - 13.0 Early milk

75 11.1 - Medium milk

77 - - Late milk

Dough Development

80 - - ---

83 - 14.0 Early dough

85 11.2 - Soft dough

87 - 15.0 Hard dough

Ripening

90 - - ---

91 11.3 - Kernel hard (difficult to
divide by thumbnail)

92 11.4 16.0 Kernel hard (can no longer
be dented by thumbnail)

93 - - Kernel loosening in daytime

94 - - Overripe, straw dead and collapsing

95 - - Seed dormant

96 - - Viable seed giving 50% germination

97 - - Seed not dormant

98 - - Secondary dormancy induced

99 - - Secondary dormancy lost

References.

- Abbott, A.** (1999). A post-genomic challenge: learning to read patterns of protein synthesis. *Nature* **402**: 715-720.
- Aebersold, R., Rist, B., and Gygi, S. P.** (2000). Quantitative proteome analysis: methods and applications. *Annals of the New York Academy of Sciences* **919**: 33-47.
- Ahn, S. J., Shin, R., and Schachtman, D. P.** (2004). Expression of KT/KUP genes in Arabidopsis and the role of root hairs in K⁺ uptake. *Plant Physiology* **134**: 1135-1145.
- Akhkha, A., Reid, I., Clarke, D., and Dominy, P.** (2001). Photosynthetic light response curves determined with the leaf oxygen electrode: minimisation of errors and significance of the convexity term. *Planta* **214**: 135-141.
- Al-Khatib, M., McNeilly, T., and Collins, J. C.** (1993). The potential of selection and breeding for improved salt tolerance in lucerne (*Medicago sativa* L.). *Euphytica* **65**: 43-51.
- Anderson, J. A., Huprikar, S. S., Kochian, L. V., Lucas, W. J., and Gaber, R. F.** (1992). Functional expression of a probable Arabidopsis thaliana potassium channel in *Saccharomyces cerevisiae*. *Proceedings of the National Academy of Sciences of the United States of America* **89**: 3736-3740.
- Apse, P. M., Aharon, G. S., Snedden, W. A., and Blumwald, E.** (1999). Salt tolerance conferred by overexpression of a vacuolar Na⁺/H⁺ antiport in *Arabidopsis*. *Sci* **285**: 1256-1258.
- Arnon, D. I. and Stout, P. R.** (1939). The essentiality of certain elements in minute quantity for plants with special reference to copper. *Plant Physiology* **14**: 371-375.
- Ashley, M. K., Grant, M., and Grabov, A.** (2006). Plant responses to potassium deficiencies: a role for potassium transport proteins. *Journal of Experimental Botany* **57**: 425-436.
- Ashraf, M.** (1994). Breeding for salinity tolerance in plants. *CRC Crit.Rev.in plant sci* **13**: 17-42.
- Assmann, S. M. and Haubrick, L. L.** (1996). Transport proteins of the plant plasma membrane. *Current Opinion in Cell Biology* **8**: 458-467.
- Ayers, A. D.** (1953). Germination and emergence of several varieties of barley in salinized soil cultures. *Agron.J.* **45**: 68-71.
- Ayers, R. S. and Westcot, D. W.** (1976). Water Quality for Agriculture. *FAO Irrigation and Drainage Paper* **29 (Rev 1)**.

- Bakker, E. P.** (1993). Low affinity K uptake systems. In EP Bakker, ed Alkali Cation transport systems. In prokaryotes. *CRC Press, Boca Raton, FL* : 253-276.
- Bañuelos, M. A., Garciadeblas, B., Cubero, B., and Rodríguez-Navarro, A.** (2002). Inventory and functional characterization of the HAK potassium transporters of rice. *Plant Physiology* **130**: 784-795.
- Bañuelos, M. A., Klein, R. D., Alexander-Bowman, S. J., and Rodríguez-Navarro, A.** (1995). A potassium transporter of the yeast *Schwanniomyces occidentalis* homologous to the Kup system of *Escherichia coli* has a high concentrative capacity. *EMBO J* **14**: 3021-3027.
- Bañuelos, M. A., Madrid, R., and Rodriguez-Navarro, A.** (2000). Individual functions of the HAK and TRK potassium transporters of *Schwanniomyces occidentalis*. *Molecular Microbiology* **37**: 671-679.
- Bauder, J. W.** (2001). "Interpretation of chemical analysis of irrigation water and water considered for land spreading." Personal communication. *Montana State University, Bozeman, Montana* .
- Bengtsson, B. O.** (1992). Barley genetics--not only here for the ? *Trends in Genetics* **8**: 3-5.
- Benton-Jones, J.** (1983). A guide for the hydroponic and soil less culture grower. *Timber press, Portland, Oregon*. 124-125.
- Berrie, A. M. M.** (1977). An Introduction to the Botany of the Major Crop Plants. *Heyden & Son Ltd* : 1-53.
- Blackman, F. F.** (1905). Optima and limitig factors. *Annals of Botany* **19**: 281-295.
- Blum, A.** (1988). Plant Breeding for Stress Environments. *CRC Press, Inc., Boca Raton, FL* .
- Blumwald, E., Aharon, G. S., and Apse, M. P.** (2000). Sodium transport in plant cells. *Biochem.Biophys.Acta* **1465**:140-151. **1465**: 140-151.
- Bole, J. B. and Wells, S. A.** (1979). Dryland soil salinity: Effect on the yield and yield components of 6-row barley, 2-row barley, wheat, and oats. *Canadian Journal of Soil Science*, **59**: 11-17.
- Brown, L. R.** (1995). Who will feed China. New York:W.W. Norton.
- Brown, R. and Nielsen, L.** (2000). Leading wildlife acadmic programs into the new millennium. **28(3)**: 495-502. *Wildlife Society Bulletin*.
- Brownell, P. F. and Crossland, C. J.** (1972). The requirements of sodium as a micronutrient by species having the C4 dicarboxylic photosynthetic pathway. *Plant Physiology* **49**: 794-797.

- Brüggemann, L., Dietrich, P., Becker, D., Dreyer, I., Palme, K., and Hedrich, R.** (1999). Channel-mediated high-affinity K⁺ uptake into guard cells from Arabidopsis. *Proceedings of the National Academy of Sciences* **96**: 3298-3302.
- Buchanan, B. B., Gruissem, W., and Jones, R. L.** (2000). Biochemistry and Molecular Biology of Plants. *American Society of Plant Physiologists, Rockville, MD*.
- Buringh, P.** (1989). Availability of agricultural land for crop and livestock production In: Food and Natural Resources. Pimentel, D. and Hall, C.W. (eds). *Academic Press, San Diego* : 69-83.
- Bush, D. S.** (1995). Calcium regulation in plant cells and its role in signaling. . *Ann.Rev, plant physiol.Mol.Biol.* **46**: 95-122.
- Carimi, F., Zottini, M., Costa, A., Cattelan, I., DE Michele, R., Terzi, M., and LO Schiavo, F.** (2005). NO signalling in cytokinin-induced programmed cell death. *Plant, Cell & Environment* **28**: 1171-1178.
- Carpenter, B. and Watson, T.** (1994). More people, more pollution,US News and world Report. **1117 (10)**: 63-65.
- Cash, P.** (2002). Proteomics: the protein revolution. *Biologist* **49**: 58-62.
- Castillo, E., Tuong, T. P., Inubushi, K., and Ismail, A.** (2004). Comparative Effects of Osmotic and Ionic Stresses on Yield and Biomass Accumulation in IR64 Rice Variety. *Soil Sci Plant Nutr* **50**: 1313-1315.
- Chambers, G., Lawrie, L., Cash, P., and Murray, G. I.** (2000). Proteomics: a new approach to the study of disease. *Journal of Pathology* **192**: 280-288.
- Chandler, P. M. and Robertson, M.** (1994). Gene expression regulated by abscisic acid and its relation to stress tolerance. *Annual Review of Plant Physiology and Plant Molecular Biology* **45**: 113-141.
- Chartier, P.** (1970). A model for CO₂ assimilation in leaf. In Rees AR, Cockshull KE, Hand DW, Hurd RG (eds) prediction and measurmentof photosynthesis productivity. *Academic Press, London*. 305-326.
- Chee, M., Yang, R., Hubbell, E., Berno, A., Huang, X. C., Stern, D., Winkler, J., Lockhart, D. J., Morris, M. S., and Fodor, S. P.** (1996). Accessing genetic information with high-density DNA arrays. *Science* **274**: 610-614.
- Cheung, V. G., Gregg, J. P., Gogolin-Ewens, K. J., Bandong, J., Stanley, C. A., Baker, L., Higgins, M. J., Nowak, N. J., Shows, T. B., Ewens, W. J., Nelson, S. F., and Spielman, R. S.** (1998). Linkage-disequilibrium mapping without genotyping. *Nature Genetics* **18**: 225-230.
- Chinnusamy, V., Jagendorf, A., and Zhu, J. K.** (2005). Understanding and Improving Salt Tolerance in Plants. *Crop Science* **45**: 437-448.

- Cho, Y. H., Yoo, S. D., and Sheen, J.** (2006). Regulatory Functions of Nuclear Hexokinase1 Complex in Glucose Signaling. *Cell* **127**: 579-589.
- Clarke, H. H.** (1967). Agricultural History Review **15**, 1-18. Cited in Barley. Ed. by Briggs, D. E. (1978). pp. 76-88. *Chapman & Hall, London*.
- Cornic, G.** (2000). Drought stress inhibits photosynthesis by decreasing stomatal aperture - not by affecting ATP synthesis. *Trends in Plant Science* **5**: 187-188.
- Corwin, D. L., Kaffka, S. R., Hopmans, J. W., Mori, Y., van Groenigen, J. W., van Kessel, C., Lesch, S. M., and Oster, J. D.** (2003). Assessment and field-scale mapping of soil quality properties of a saline-sodic soil. *Geoderma* **114**: 231-259.
- Cramer, G. R., Epstein, E., and Läuchli, A.** (1989). Na-Ca interactions in barley seedlings: relationship to transport and growth. *Plant Cell Environ* **12**: 551-558.
- Cramer, G. R., Läuchli, A., and Epstein, E.** (1987). Influx of Na⁺ effects of supplemental Ca²⁺. *Plant Physiol.* **83**: 510-516.
- Cramer, G. R., Läuchli, A., and Polito, V. S.** (1985). Displacement of Ca²⁺ by Na⁺ from the plasmalemma of root cells. A primary response to salt stress? *Plant Physiol.* **79**: 202-211.
- de Saizieu, A., Certa, U., Warrington, J., Gray, C., Keck, W., and Mous, J.** (1998). Bacterial transcript imaging by hybridization of total RNA to oligonucleotide arrays. *Nature Biotechnology* **16**: 45-48.
- Donovan, T. R. and Day, A. D.** (1969). Some effects of high salinity on germination and emergence of barley (*Hordeum vulgare* L. emend Lam.). *Agron.J.* **61**: 236-238.
- Doos, B. R.** (1994). Environmental degradation, global food production, and risk for larger-scale migrations. *Ambio* **23(2)**: 124-130.
- Edwards, K., Johnstone, C., and Thompson, C.** (1991). A simple and rapid method for the preparation of plant genomic DNA for PCR analysis. *Oxford University Press, Nucleic Acids Research* **19**: 1349-1349.
- Epstein, E.** (1961). The essential role of calcium in selective cation transport by plant cells. *Plant Physiol.* **36**: 437-444.
- Epstein, E.** (1965). Mineral metabolism. In: Plant biochemistry, J. Bonnet, J.E. Varner, eds. *New York: Academic Press* : 438-466.
- Epstein, E.** (1966). Dual Pattern of Ion Absorption by Plant Cells and by Plants. *Nature* **212**: 1324-1327.
- Epstein, E., Rains, D. W., and Elzam, O. E.** (1963). Resolution of dual mechanisms of potassium absorption by barley roots. *Proc Natl Acad Sci U S A* **49 (5)**: 684-692.

- Fageria, N. K.** (1992). Maximising crop yields. pp. 189. *Marcel Deker, New York* : 189-193.
- Fairbairn, D. J., Liu, W., Schachtman, D. P., Gomez-Gallego, S., Day, S. R., and Teasdale, R. D.** (2000). Characterisation of two distinct HKT1-like potassium transporters from *Eucalyptus camaldulensis*. *Plant Molecular Biology* **43**: 515-525.
- FAO** (1990). An international action program on water and sustainable agricultural development. A Strategy for the Implementation of the Mar del Pintos Action Plan of the 1990s. *Rome, Italy:FAO* .
- FAO** (1991). Food balance sheets (Rome).
- FAO** (2002). the state of food and agriculture 2002.(Rome, FAO).
- Farquhar, G. D. and Sharkey, T. D.** (1982). Stomatal conductance and photosynthesis. *Annu.Rev.Plant Physiol.* **33**: 317-345.
- Farquhar, G. D., von Caemmerer, S., and Berry, J. A.** (1980). A Biochemical Model of Photosynthetic CO₂ Assimilation in Leaves of C₃ Species. *Planta* **149**: 78-90.
- Fernandez-Ballester, G., Garcia-Sanchez, F., Cerda, A., and Martinez, V.** (2003). Tolerance of citrus root stock seedling to saline stress based on their ability to regulate ion uptake and transport. *Tree Physiology* **23**: 265-271.
- Findlay, G. P., Tyerman, S. D., Garrill, A., and Skerrett, M.** (1994). Pump and K⁺ inward rectifiers in the plasmalemma of wheat root protoplasts. *Journal of Membrane Biology* **139**: 103-116.
- Flexas, J. and Medrano, H.** (2002). Drought-inhibition of photosynthesis in C₃ plants: stomatal and non-stomatal limitations revisited. *Annals of Botany* **89**: 183-189.
- Flower, T. J., Troke, P. F., Yeo, and A.R.** (1977). The mechanism of salt tolerance in halophytes. *Annual Review of Plant Physiology* **28**: 89-121.
- Flowers, T. J. and Lauchli, A.** (1983). Sodium versus potassium: Substitution and compartmentation. *In Encyclopedia of Plant Physiology New Series. In: Lauchli and RL, Bielecki* **15 B. Eds**: 651-681.
- Frova, C.** (2003). The plant glutathione transferase gene family: genomic structure, functions, expression and evolution. *Physiologia Plantarum* **119**: 469-479.
- Fu, H. and Luan, S.** (1998). AtKUP1: A Dual-Affinity K⁺ Transporter from Arabidopsis. *Plant Cell* **10**: 63-74.
- Fukuda, A., Nakamura, A., and Tanaka, Y.** (1999). Molecular cloning and expression of the Na⁺/H⁺ exchanger gene in *Oryza sativa*. *Biochimica et Biophysica Acta* **1446**: 149-155.
- Garciadeblas, B., Benito, B., and Rodríguez-Navarro, A.** (2002). Molecular cloning and functional expression in bacteria of the potassium transporters CnHAK1 and

CnHAK2 of the seagrass *Cymodocea nodosa*. *Plant Molecular Biology* **50**: 623-633.

Gassmann, W., Rubio, F., and Schroeder, J. I. (1996). Alkali cation selectivity of the wheat root high-affinity potassium transporter HKT1. *The Plant Journal* **10**: 869-882.

Gassmann, W. and Schroeder, J. I. (1994). Inwardrectifying K⁺ channel currents in root hairs of wheat: A mechanism for aluminum-sensitive low-affinity K⁺ uptake and membrane potential control. *Plant Physiol.* **105**: 1399-1408.

Gaxiola, R. A., Li, J., Undurraga, S., Dang, L. M., Allen, G. J., Alper, S. L., and Fink, G. R. (2001). Drought- and salt-tolerant plants result from overexpression of the AVP1 H⁺-pump. *Proceedings of the National Academy of Sciences of the United States of America* **98**: 11444-11449.

Gaxiola, R. A., Rao, R., Sherman, A., Grisafi, P., Alper, S. L., and Fink, G. R. (1999). The *Arabidopsis thaliana* proton transporters, AtNhx1 and Avp1, can function in cation detoxification in yeast. *Proceedings of the National Academy of Sciences* **96**: 1480-1485.

Gierth, M., Maser, P., and Schroeder, J. I. (2005). The potassium transporter AtHAK5 functions in K⁺ deprivation-induced high-affinity K⁺ uptake and AKT1 K⁺ channel contribution to K⁺ uptake kinetics in *Arabidopsis* roots. *Plant Physiology* **137**: 1105-1114.

Glenn, E., Brown, J. J., and Blumwald, E. (1999). Salt-tolerant mechanisms and crop potential of halophytes. *Critical Reviews in Plant Sciences* **18**: 227-255.

Gómez, J., Sánchez-Martínez, D., Stiefel, V., Rigau, J., Puigdomènech, P., and Pagès, M. (1988). A gene induced by the plant hormone abscisic acid in response to water stress encodes a glycine-rich protein. *Nature* **334**: 262-264.

Gong, Z., Koiwa, H., Cushman, M. A., Ray, A., Bufford, D., Kore-eda, S., Matsumoto, T. K., Zhu, J., Cushman, J. C., Bressan, R. A., and Hasegawa, P. M. (2001). Genes that are uniquely stress regulated in salt overly sensitive (sos) mutants. *Plant Physiology* **126**: 363-375.

Gorg, A., Obermaier, C., Boguth, G., Harder, A., Scheibe, B., Wildgruber, R., and Weiss, W. (2000). The current state of two-dimensional electrophoresis with immobilized pH gradients. *Electrophoresis* **21**: 1037-1053.

Gorham, J. (1992a). Salt tolerance of plants. *Sci.Prog.Oxf.* **76**: 273-285.

Gorham, J. (1992b). Stress Tolerance and Mechanisms behind Tolerance in Barley. *Barley Genetics*, 1035-1949.

Graveley, B. R. (2001). Alternative splicing: increasing diversity in the proteomic world. *Trends in Genetics* **17**: 100-107.

Greenway, H. and Munns, R. (1980). Mechanisms of salt tolerance in nonhalophytes. *Annu.Rev.Plant Physiol.* **31**: 149-190.

- Guo, Y., Halfter, U., Ishitani, M., and Zhu, J. K.** (2001). Molecular characterization of functional domains in the protein kinase SOS2 that is required for plant salt tolerance. *Plant Cell* **13**: 1383-1400.
- Gygi, S. P. and Aebersold, R.** (2000). Mass spectrometry and proteomics. *Current Opinion in Chemical Biology* **4**: 489-494.
- Gygi, S. P., Rist, B., and Aebersold, R.** (2000). Measuring gene expression by quantitative proteome analysis. *Current Opinion in Biotechnology* **11**: 396-401.
- Gygi, S. P., Rochon, Y., Franza, B. R., and Aebersold, R.** (1999). Correlation between protein and mRNA abundance in yeast. *Molecular & Cellular Biology* **19**: 1720-1730.
- Hacia, J. G., Makalowski, W., Edgemon, K., Erdos, M. R., Robbins, C. M., Fodor, S. P., Brody, L. C., and Collins, F. S.** (1998). Evolutionary sequence comparisons using high-density oligonucleotide arrays. *Nature Genetics* **18**: 155-158.
- Halfter, U., Ishitani, M., and Zhu, J. K.** (2000). The Arabidopsis SOS2 protein kinase physically interacts with and is activated by the calcium-binding protein SOS3. *Proceedings of the National Academy of Sciences of the United States of America* **97**: 3735-3740.
- Hanson, B., Grattan, S. R., and Fulton, A.** (1999). "Agricultural Salinity and Drainage." University of California Irrigation Program. . *University of California, Davis* .
- Harlan, J. R.** (1995). Barley. In: Evolution of crop plants. Eds. *Smartt, J. & Simmonds, N.W.* London Longman. 140-147.
- Harlan, J. R. and Zohary, D.** (1966). *Science*, **153**, 1074-1080. Cited in Barley. Ed. by Briggs, D. E. (1978). pp. 78-88. *Chapman & Hall, London* .
- Haro, R., Sainz, L., Rubio, F., and Rodriguez-Navarro, A.** (1999). Cloning of two genes encoding potassium transporters in *Neurospora crassa* and expression of the corresponding cDNAs in *Saccharomyces cerevisiae*. *Molecular Microbiology* **31**: 511-520.
- Harrison, P. M. and Arosio, P.** (1996). The ferritins : molecular properties, iron storage, function and cellular regulation. *Biochimica et Biophysica Acta* **1275**: 161-203.
- Hayashi, M. and Nishimura, M.** (2006). *Arabidopsis thaliana*--A model organism to study plant peroxisomes. *Biochimica et Biophysica Acta (BBA) - Molecular Cell Research* **1763**: 1382-1391.
- Heakal, M. S., El-abasiri, A., Abo-Elenin, R. A., and Gomma, A. S.** (1981). Studies on salt-tolerance in barley and wheat. I. Screening techniques. In *Proceedings of the 4th International. Barley Genetics Symposium. Edinburgh*, 394-401.

- Heazlewood, J. L., Tonti-Filippini, J. S., Gout, A. M., Day, D. A., Whelan, J., and Millar, A. H.** (2004). Experimental Analysis of the Arabidopsis Mitochondrial Proteome Highlights Signaling and Regulatory Components, Provides Assessment of Targeting Prediction Programs, and Indicates Plant-Specific Mitochondrial Proteins. *THE PLANT CELL* **16**: 241-256.
- Hoagland, D. R. and Arnon, D. I.** (1950). The water culture method of growing plants without soil. California Agricultural. *Experiment Station circular* : 347-360.
- Huang, J., Pray, C., and Rozelle, S.** (2002). Enhancing the crops to feed the poor. *Nature* **418**: 678-684.
- Huang, Y. Z., Zhang, G. G., Wu, F. B., Chen, I. X., and Zhou, M. X.** (2006). Differences in Physiological Traits Among Salt-Stressed Barley Genotypes. *Communications in Soil Science and Plant Analysis* **37**: 557-570.
- Husain, S., Munns, R., and Condon, A. G.** (2003). Effect of sodium exclusion trait on chlorophyll retention and growth of durum wheat in saline soil. *Aust.J.Agric.Res.* **54(6)**: 589-597.
- Jacoby, B.** (1964). Sodium retention in excised bean stems. *Physiologia planlarum* **18**: 730-739.
- James, R. A., Rivelli, A. R., Munns, R., and von Caemmerer, S.** (2002). Factors affecting CO₂ assimilation, leaf injury and growth in salt-stress durum wheat. *Funct Plant Biol* **29**: 1393-1403.
- Jayne, V.** (1999). Economies of ecology. *New Zealand Management* **46(3)**: 26-30.
- Jiang, X. S., Tang, L. Y., Dai, J., Zhou, H., Li, S. J., Xia, Q. C., Wu, J. R., and Zeng, R.** (2005). Quantitative analysis of severe acute respiratory syndrome (SARS)-associated coronavirus-infected cells using proteomic approaches: implications for cellular responses to virus infection. *Molecular & Cellular Proteomics* **4**: 902-913.
- Jones, R. A.** (1992). Developing crops better adapted to saline environment: progress, puzzles, and constraints. *Acta Hort.(wageningen)* **323**: 461-473.
- Kamei, A., Seki, M., Umezawa, T., Ishida, J., Satou, M., Akiyama, K., Zhu, J. K., and Shinozaki, K.** (2005). Analysis of gene expression profiles in Arabidopsis salt overly sensitive mutants *sos2-1* and *sos3-1*. *Plant, Cell & Environment* **28**: 1267-1275.
- Keunecke, M., Lindner, B., Seydel, U., Schulz, A., and Hansen, U. P.** (2001). Bundle sheath cells of small veins in maize leaves are the location of uptake from the xylem. *Journal of Experimental Botany* **52**: 709-714.
- Kim, E. J., Kwak, J. M., Uozumi, N., and Schroeder, J. I.** (1998). AtKUP1: an Arabidopsis gene encoding high-affinity potassium transport activity. *Plant Cell* **10**: 51-62.

- Kishore, G. M. and Shewmaker, C.** (1999). Biotechnology: enhancing human nutrition in developing and developed worlds. *Proceedings of the National Academy of Sciences of the United States of America* **96**: 5968-5972.
- Klein, E. M., Mascheroni, L., Pompa, A., Ragni, L., Weimar, T., Lilley, K. S., Dupree, P., and Vitale, A.** (2006). Plant endoplasmic reticulum supports the protein secretory pathway and has a role in proliferating tissues. *The Plant Journal* **48**: 657-673.
- Kramer, P. J. and Boyer, J. S.** (1995). Water Relations of Plants and Soils. *Academic Press, San Diego, CA-USA*.
- LaHaye, P. A. and Epstein, E.** (1971). Calcium and salt tolerance by bean plants. *Plant Physiol.* **25**: 213-218.
- LaRosa, P., Rhodes, D., Clithero, J., Watad, A., and Bressan, R.** (1987). Abscisic acid stimulated osmotic adjustment and its involvement in adaptation of tobacco cells to NaCl. *Plant Physiology* **85**: 174-181.
- Läuchli, A.** (1984). Salt exclusion: An adaptation of legumes for crops and pastures under saline conditions. In Salinity tolerance in plants. Strategies for crop improvement. Eds. *R C Staples and GH Toenniessen John Wiley and Sons, New York* : 171-187.
- Laurie, D. A., Pratchett, N., Bezant, J. H., and Snape, J. W.** (1995). RFLP mapping of five major genes and eight quantitative trait loci controlling flowering time in a winter × spring barley (*Hordeum vulgare* L.). *Genome* **38**: 575-585.
- Lawlor, D. W.** (1995). The effects of water deficit on photosynthesis. In Environmental and Plant Metabolism: Flexibility and Acclimation (ed. N. Smirnov). *BIOS Scientific Publishers, Oxford, UK*. 129-160.
- Le Naour, F., Hohenkirk, L., Grolleau, A., Misek, D. E., Lescure, P., Geiger, J. D., Hanash, S., and Beretta, L.** (2001). Profiling changes in gene expression during differentiation and maturation of monocyte-derived dendritic cells using both oligonucleotide microarrays and proteomics. *Journal of Biological Chemistry* **276**: 17920-17931.
- Le Roch, K. G., Johnson, J. R., Florens, L., Zhou, Y., Santrosyan, A., Grainger, M., Yan, S. F., Williamson, K. C., Holder, A. A., Carucci, D. J., Yates, J. R., III, and Winzler, E. A.** (2004). Global analysis of transcript and protein levels across the *Plasmodium falciparum* life cycle. *Genome Research* **14**: 2308-2318.
- Lessani, H. and Marschner, H.** (1978). Relation Between Salt Tolerance and Long-Distance Transport of Sodium and Chloride in Various Crop Species. *Australian Journal of Plant Physiology* **5**: 27-37.
- Leverenz, J. W.** (1987). Chlorophyll content and the light response curve of shade-adapted conifer needles. *Physiol. Plant* **71**: 20-29.

- Leverenze, J. W.** (1988). The effects of illumination sequence, CO₂ concentration, temperature and acclimation on the convexity of the photosynthetic light response curve. *Physiol.Plan* **74**: 332-341.
- Lewis, L. N.** (1984). A vital resource in danger. *Calif Agric. Calif.Agric.* **38 (10)**: 33-34.
- Lister, R., Chew, O., Lee, M. N., Heazlewood, J. L., Clifton, R., Parker, K. L., Millar, A. H., and Whelan, J.** (2004). A Transcriptomic and Proteomic Characterization of the Arabidopsis Mitochondrial Protein Import Apparatus and Its Response to Mitochondrial Dysfunction. *Plant Physiology* **134**: 777-789.
- Liu, J. and Zhu, J. K.** (1998). A calcium sensor homolog required for plant salt tolerance. *Science* **280**: 1943-1945.
- Liu, W., Fairbairn, D. J., Reid, R. J., and Schachtman, D. P.** (2001). Characterization of two *HKT1* homologues from *Eucalyptus camaldulensis* that display intrinsic osmosensing capability. *Plant Physiol.* **127**: 283-294.
- Maas, E. V.** (1986). Salt tolerance of plants. *Appl.Agric.Res* **1**: 12-25.
- Maas, E. V. and Hoffman, G. J.** (1977). Crop Salt Tolerance-Current Assessment. *Journal of the Irrigation and Drainage Division* **103**: 115-134.
- Maathuis, F. J. and Sanders, D.** (1995). Contrasting roles in ion transport of two K⁺ - channel types in root cells of *Arabidopsis thaliana*. *Planta* **197**: 456-464.
- Maathuis, F. J. and Sanders, D.** (2001). Sodium uptake in Arabidopsis roots is regulated by cyclic nucleotides. *Plant Physiology* **127**: 1617-1625.
- Maathuis, F. J. M., Ichida, A. M., Sanders, D., and Schroeder, J. I.** (1997). Roles of higher plant K⁺ channels. *Plant Physiol.* **114**: 1141-1149.
- Maeshima, M.** (2001). Tonoplast transporters: Organization and Function. *Annual Review of Plant Physiology and Plant Molecular Biology* **52**: 469-497.
- Magnotta, S. and Gogarten, J.** (2002). Multi site polyadenylation and transcriptional response to stress of a vacuolar type H⁺-ATPase subunit A gene in *Arabidopsis thaliana*. *BMC Plant Biology* **2**: 3-13.
- Malcolm, C. V.** (1982). Wheatbelt Salinity: A Review of the Salt Land Problem in South Western Australia. *WA-Dep.Agric.Tech.Bul.* 52-56.
- Marschner, H.** (1995). Mineral Nutrition of Higher Plants. *Academic Press, London.*
- Marshall, B. and Biscoe, P. V.** (1980). A model for C-3 leaves describing the dependence of net photosynthesis on irradiance: I- Derivation. *J Exp Bot* **31**: 29-39.
- Martinez-Cordero, M. A., Martinez, V., and Rubio, F.** (2005). High-affinity K⁺ uptake in pepper plants. *Journal of Experimental Botany* **56**: 1553-1562.

- Mäser, P., Thomine, S., Schroeder, J. I., Ward, J. M., Hirschi, K., Sze, H., Talke, I. N., Amtmann, A., Maathuis, F. J., Sanders, D., Harper, J. F., Tchieu, J., Gribskov, M., Persans, M. W., and Salt, D. E.** (2001). Phylogenetic relationships within cation transporter families of Arabidopsis. *Plant Physiology* **126**: 1646-1667.
- Mass, E. V. and Grieve, C. M.** (1987). Sodium-induced calcium deficiency in salt-stressed corn. *Plant Cell Environ* **10**: 559-564.
- Massoud, F. I.** (1974). Salinity and alkalinity as soil degradation hazards. Rept. FAO/UNEP. Expert Consultation on soil degradation. *FAO, Rome* .
- May, M. J. and Leaver, C. J.** (1993). Oxidative Stimulation of Glutathione Synthesis in Arabidopsis-Thaliana Suspension-Cultures. *Plant Physiology* **103**: 621-627.
- McCabe, P. F. and Leaver, C. J.** (2000). Programmed cell death in cell cultures. *Plant Molecular Biology* **44**: 359-368.
- Mengel, K. and Kirkby, E. A.** (1982). Principles of plant nutrition. Worbiaufen-Berne, Switzerland: International Potash Institute. *International Potash Institute*. 655-656.
- Molloy, M. P.** (2000). Two-dimensional electrophoresis of membrane proteins using immobilized pH gradients. *Analytical Biochemistry* **280**: 1-10.
- Morpurgo, R.** (1991). Correlation between Potato Clones Grown in vivo and in vitro under Sodium Chloride Stress Conditions. *Plant Breeding* **107**: 80-82.
- Moya, J. L., Gomez-Codenas, A., Primo-Millo, E., and Talon, M.** (2003). Chloride absorption in salt-sensitive Carrizo citrange and salt-tolerant Cleopatra mandarin citrus rootstocks is linked to water use. *Journal of Experimental Botany* **54**: 825-833.
- Munns, R.** (1993). Physiological processes limiting plant growth insaline soils: some dogmas and hypotheses. *Plant, Cell and Environment* **16**: 15-24.
- Munns, R.** (2002). Comparative physiology of salt and water stress. *Plant Cell Environ.* **25**: 239-250.
- Munns, R.** (2005). Genes and salt tolerance: bringing them together. *New Phytologist* **167**: 645-663.
- Munns, R., Schachtman, D. P., and Condon, A. G.** (1995). The significance of a two-phase growth response to salinity in wheat end barley. *Aust.J.plant physiol* **22**: 561-569.
- Nito, K., Hayashi, M., and Nishimura, M.** (2002). Direct Interaction and Determination of Binding Domains among Peroxisomal Import Factors in Arabidopsis thaliana. *Plant and Cell Physiology* **43**: 355-366.
- Nito, K., Kamigaki, A., Kondo, M., Hayashi, M., and Nishimura, M.** (2007). Functional Classification of Arabidopsis Peroxisome Biogenesis Factors

Proposed from Analyses of Knockdown Mutants. *Plant and Cell Physiology* **48**: 763-774.

O'Farrell, P. H. (1975). High resolution two-dimensional electrophoresis of proteins. *Journal of Biological Chemistry* **250**: 4007-4021.

Ogren, E. (1993). Convexity of the photosynthetic light-response curve in relation to intensity and direction of light during growth. *Physiol. Plant* **101**: 1013-1019.

Ogren, E. and Evans, J. R. (1993). Photosynthetic light-response curves :I. The influence of CO₂ partial pressures and leaf inversion. *Planta* **189**: 182-190.

Palzkill, T. (2002). Proteomics. Springer. Kluwer Academic Publishers. *Kluwer Academic* .

Pardossi, A., Vernieri, P., and Tognoni, F. (1991). Evaluation of the pressure chamber method for the assessment of water status in chilled plant. *Plant, Cell and Environment* **14**: 675-682.

Pessaraki, M. and Marcum, K. B. (2000). Growth responses and Nitrogen-15 absorption of *Distichlis* under sodium chloride stress. ASA-CSSA-SSSA Annual Meetings, Nov. 5-9, 2000, Minneapolis, Minnesota. (*Agronomy abstracts*) .

Pessaraki, M., Marcum, K. B., and Kopec, D. M. (2001). Growth responses of desert saltgrass (*Distichlis spicata* L.) under salt stress. Turfgrass Landscape and Urban IPM Research Summary 2001, Cooperative Extension, Agricultural Experiment Station, The University of Arizona, Tucson, U.S. *Department of Agriculture, AZ1246 Series P-126* : 70-73.

Petit, J. M., Briat, J. F., and Lobréaux, S. (2001). Structure and differential expression of the four members of the *Arabidopsis thaliana* ferritin gene family. *Biochemical Journal* **359**: 575-582.

Pimental, D., Huang, X., Cordova, A., and Pimental, M. (1997). Impact of population growth on food supplies and environment. *Population and Environment* **19**: 9-14.

Plant, J., Smith, D., and Williams, L. (2000). Environmental geochemistry at the global scale. *Journal of the Geological Society* **157(4)**: 837-849.

Price, J. (2005). An investigation into halotolerance mechanisms in *Arabidopsis thaliana*. *PhD thesis University of Glasgow*.

Qiu, Q. S., Guo, Y., Dietrich, M. A., Schumaker, K. S., and Zhu, J. K. (2002). Regulation of SOS1, a plasma membrane Na⁺/H⁺ exchanger in *Arabidopsis thaliana*, by SOS2 and SOS3. *Proceedings of the National Academy of Sciences of the United States of America* **99**: 8436-8441.

Quintero, F. J., Ohta, M., Shi, H., Zhu, J. K., and Pardo, J. M. (2002). Reconstitution in yeast of the *Arabidopsis* SOS signaling pathway for Na⁺ homeostasis. *Proceedings of the National Academy of Sciences of the United States of America* **99**: 9061-9066.

- Quintero, F. J. and Blatt, M. R.** (1997). A new family of K⁺ transporters from Arabidopsis that are conserved across phyla. *FEBS Letters* **415**: 206-211.
- Rabinowich, E. I.** (1951). Photosynthesis and related processes. *Wiley, New York* vol. **2**: 831-1191.
- Rains, D. W.** (1972). Salt transport by plants in relation to salinity. *Annu.Rev.Plant Physiol.* **23**: 367-388.
- Rains, D. W. and Epstein, E.** (1965). Transport of sodium in plant tissue. *Science* **148**: 1611-1620.
- Ramos, J., Alijo, R., Haro, R., and Rodriguez-Navarro, A.** (1994). TRK2 is not a low-affinity potassium transporter in *Saccharomyces cerevisiae*. *J.Bacteriol* **176**: 249-252.
- Ramos, J., Contreras, P., and Rodriguez-Navarro, A.** (1985). A potassium transport mutant of *Saccharomyces cerevisiae*. *Arch.Microbiol* **143**: 88-93.
- Rawson, H. M., Richard, R. A., and Munns, R.** (1988). An examination of selection criteria for salt tolerance in wheat, barley and triticale genotypes. *Australian Journal of Agricultural Research* **39**: 759-771.
- Rengel, Z.** (1992). The role of calcium in salt toxicity. *Plant Cell Environ.* **15**: 625-632.
- Rhoades, J. D.** (1977). "Potential for using saline agricultural drainage waters for irrigation." Proceedings from Water Management for Irrigation and Drainage. *American Society of Civil Engineers.Reno, Nevada.* 20-22.
- Richard, R. A., Dennet, C. W., Qualset, C. O., Epstein, E., Norlyn, J. D., and Winslow, M. D.** (1987). Variation in yield of grain and biomass in wheat, barley and triticale in a saltaffected field. *Field Crops Research*, **15**: 277-288.
- Roberts, S. K. and Tester, M.** (1995). Inward and outward K⁺-selective currents in the plasma membrane of protoplasts from maize root cortex and stele. *PlantJ.* **8**: 811-825.
- Rodriguez-Navarro, A.** (2000). Potassium transport in fungi and plants. *Biochimica et Biophysica Acta* **1469**: 1-30.
- Rodriguez-Navarro, A., Quintero, F. J., and Garciadeblas, B.** (1994). Na⁺-ATPases and Na⁺/H⁺ antiporters in fungi. *Biochimica et Biophysica Acta* **1187**: 203-205.
- Rodriguez-Navarro, A. and Ramos, A.** (1984). Dual system potassium transport in *Saccharomyces cerevisiae*. *J.Bacteriol.* **159**: 940-945.
- Rodriguez-Navarro, A. and Rubio, F.** (2006). High-affinity potassium and sodium transport systems in plants. *Journal of Experimental Botany* **57**: 1149-1160.
- Rubio, F., Gassmann, W., and Schroeder, J. I.** (1995). Sodium-driven potassium uptake by the plant potassium transporter HKT1 and mutations conferring salt tolerance. *Science* **270**: 1660-1663.

- Rubio, F., Santa-Maria, G. E., and Rodriguez-Navarro, A.** (2000). Cloning of *Arabidopsis* and barley cDNAs encoding HAK potassium transporters in root and shoot cells. *Physiologia Plantarum* **109** (1), 34-43. **109** (1): 34-43.
- Russell, R. B.** (2002). Genomics, proteomics and bioinformatics: all in the same boat. *Genome Biology* **3**: REPORTS4034-4035.
- Sambrook, J. and Russell, D. W.** (2001). *Molecular Cloning - A Laboratory Manual, Third Edition*. Cold Spring Harbour Laboratory Press, New York. p. A 1.2-A 1.30.
- Santa-Maria, G. E., Rubio, F., Dubcovsky, J., and Rodriguez-Navarro, A.** (1997). The HAK1 gene of barley is a member of a large gene family and encodes a high-affinity potassium transporter. *Plant Cell* **9**: 2281-2289.
- Sapolsky, R. J. and Lipshutz, R. J.** (1996). Mapping genomic library clones using oligonucleotide arrays. *Genomics* **33**: 445-456.
- Schachtman, D. P., Kumar, R., Schroeder, J. I., and Marsh, E. L.** (1997). Molecular and functional characterization of a novel low-affinity cation transporter (LCT1) in higher plants. *Proceedings of the National Academy of Sciences of the United States of America* **94**: 11079-11084.
- Schaller, C. W., Berdegve, J. A., Dennett, C. W., Richards, R. A., and Winslow, M. D.** (1981). Screening the world barley collection for salt tolerance. Proc. 4th Intern. *Barley Gen.Syrup.* 389-393.
- Schena, M., Shalon, D., Davis, R. W., and Brown, P. O.** (1995). Quantitative monitoring of gene expression patterns with a complementary DNA microarray.[see comment]. *Science* **270**: 467-470.
- Schroeder, J. I., Ward, J. M., and Gassmann, W.** (1994). Perspectives on the physiology and structure of inward-rectifying K⁺ channels in higher plants: biophysical implications for K⁺ uptake. *Annual Review of Biophysics & Biomolecular Structure* **23**: 441-471.
- Senn, M. E., Rubio, F., Bañuelos, M. A., and Rodríguez-Navarro, A.** (2001). Comparative functional features of plant potassium HvHAK1 and HvHAK2 transporters. *Journal of Biological Chemistry* **276**: 44563-44569.
- Sentenac, H., Bonneaud, N., Minet, M., Lacroute, F., Salmon, J. M., Gaymard, F., and Grignon, C.** (1992). Cloning and expression in yeast of a plant potassium ion transport system. *Science* **256**: 663-665.
- Serrano, R. and Gaxiola, R.** (1994). Microbial models and salt stress tolerance in plants. *Crit.Rev.in plant.Sci.* **13**(2): 121-138.
- Shannon, M. C.** (1984). Breeding, selection and the genetics of salt tolerance. In *Salinity Tolerance in Plants*. Eds. R C Staples and G H Toenniessen. *John Wiley and Sons, New York*. 231-254.

- Shi, H., Ishitani, M., Kim, C., and Zhu, J. K.** (2000). The Arabidopsis thaliana salt tolerance gene SOS1 encodes a putative Na⁺/H⁺ antiporter. *Proceedings of the National Academy of Sciences of the United States of America* **97**: 6896-6901.
- Shi, H., Lee, B. H., Wu, S. J., and Zhu, J. K.** (2003). Overexpression of a plasma membrane Na⁺/H⁺ antiporter gene improves salt tolerance in Arabidopsis thaliana. *Nature Biotechnology* **21**: 81-85.
- Shi, H., Xiong, L., Stevenson, B., Lu, T., and Zhu, J. K.** (2002). The Arabidopsis salt overly sensitive 4 mutants uncover a critical role for vitamin B6 in plant salt tolerance. *Plant Cell* **14**: 575-588.
- Shi, H. and Zhu, J. K.** (2002). Regulation of expression of the vacuolar Na⁺/H⁺ antiporter gene AtNHX1 by salt stress and abscisic acid. *Plant Molecular Biology* **50**: 543-550.
- Shinozaki, K. and Shinozaki-Yamaguchi, K.** (1996). Molecular responses to drought and cold stress. *Current Opinion in Biotechnology* **7**: 161-167.
- Shoemaker, D. D., Lashkari, D. A., Morris, D., Mittmann, M., and Davis, R. W.** (1996). Quantitative phenotypic analysis of yeast deletion mutants using a highly parallel molecular bar-coding strategy. *Nature Genetics* **14**: 450-456.
- Shone, M. G. T., Shone, M. G. T., and Sanderson, J.** (1969). The absorption and translocation of sodium by maize seedlings. *Planta* **86**: 301-314.
- Singh, N. K., Larosa, P. C., Handa, A. K., Hasegawa, P. M., and Bressan, R. A.** (1987). Hormonal regulation of protein synthesis associated with salt tolerance in plant cells. *Proceedings of the National Academy of Sciences of the United States of America* **84**: 739-743.
- Smith, G. S., Middleton, K. R., and Edmonds, A. S.** (1980). Sodium nutrition of pasture plants. I. Translocation of sodium and potassium in relation to transpiration rates. *New Phytologist* **84**: 603-612.
- Srivastava, J. P. and Jana, S.** (1984). Screening wheat and barley germplasm for salt tolerance. In *Salinity Tolerance in Plants*. Eds. R C Staples and G H Toenniessen. *John Wiley and Sons, New York*. 273-283.
- Street, H. E. and Opik, H.** (2006). The physiology of flowering plants. Their growth and development. *3rd ed., Baltimore, MD*.
- Su, H., Balderas, E., Vera-Estrella, R., Gollack, D., Quigley, F., Zhao, C., Pantoja, O., and Bohnert, H. J.** (2003). Expression of the cation transporter McHKT1 in a halophyte. *Plant Molecular Biology* **52**: 967-980.
- Subbarao, G. V., Ito, O., Berry, W. L., and Wheeler, R. M.** (2003). Sodium--A Functional Plant Nutrient. *Critical Reviews in Plant Sciences* **22**: 391-416.
- Sung, D. Y., Vierling, E., and Guy, C. L.** (2001). Comprehensive Expression Profile Analysis of the Arabidopsis Hsp70 Gene Family. *Plant Physiology* **126**: 789-800.

- Sweetlove, L. J., Heazlewood, J. L., Herald, V., Holtzapffel, R., Day, D. A., Leaver, C. J., and Millar, A. H.** (2002). The impact of oxidative stress on Arabidopsis mitochondria. *The Plant Journal* **32**: 891-904.
- Szabolcs, I.** (2004). Prospects of soil salinity for the 21st Century. *ISSS, 15th World Congress of Soil Science*, **1**: 123-141, Acapulco.
- Taiz, L.** (1992). The plant vacuole. *Journal of Experimental Biology* **172**: 113-122.
- Teichmann, S. A., Park, J., and Chothia, C.** (1998). Structural assignments to the Mycoplasma genitalium proteins show extensive gene duplications and domain rearrangements. *Proceedings of the National Academy of Sciences* **95**: 14658-14663.
- Terashima, I. and Saeki, T.** (1983). Light environment within a leaf 1. Optical-properties of paradermal sections of *Camellia* leaves with special reference to differences in the optical-properties of palisade and spongy tissues. *Plant & Cell Physiology* **24**: 1493-1501.
- Tezara, W., Mitchell, V. J., Driscoll, S. D., and Lawlor, D. W.** (1999). Water stress inhibits plant photosynthesis by decreasing coupling factor and ATP. *Nature* **401**: 914-917.
- Theodoulou, F. L.** (2000). Plant ABC transporters. *Biochimica et Biophysica Acta (BBA) - Biomembranes* **1465**: 79-103.
- Thornley, J. H. M.** (1976). Photosynthesis. In: Sutcliffe JF, Mahlberg P (eds) Mathematical models in plant physiology. *Academic Press, London* : 92-110.
- Toenniessen, G. H., O'Toole, J. C., and DeVries, J.** (2003). Advances in plant biotechnology and its adoption in developing countries. *Current Opinion in Plant Biology* **6**: 191-198.
- Tournaire, C., Kushnir, S., Bauw, G., Inze, D., de la Serve, B. T., and Renaudin, J. P.** (1996). A Thiol Protease and an Anionic Peroxidase Are Induced by Lowering Cytokinins during Callus Growth in Petunia. *Plant Physiology* **111**: 159-168.
- Troeh, R. F., Hobbs, J. A., and Donahue, Rl.** (1980). Irrigation and reclamation. In: soil and water conservation for productivity and environmental prentic- Hall. Inc.. *Englewood Cliffs, New Jersey* : 560-564.
- Turner, A., Beales, J., Faure, S., Dunford, R. P., and Laurie, D. A.** (2005). The Pseudo-Response Regulator Ppd-H1 Provides Adaptation to Photoperiod in Barley. *Science* **310**: 1031-1034.
- United States Bureau of the Census** (1996). Statistical abstract of the United States ed. Washinton, DC:U.S. Dep. of the United States1993. *U.S.Goverment Printing Office* **200th** .

- United States Salinity Laboratory UC Riverside, C.** (1954). Diagnosis and improvement of saline and alkali soils. *Handbook No.60, U.S.Dept.of Agriculture*.
- Unlu, M., Morgan, M. E., and Minden, J. S.** (1997). Difference gel electrophoresis: a single gel method for detecting changes in protein extracts. *Electrophoresis* **18**: 2071-2077.
- Uozumi, N., Kim, E. J., Rubio, F., Yamaguchi, T., Muto, S., Tsuboi, A., Bakker, E. P., Nakamura, T., and Schroeder, J. I.** (2000). The Arabidopsis HKT1 Gene Homolog Mediates Inward Na⁺ Currents in *Xenopus laevis* Oocytes and Na⁺ Uptake in *Saccharomyces cerevisiae*. *Plant Physiology* **122**: 1249-1260.
- US Census Bureau** (2004). Global population at a glance: 2002 and beyond, International Brief, Washington, DC: US Census Bureau. US Census Bureau.
- USDA, N. R. C. S.** (2002). Soil Conservationists. Salinity Management Guide - Salt Management. Available at. <http://www.launionsweb.org/salinity.htm>.
- Véry, A. A. and Sentenac, H.** (2003). Molecular mechanisms and regulation of K⁺ transport in higher plants. *Annual Review of Plant Biology* **54**: 575-603.
- Vogelzang, S. A. and Prins, H. B. A.** (1994). Patch clamp analysis of the dominant plasma membrane K⁺ channel in root cell protoplasts of *Plantago media* L: Its significance for the P and K state. *Journal of Membrane Biology* **141**: 113-122.
- Wagner, U., Edwards, R., Dixon, D. P., and Mauch, F.** (2002). Probing the Diversity of the Arabidopsis glutathione S-Transferase Gene Family. *Plant Molecular Biology* **V49**: 515-532.
- Wang, D. G., Fan, J. B., Siao, C. J., Berno, A., Young, P., Sapolsky, R., Ghandour, G., Perkins, N., Winchester, E., Spencer, J., Kruglyak, L., Stein, L., Hsie, L., Topaloglou, T., Hubbell, E., Robinson, E., Mittmann, M., Morris, M. S., Shen, N., Kilburn, D., Rioux, J., Nusbaum, C., Rozen, S., Hudson, T. J., Lipshutz, R., Chee, M., and Lander, E. S.** (1998). Large-scale identification, mapping, and genotyping of single-nucleotide polymorphisms in the human genome. *Science* **280**: 1077-1082.
- Wegner, L. H. and Raschke, K.** (1994). Ion channels in the xylem parenchyma of barley roots. *Plant Physiol.* **105**: 977-813.
- Western Fertilizer Handbook** (1995). Produced by the Soil Improvement Committee of the California Fertilizer Association. *Interstate Publishers, Inc., Sacramento, California* .
- White, P. J. and Broadley, M. R.** (2001). Chloride in soils and its uptake and movement within the plant. *A Review. Ann.Bot* **88**: 967-988.
- Whitehead, D. C. and Jones, L. H. P.** (1972). The effect of replacing potassium by sodium on cation uptake and transport to the shoots in four legumes and Italian ryegrass. *Ann.Appl.Biol.* **71**: 81-89.

- World Resources Institute** (1992). World Resources. ed. New York. Oxford University Press.
- World Resources Institute** (1994). World Resources 1994-95. Washington, DC, WRI .
- Wu, W., Hu, W., and Kavanagh, J. J.** (2002). Proteomics in cancer research. *International Journal of Gynecological Cancer* **12**: 409-423.
- Wyn Jones, R. G. and Pollard, A.** (1983). Encyclopedia of Plant Physiology. (Lauchl, A., and Pirson, A., eds.), New Ser. Springer-Verlag, Berlin **15B**: 528-562.
- Yan, L., Loukoianov, A., Tranquilli, G., Helguera, M., Fahima, T., and Dubcovsky, J.** (2003). Positional cloning of the wheat vernalization gene VRN1. *Proceedings of the National Academy of Sciences* **100**: 6263-6268.
- Yan, L., Loukoianov, A., Blechl, A., Tranquilli, G., Ramakrishna, W., SanMiguel, P., Bennetzen, J. L., Echenique, V., and Dubcovsky, J.** (2004). The Wheat VRN2 Gene Is a Flowering Repressor Down-Regulated by Vernalization. *Science* **303**: 1640-1644.
- Yanagida, M.** (2002a). Functional proteomics; current achievements. *Journal of Chromatography B: Analytical Technologies in the Biomedical & Life Sciences* **771**: 89-106.
- Yanagida, M.** (2002b). Functional proteomics; current achievements. [Review] [115 refs]. *Journal of Chromatography B: Analytical Technologies in the Biomedical & Life Sciences* **771**: 89-106.
- Yeo, A.** (1998). Review article. Molecular biology of salt tolerance in the context of whole-plant physiology. *Journal of Experimental Botany* **49**: 951-929.
- Yeo, M. E., Yeo, A. R., and Flowers, T. J.** (1994). Photosynthesis and photorespiration in the genus *Oryza*. *Journal of Experimental Botany* **45**: 553-560.
- Zadoks, J. C., Chang, T. T., and Konzak, B. F.** (1974). A decimal code for the growth stages of cereals. *Weed Res* **14**: 415-421.
- Zandt, P. A. V. and Mopper, S.** (2002). Delayed and carryover effects of salinity on flowering in *Iris hexagona* (Iridaceae). *American Journal of Botany* **89**: 1847-1851.
- Zhang, C. G., Chromy, B. A., and McCutchen-Maloney, S. L.** (2005). Host-pathogen interactions: a proteomic view. *Expert Review of Proteomics* **2**: 187-202.
- Zhang, H. X. and Blumwald, E.** (2001). Transgenic salt-tolerant tomato plants accumulate salt in foliage but not in fruit. *Nature Biotechnology* **19**: 765-768.
- Zhang, Y., Wang, L., Liu, Y., Zang, Q., Wei, Q., and Zhang, W.** (2006). Nitric oxide enhances salt tolerance in maize seedlings through increasing activities of proton-pump and Na⁺/H⁺ antiport in the tonoplast. *Planta* **224**: 545-555.

- Zhao, L., Zhang, F., Guo, J., Yang, Y., Li, B. i., and Zhang, L.** (2004). Nitric Oxide Functions as a Signal in Salt Resistance in the Calluses from Two Ecotypes of Reed. *Plant Physiology* **134**: 849-857.
- Zhu, J. K.** (2001). Plant salt tolerance. *Trends in Plant Science* **6**: 66-71.
- Zhu, J. K.** (2003). Regulation of ion homeostasis under salt stress. *Current Opinion in Plant Biology* **6**: 441-445.
- Zhu, J. K., Liu, J., and Xiong, L.** (1998). Genetic analysis of salt tolerance in arabidopsis. Evidence for a critical role of potassium nutrition. *Plant Cell* **10**: 1181-1191.
- Zohary, D.** (1969). The progenitors of wheat and barley in relation to domestication and agriculture dispersal in the world. In: The domestication and exploitation of plants and animals. Ed. by Ucko, P. J. & Dimbleby, G. W. Cited in Zohary and Hopf, 1994. *Duck Worth, London.* 47-66.